UNIVERSITÉ DE STRASBOURG

ÉCOLE DOCTORALE DES SCIENCES CHIMIQUES

Institut de Chimie, UMR 7177

THÈSE présentée par :

Xiaoyu REN

soutenue le : **17 Novembre 2017**

pour obtenir le grade de : **Docteur de l'université de Strasbourg**

Discipline/ Spécialité : Chimie

Synthèse et réactivité de complexes métalliques porteurs de ligands carbéniques N-hétérocycliques fonctionnels

THÈSE dirigée par :

M. BRAUNSTEIN Pierre	Directeur de recherche émérite, CNRS, Université de Strasbourg
M. WESOLEK Marcel	Chargé de recherche, CNRS, Université de Strasbourg

RAPPORTEURS :

M. GUILARD Roger	Professeur, Université de Bourgogne
M. KNOCHEL Paul	Professeur, Ludwig-Maximilians-Universität München (Germany)

AUTRES MEMBRES DU JURY :

M. MEYER Franc	Professeur, Georg-August University Göttingen (Germany)

Acknowledgements

This work was carried out in the Laboratoire de Chimie de Coordination (UMR 7177 CNRS) of the Université de Strasbourg, directed by Prof. Pierre Braunstein and Dr. Marcel Wesolek. I am very grateful to all the kind people around me because it would not have been possible for me to finish my doctoral thesis without their help and support.

Firstly, I wish to thank my supervisor Prof. Pierre Braunstein. He is a very nice and respected supervisor and his vast experience and profound knowledge in the area has helped me durting my PhD search. He always gave me constant encouragements and suggestions in spite of his busy agenda. In addtion, he also helped me deal with other problems, such as introducing some doctors who could speak English, etc. It has been my honor to be his PhD student.

Then I would like to express my sincere thanks to my co-supervisor Dr. Marcel Wesolek. He is very a kind and diligent researcher with constructive thoughts. He taught me a lot of experimental skills and guided me in the research of my thesis.

I would like to express my sincere gratitude to the members of jury, Prof. Guilard Roger, Prof. Knochel Paul, and Prof. Meyer Franc, for agreeing to be the external evaluators and participate in the defense of this thesis.

I thank Dr. Christophe Gourlaouen (Institut de Chimie, Strasbourg) for his contributuion to the theoretical calculations. I would like to thank all the members of the NMR, X-ray crystallography (Lydia Karmazin and Corinne Bailly), Elemental Analysis and Mass Spectroscopy services of the Université de Strasbourg fo their contribution and assistance.

I am grateful to the present and former secretaries for all their help : Nadia Bouaouina, Sandrine Garcin. I also thank the present and former members in our lab (in random order) : Dr. Jacky Rosé ; Dr. Andreas Danopoulos, Dr. Lucie Routaboul, Dr. Beatrice Jacques, Dr. Pierre de Fremont, Melanie Boucher, Marc Mermillon-Fournier, Alessio Ghisolfi, Sophie Hameury, Martin Jagenbrein, Paulin Buchwalter, Valentine Charra. In particular, I want to thank Thomas Simler, Pengfei Ai, Minghui Yuan and Fan He, we spent more than one year together and they helped me a lot when I came to France in 2014.

I want to express my thanks to all my Chinese friends in Strasbourg. Without

them, my life abroad would not be so interesting.

Lastly, I would like to thank my parents for all their encouragements and support.

感谢父母对我多年的支持和鼓励，我会继续努力，我爱你们。

Xiaoyu REN

Strasbourg

Octobre, 2017

ABBREVIATIONS

δ	chemical shift
Ad	adamantly
anal. calcd.	analysis calculated
Bn	benzyl
CCDC	Cambridge Crystallographic Data Center
CIF	crystallographic information files
cod	cycloocta-1,5-diene
COSY	correlation spectroscopy
Cy	cyclohexyl
Dipp	2,6-diisopropylphenyl
dme	dimethoxyethane
DMSO	dimethylsulfoxide
EADC	ethylaluminium dichloride
equiv.	(mole) equivalent
ESI	electronic supplementary information
ESI+/-	electrospray ionization (+/- mode)
GC	gas chromatography
HMBC	heteronuclear multiple-bond correlation
HSQC	heteronuclear single-quantum correlation
Im	imidazolium
KHMDS	potassium bis(trimethylsilyl)amide
MAO	methylaluminoxane
Mes	mesityl
MS	mass spectrometry
MS 3/4 Å	molecular sieves (pore size of 3/4 Å)
NHC	*N*-heterocyclic carbene
ORTEP	Oak Ridge thermal ellipsoid
Ph	phenyl
ppm	parts per million
r.t.	room temperature
THF	tetrahydrofuran

TABLE DES MATIERES

INTRODUCTION GÉNÉRALE 1

1. Bref historique et introduction des carbènes complexés avec les métaux de transition 2
2. Hémilabilité 3
3. L'oligomérisation de l'éthylène 5
   - 3.1 Production de oléfines linéaires dans l'industrie 5
   - 3.2 Utilisation de ligands carbènes N-hétérocycliques dans la réaction d'oligomérisation de l'éthylène 6
4. Complexes des métaux de transition de type pinceur 7
5. Objectifs de la thèse 9
6. References 11

CHAPITRE 1 14

1. Résumé en français 16
2. Abstract 18
3. Introduction 19
4. Results and discussion 20
5. Conclusions 37
6. Experimental section 38
7. Acknowledgements 45
8. References 46
9. Supporting Information 48

CHAPITRE 2 56

1. Résumé en français 58
2. Abstract 59
3. Introduction 59
4. Results and discussion 61
5. Conclusion 74
6. Experimental section 74
7. Acknowledgements 80

8. References 81
9. Supporting Information 83

CHAPITRE 3 89

1. Résumé en français 91
2. Supporting Information 97
3. Experimental Procedures & Results and Discussion 98
4. X-ray crystallography 108
5. Modelisation 111
6. References 115

CHAPITRE 4 116

1. Résumé en français 118
2. Abstract 119
3. Introduction 119
4. Results and discussion 121
5. Conclusion 131
6. Experimental section 132
7. Acknowledgements 137
8. References 139
9. Supporting Information 142

CONCLUSION GÉNÉRALE 147

INTRODUCTION GÉNÉRALE

1. Bref historique et introduction des carbènes complexés avec les métaux de transition

Les carbènes sont définis comme des composés neutres insaturés constitués d'un atome de carbone divalent et entouré par 6 électrons de valence. Ils peuvent participer à la constitution de complexes avec les métaux de transition. Fischer a isolé le premier complexe métal-carbène en 1964.[1]

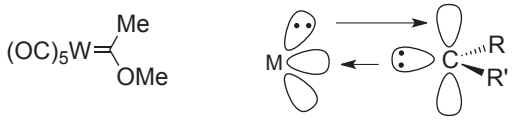

Schéma 1. Carbène singulet de type Fisher.

On retrouve ce type de carbène singulet avec les métaux de transition à bas degré d'oxydation tels que Fe(0), Mo(0), Cr(0)…

Un autre type de carbène triplet cette fois se retrouve dans le complexe du tantale à haut degré d'oxydation et a été synthétisé par R. R. Schrock en 1974.[2] Les métaux les plus fréquemment impliqués avec ce type de carbène sont le Mo, le W et le Ru.

Schéma 2. Carbène triplet de type Schrock.

Entre-temps des complexes métalliques possédant des ligands carbènes N-hétérocycliques singulet (abrégé par la suite en NHCs) ont été décrits indépendamment par Öfele[3] et Wanzlick[4] en 1968.

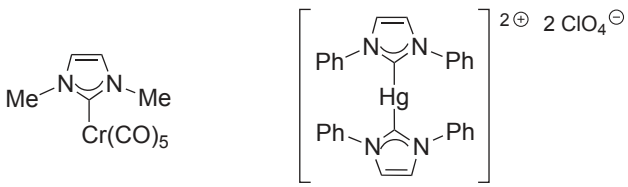

Schéma 3. Complexes de Öfele et Wanzlick avec des carbènes NHC.

Mais ce n'est qu'en 1991 que le premier NHC stable fut isolé par Arduengo 1,3-di(adamantyl)imidazol-2-ylidène.[5] Depuis, une très grande diversité de ligands NHCs a été synthétisée et on assiste à une véritable explosion du nombre d'études expérimentales, car ils mettent en œuvre non seulement les métaux de transitions mais aussi les éléments p.

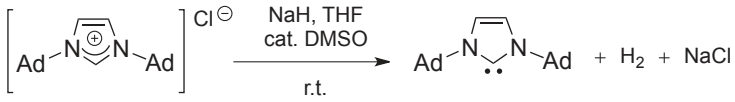

Schéma 4. Isolation du premier NHC stable.

La caractéristique des NHCs est une configuration électronique singulet avec carbone d'hybridisation sp^2 qui contient deux électrons appariés et une orbitale p vide. Les atomes d'azote adjacents de par leurs propriétés σ–électro attracteur et π donneur stabilisent par effet inductif (en abaissant l 'énergie de l'orbitale occupée s) et par effet mésomérique (en donnant de la densité électronique dans l'orbitale vide p) (Scheme 5). En comparaison avec les ligands phosphines, les NHCs exhibent un pouvoir σ donneur plus important et un pouvoir π accepteur plus faible.

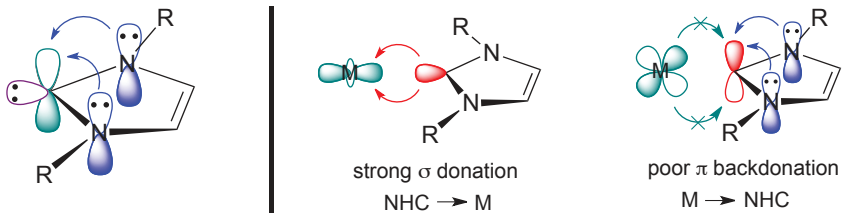

Schéma 5. Carbène-N-hétérocyclique, interaction avec le métal.

2. Hémilabilité

Le terme « ligand hémilabile » a été introduit pour la première fois par Jeffrey Rauchfuss en 1979,[6] bien que quelques exemples de ligands bi-fonctionnels possédant un mode mixte de liaison ont déjà été observés auparavant.[7] Les ligands hémilabiles sont représentés par des chélates polydentes qui possèdent au moins deus différents types de donneurs , le donneur non substituable (**D**) lié fermement au métal tandis que

le donneur (**Z**) lié de façon moins forte et de ce fait labile peut être facilement déplacé de façon réversible par d'autres ligands ou molécules de solvant (**Y**).(Schéma 6)

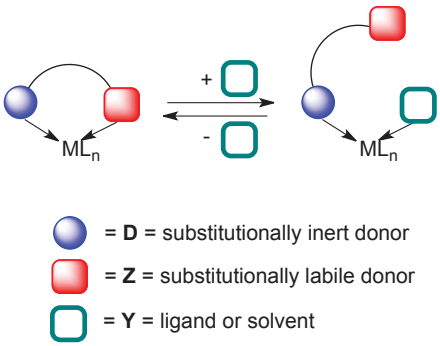

Schéma 6. Propriétés générales des ligands hémilabiles.

Les ligands hybrides qui contiennent au moins deux donneurs avec des fonctionnalités différentes peuvent se lier au métal de différentes manières du fait des interactions des différentes fonctions avec le ou les centres métalliques. Il y a trois modes de liaisons différents représenté dans le schéma 7 :1) coordination monodente, seul un donneur se coordine au centre métallique ; 2) mode chélate, deux différents donneurs se coordinent au même centre métallique par deux interactions différentes ;3) mode pontant, chaque donneur se coordine à un seul centre métallique qu'il y ait interaction entre les métaux ou non.

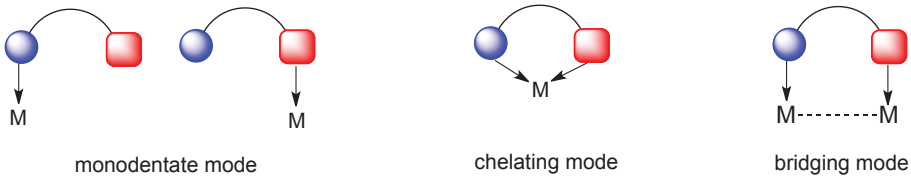

Schéma 7. Modes de liaison des ligands hybrides.

Les ligands hémilabile donnent accès à un site de coordination envers le métal durant une réaction et peuvent stabiliser des intermédiaires réactifs. Initialement l'intérêt était axé sur la coordination réversible, l'activation stoechiométrique ou catalytique et le transport de petites molécules. C'est pourquoi les complexes contenant des ligands hémilabiles se trouvaient être actives catalytiquement dans une large gamme de réactions incluant l'hydrogénation, la carbonylation ou leurs réactions inverses, l'hydroformylation des alcènes, l'époxydation des alcènes, la codimérisation et la

copolymérisation des alcènes, la métathèse par ouverture de chaîne pour donner des polymères (ROMP) etc.[8]

3. L'oligomérisation de l'éthylène

3.1 Production de oléfines linéaires dans l'industrie

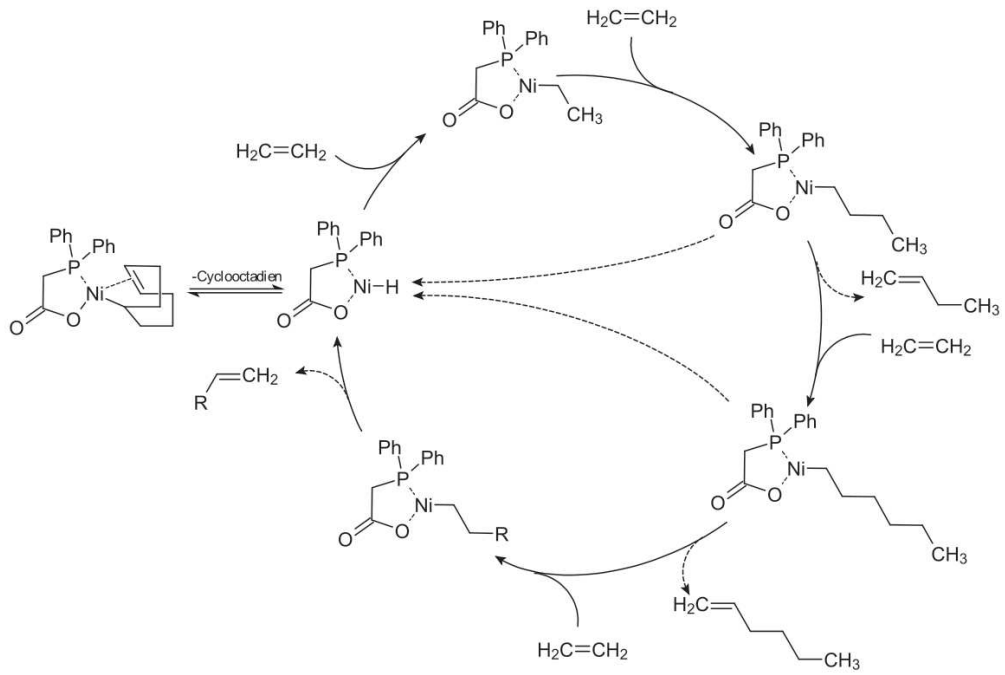

Schéma 8. Mécanisme catalytique de type SHOP (Shell Higher Olefin Process)

L'oligomérisation des alcènes et de l'éthylène en particulier pour donner des α–oléfines linéaires de courtes chaînes $C_{6\text{-}20}$ (LAOs) continue d'être un sujet d'études tant sur le plan de la recherche académique que dans l'industrie. Les alcènes terminaux en tant que produit principal de l'oligomérisation de l'éthylène sont des composés de départs pour un large éventail de produits industriels et de produits de consommation incluant les détergents biodégradables ainsi que de nouveaux types de polymères, des lubrifiants et beaucoup d'autres produits chimiques industriellement intéressants.[9] Les catalyseurs de métaux de transition et l'aluminium sont utilisés de façon prédominante pour donner une distribution offrant une gamme complète d'oligomères. Généralement deux mécanismes de croissance de chaînes sont considérés :1) via une insertion linéaire migratoire comme dans le catalyseur du

nickel dans le procédé SHOP[9a, b] (Shell Higher Olefin Process) (schéma 8) (distribution Schulz-Flory) : 2) via des intermédiaires métallacycliques (Schéma 9), dans la production de copolymères pour les « linear low-density polyethylene » (LLDPE). Du fait que les LAO avec des distributions larges ne correspondent pas à la réalité du marché[10] et d'une demande croissante pour des oligomères à chaînes courtes (en particulier 1-butène, 1-hexène et 1-octène), les technologies permettant l'oligomérisation sélective ont attiré beaucoup l'attention.[9c, 11]

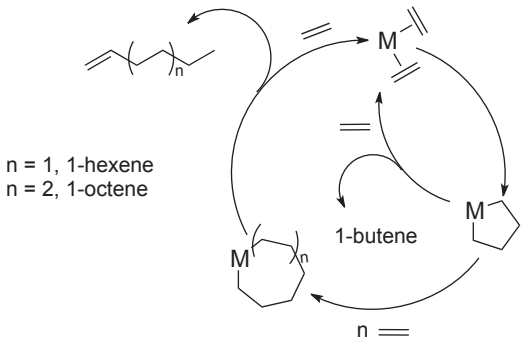

Schéma 9. Mécanisme simplifié du type métallacycle concernant plutôt les complexes du chrome

3.2 Utilisation de ligands carbènes N-hétérocycliques dans la réaction d'oligomérisation de l'éthylène

Malgré leur popularité en catalyse, les complexes NHC sont sous-représentés dans la réaction d'oligomérisation de l'éthylène. On trouve seulement quelques complexes du chrome(III),[12] ruthénium(II),[13] nickel(II),[14] zirconium(IV),[15] rhodium(I),[16] et du palladium(II)[17] dans la littérature. Notamment, les complexes du Cr(III) décrits par McGuiness *et al.* ont révélés une bonne activité en oligomérisation de l'éthylène. La catalyse avec les composés du chrome passe par un mécanisme de type métallacycle.[18]

Dans un premier temps nous nous sommes intéressé au nickel. La plupart des complexes de nickel testés ont des activités faibles à modérées et sont plutôt sélectifs pour la dimérisation de l'éthylène.[14a-d] L'élimination réductrice facile des ligands NHC a été mise en cause.[19] Le complexe indényle du nickel (Schéma 10) ne donne

qu'une faible activité catalytique en oligomérisation de l'éthylène (260 g C_2H_4/g Ni) après activation avec du MMAO dans le toluène.[14c] D'autres systèmes étudiés ont aussi montré des faibles, voire très faibles activités, par exemple, le complexe

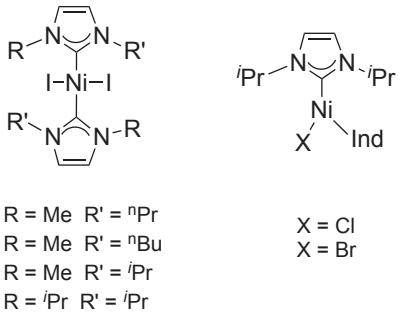

Schéma 10. Exemples de complexes du nickel testés en catalyse

$[NiI_2(NHC)_2]$ (Schéma 10), après activation, avec $AlEt_2Cl_2$ cette fois, présente un TON maximal de seulement 50 mol C_4H_{10}/mol Ni pour la dimérisation en 1-butène.[20]

4. Complexes des métaux de transition de type pinceur

Depuis que Shaw et Moulton[21] ont mis en évidence la stabilisation de complexes de métaux de transition avec des chélates tridente (système du type **PCP,** schéma 11), les plateformes pinceur[22] dans laquelle le donneur **C** lié par une liaison σ est flanqué de deux bras avec une fonctionnalité **E** (architecture typique **ECE**, schéma 11), ont été développées intensivement. En effet ces **ECE** contribuent à la stabilité et aux propriétés électroniques des complexes des métaux de transition qui les incorporent. Les donneurs neutres sont souvent utilisés en tant que **E** avec les atomes d'oxygène, soufre, phosphore, azote et NHCs[23].

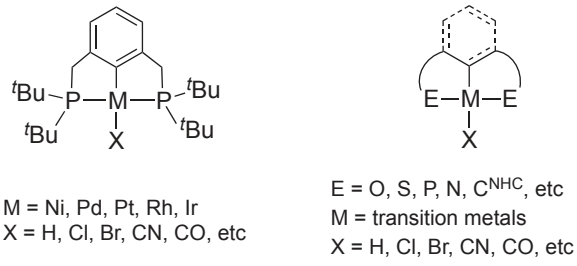

Scheme 11. Représentation des systèmes pinceurs **PCP** et **ECE**

Complexes des métaux de transition de type pinceur non-symétriques ou tritopiques.

La modification du ligand pinceur classique **ECE** peut conduire à un ligand pinceur non-symétrique ou tritopique (**EYE'**) en utilisant des donneurs **E** différents (**E** ≠ **E'**) et en remplaçant le site central carbanion par un atome d'azote ou par un NHC. (Schéma 12).

Y = C^-, N, C^{NHC}
E ≠ E'= O, S, P, N, C^{NHC}, etc
M = transition metals

Schéma 12. Représentation d'un système de ligand pinceur tritopique **EYE'**

En raison des diverses possibilités de transformation fine de leur effets stériques et électroniques les NHCs ont été incorporés de façon croissante dans les systèmes de type pinceur et cette entreprise a généré de nouvelles perspectives dans le domaine des ligands hybrides non symétriques ou tritopiques combinant un C^{NHC} central avec différents groupes donneurs en chimie organométallique et en catalyse[4].

5. Objectifs de la thèse

Ces dernières années notre laboratoire s'est plus particulièrement intéressé à la synthèse et l'étude des propriétés catalytiques de complexes des métaux de transition possédant des ligands NHC fonctionnalisés. Différents types de ligands multidentes ont été développés avec une variété de fonctions contenant l'oxygène, l'azote ou le phosphore.

Représenté dans le schéma x ci-dessous notre groupe a publié la formation d'un complexe très particulier, le *cis*-bis-NHC du nickel(II) avec deux molécules d'eau coordinées au centre métallique (Schéma 13). La coordination de l'oxygène au centre métallique ainsi que les interactions impliquant des liaisons hydrogène nous ont suggéré qu'en augmentant le groupe espaceur, on pourrait obtenir un chélate à sept chaînons avec coordination du groupe éther. De plus cette fonction donneur éther nous paraissait être un bon candidat pour participer dans le processus catalytique comme un groupement hémilabile.

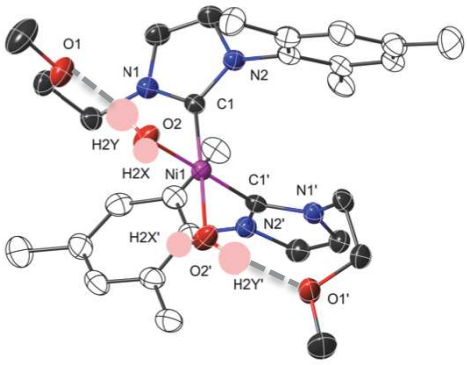

Schéma 13. Complexe $[Ni\{ImMes(C_2OMe)\}_2(H_2O)_2\}][PF_6]_2$ les contre-anions ne sont pas représentés

Après l'étude du ligand bidente $C^{NHC}O^{ether}$ possédant un espaceur C_3 pouvant conduire à un chélate à sept chaînons nous avons, dans cette thèse, entrepris l'étude des ligands de type pinceur tridente avec différents groupes fonctionnels conduisant à des ligands pinceur non symétriques ou tritopiques. Nous avons développé en particulier deux nouveaux ligands pinceurs tritopiques $N^{imine}C^{NHC}N^{amine}$ et $N^{imine}C^{NHC}O^{ether}$ possédant un donneur central NHC flanqué de deux donneurs différents et nous avons joué sur la longueur de l'espaceur quand cela était possible.

La complexation de différents métaux (Ag, Cu, Ni, Cr, Ir) et l'étude des complexes obtenus nous a permis d'avoir une idée du comportement des différents groupes donneurs. Les propriétés catalytiques des complexes du nickel et du chrome ont aussi été étudiées dans la réaction d'oligomérisation de l'éthylène.

6. References

(1) E. O. Fischer, A. Maasböl, *Angew. Chem. Int. Ed. Engl.* **1964**, *3*, 580-581.

(2) R. R. Schrock, *J. Am. Chem. Soc.* **1975**, *97*, 6577-6578.

(3) K. Öfele, *J. Organomet. Chem.* **1968**, *12*, P42-P43.

(4) H. W. Wanzlick, H. J. Schoenherr, *Angew. Chem., Int. Ed. Engl.* **1968**, *7*, 141-142.

(5) A. J. Arduengo, R. L. Harlow, M. Kline, *J. Am. Chem. Soc.* **1991**, *113*, 361-363.

(6) J. C. Jeffrey, T. B. Rauchfuss, *Inorg. Chem.* **1979**, *18*, 2658-2666.

(7) P. Braunstein, D. Matt, F. Mathey, D. Thavard, *J. Chem. Res. Synop.* **1978**, 232; P. Braunstein, D. Matt, F. Mathey, D. Thavard, *J. Chem. Res. Miniprint* **1978**, 3041.

(8) a) A. Bader, E. Lindner, *Coord. Chem. Rev.* **1991**, *108*, 27; b) For recent catalytic applications of P,O and P,N ligands, see e.g.: asymmetric hydrogenation of olefins: J. Holz, R. Kadyrov, S. Borns, D. Heller, A. Börner, *J. Organomet. Chem.* **2000**, *603*, 61; asymmetric transfer hydrogenation of ketones: J.-X. Gao, X.-D. Yi, P.-P. Xu, C.-L. Tang, H.-L. Wan, T. Ikariya, *J. Organomet. Chem.* **1999**, *592*, 290 ; silylation of aryl halides : E. Shirakawa, T. Kurahashi, H. Yoshida, T. Hiyama, *Chem. Commun.* **2000**, *1895*; ethylene dimeri- zation: J. Andrieu, P. Braunstein, F. Naud, R. D. Adams, *J. Organomet. Chem.* **2000**, *601*, 43; alternating CO/olefin copolymerization: E. Lindner, M. Schmid, P. Wegner, C. Nachtigal, M. Steimann, R. Fawzi, *Inorg. Chim. Acta* **1999**, *296*, 103; J. Andrieu, P. Braunstein, F. Naud, R. D. Adams, *J. Organomet. Chem.* **2000**, *601*, 43 ; P. Braunstein, M.D. Fryzuk, M. LeDall, F. Naud, S.J. Rettig, F. Speiser, *J. Chem. Soc. Dalton Trans.* **2000**, 1067; ring-opening metathesis polymerization: E. Lindner, S. Pautz, R. Fawzi, M. Steimann, *Organometallics* **1998**, *17*, 3006; hydroformylation of olefins : S. Gladiali, S. Medici, T. KeÂ gl, L. KollaÁ r, *Monatsh. Chem.* **2000**, *131*, 1351; hydroformylation of epoxides: R. Weber, U. Englert, B. Ganter, W. Keim, M. Möthrath, *Chem. Commun.* **2000**, 1419; asymmetric ring opening of epoxides: J.-M. Brunet, O. Legrand, S. Reymond, G. Buono, *Angew. Chem.* **2000**, *112*, 2654; *Angew. Chem. Int. Ed.* **2000**, *39*, 2554; animation of aromatic olefins: A.

Tillack, H. Trauthwein, C. G. Hartung, M. Eichberger, S. Pitter, A. Jansen, M. Beller, *Monatsh. Chem.* **2000**, *131*, 1327.

(9) a) J. Skupinska, *Chem. Rev.* **1991**, *91*, 613-648; b) D. Vogt, in *Applied Homogeneous Catalysis with Organometallic Compounds, Vol. 1* (Eds.: B. Cornils, W. A. Herrmann), Wiley-VCH, Weinheim, **2002**, p. 245; c) A. Forestière, H. Olivier-Bourbigou, L. Saussine, *Oil & Gas Science and Technology* **2009**, *64*, 649-667.

(10) Eur. Chem. News **2004**, *80*, 16.

(11) a) J. T. Dixon, M. J. Green, F. M. Hess, D. H. Morgan, *J. Organomet. Chem.* **2004**, *689*, 3641-3668; b) D. F. Wass, *Dalton Trans.* **2007**, 816-819.

(12) a) D. S. McGuinness, V. C. Gibson, D. F. Wass and J. W. Steed *J. Am. Chem. Soc.* **2003**, *125*, 12716-12717; b) D. S. McGuinness, J. A. Suttil, M. G. Gardiner and N. W. Davies *Organometallics* **2008**, *27*, 4238-4247; c) D. McGuinness *Dalton Trans.* **2009**, 6915-6923; d) D. S. McGuinness *Organometallics* **2009**, *28*, 244-248.

(13) a) P. Csabai, F. Joó, A. M. Trzeciak and J. J. Ziółkowski *J. Organomet. Chem.* **2006**, *691*, 3371- 3376; b) S. T. Diver, A. A. Kulkarni, D. A. Clark and B. P. Peppers *J. Am. Chem. Soc.* **2007**, *129*, 5832-5833.

(14) a) D. S. McGuinness, W. Mueller, P. Wasserscheid, K. J. Cavell, B. W. Skelton, A. H. White and U. Englert *Organometallics* **2002**, *21*, 175-181; b) A. L. MacKinnon and M. C. Baird *J. Organomet. Chem.* **2003**, *683*, 114-119; c) H. M. Sun, Q. Shao, D. M. Hu, W. F. Li, Q. Shen and Y. Zhang *Organometallics* **2005**, *24*, 331-334; d) W.-F. Li, H.-M. Sun, M.-Z. Chen, Q. Shen and Y. Zhang *J. Organomet. Chem.* **2008**, *693*, 2047-2051; e) L. Benıt́ ez Junquera, M. C. Puerta and P. Valerga *Organometallics* **2012**, *31*, 2175-2183.

(15) S. Dagorne, S. Bellemin-Laponnaz and C. Romain *Organometallics* **2013**, *32*, 2736-2743.

(16) W. Gil, T. Lis, A. M. Trzeciak and J. J. Ziółkowski *Inorg. Chim. Acta* **2006**, *359*, 2835-2841.

(17) V. Khlebnikov, A. Meduri, H. Mueller-Bunz, T. Montini, P. Fornasiero, E. Zangrando, B. Milani and M. Albrecht *Organometallics* **2012**, *31*, 976-986.

(18) a) D. S. McGuinness, J. A. Suttil, M. G. Gardiner and N. W. Davies *Organometallics* **2008**, *27*, 4238-4247; b) D. S. McGuinness *Organometallics*

2009, *28*, 244-248.

(19) K. J. Cavell and D. S. McGuinness *Coord. Chem. Rev.* **2004**, *248*, 671-681.

(20) D. S. McGuinness, W. Mueller, P. Wasserscheid, K. J. Cavell, B. W. Skelton, A. H. White and U. Englert *Organometallics* **2002**, *21*, 175-181.

(21) M. Albrecht, G. van Koten, *Angew. Chem. Int. Ed.* **2001**, *40*, 3750-3781.

(22) a) D. Morales-Morales, C. G. M. Jensen, *The Chemistry of Pincer Compounds*, Elsevier Science, **2011**; b) G. van Koten, R. A. Gossage, *The Privileged Pincer-Metal Platform: Coordination Chemistry & Applications*, Springer International Publishing, **2015**.

(23) a) S. Hameury, P. de Fremont, P. Braunstein, *Chem. Soc. Rev.* **2017**, *46*, 632-733; b) J. B. Smith, A. J. M. Miller, *Organometallics* **2015**, *34*, 4669-4677; c) T. Simler, A. A. Danopoulos, P. Braunstein, *Chem. Commun.* **2015**, *51*, 10699-10702; d) B. Mougang-Soumé, F. Belanger-Gariépy, D. Zargarian, *Organometallics* **2014**, *33*, 5990-6002; e) D. Pugh, A. A. Danopoulos, *Coord. Chem. Rev.* **2007**, *251*, 610-641; f) M. E. van der Boom, D. Milstein, *Chem. Rev.* **2003**, *103*, 1759-1792.

CHAPITRE 1

Synthesis and Characterization of Nickel(II) Complexes with Oxygen- or Nitrogen-Functionalized NHC Hybrid Ligands and Catalytic Ethylene Oligomerization

This chapter is written in the form of a publication draft, more work being currently in progress. Some characterization data are still missing at this stage of the work.

My contribution to this work consisted of the bibliographic search, the experimental work and the preparation of the draft of the publication.

Synthesis and Characterization of Nickel(II) Complexes with Oxygen- or Nitrogen-Functionalized NHC Hybrid Ligands and Catalytic Ethylene Oligomerization

Xiaoyu Ren,[a] Marcel Wesolek*[a] and Pierre Braunstein*[a]

[a] Laboratoire de Chimie de Coordination, Institut de Chimie (UMR 7177 CNRS), Université de Strasbourg, 4 rue Blaise Pascal, 67081 Strasbourg Cedex (France)

E-mail: braunstein@unistra.fr

Synopsis

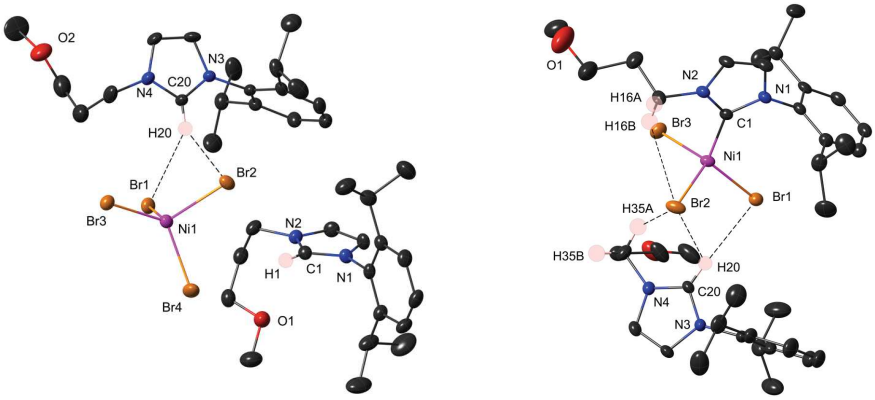

1. Résumé en français

Des ligands hybrides potentiellement bidentes formés d'un donneur carbène N-hétérocyclique (NHC) associé à un groupement éther ou amine ont été préparés et coordinés au Ni(II). L'influence de la longueur de la chaine alkyle -$(CH_2)_2$- ou –$(CH_2)_3$- reliant les fonctions éther ou amine avec un atome d'azote de l'hétérocycle a été étudiée. Un ligand hybride possédant une fonction carbène libre, sensible à l'air, associée à un groupement éther, (Dipp)(C_3OMe)imidazole-ylidene (**4**), a été isolé sous forme cristalline et sa structure a été confirmée par diffraction des rayons X. Les complexes du Ni(II) avec les ligands $C^{NHC}O^{ether}$ ont été préparés soit par déprotonation du sel d'imidazolium correspondant suivi de l'addition de [$NiCl_2$(dme)] ou par transmétallation d'un complexe NHC de l'argent. Des complexes mono- ou bis-NHC du Ni(II) ont ainsi été obtenus. Les complexes correspondants de l'argent [AgCl{ImDipp(C_3OMe)}$_2$] (**8**), [AgCl{ImMes(C_3OMe)}$_2$] (**9**), [AgCl{ImMe(C_3OMe)}$_2$] (**10**) ont été préparés avec de bons rendements. Les complexes du Ni(II) *trans*-[$NiCl_2${ImDipp(C_3OMe)}$_2$] (**5**), *trans*-[$NiCl_2${ImMes(C_3OMe)}$_2$] (**6**), et *trans*-[$NiCl_2${ImMe(C_3OMe)}$_2$] (**7**) ont été obtenus sous forme de poudre orange diamagnétique stable à l'air. Les complexes de coordination plan carré contenant deux ligands acétonitrile, c*is*-[Ni{ImDipp(C_3OMe)}$_2$(NCMe)$_2$](PF_6)$_2$ (**14**), et *cis*-[Ni{ImMes(C_3OMe)}$_2$(NCMe)$_2$](PF_6)$_2$ (**15**) ont été obtenus avec R = Dipp ou Mes respectivement. De plus, un procédé indirect consistant dans la formation d'un sel de bis-imidazolium associé à $[NiX_4]^{2-}$ suivie par une déprotonation a aussi été utilisé pour la synthèse de complexes mono- ou bis-NHC du Ni(II). Les sels de bis-imidazolium contenant le dianion $[NiX_4]^{2-}$, [(ImH)Dipp(C_3OMe)]$_2$[$NiCl_4$] (**11**), [(ImH)Mes(C_3OMe)]$_2$[$NiCl_4$] (**12**) et [(ImH)Me(C_3OMe)]$_2$[$NiCl_4$] (**13**) furent obtenus sous forme de poudre bleu et sont paramagnétiques.

Les complexes du nickel mono-NHC, [(ImH)Dipp(C_3OMe)][$NiCl_3${ImDipp(C_3OMe)}] (**16**) et [(ImH)Dipp(C_3OMe)][$NiBr_3${ImDipp(C_3OMe)}] (**18**), furent préparés par déprotonation des sels d'imidazolium [(ImH)Dipp(C_3OMe)]$_2$[$NiCl_4$] (**11**) et [(ImH)Dipp(C_3OMe)]$_2$[$NiBr_4$] (**17**), respectivement, et l'analyse par diffraction des rayons X du complexe **18** confirme la présence d'interactions hydrogène à l'état solide.

Les ligands bidentes $C^{NHC}N^{amine}$ [(ImH)Dipp(C_2N(H)Me$_2$)]Cl_2 (**22**) et [(ImH)Dipp(C_3N(H)Me$_2$)]Cl_2 (**23**) et leur complexes correspondants de l'argent [AgCl{ImDipp(C_2NMe$_2$)}] (**24**) et [AgCl{ImDipp(C_3NMe$_2$)}] (**25**) furent préparés en vu de la synthèse de complexes du Ni(II). Les complexes du Ni(II) [$NiBr_2${κ*N*^{amine},κ*C*^{NHC}-(ImH)Dipp(C_2NMe$_2$)}] (**26**) et [$NiBr_2${κ*N*^{amine},κ*C*^{NHC}-(ImH)Dipp(C_3NMe$_2$)}] (**27**) contiennent des chélates $C^{NHC}N^{amine}$ avec,

respectivement, des cycles à six ou sept chainons et ont été caractérisés par diffraction des rayons X.

En plus de ces ligands $C^{NHC}O^{ether}$ et $C^{NHC}N^{amine}$, un ligand potentiellement tridente avec un donneur NHC associé à des fonctions éther et imine [Im(H)(C(Me)(=NDipp))(C_3OMe)]Cl (**19**) a été préparé et complexé à Ag(I) pour donner [AgCl{Im(C(Me)(=NDipp))(C_3OMe)}] (**21**) où seul le C^{NHC} est coordiné, bien que les deux groupes donneurs soient orientés vers le centre métallique. Un sel de bis-imidazolium avec $[NiX_4]^{2-}$ comme dianion [Im(H)(C(Me)(=NDipp))(C_3OMe)]$_2$[$NiCl_4$] (**20**) a été synthétisé pour former les complexes mono- ou bis-NHC Ni(II) par réaction de déprotonation.

Synthesis and Characterization of Nickel(II) Complexes with Oxygen- or Nitrogen-Functionalized NHC Hybrid Ligands and Catalytic Ethylene Oligomerization

Xiaoyu Ren,[a] Marcel Wesolek[*a] and Pierre Braunstein*[*a]*

[a] *Laboratoire de Chimie de Coordination, Institut de Chimie (UMR 7177 CNRS), Université de Strasbourg, 4 rue Blaise Pascal, 67081 Strasbourg Cedex (France)*

E-mail: braunstein@unistra.fr

2. Abstract

Potentially bidentate hybrid ligands containing a N-heterocyclic carbene (NHC) donor associated with an ether or an amine have been prepared and used for coordination to Ni(II). The influence of length of the alkyl chain, -$(CH_2)_2$- or –$(CH_2)_3$- connecting the ether or the amine group to the heterocycle was examined. An air-sensitive NHC ligand with an ether donor, (Dipp)(C_3OMe)imidazole-ylidene (**4**), was isolated in crystalline form and its structure was confirmed by X-ray diffraction analysis. The Ni(II) complexes with $C^{NHC}O^{ether}$ ligands were prepared either by deprotonation of the corresponding imidazolium salts followed by addition of [$NiCl_2$(dme)] or by transmetalation from a NHC silver complex. Mono- or bis-NHC Ni(II) complexes were obtained. The corresponding Ag-NHC complexes [AgCl{ImDipp(C_3OMe)}$_2$] (**8**), [AgCl{ImMes(C_3OMe)}$_2$] (**9**), [AgCl{ImMe(C_3OMe)}$_2$] (**10**) were prepared in good yields. The Ni(II) complexes *trans*-[$NiCl_2${ImDipp(C_3OMe)}$_2$] (**5**), *trans*-[$NiCl_2${ImMes(C_3OMe)}$_2$] (**6**), and *trans*-[$NiCl_2${ImMe(C_3OMe)}$_2$] (**7**) were obtained as orange, diamagnetic, air-stable powders. The dicationic, square-planar acetonitrile-coordinated complexes c*is*-[Ni{ImDipp(C_3OMe)}$_2$(NCMe)$_2$](PF_6)$_2$ (**14**) and *cis*-[Ni{ImMes(C_3OMe)}$_2$(NCMe)$_2$](PF_6)$_2$ (**15**) were obtained with R = Dipp or Mes, respectively. Furthermore, an indirect procedure consisting in the formation of bis-imidazolium salts associated with $[NiX_4]^{2-}$ followed by deprotonation was also used for the synthesis of mono- or bis-NHC nickel complexes. The bis-imidazolium salts containing $[NiX_4]^{2-}$ dianions [(ImH)Dipp(C_3OMe)]$_2$[$NiCl_4$] (**11**), [(ImH)Mes(C_3OMe)]$_2$[$NiCl_4$] (**12**) and [(ImH)Me(C_3OMe)]$_2$[$NiCl_4$] (**13**) were obtained as blue, paramagnetic powders.

The mono-NHC nickel complexes [(ImH)Dipp(C_3OMe)][$NiCl_3${ImDipp(C_3OMe)}] (**16**) and [(ImH)Dipp(C_3OMe)][$NiBr_3${ImDipp(C_3OMe)}] (**18**) were prepared by deprotonation of the corresponding imidazolium salts [(ImH)Dipp(C_3OMe)]$_2$[$NiCl_4$] (**11**) and

[(ImH)Dipp(C_3OMe)]$_2$[NiBr$_4$] (**17**), and an X-ray diffraction analysis of complex **18** established the presence of intramolecular hydrogen-bonding interactions.

The bidentate $C^{NHC}N^{amine}$ ligands [(ImH)Dipp(C_2N(H)Me$_2$)]Cl$_2$ (**22**) and [(ImH)Dipp(C_3N(H)Me$_2$)]Cl$_2$ (**23**) and their corresponding silver complexes [AgCl{ImDipp(C_2NMe$_2$)}] (**24**) and [AgCl{ImDipp(C_3NMe$_2$)}] (**25**) were prepared with the aim to synthesize Ni(II) complexes. Thus, the Ni(II) complexes [NiBr$_2${κ*N*^{amine},κ*C*^{NHC}-(ImH)Dipp(C_2NMe$_2$)}] (**26**) and [NiBr$_2${κ*N*^{amine},κ*C*^{NHC}-(ImH)Dipp(C_3NMe$_2$)}] (**27**) were obtained and characterized by X-ray diffraction. They contain a six- or a seven-membered $C^{NHC}N^{amine}$ chelate, respectively. In addition to these $C^{NHC}O^{ether}$ and $C^{NHC}N^{amine}$ ligands, a potentially $N^{imine}C^{NHC}O^{ether}$ tridentate ligand containing a NHC donor flanked with an ether and an imine function, [Im(H)(C(Me)(=NDipp))(C_3OMe)]Cl (**19**), was prepared and coordinated to Ag(I) to give the complex [AgCl{Im(C(Me)(=NDipp))(C_3OMe)}] (**21**), where only the C^{NHC} is coordinated, although the two other donor groups are oriented toward the metal center. A bis-imidazolium salt with $[NiX_4]^{2-}$ dianions [Im(H)(C(Me)(=NDipp))(C_3OMe)]$_2$[NiCl$_4$] (**20**) was synthesized to form the mono- or bis-NHC Ni(II) complexes by deprotonation reactions.

3. Introduction

Following the report of the first complexes containing *N*-heterocyclic carbene (NHC) ligands[1] and the isolation of the first stable NHC ligands,[2] a rapidly growing interest developed for this class of ligands and their metal complexes, largely triggered by their often unique properties and wide range of applications.[3] The NHC donor group has also been included in bi- or multidentate hybrid ligands, which associate at least two different functionalities within the same molecule.[4] One such family of ligands combine NHC and oxygen-donor groups and depending on their stereoelectronic properties and on the length and type of spacer connecting a NHC nitrogen atom and the oxygen-donor, monodentate, chelating and bridging behavior have been observed.[5]

In the course of our studies on the synthesis of bis(ether-functionalized NHC) Ni(II) complexes aimed at examining the consequences of oxygen chelation on the structure and properties of the corresponding metal complexes,[6] we found that only monodentate behavior through the NHC function was observed in the case of the $C^{NHC}O^{ether}$ hybrid ligands studied, although alcoholate-functionalized NHC ligands with a similar –CH_2CH_2– (C_2) spacer connecting the NHC nitrogen atom and the oxygen-donor led to mononuclear chelated complexes or to oxygen-bridged dinuclear NHC complexes.[7] We thus wondered whether in the $C^{NHC}O^{ether}$ systems, formation of

NHC,*O*-chelates could be favored by increasing the length of the spacer from C_2 to C_3. For comparison, $C^{NHC}N^{amine}$ hybrid ligands containing an amino group and a C_3 spacer were also investigated and these studies are reported here. Owing to the impressive developments of the research on transition metal complexes with pincer ligands[8] and in view of our previous works on NCN-based pincer ligands,[9] the coordination to nickel of a potentially tridentate $N^{imine}C^{NHC}O^{ether}$ pincer ligand was also investigated. Other transition metal complexes stabilized by NCO pincer ligands have been recently reported.[10] In addition to the synthetic and structural features associated with new complexes containing NHC-type ligands, we were also interested in evaluating the catalytic properties of the nickel complexes for ethylene oligomerization. Triggered by industrial market requirements, olefin oligomerization plays an important role in the field of petrochemistry, and investigations on new catalysts, technology, and process developments remains of considerable academic and industrial interest.[11] Considerable research has been devoted to the synthesis and catalytic study of transition metal complexes to enhance catalytic productivity, selectivity and sustainability,[11a] and nickel complexes have long been known as privileged catalysts for olefin oligomerization.[12]

4. Results and discussion

Syntheses and Structures.

We prepared 1-(2,6-diisopropylphenyl)-3-(3-methoxypropyl)-1*H*-imidazol-3-ium chloride, [(ImH)Dipp(C_3OMe)]Cl (**1**), 1-mesityl-3-(3-methoxypropyl)-1*H*-imidazol-3-ium chloride, [(ImH)Mes(C_3OMe)]Cl (**2**), and 1-methyl-3-(3-methoxypropyl)-1*H*-imidazol-3-ium chloride, [(ImH)Me(C_3OMe)]Cl (**3**) in good yields according to the reactions of eq. 1.[6b]

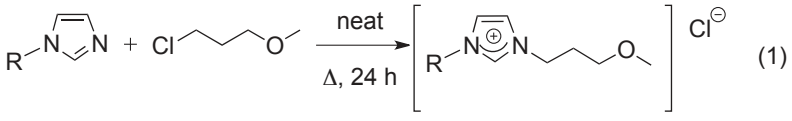

(1)

1 R = Dipp
2 R = Mes
3 R = Me

The bis(ether-functionalized NHC) nickel complexes were obtained following typical approaches described in the literature, by deprotonation of these imidazolium salts followed by direct addition of $[NiCl_2(dme)]$ or by transmetalation using a NHC silver complex as precursor (Scheme 1). An indirect pathway consisting firstly in the formation of $[NiX_4]^{2-}$ bis-imidazolium salts followed by deprotonation with 2 equiv. of base was also applied. The addition of a slight

excess of NaO^{t}Bu (2.2 equiv.) to the $[NiX_4]^{2-}$ bis-imidazolium salt led to an improved yield.

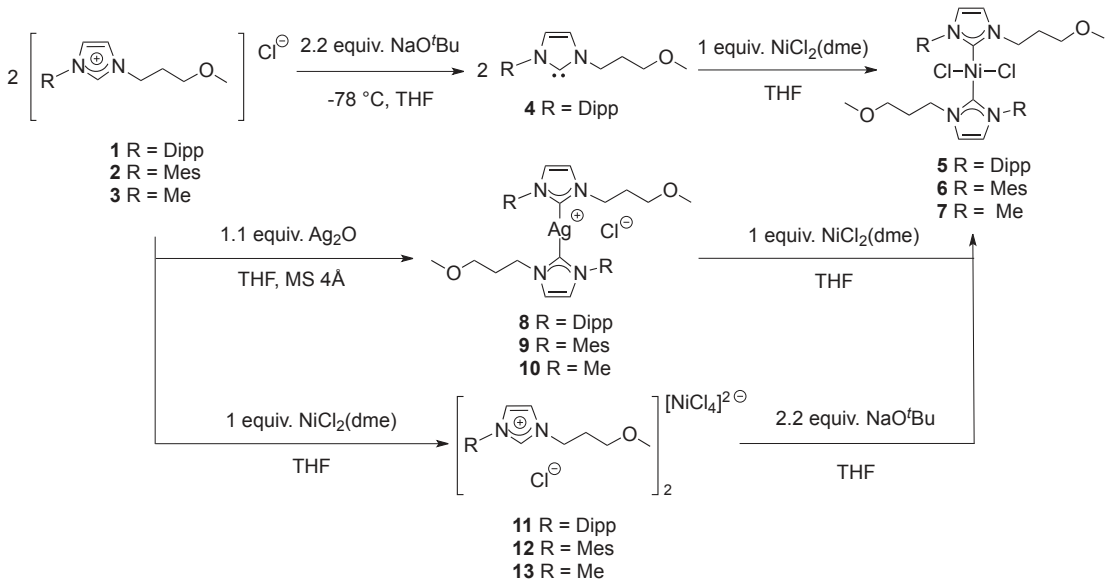

Scheme 1. Synthesis of bis-ether-functionalized *trans*-coordinated NHC Ni(II) complexes

To isolate the free carbene 1-(2,6-diisopropylphenyl)-3-(3-methoxypropyl)-1*H*-imidazol-2(3*H*)-ylidene (**4**), a THF solution of NaO^{t}Bu was added dropwise to a THF suspension of the corresponding imidazolium salt at –78 °C and colorless crystals were obtained. An X-ray diffraction analysis was performed on single crystals grown from a saturated Et_2O solution at –30 °C (Scheme 1, Figure 1). Compound **4** crystallizes in the monoclinic system ($P2_1/c$ space group).

The Ni(II) complexes dichlorobis[1-(2,6-diisopropylphenyl)-3-(3-methoxypropyl)-1*H*-imidazol-2(3*H*)-ylidene] nickel, $[NiCl_2\{ImDipp(C_3OMe)\}_2]$ (**5**), dichlorobis[1-mesityl-3-(3-methoxypropyl)-1*H*-imidazol-2(3*H*)-ylidene]nickel, $[NiCl_2\{ImMes(C_3OMe)\}_2]$ (**6**), and dichlorobis[1-methyl-3-(3-methoxypropyl)-1*H*-imidazol-2(3*H*)-ylidene]nickel, $[NiCl_2\{ImMe(C_3OMe)\}_2]$ (**7**), were obtained as orange, diamagnetic, air-stable powders in good yield according to the reactions shown in Scheme 1. Complexes **5** and **7** were characterized by X-ray diffraction (Figure 2), they crystallize in the monoclinic system ($P2_1/c$ space group). The nickel center displays a square planar coordination environment with two trans chlorides and two trans NHC ligands. The ether groups remain dangling, as previously observed when the shorter spacer $–CH_2CH_2-$ was used between the N and O atoms.[6b] Moreover, a minor isomer is always present in solution as indicated by ^{1}H NMR spectroscopy which could not be unambiguously

identified but we suggest that it corresponds to different mutual orientations of the NHC ligands in complex **5** (see Experimental section). A similar observation was recently made in related nickel complexes.[6b]

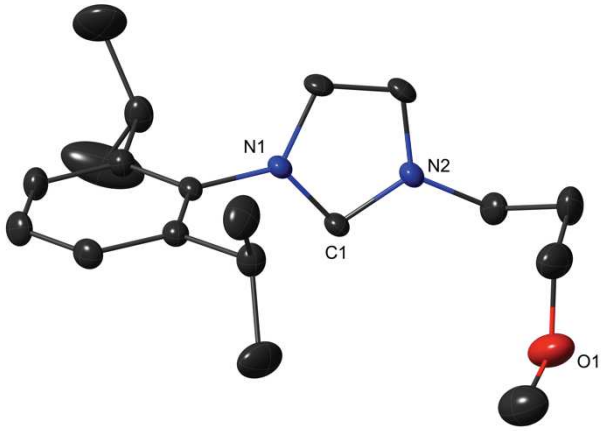

Figure 1. Structure of the $C^{NHC}O^{ether}$ ligand **4** with H atoms omitted for clarity. Thermal ellipsoids at the 30% probability level. Selected bond lengths (Å) and angles (deg): C1−N1 1.367(2), C1−N2 1.363(2), N1−C1−N2 101.7(1).

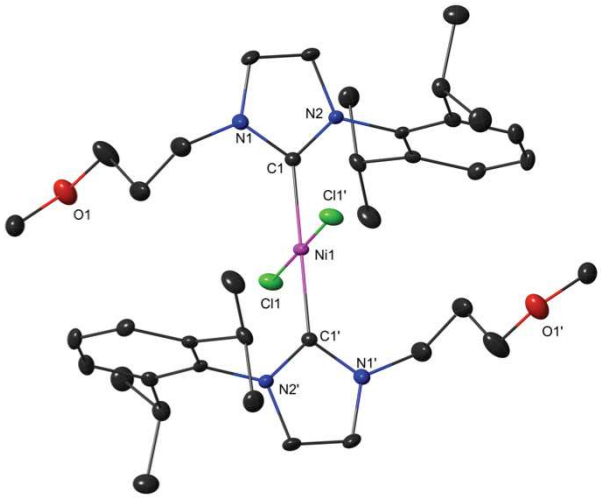

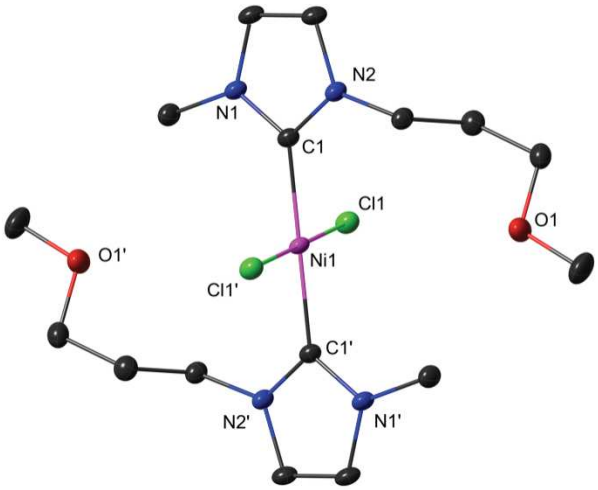

Figure 2. Structures of the *trans*-Ni(II) complexes **5** (top) and **7** (bottom) with H atoms omitted for clarity. Thermal ellipsoids at the 30% probability level. Selected bond lengths (Å) and angles (deg): in **5** Ni1−C1 1.918(3), Ni1−Cl1 2.190(7), C1−N1 1.355(3), C1−N2 1.352(3), C1−Ni1−Cl1 87.5(8), C1−Ni1−Cl1' 92.5(8), N1−C1−Ni1 131.1(2), N2−C1−Ni1 124.4(2), N1−C1−N2 104.3(2); in **7** Ni1−C1 1.923(2), Ni1−Cl1 2.199(4), C1−N1 1.350(2), C1−N2 1.351(2), C1−Ni1−Cl1 90.0(5), C1−Ni1−Cl1' 90.0(5), N1−C1−Ni1 127.8(1), N2−C1−Ni1 127.2(1), N1−C1−N2 104.8(1).

In order to promote chelation of the ether group, halogen abstraction was performed on **5** and **6** with $AgPF_6$ or $TlPF_6$, the latter being used in order to prevent redox side reactions. When THF was used as a solvent, a yellow compound was formed that could not be fully identified. We then carried out the same reaction in the presence of very small amounts of water, as in a previous work where a Ni(II) complex was isolated with a stabilizing coordinated water molecule.[6b] However, we could not characterize such a species, but after dissolution of the complex in acetonitrile, the complexes with coordinated acetonitrile molecules, *cis*-[Ni{ImDipp(C_3OMe)}$_2$(NCMe)$_2$](PF_6)$_2$ (**14**) and *cis*-[Ni{ImMes(C_3OMe)}$_2$(NCMe)$_2$](PF_6)$_2$ (**15**), were obtained with R = Dipp or Mes, respectively. Pale yellow crystals were grown by slow diffusion of ether into an acetonitrile solution containing the product **15**, which were characterized by X-ray diffraction (Figure 3). When the crude product obtained from the halide abstraction reaction performed in dry THF on **5** or **6** was treated with acetonitrile, formation of the acetonitrile-coordinated complexes was not observed by NMR. However, if halide abstraction was carried out in dry acetonitrile, complexes **14** and **15** were obtained directly (eq. 2). The ^{1}H NMR spectra indicated the diastereotopicity of the *gem*-protons on the ether arms -NC*H*$_2$C*H*$_2$C*H*$_2$OMe because of the *cis*-coordination geometry of the two NHC ligands. As shown in Figure 3, the nickel center adopts a square planar coordination geometry defined by two molecules of acetonitrile and two NHCs; the carbene ligands are almost orthogonal

to each other (88.74°) in order to minimize steric repulsions.

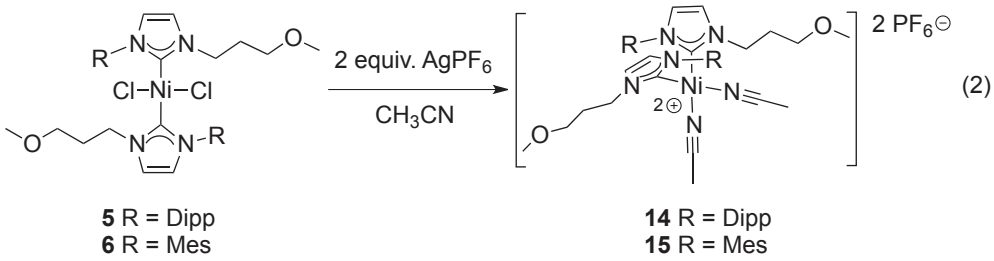

5 R = Dipp
6 R = Mes

14 R = Dipp
15 R = Mes

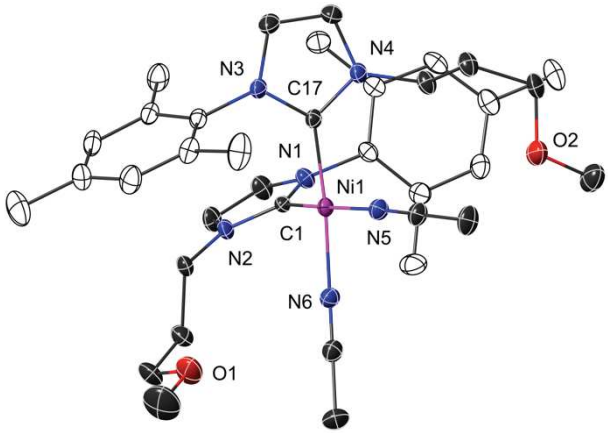

Figure 3. Structure of the Ni(II) complexes **15** with H atoms and PF_6 anions omitted for clarity. Thermal ellipsoids at the 40% probability level. Selected bond lengths (Å) and angles (deg): Ni1−C1 1.884(2), Ni1−C17 1.884(2), Ni1−N5 1.898(2), Ni1−N6 1.906(2), C1−N1 1.364(3), C1−N2 1.349(3), C17−N3 1.359(3), C17−N4 1.348(3), C1−Ni1−C17 89.8(9), C1−Ni1−N6 92.8(8), C17−Ni1−N5 91.0(8), N5−Ni1−N6 87.4(8), C1−Ni1−N5 172.4(9), C17−Ni1−N6 172.7(9), N1−C1−N2 105.2(2), N3−C17−N4 105.5(2).

To examine the possibility of forming Ni(II) complexes by transmetallation reaction, the corresponding Ag(I) complexes were synthesized as shown in Scheme 1. X-ray quality crystals of the complex [Ag{ImDipp(C_3OMe)}$_2$]Cl (**8**) were obtained by slow diffusion of pentane into its THF solution. It crystallizes in the monoclinic system (*C*2/c space group) (Figure 4). The coordination geometry about silver is nearly linear (the $C_{carbene}$−Ag−$C_{carbene}$ angle = 174.4(7)°) and the mean planes of the two NHC ligands make an angle of 40.53° to each other, most likely for steric reasons. The Ag−$C_{carbene}$ distance of 2.095(1) Å is in good agreement with data reported for homoleptic cationic bis-(NHC) Ag(I) complexes. In the crystal, the Ag−Cl separation of 2.8775(6) Å is similar to that observed in related complexes,[13] and could result from an electrostatic interaction between the silver cation and the halide anion.[3]

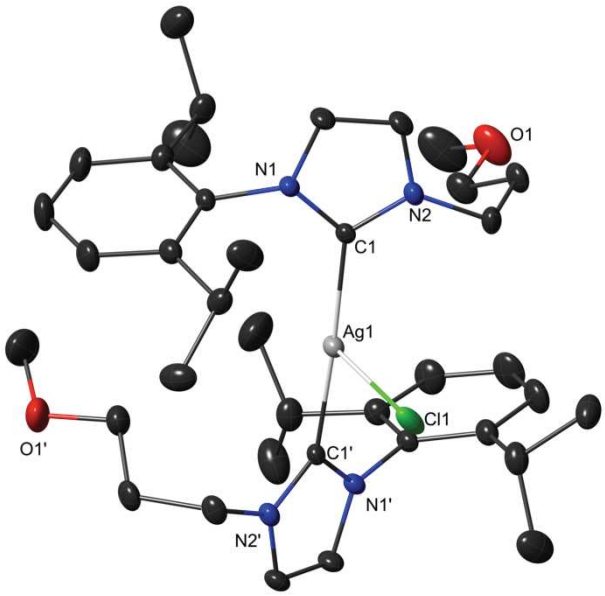

Figure 4. Structure of the Ag(I) complex **8** with H atoms omitted for clarity. Thermal ellipsoids at the 30% probability level. Selected bond lengths (Å) and angles (deg): Ag1−C1 2.095(1), Ag1−Cl1 2.878(6), C1−N1 1.358(2), C1−N2 1.351(2), C1−Ag1−Cl1 92.8(3), C1−Ag1−C1' 174.4(7), N1−C1−Ag1 128.9(9), N2−C1−Ag1 127.0(9), N1−C1−N2 103.8(1).

Among the three different methods mentioned above for the synthesis of bis-NHCs nickel complexes (Scheme 1), the indirect approach involving first formation of the bis-imidazolium salt of $[NiX_4]^{2-}$ followed by its deprotonation with 2 equiv. of NaO^{t}Bu presented clear advantages: shorter reaction times and no need to involve air-sensitive, free carbenes. High yields of these salts, $[(ImH)Dipp(C_3OMe)]_2[NiCl_4]$ (**11**) and $[(ImH)Me(C_3OMe)]_2[NiCl_4]$ (**13**), were obtained by reaction of 2 equiv. of the corresponding imidazolium chloride with 1 equiv. of $[NiCl_2(dme)]$. Blue powders were isolated which are soluble in MeCN or CH_2Cl_2, but insoluble in THF. Crystallographic analyses of **11** and **13** confirmed the presence of $[NiX_4]^{2-}$ dianions associated with two imidazolium cations (Figure 5). The nickel center is in a tetrahedral environment constituted by four chlorides. Complex **11** crystalizes in the orthorhombic system ($P2_12_12_1$ space group), and the H1···Cl2 and H1···Cl4 distances of 2.673 Å and 2.952 Å, respectively, reveal weak hydrogen-bonding interactions. Complex **13** crystallizes in the monoclinic system ($C2/c$ space group). The asymmetric unit contains one molecule of the ligand and half a $[NiCl_4]^{2-}$ dianion and the nickel atom is in a special position (population 50%).

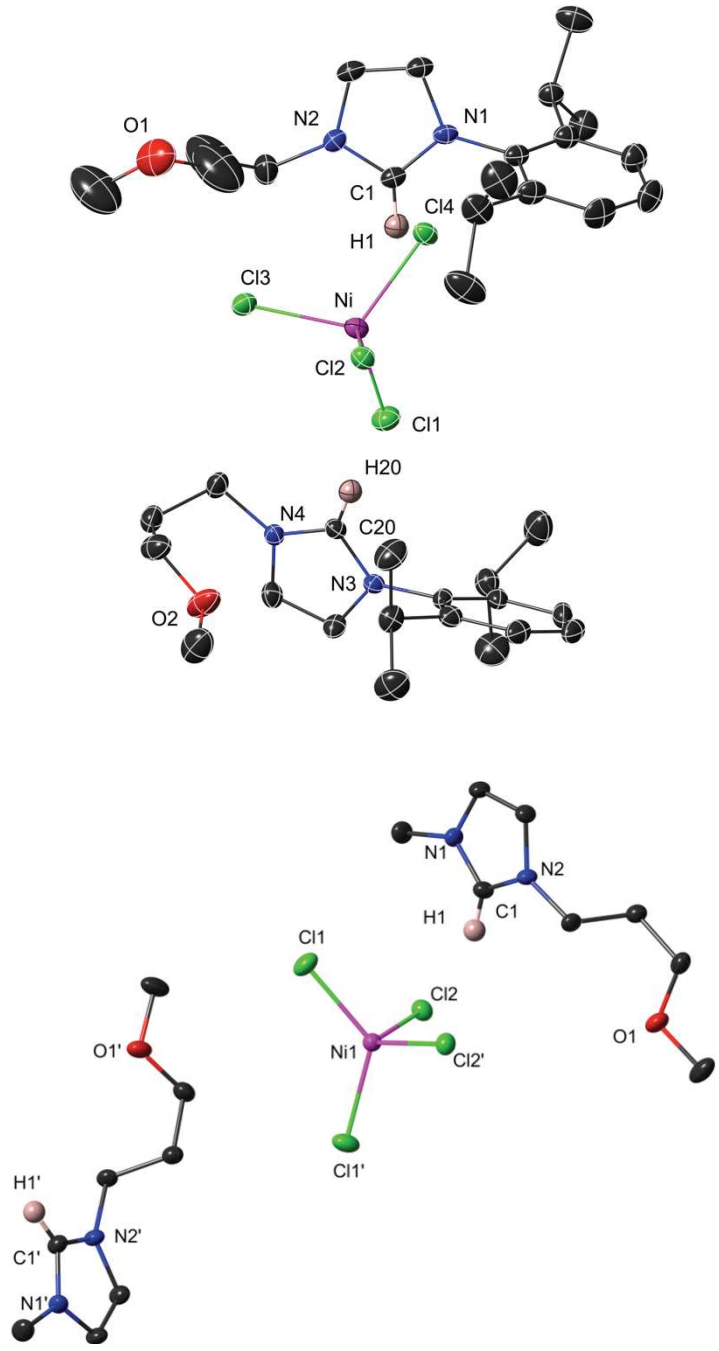

Figure 5. Structures of the complexes **11** (top) and **13** (bottom) with H atoms omitted for clarity, except the NC*H*N hydrogen atoms. Thermal ellipsoids at the 40% (**11**) and 30% (**13**) probability level. Selected bond lengths (Å) and angles (deg): in **11** Ni1−Cl1 2.245(1), Ni1−Cl2 2.282(9), Ni1−Cl3 2.275(9), Ni1−Cl4 2.266(9), C1−N1 1.331(4), C1−N2 1.331(4), C20−N3 1.334(4), C20−N4 1.317(4), N1−C1−N2 109.2(3), N3−C20−N4 109.0(3); in **13** Ni1−Cl1 2.250(1), Ni1−Cl2 2.277(1), C1−N1 1.332(4), C1−N2 1.322(5), N1−C1−N2 108.8(3).

When the salt **11** was used for the synthesis of the corresponding bis(NHC) Ni(II) complex, we obtained unexpectedly a few dark blue crystals of the Ni(II) complex **16**. Similar blue crystals have been previously isolated in a non-reproducible manner.[6b] An X-ray diffraction analysis revealed the presence of a tetrahedral Ni(II) complex coordinated by three chlorides and one NHC ligand, the negative charge being compensated by an imidazolium cation. Surprisingly, as shown in Figure 6, this paramagnetic nickel complex **16** presented a ^{1}H NMR spectrum with rather sharp peaks between -32 and 92 ppm.

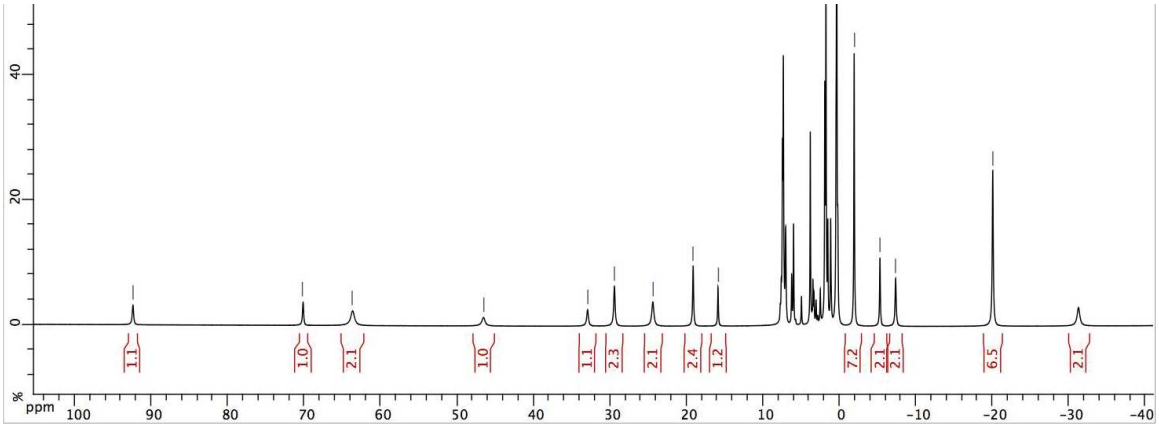

Figure 6. ^{1}H Paramagnetic spectrum of **16**

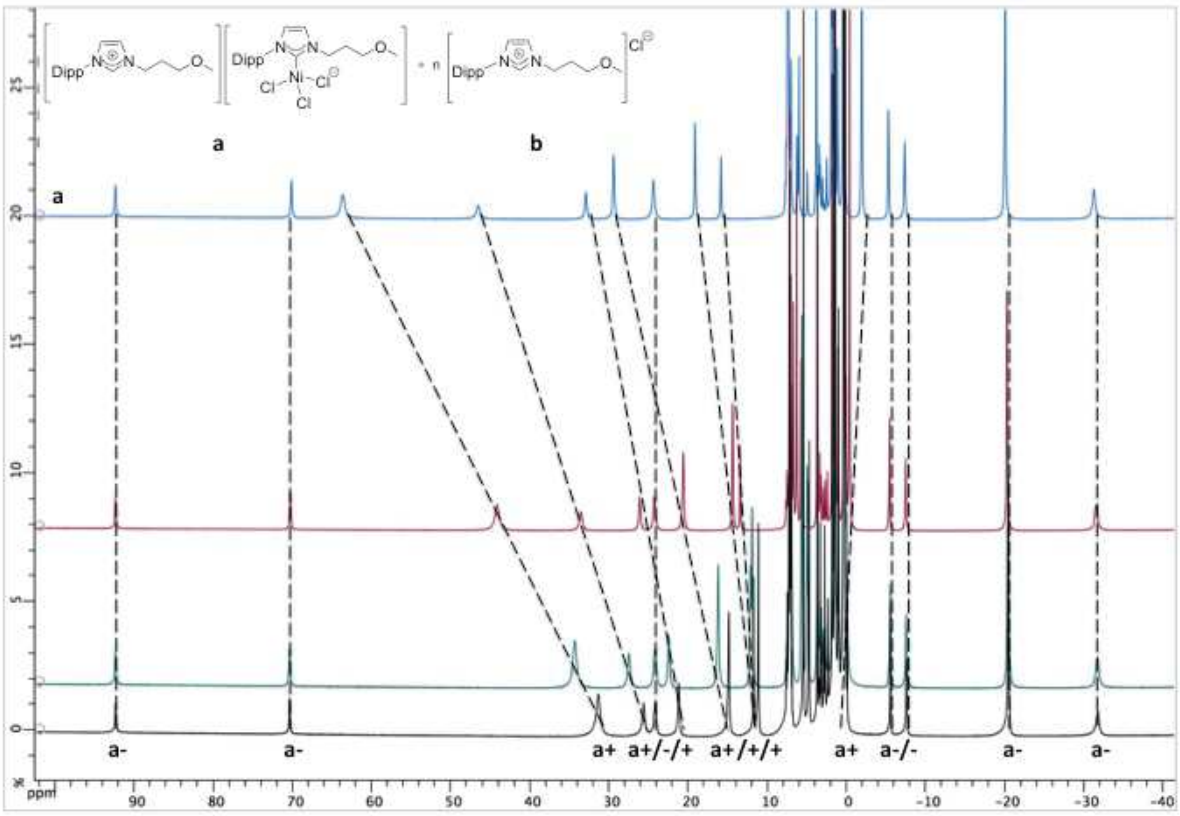

Figure 7. Changes in the ^{1}H NMR spectrum of **16** upon addition of increasing amounts of the corresponding imidazolium salt, [**a**+] represents the peaks assigned to $[(ImH)Dipp(C_3OMe)]^+$ and [**a**-] those assigned to $[NiCl_3\{ImDipp(C_3OMe)\}]^-$.

Because of the presence of an ether-functionalized NHC ligand in both the cationic and anionic fragments, we performed ^{1}H NMR investigations in order to assign them. As shown in Figure 7, the blue spectrum (top) presents the ^{1}H NMR features of $[(ImH)Dipp(C_3OMe)][NiCl_3\{ImDipp(C_3OMe)\}]$ (**16 = a**), and the three spectra below illustrate the shifts resulting from the addition of increasing amount of imidazolium salt (**1** = $\mathbf{b^+Cl^-}$) to **16**. Some peaks ($\mathbf{a^-}$) retained their chemical shift but other ($\mathbf{a^+}$) were significantly shifted. The $\mathbf{a^-}$ peaks belong to the anionic part of the complex with the carbene ligand bound to the nickel center; whereas the $\mathbf{a^+}$ peaks belong to the imidazolium cation that interacts by hydrogen bonding with the paramagnetic nickel fragment. In solution, we could not distinguish the $\mathbf{a^+}$ and $\mathbf{b^+}$.

The isolation of the mono-NHC nickel complex **16** suggested that it may be prepared in better yield by decreasing the quantity of base from 2 equiv. to 1 equiv. (eq. 3).

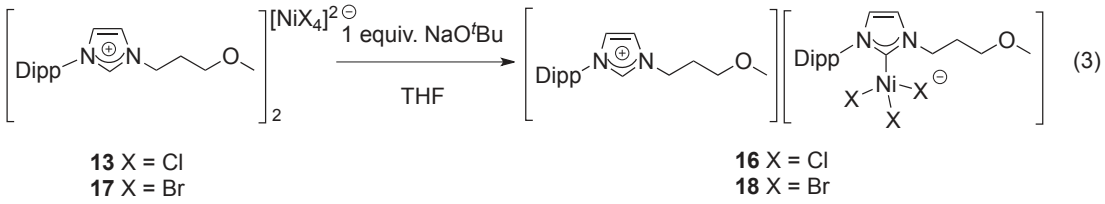

13 X = Cl
17 X = Br

16 X = Cl
18 X = Br

Addition of ether to a toluene solution of the product afforded dark blue, paramagnetic, air-stable crystals, but these crystals were not suitable for crystallographic analysis. As a result, the bromide analogue mono(NHC) nickel complex [(ImH)Dipp(C_3OMe)][$NiBr_3${ImDipp(C_3OMe)}] (**18**) was prepared from the imidazolium salt [(ImH)Dipp(C_3OMe)]$_2$[$NiBr_4$] (**17**) under similar reaction conditions and isolated in good yield. Single crystals of complexes **17** and **18** suitable for X-ray diffraction analysis were obtained (eq. 3, Figure 8). These complexes are similar to their chloride analogues and the structure of **17** displays weak hydrogen-bonding interactions (H20−Br1 = 2.943 Å and H20−Br2 = 2.876 Å). Complex **18** crystallized in the monoclinic system ($P2_1/c$ space group). The nickel center is surrounded by three bromides and one NHC ligand forming a tetrahedral coordination environment. The distances H20−Br1 (2.735 Å), H20−Br2 (3.043 Å), H16B−Br2 (2.911 Å) and H35A−Br2 (3.127 Å) are indicative of weak hydrogen-bonding interactions in **18**.

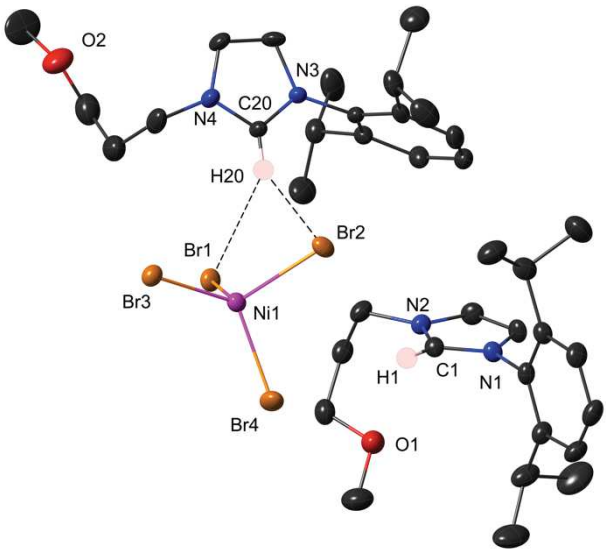

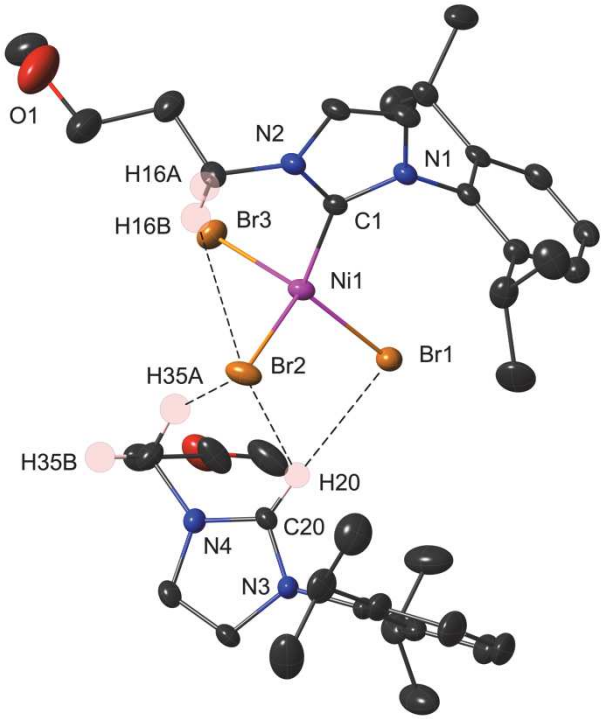

Figure 8. Structures of the complexes in **17** (top) and **18** (bottom) with H atoms omitted for clarity, except those involved in H-bonding interactions. Thermal ellipsoids at the 30% probability level. Selected bond lengths (Å) and angles (deg): in **17** Ni1−Br1 2.394(8), Ni1−Br2 2.401(7), Ni1−Br3 2.404(8), Ni1−Br4 2.376(9), C1−N1 1.333(6), C1−N2 1.323(6), C20−N3 1.315(6), C20−N4 1.317(6), N1−C1−N2 108.6(4), N3−C20−N4 109.8(4); in **18** Ni1−Br1 2.402(5), Ni1−Br2 2.405(5), Ni1−Br3 2.424(5), Ni1−C1 1.985(3), C1−N1 1.372(3), C1−N2 1.354(3), C20−N3 1.331(3), C20−N4 1.327(3), C1−Ni1−Br1 120.7(8), C1−Ni1−Br2 103.2(8), C1−Ni1−Br3 104.1(8), Br1−Ni1−Br2 109.0(2), Br1−Ni1−Br3 107.4(2), Br2−Ni1−Br3 112.5(2), N1−C1−Ni1 129.0(2), N2−C1−Ni1 127.0(2), N1−C1−N2 104.0(2), N3−C20−N4 108.5(2).

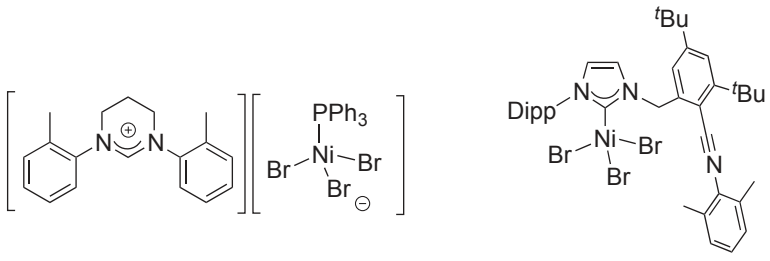

Whittlesey **Fout**

Figure 9. Ni(II) complexes containing a $[NiBr_3]^-$ moiety (see text)

Owing to the quality of the ^{1}H NMR spectrum of the paramagnetic compound **16**, we searched for other nickel complexes possessing a $[NiX_3]^-$ moiety for comparison. In 2014, Whittlesey and

co-workers reported a complex containing the Ni(II) anion $[Ni(PPh_3)Br_3]^-$, as a byproduct in the formation of a Ni(II) NHC complex by deprotonation of a N-aryl substituted six-membered imidazolium ring followed by the addition of $[Ni(PPh_3)_2Br_2]$.[14] ^1H NMR resonances between 19.55 and -4.85 ppm were observed. Similarly, a Ni(II) complex with an NHC ligand bound to $[NiCl_3]^-$ was found as a reaction byproduct.[6b] In 2017, Fout and co-workers isolated a $[Ni(NHC)Br_3]^-$,complex from the chemical oxidation of a bidentate NHC-η^2-iminoacyl Ni(II) complex by $[Ph_3CBr]$.[15] Interestingly, their ^1H NMR chemical shifts ranged from 87.29 to -22.21 ppm, but the signals were not as sharp as in our case.

Since Ni(II) binds to the potential $C^{NHC}O^{ether}$ bidentate ligands in a monodentate mode via C^{NHC} while the oxygen-function remains dangling, we considered introducing a N^{imine} donor to form a potentially $N^{imine}C^{NHC}O^{ether}$ tridentate ligand and investigate the properties of its corresponding nickel complexes. The imidazolium salt $[(ImH)\{C(Me)=NDipp\}(C_3OMe)]Cl$ (**19**) (eq. 4) was isolated as a white powder and used for the direct synthesis of Ni(II) NHC complexes. Deprotonation of **19** followed by the addition of $[NiCl_2(dme)]$ an intractable mixture. The indirect pathway mentioned above consisting in the formation of the $[NiCl_4]^{2-}$ bis-imidazolium salt $[(ImH)\{C(Me)=NDipp\}(C_3OMe)]_2[NiCl_4]\}]$ (**20**) (eq. 5), followed by deprotonation with 1 or 2 equiv. of base, led to better results.

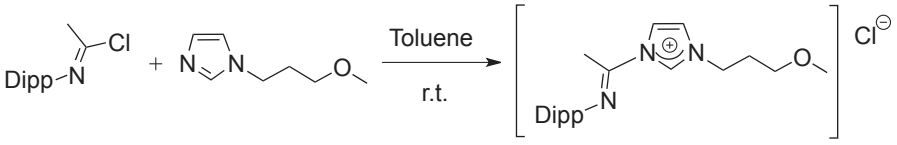

19 (4)

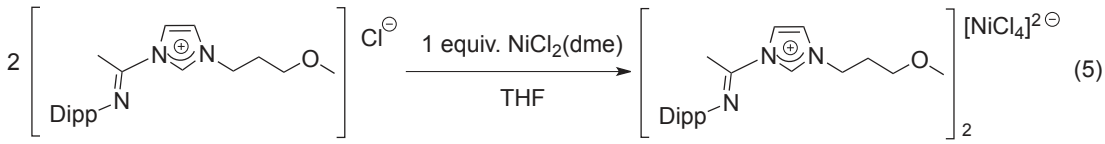

19 **20** (5)

As shown in Figure 10, the salt **20** crystallizes in the monoclinic system (*C*2/c space group). The asymmetric unit contains one molecule of the ligand and half a molecule of $[NiCl_4]^{2-}$ and the nickel atom is in a special position (population 50%), as in compound **13**. A green, paramagnetic complex was obtained by deprotonation of **20** with 1 equiv. NaO^tBu but no crystals formed. From the ^1H NMR spectroscopy analysis, no formation of the analogous compound containing the

$[Ni(NHC)Cl_3]^-$ moiety could be observed.

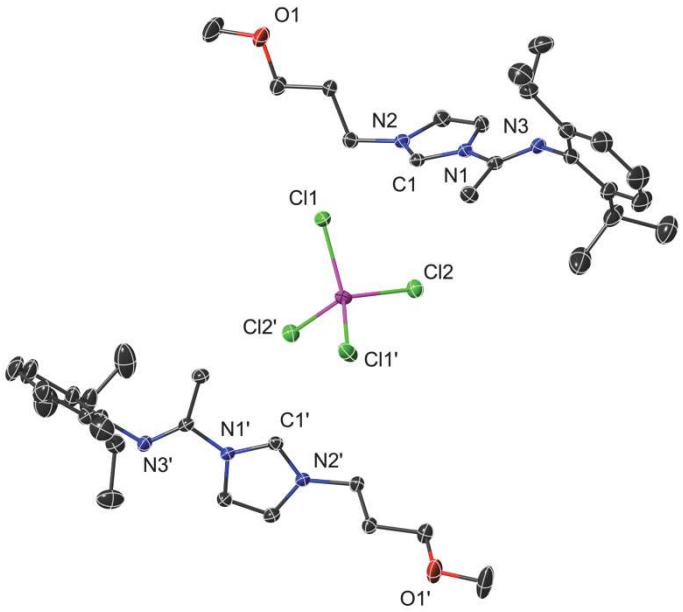

Figure 10. Structure of complex **20** with H atoms omitted for clarity, except the NC*H*N hydrogen atoms. Thermal ellipsoids at the 40% probability level. Selected bond lengths (Å) and angles (deg): Ni1−Cl1 2.263(4), Ni1−Cl2 2.271(4), C1−N1 1.340(2), C1−N2 1.324(2), N1−C1−N2 108.3(1).

Considering that silver(I) complexes are widely used as transmetalating agents in the synthesis of transition metal NHC complexes, the silver complex [AgCl{C(Me)=NDipp}(C_3OMe)] (**21**) was prepared (eq. 6, Figure 11) and used for transmetallation reactions to Ni(II). Its crystallographic analysis reveals for the metal a nearly linear coordination geometry (C1−Ag1−Cl1 angle of 177.1(4) Å), a monodentate NHC ligand with pendent N^{imine} and O^{ether} groups but with the N and O atoms directed toward the Ag atom; however, the Ag1···N3 (2.801 Å) and Ag1···O1 (3.334 Å) distances are too long to represent significant bonding interactions.

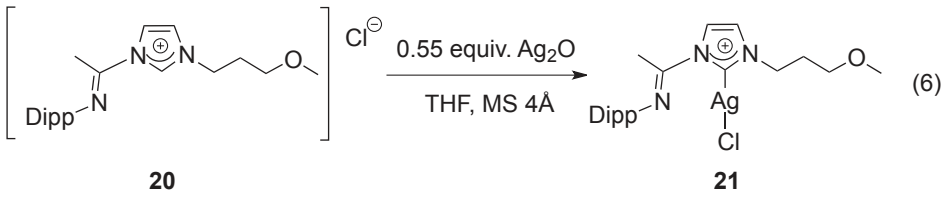

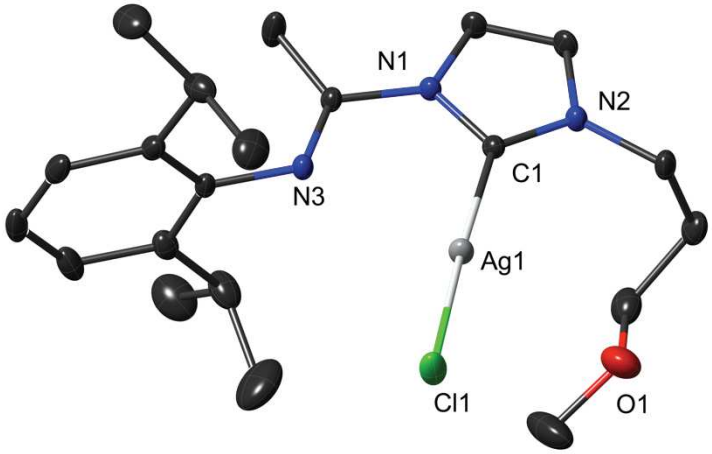

Figure 11. Structure of the Ag(I) complex **21** with H atoms omitted for clarity. Thermal ellipsoids at the 30% probability level. Selected bond lengths (Å) and angles (deg): Ag1−C1 2.080(1), Ag1−Cl1 2.332(4), C1−N1 1.366(2), C1−N2 1.346(2), C1−Ag1−Cl1 177.1(4), N1−C1−Ag1 125.1(1), N2−C1−Ag1 130.6(1), N1−C1−N2 104.3(1).

Using $[NiCl_2(dme)]$ as precursor to form a Ni(II) complex by transmetallation, a green oil was obtained from the reaction in THF but could not be analyzed owing to its paramagnetic nature. The low solubility of $[NiCl_2(dme)]$ that could favor formation of the bis-NHC complex prompted us to use a more soluble precursor. Therefore, $[Ni(NCMe)_6](BF_4)_2$ was employed with a Ni/Ag-NHC ratio of 1:1 or 2:1 to form a mono- or bis-NHC Ni(II) complex. Similar results were obtained with both ratios according to ^{1}H NMR spectroscopy, but the product could not be crystallized.

Since it was not possible to coordinate the ether function in a mono-NHC neutral complex or by halide abstraction from a bis-NHC dihalide complex using $AgBF_4$ or $TlPF_6$, we introduced a stronger amine donor in place of the ether to investigate the possibility of forming a $C^{NHC}N^{amine}$ chelate. We prepared the protonated salts $[(ImH)Dipp(C_2NHMe_2)]Cl_2$ (**22**) and $[(ImH)Dipp(C_3NHMe_2)]Cl_2$ (**23**) according to eq. 7 and reacted them with 2 equiv. of base and then with $[NiBr_2(dme)]$. We also prepared the Ag(I) complexes $[Ag\{(ImH)Dipp(C_2NMe_2)\}Cl]$ (**24**) and $[Ag\{(ImH)Dipp(C_3NMe_2)\}Cl]$ (**25**) for transmetallation purpose, using a nickel/ligand ratio of 1:1 (Scheme 2). In both cases, purple crystals could be isolated and their analysis by X-ray diffraction established their nature as $[NiCl_2\{\kappa N^{amine},\kappa C^{NHC}\text{-}(ImH)Dipp(C_2NMe_2)\}]$ (**26**) (Figure 12). It crystallizes in the monoclinic system ($P2_1/c$ space group). The nickel center is in a tetrahedral coordination environment consisting of two bromides, the NHC and the amine donor groups. Formation of a $C^{NHC}N^{amine}$ chelate Ni complex is consistent with an amine group coordinating more readily to Ni(II) than an ether group owing to its stronger donor ability. Broadening the

investigation to the $C^{NHC}N^{amine}$ ligand with the C3 spacer connecting the N^{NHC} and the N^{amine} donor, a purple Ni(II) complex [$NiCl_2\{\kappa N^{amine},\kappa C^{NHC}$-(ImH)Dipp($C_3NMe_2$)}] (**27**) was isolated which contains a seven-membered ring $C^{NHC}N^{amine}$ chelate. Its crystallographic characterization revealed that the nickel center adopts the same coordination geometry as in **26**, with similar bond distances and angles, except for the C1−Ni1−N3 angle (104.7(3)° in **27**, 94.8(2)° in **26**).

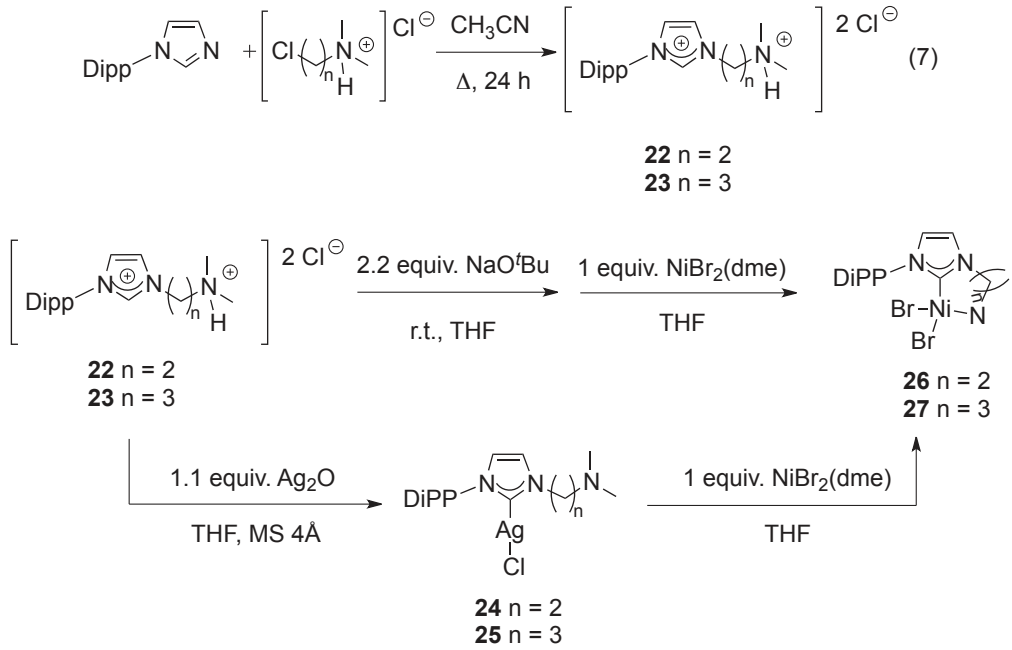

Scheme 2. Synthesis of the mono-amine-functionalized NHC Ag(I) and Ni(II) complexes **24**-**27**

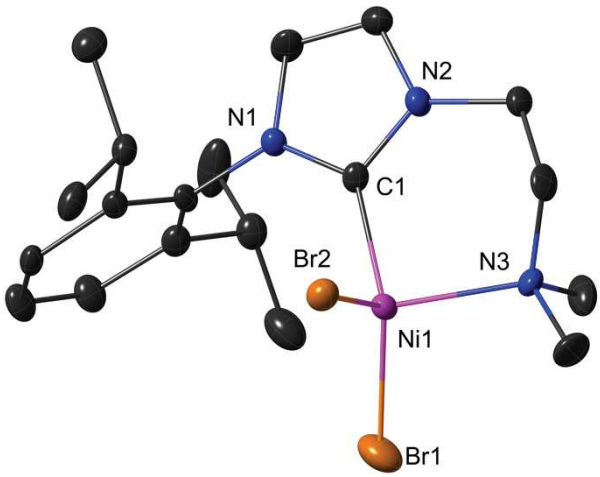

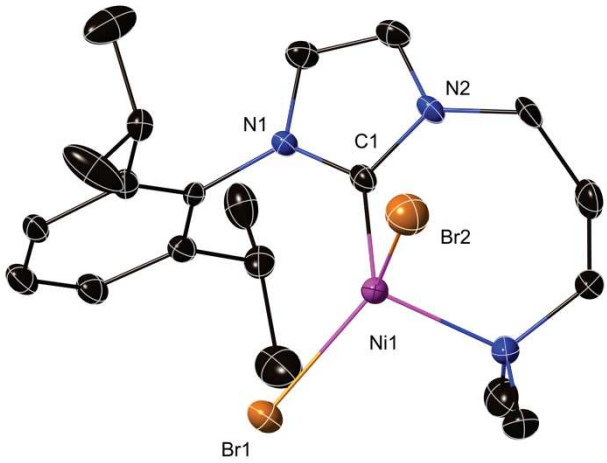

Figure 12. Structures of complex **26** (top) and **27** (bottom) with H atoms omitted for clarity. Thermal ellipsoids at the 30% probability level. Selected bond lengths (Å) and angles (deg): in **26** Ni1−Br1 2.342(1), Ni1−Br2 2.397(1), Ni1−C1 1.970(6), Ni1−N3 2.042(5), C1−N1 1.358(8), C1−N2 1.343(8), C1−Ni1−Br1 124.3(2), C1−Ni1−Br2 103.4(2), C1−Ni1−N3 94.8(2), Br1−Ni1−Br2 122.2(5), Br1−Ni1−N3 102.4(2), Br2−Ni1−N3 104.2(2), N1−C1−N2 104.5(5), N1−C1−Ni1 130.9(5), N2−C1−Ni1 124.6(5); in **27** Ni1−Br1 2.353(2), Ni1−Br2 2.348(2), Ni1−C1 1.989(9), Ni1−N3 2.056(8), C1−N1 1.352(1), C1−N2 1.362(1), C1−Ni1−Br1 118.1(2), C1−Ni1−Br2 101.2(2), C1−Ni1−N3 104.7(3), Br1−Ni1−Br2 123.6(8), Br1−Ni1−N3 104.6(2), Br2−Ni1−N3 102.2(2), N1−C1−N2 104.5(7), N1−C1−Ni1 129.2(6), N2−C1−Ni1 125.3(6).

Ethylene oligomerization catalysis

In continuation of previous investigations in our group on the catalytic properties of Ni NHC complexes in ethylene oligomerization, we examined the catalytic properties of complexes **5**, **6**, **11**, **13**, **18**, **26** and **27** in toluene or in a mixture of toluene and chlorobenzene in the presence of 10 equiv. ethylaluminum dichloride (EADC) as co-catalyst. The influence of the *N*-substituents (R = Dipp, Mes, Me) and *N*-functionality (C_3OMe, C_2NMe_2 and C_3NMe_2) on the NHC ligands, the quantity of cocatalyst and the different cations present in the salts containing $[NiCl_4]^{2-}$ dianion could thus be evaluated.

The neutral bis-NHC Ni(II) complexes **5** and **6** with the C_3OMe *N*-functionality displayed similar activities with R = Dipp or Mes (productivity: 3500 g C_2H_4/(g Ni•h) of **5** and 3100 g C_2H_4/(g Ni•h) of **6**, entries 2, 3), that are also similar to those previously reported for the complex containing the C_2OMe substituent in place of C_3OMe (4600 g C_2H_4/(g Ni•h) of **ref 1**, entry 1). Another neutral mono-Ni(II) species with the C_2NMe_2 or C_3NMe_2 *N*-functionality was investigated under similar catalytic conditions and exhibited more than twice higher productivities than the samples with the

C_3OMe arm (15600 g C_2H_4/(g Ni•h) of **26** and 13300 g C_2H_4/(g Ni•h) of **27**, entries 4, 5). To estimate the influence of the quantity of cocatalyst on catalytic activity, a lower amount (4 equiv.) of EADC was employed but much lower ethylene consumption and activity were obtained (productivity: 2000 g C_2H_4/(g Ni•h) of **27**[f], entry 6). Butenes were the major products, with a selectivity ranging from 66% to 81%, and the formation of 1-butene being more selective when the catalytic productivity is lower (1-butene selectivity: 51% of **5**, 48% of **6** and 32% of **27**[f], respectively, 8% of **26** and 9% of **27**).

Moreover, we applied the same catalysis procedure with the monoanionic NHC Ni(II) complex ([(ImH)Dipp(C_3OMe)][$NiBr_3${ImDipp(C_3OMe)}]) (**18**). On the one hand, the productivity of **18** (12300 g C_2H_4/(g Ni•h), entry 7) was more than 2 times higher than with the neutral bis-NHC Ni(II) complexes (**5** and **6**, entries 2, 3) but similar to that of the neutral mono-NHC Ni(II) complexes (**26** and **27**, entries 4, 5). On the other hand, the selectivity of **18** for the formation of butenes (80%) and hexenes (19%) was similar to that of the former samples (butenes: 66%-81%, hexenes: 17%-28%).

In comparison with the neutral and monoanion complexes, the dianion Ni(II) complexes exhibited higher ethylene consumption and productivities (productivity: 16900 g C_2H_4/(g Ni•h) of **11** and 18000 g C_2H_4/(g Ni•h) of **13**, entries 8, 9) in ethylene oligomerization. It is noteworthy that the dianion Ni(II) complex associated with the ammonium cation has the best productivity (19900 g C_2H_4/(g Ni•h), **ref 2**, entry 10) among the dianion nickel complexes. Butenes are the major products, similar to the other nickel complexes discussed above.

					selectivity[c]					
entry		complex	ethylene consumed[a]	productivity[b]	C_4	C_6	C_8 +	1-butene[d]	1-hexene[d]	linear C_6[e]
1	**ref 1**	[$NiCl_2${ImDipp(C_2OMe)}$_2$]	6.3	4600	64	32	4	52	3	17
2	**5**	[$NiCl_2${ImDipp(C_3OMe)}$_2$]	4.8	3500	73	23	3	51	5	
3	**6**	[$NiCl_2${ImMes(C_3OMe)}$_2$]	4.2	3100	81	17	2	48	6	
4	**26**	[$NiBr_2${ImDipp(C_2NMe_2)}]	21.3	15600	71	26	3	9	1	
5	**27**	[$NiBr_2${ImDipp(C_3NMe_2)}]	18.2	13300	74	24	2	8	1	
6	**27**[f]	[$NiBr_2${ImDipp(C_3NMe_2)}]	2.8	2000	66	28	6	32	2	
7	**18**	[(ImH)Dipp(C_3OMe)][$NiBr_3${ImDipp(C_3OMe)}]	15.3	12300	80	19	1	9	1	

8	**11**	[(ImH)Dipp(C_3OMe)]$_2$[$NiCl_4$]	23.2	16900	68	29	3	5	1
9	**13**	[(ImH)Me(C_3OMe)]$_2$[$NiCl_4$]	24.7	18000	72	26	2	7	1
10	**ref 2**	[(Et_4N)$_2$[$NiBr_4$]	27.2	19900	67	30	3	7	1

Conditions: amount of catalyst: 4×10^{-5} mol, amount of cocatalyst (EADC): 4×10^{-4} mol (10 equiv.), T = 30–35 °C, solvent: toluene (except for **11, 13** and **ref** in chlorobenzene for solubility issues), total volume: 15 mL, 10 bar C_2H_4, reaction time 35 min., every test was repeated at least twice.

[a] equal to the quantity of ethylene introduced minus the unreacted ethylene collected at the end of the reaction (see experimental), expressed in g;

[b] expressed in g C_2H_4/(g Ni·h);

[c] expressed in %, calculated by GC analysis;

[d] selectivity for a within the C_4 or C_6 fraction, expressed in % mol;

[e] selectivity for linear olefins within the C_6 fraction;

[f] amount of cocatalyst (EADC): 1.6×10^{-4} mol (4 equiv.).

5. Conclusions

A series of $C^{NHC}O^{ether}$ hybrid ligands with different *N*-substituents (R = Dipp, Mes, Me) has been investigated and revealed a monodentate coordinative behavior with both silver and nickel precursors. An indirect synthetic method to selectively access mono-, or bis-NHC nickel complexes has been described which proceeds in two steps: formation of bis-imidazolium salts with a $[NiX_4]^{2-}$ dianions, followed by deprotonation of this salt by a base. The procedure avoids the isolation of a sensitive, free carbene and it is noteworthy that the formation of mono-, or bis-NHC Ni(II) complexes could be simply controlled by the quantity of base used. Interestingly, the mono-NHC nickel complex with the $[NiCl_3]^-$ moiety exhibited a paramagnetic ^{1}H NMR spectrum with sharp peaks ranging from 93 to -32 ppm, probably due to the hydrogen bond interaction between the imidazolium cation and $[NiCl_3]^-$ anion. Detailed ^{1}H NMR spectroscopic analyses allowed assignment of the resonances in both cationic and anionic fragments, by adding increasing amount of the corresponding imidazolium salt [(ImH)Dipp(C_3OMe)]Cl (**1**) to the nickel complex [(ImH)Dipp(C_3OMe)][$NiCl_3${ImDipp(C_3OMe)}] (**16**). The peaks remained in the same chemical shift range to those of the anionic fragment [$NiCl_3${ImDipp(C_3OMe)}]$^-$.

For comparison with the ether-functionalized ligand, the $C^{NHC}N^{amine}$ hybrid ligands chelate the

tetrahedral Ni(II) center, two bromides completing the coordination sphere. These complexes showed normal paramagnetic ^{1}H NMR spectra with broad peaks.

This study has shown that with hybrid ligands containing a NHC donor, the additional function present in the ligand does not always coordinated to the metal and that changes in its chemical nature and in the length of the spacer used represent useful parameters to increase and eventually control their coordination chemistry.

6. Experimental section

General methods

All manipulations involving organometallics were performed under nitrogen or argon in a Braun glove-box or using standard Schlenk techniques. Solvents were dried using standard methods and distilled under nitrogen prior use or passed through columns of activated alumina and subsequently purged with nitrogen or argon. The starting materials **X** were prepared according to the literature. NMR spectra were recorded on Bruker spectrometers (AVANCE I − 300 MHz, AVANCE III − 400 MHz or AVANCE I − 500 MHz equipped with a cryogenic probe). Elemental analyses were performed by the "Service de microanalyses", Université de Strasbourg.

Preparation of [(ImH)Dipp(C_3OMe)]Cl (1)

A mixture of 1-(2,6-diisopropylphenyl)-1*H*-imidazole (5.000 g, 21.9 mmol) and 1-chloro-3-methoxypropane (12 mL, 109.5 mmol) was refluxed for 1.5 days. The unreacted 1-chloro-3-methoxypropane was removed under reduced pressure. The resulting sticky solid was triturated twice with Et_2O. It was then stirred in Et_2O for 16 h and collected by filtration to afford **1** as a white solid (7.260 g, 98%). ^{1}H NMR (500 MHz, CD_2Cl_2) δ: 10.32 (br, 1H, $CH^{imidazole}$), 7.95 (br, 1H, $CH^{imidazole}$), 7.57 (t, ^{3}J = 7.8 Hz, 1H, $CH^{p\text{-}Ar}$), 7.34 (d, ^{3}J = 7.8 Hz, 2H, $CH^{m\text{-}Ar}$), 7.21 (br, 1H, $CH^{imidazole}$), 4.79 (t, ^{3}J = 6.7 Hz, 2H, C*H*$_2$CH$_2$CH$_2$OMe), 3.51 (t, ^{3}J = 5.6 Hz, 2H, CH$_2$CH$_2$C*H*$_2$OMe), 3.28 (s, 3H, CH$_2$CH$_2$CH$_2$O*Me*), 2.33-2.26 (m, 4H, CH$_2$C*H*$_2$CH$_2$OMe overlapped with CH^{iPr}), 1.22 (d, ^{3}J = 6.7 Hz, 6H, $CH_3{}^{iPr}$), 1.16 (d, ^{3}J = 6.7 Hz, 6H, $CH_3{}^{iPr}$). ^{13}C NMR (126 MHz, CD_2Cl_2) δ: 145.8 ($C^{o\text{-}Ar}$), 138.7($C^{imidazole}$), 132.1($C^{p\text{-}Ar}$), 130.6 ($C^{ipso\text{-}Ar}$), 125.0 ($C^{m\text{-}Ar}$), 124.2 ($C^{imidazole}$), 123.9 ($C^{imidazole}$), 69.5 (*C*H$_2$CH$_2$CH$_2$OMe), 59.0 (CH$_2$CH$_2$CH$_2$O*Me*), 48.6 (CH$_2$CH$_2$*C*H$_2$OMe), 30.7 (CH$_2$*C*H$_2$CH$_2$OMe), 29.0 (CH^{iPr}), 24.5 ($CH_3{}^{iPr}$), 24.3 ($CH_3{}^{iPr}$)

Preparation of [(ImH)Mes(C_3OMe)]Cl (2)

A mixture of 1-(2,6-diisopropylphenyl)-1*H*-imidazole (5.000 g, 21.9 mmol) and

1-chloro-3-methoxypropane (12 mL, 109.5 mmol) was refluxed for 1.5 days. The unreacted 1-chloro-3-methoxypropane was removed under reduced pressure. The resulting sticky solid was triturated twice with Et_2O. It was then stirred in Et_2O for 16 h and the solid was collected by filtration to afford **1** as a white solid (7.260 g, 98%). ^{1}H NMR (500 MHz, CD2Cl2) δ: 10.79 (br, 1H, $CH^{imidazole}$), 7.79 (br, 1H, $CH^{imidazole}$), 7.20 (br, 1H, $CH^{imidazole}$), 7.04 (s, 2H, $CH^{m\text{-}Ar}$), 4.70 (t, ^3J = 6.7 Hz, 2H, $CH_2CH_2CH_2OMe$), 3.48 (t, ^3J = 5.6 Hz, 2H, $CH_2CH_2CH_2OMe$), 3.27 (s, 3H, $CH_2CH_2CH_2OMe$), 2.34(s, 3H, Me-^{para}), 2.08 (s, 6H, Me-^{ortho}) ^{13}C NMR (126 MHz, CD_2Cl_2) δ:141.5 ($C^{p\text{-}Ar}$), 139.4 ($C^{imidazole}$), 134.7 ($C^{o\text{-}Ar}$), 131.3 ($C^{ipso\text{-}Ar}$), 130.0 ($C^{m\text{-}Ar}$), 123.4 ($C^{imidazole}$), 123.1($C^{imidazole}$), 69.5 ($CH_2CH_2CH_2OMe$), 58.9 ($CH_2CH_2CH_2OMe$), 48.3 ($CH_2CH_2CH_2OMe$), 30.6 ($CH_2CH_2CH_2OMe$), 21.2 ($Me^{\text{para-Mes}}$), 17.7 ($Me^{\text{ortho-Mes}}$),

Preparation of [(ImH)Me(C_3OMe)]Cl (3)

A mixture of 1-methyl-1*H*-imidazole (5.000 g, 60.9 mmol) and 1-chloro-3-methoxypropane (20 mL, 184.2 mmol) was refluxed overnight. The unreacted 1-chloro-3-methoxypropane was removed under reduced pressure. The resulting sticky liquid was triturated twice with Et_2O to give a solid that was then washed with THF and collected by filtration to afford **3** as a white solid (9.075 g, 96%). ^{1}H NMR (500 MHz, $CDCl_3$) δ: 10.76 (br, 1H, $CH^{imidazole}$), 7.56 (br, 1H, $CH^{imidazole}$), 7.47 (br, 1H, $CH^{imidazole}$), 4.37 (t, ^3J = 7.0 Hz, 2H, $CH_2CH_2CH_2OMe$), 4.04 (s, 3H, $Me^{N\text{-}im}$), 3.37 (t, ^3J = 5.8 Hz, 2H, $CH_2CH_2CH_2OMe$), 3.26 (s, 3H, $CH_2CH_2CH_2OMe$), 2.17-2.12 (m, 2H, $CH_2CH_2CH_2OMe$). ^{13}C NMR (126 MHz, CD_2Cl_2) δ: 138.6($C^{imidazole}$), 123.4($C^{imidazole}$), 122.6($C^{imidazole}$), 68.6 ($CH_2CH_2CH_2OMe$), 58.8($Me^{N\text{-}Im}$), 47.4 ($CH_2CH_2CH_2OMe$), 36.6 ($CH_2CH_2CH_2OMe$), 30.42 ($CH_2CH_2CH_2OMe$)

Preparation of (Dipp)(C_3OMe)imidazole-ylidene (4)

To a suspension of the imidazolium salt [(ImH)Dipp(C_3OMe)]Cl (0.250 g, 0.74 mmol) in THF (5 ml) at -40 ^{o}C was added dropwise a solution of sodium hexamethyldisilazide (0.177 g, 0.96 mmol) in THF (8 ml). The reaction mixture was allowed to warm to room temperature and stirred for 30 min. Evaporation of the solvent under reduced pressure, extraction of the residue into pentane (3×20 ml), evaporation of the extracts to dryness and washing of the solid residue with pentane (5 ml) at -30 ^{o}C gave **4** as a colorless powder (0.102 g, 46%). X-ray quality crystals were obtained by slow cooling (-30 ^{o}C) of dilute pentane solutions for two days.

Preparation of [$NiCl_2${ImDipp(C_3OMe)}$_2$] (5).

Method A: To a solution of the imidazolium salt [(ImH)Dipp(C_3OMe)]Cl (0.200 g, 0.59 mmol) in THF (8 mL) was added a solution of NaO^{t}Bu (0.418 g, 0.60 mmol) in THF (5 mL). The reaction mixture was stirred for 1 h and to this solution was then added [$NiCl_2$(dme)] (0.065 g, 0.30 mmol). The reaction mixture was stirred for 3 h.

Method B: To a solution of the [(ImH)Dipp(C_3OMe)]$_2$[$NiCl_4$] (0.200 g, 0.25 mmol) in THF (8 mL) was added a solution of NaO^{t}Bu (0.055 g, 0.57 mmol) in THF (5 mL). The reaction mixture was stirred for 3 h. The orange solution was then filtered through a Celite pad and the filtrate was evaporated under reduced pressure. The complex was precipitated from THF/Et_2O and washed with Et_2O to afford an orange powder (0.165-0.179 g, 77-83%). X-ray quality crystals were obtained by slow diffusion of Et_2O into THF solution. *Anti*-form (82 %): ^{1}H NMR (500 MHz, $CDCl_3$): δ 7.56 (t, ^3J = 7.8 Hz, 1H, CH$^{p\text{-Ar}}$), 7.40 (d, ^3J = 7.8 Hz, 2H, CH$^{m\text{-Ar}}$), 6.78 (d, ^3J = 1.5 Hz, 1H, CH$^{\text{imidazole}}$), 6.62 (d, ^3J = 1.5 Hz, 1H, CH$^{\text{imidazole}}$), 4.80 (t, ^3J = 7.2 Hz, 2H, C*H*$_2$CH$_2$CH$_2$OMe), 3.32 (s, 3H, CH$_2$CH$_2$CH$_2$O*Me*), 3.17 (t, ^3J = 5.8 Hz, 2H, CH$_2$CH$_2$C*H*$_2$OMe), 2.71 (sept, ^3J = 6.9 Hz, 2H, CH$^{i\text{Pr}}$), 2.29 (apparent quit, ^3J = 7.2-5.8 Hz, 2H, CH$_2$*CH*$_2$CH$_2$OMe), 1.30 (d, ^3J = 6.9 Hz, 6H, CH$_3^{i\text{Pr}}$), 0.91 (d, ^3J = 6.9 Hz, 6H, CH$_3^{i\text{Pr}}$).^{13}C NMR (126 MHz, $CDCl_3$) δ: 168.9 (C$^{\text{carbene}}$), 148.0 (C$^{o\text{-Ar}}$), 136.0 (C$^{ipso\text{-Ar}}$), 129.9 (C$^{\text{imidazole}}$), 123.9 (C$^{p\text{-Ar}}$), 123.7 (C$^{m\text{-Ar}}$), 120.8 (C$^{\text{imidazole}}$), 69.5 (*C*H$_2$CH$_2$CH$_2$OMe), 58.7 (CH$_2$CH$_2$CH$_2$O*Me*), 47.8 (*C*H$_2$CH$_2$*C*H$_2$OMe), 30.3 (*C*H$_2$*C*H$_2$CH$_2$OMe), 28.4 (CH$^{i\text{Pr}}$), 26.7 (CH$_3^{i\text{Pr}}$), 22.8 (CH$_3^{i\text{Pr}}$). *Syn*-form (18 %): ^{1}H NMR (500 MHz, $CDCl_3$) δ: 7.41 (overlapped with the anti-form) (t, ^3J = 7.8 Hz, 1H, CH$^{p\text{-Ar}}$), 7.14 (d, ^3J = 7.8 Hz, 2H, CH$^{m\text{-Ar}}$), 6.87 (d, ^3J = 1.8 Hz, 1H, CH$^{\text{imidazole}}$), 6.54 (d, ^3J = 1.8 Hz, 1H, CH$^{\text{imidazole}}$), 5.54 (t, ^3J = 7.2 Hz, 2H, C*H*$_2$CH$_2$CH$_2$OMe), 3.62 (t, ^3J = 5.8 Hz, 2H, CH$_2$CH$_2$C*H*$_2$OMe), 3.44 (s, 3H, CH$_2$CH$_2$CH$_2$O*Me*), 2.65 (partly overlapped with the anti-form) (apparent quit, ^3J = 7.2-5.8 Hz, 2H, CH$_2$*CH*$_2$CH$_2$OMe), 2.46 (sept, ^3J = 6.9 Hz, 2H, CH$^{i\text{Pr}}$), 0.92 (partly overlapped with the anti-form) (d, ^3J = 6.9 Hz, 6H, CH$_3^{i\text{Pr}}$), 0.84 (d, ^3J = 6.9 Hz, 6H, CH$_3^{i\text{Pr}}$). ^{13}C NMR (126 MHz, $CDCl_3$) δ: not seen (C$^{\text{carbene}}$), 146.9 (C$^{o\text{-Ar}}$), 135.6 (C$^{ipso\text{-Ar}}$), 129.4 (C$^{\text{imidazole}}$), 124.4 (C$^{p\text{-Ar}}$), 123.9 (C$^{m\text{-Ar}}$), 120.2 (C$^{\text{imidazole}}$), 69.9 (*C*H$_2$CH$_2$CH$_2$OMe), 58.9 (CH$_2$CH$_2$CH$_2$O*Me*), 48.2 (*C*H$_2$CH$_2$*C*H$_2$OMe), 31.2 (*C*H$_2$*C*H$_2$CH$_2$OMe), 28.1 (CH$^{i\text{Pr}}$), 26.4 (CH$_3^{i\text{Pr}}$), overlapped with the anti-form (CH$_3^{i\text{Pr}}$). Anal. calcd. for $C_{38}H_{56}Cl_2N_4NiO_2$: C, 62.48; H, 7.73; N, 7.67%; found: C, 62.16; H, 7.67; N, 7.71%.

Preparation of [$NiCl_2${ImMes(C_3OMe)}$_2$] (6).

To a solution of the [(ImH)Mes(C_3OMe)]$_2$[$NiCl_4$] (0.200 g, 0.28 mmol) in THF (8 mL) was added a solution of NaO^{t}Bu (0.054 g, 0.56 mmol) in THF (5 mL). The reaction mixture was stirred for 3 h. The orange solution was then filtered through a Celite pad and the filtrate was evaporated under

reduced pressure. The complex was precipitated from THF/Et_2O and washed with Et_2O to afford an orange powder. (0.145 g, 80%). X-ray quality crystals were obtained by slow diffusion of Et_2O into THF solution.

Preparation of [$NiCl_2${$Me(C_3OMe)$}$_2$] (7).

To a solution of the [(ImH)$Me(C_3OMe)]_2[NiCl_4]$ (0.100 g, 0.20 mmol) in THF (8 mL) was added a solution of NaO^tBu (0.042 g, 0.44 mmol) in THF (5 mL). The reaction mixture was stirred for 3 h. The orange solution was then filtered through a Celite pad and the filtrate was evaporated under reduced pressure. The complex was precipitated from THF/ether and washed with Et_2O to afford an orange powder (0.055 g, 63%). X-ray quality crystals were obtained by slow diffusion of Et_2O into THF solution.

Preparation of [AgCl{ImDipp(C_3OMe)}$_2$] (8).

A mixture of the imidazolium salt [(ImH)Dipp(C_3OMe)]Cl (0.420 g, 1.25 mmol), Ag_2O (0.159 g, 0.69 mmol) and molecular sieves in THF (10 mL) was stirred overnight under exclusion of light. The beige reaction mixture was then filtered through Celite and the filtrate was dried under reduced pressure. The resulting solid was washed with Et_2O to give as a beige powder (0.359 g, 77%). X-ray quality crystals were obtained by slow diffusion of pentane into THF solution. ^{1}H NMR (CD_2Cl_2, 500 MHz): δ 7.47 (t, ^3J = 7.8 Hz, 1H, $CH^{p\text{-Ar}}$), 7.44 (t, ^3J(H-H) = 1.5 Hz, ^4J(H-Ag) = 1.5 Hz, 1H, $CH^{imidazole}$), 7.23 (d, ^3J = 7.8 Hz, 1H, $CH^{m\text{-Ar}}$), 7.00 (t, ^3J(H-H) = 1.5 Hz, ^4J(H-Ag) = 1.5 Hz, 1H, $CH^{imidazole}$), 4.01 (t, ^3J = 7.0 Hz, 2H, $CH_2CH_2CH_2OMe$), 3.26 (s, 3H, $CH_2CH_2CH_2OMe$), 3.21 (t, ^3J = 5.8 Hz, 2H, $CH_2CH_2CH_2OMe$), 2.25 (sept, ^3J = 6.9 Hz, 2H, $CH^{i\text{Pr}}$), 1.85 (apparent quintet, ^3J = 7.0-5.8 Hz, 2H, $CH_2CH_2CH_2OMe$), 1.08 (d, ^3J = 6.9 Hz, 6H, $CH_3^{i\text{Pr}}$), 0.98 (d, ^3J = 6.9 Hz, 6H, $CH_3^{i\text{Pr}}$). ^{13}C NMR (126 MHz, CD_2Cl_2) δ: 181.2 (d, $^1J(^{13}C\text{-}^{107}Ag)$ = 182 Hz, $^1J(^{13}C\text{-}^{109}Ag)$ = 210 Hz, $C^{carbene}$), 145.9 ($C^{o\text{-Ar}}$), 134.9 ($C^{ipso\text{-Ar}}$), 130.5 ($C^{p\text{-Ar}}$), 124.1 ($C^{m\text{-Ar}}$), 123.8 (^3J(C-Ag) = 5.6 Hz, $C^{imidazole}$), 122.4 (^3J(C-Ag) = 5.6 Hz, $C^{imidazole}$), 68.5 ($CH_2CH_2CH_2OMe$), 58.5 ($CH_2CH_2CH_2OMe$), 48.7 ($CH_2CH_2CH_2OMe$), 31.4 ($CH_2CH_2CH_2OMe$), 28.2 ($CH^{i\text{Pr}}$), 24.4 ($CH_3^{i\text{Pr}}$), 23.9 ($CH_3^{i\text{Pr}}$). Anal. calcd. for $C_{38}H_{56}N_4O_2AgCl$: C, 61.33; H, 7.58; N, 7.53%; found: C, 60.87; H, 7.67; N, 7.08%. Despite numerous attempts, no better elemental analysis data could be obtained.

Preparation of [AgCl{ImMes(C_3OMe)}$_2$] (9).

A mixture of the imidazolium salt [(ImH)Mes(C_3OMe)]Cl (0.500 g, 1.70 mmol), Ag_2O (0.216 g, 0.94 mmol) and molecular sieves in THF (10 mL) was stirred overnight under exclusion of light.

The beige reaction mixture was then filtered through Celite and the filtrate dried under reduced pressure. The resulting solid was washed with Et_2O to give a beige powder (0.454 g, 81%). X-ray quality crystals were obtained by slow diffusion of pentane into THF solution.

Preparation of [AgCl{ImMe(C_3OMe)}$_2$] (10).

A mixture of the imidazolium salt [(ImH)Me(C_3OMe)]Cl (0.500 g, 2.62 mmol), Ag_2O (0.334 g, 1.44 mmol) and molecular sieves in THF (10 mL) was stirred overnight under exclusion of light. The beige reaction mixture was then filtered through Celite and the filtrate was dried under reduced pressure. The resulting solid was washed with Et_2O to give a beige powder (0.462 g, 78%). X-ray quality crystals were obtained by slow diffusion of pentane into THF solution.

Preparation of [(ImH)Dipp(C_3OMe)]$_2$[$NiCl_4$] (11).

A mixture of the imidazolium salt [(ImH)Dipp(C_3OMe)]Cl (1.000 g, 2.97 mmol) and [$NiCl_2$(dme)] (0.327 g, 1.49 mmol) in THF was stirred overnight. The solvent was evaporated under reduced pressure. The blue slurry was then triturated with Et_2O until a blue powder was obtained (1.027 g, 86%). X-ray quality crystals were obtained by slow diffusion of Et_2O into CH_3CN solution.

Preparation of [(ImH)Mes(C_3OMe)]$_2$[$NiCl_4$] (12).

A mixture of the imidazolium salt [(ImH)Mes(C_3OMe)]Cl (0.200 g, 0.68 mmol) and [$NiCl_2$(dme)] (0.075 g, 0.34 mmol) in THF was stirred overnight. The solvent was evaporated under reduced pressure. The blue slurry was then triturated with Et_2O until a blue powder was obtained (0.208 g, 85%). X-ray quality crystals were obtained by slow diffusion of Et_2O into CH_3CN solution.

Preparation of [(ImH)Me(C_3OMe)]$_2$[$NiCl_4$] (13).

A mixture of the imidazolium salt [(ImH)Me(C_3OMe)]Cl (0.200 g, 1.05 mmol) and [$NiCl_2$(dme)] (0.115 g, 0.53 mmol) in THF was stirred overnight. The solvent was evaporated under reduced pressure. The blue slurry was then triturated with Et_2O until a blue powder was obtained (0.203 g, 75%). X-ray quality crystals were obtained by slow diffusion of Et_2O into CH_3CN solution.

Preparation of [(ImH)Dipp(C_3OMe)]$_2$[$NiBr_4$] (17).

To a solution of the imidazolium salt [(ImH)Dipp(C_3OMe)]Br (1.000 g, 2.62 mmol) in THF was added [$NiBr_2$(dme)] (0.405 g, 1.31 mmol). The reaction mixture was stirred overnight. The solvent was evaporated under reduced pressure. The blue slurry was then triturated with Et_2O until a purple

powder was obtained (1.073 g, 83%). X-ray quality crystals were obtained by slow diffusion of Et_2O into CH_3CN solution.

Preparation of [(ImH)Dipp(C_3OMe)][$NiBr_3${ImDipp(C_3OMe)}] (18).

To a solution of the [(ImH)Dipp(C_3OMe)]$_2$[$NiBr_4$] (0.200 g, 0.20 mmol) in THF (8 mL) was added a solution of NaO^{t}Bu (0.020 g, 0.21 mmol) in THF (5 mL). The reaction mixture was stirred for 3 h. The dark blue solution was then filtered through a Celite pad and the filtrate was evaporated under reduced pressure. The complex was precipitated from THF/Et_2O and washed with Et_2O to afford a blue powder (0.101 g, 55%). X-ray quality crystals were obtained by slow diffusion of a mixture of Et_2O and pentane into THF solution. Anal. calcd. for $C_{38}H_{57}Br_3N_4NiO_2$: C, 50.70; H, 6.38; N, 6.22%; found: C, 50.61; H, 6.44; N, 6.20%.

Preparation of [(ImH){C(Me)=NDipp}(C_3OMe)]Cl (19)

To a solution of 1-(3-methoxypropyl)-1*H*-imidazole (1.410 g, 10.1 mmol) in toluene (10 mL) was added dropwise (*E*)-*N*-(2,6-diisopropylphenyl)acetimidoyl chloride (2.39g, 10.1 mmol). The reaction mixture was stirred overnight at room temperature. Then the resulting precipitate was collected by filtration, and washed with Et_2O to give a white powder (3.17 g, 83%).

Preparation of [(ImH){C(Me)=NDipp}(C_3OMe)]$_2$[$NiCl_4$] (20).

A mixture of the imidazolium salt [(ImH){C(Me)=NDipp}(C_3OMe)]Cl (0.100 g, 0.27 mmol) and [$NiCl_2$(dme)] (0.029 g, 0.13 mmol) in THF was stirred overnight. The solvent was evaporated under reduced pressure. The blue slurry was then triturated with Et_2O until a blue powder was obtained (0.096 g, 83%). X-ray quality crystals were obtained by slow diffusion of Et_2O into CH_3CN solution.

Preparation of [AgCl{Im[C(Me)=NDipp](C_3OMe)}] (21).

A mixture of the imidazolium salt [(ImH){C(Me)=NDipp}(C_3OMe)]Cl (0.100 g, 0.27 mmol), Ag_2O (0.034 g, 0.15 mmol) and molecular sieves in THF (10 mL) was stirred overnight under exclusion of light. The beige reaction mixture was then filtered through Celite and the filtrate was dried under reduced pressure. The resulting solid was washed with Et_2O to give a beige powder (0.101 g, 77%). X-ray quality crystals were obtained by slow diffusion of pentane into THF solution.

Preparation of [(ImH)Dipp(C_2NHMe$_2$)]Cl$_2$ (22)

A mixture of 1-(2,6-diisopropylphenyl)-1*H*-imidazole (2.000 g, 8.8 mmol) and 2-chloro-*N*,*N*-dimethylethanamine hydrochloride (1.261 g, 8.8 mmol) in CH_3CN (30 mL) was refluxed for overnight. After filtration and washed with Et_2O, a white powder was obtained (2.064 g, 63%).

Preparation of [(ImH)Dipp(C_3NHMe_2)]Cl_2 (23)

A mixture of 1-(2,6-diisopropylphenyl)-1*H*-imidazole (2.283 g, 10.0 mmol) and 3-dimethylamino-1-propyl chloride hydrochloride (1.580 g, 10.0 mmol) in CH_3CN (30 mL) was refluxed for overnight. After filtration and washed with Et_2O, a white powder was obtained (2.202 g, 57%).

Preparation of [AgCl{ImDipp(C_2NMe_2)}] (24).

A mixture of the imidazolium salt [(ImH)Dipp(C_2NHMe_2)]Cl_2 (0.300 g, 0.81 mmol), Ag_2O (0.131 g, 0.57 mmol) and molecular sieves in THF (10 mL) was stirred overnight under exclusion of light. The beige reaction mixture was then filtered through Celite and the filtrate evaporated under reduced pressure. The resulting solid was washed with Et_2O to give as a beige powder (0.226 g, 63%). X-ray quality crystals were obtained by slow diffusion of pentane into THF solution.

Preparation of [AgCl{ImDipp(C_3NMe_2)}] (25).

A mixture of the imidazolium salt [(ImH)Me(C_3OMe)]Cl (0.300 g, 0.78 mmol), Ag_2O (0.126 g, 0.54 mmol) and molecular sieves in THF (10 mL) was stirred overnight under exclusion of light. The beige reaction mixture was then filtered through Celite and the filtrate evaporated under reduced pressure. The resulting solid was washed with Et_2O to give as a beige powder (0.242 g, 68%). X-ray quality crystals were obtained by slow diffusion of pentane into THF solution.

Preparation of [$NiBr_2${ImDipp(C_2NMe_2)}] (26).

To a solution of [AgCl{ImDipp(C_2NMe_2)}] (0.100 g, 0.226 mmol) in THF (10 mL) was added dropwise a THF solution of [$NiBr_2$(dme)] (0.070g, 0.226 mmol). The reaction mixture was stirred overnight at room temperature. A purple solution and white precipitates were obtained. Then the purple solution was collected by filtration, and concentrated to 5 mL. X-ray quality crystals were obtained by slow diffusion of pentane into THF solution (0.088 g, 75%).

Preparation of [$NiBr_2${ImDipp(C_3NMe_2)}] (27).

To a solution of [AgCl{ImDipp(C_3NMe_2)}] (0.100 g, 0.219 mmol) in THF (10 mL) was added dropwise a THF solution of [$NiBr_2$(dme)] (0.068g, 0.219 mmol). The reaction mixture was stirred overnight at room temperature. A purple solution and white precipitates were obtained. Then the purple solution was collected by filtration, and concentrated to 5 mL. X-ray quality crystals were obtained by slow diffusion of pentane into THF solution (0.094 g, 81%).

7. Acknowledgements

We are grateful to the China Scholarship Council for a PhD grant to X.R. We thank Marc Mermillon-Fournier for technical assistance, the CNRS and the MESR (Paris) for funding and Lydia Karmazin and Corinne Bailly from the Service de Radiocristallographie (UdS) for the determination of the crystal structures.

8. References

(1) (a) H. W. Wanzlick, H. J. Schoenherr, *Angew. Chem., Int. Ed. Engl.* **1968**, *7*, 141-142. (b) K. *J.* Öfele, *Organomet. Chem.* **1968**, *12*, P42-P43.

(2) A. J. Arduengo, R. L. Harlow, M. Kline, *J. Am. Chem. Soc.* **1991**, *113*, 361-363.

(3) (a) W. A. Herrmann, C. Köcher, *Angew. Chem. Int. Ed. Engl.* **1997**, *36*, 2162-2187. (b) D. Bourissou, O. Guerret, F. P. Gabbaï, G. Bertrand, *Chem. Rev.* **2000**, *100*, 39-92. (c) W. A. Herrmann, *Angew. Chem. Int. Ed.* **2002**, *41*, 1290-1309. (d) C. M. Crudden, D. P. Allen, *Coord. Chem. Rev.* **2004**, *248*, 2247-2273. (e) F. E. Hahn, *Angew. Chem. Int. Ed.* **2006**, *45*, 1348-1352. (f) D. Pugh, A. A. Danopoulos, *Coord. Chem. Rev.* **2007**, *251*, 610-641. (g) F. E. Hahn, M. C. Jahnke, *Angew. Chem. Int. Ed.* **2008**, *47*, 3122-3172. (h) P. de Frémont, N. Marion, S. P. Nolan, *Coord. Chem. Rev.* **2009**, *253*, 862-892. (i) S. Díez-González, N. Marion, S. P. Nolan, *Chem. Rev.* **2009**, *109*, 3612-3676. (j) D. G. Gusev, *Organometallics* **2009**, *28*, 763-770. (k) H. Jacobsen, A. Correa, A. Poater, C. Costabile, L. Cavallo, *Coord. Chem. Rev.* **2009**, *253*, 687-703. (l) C. S. Cazin, J., *N-Heterocyclic Carbenes in Transition Metal Catalysis and Organocatalysis*, Springer Netherlands, **2010**. (m) M. N. Hopkinson, C. Richter, M. Schedler, F. Glorius, *Nature* **2014**, *510*, 485-496. (n) D. M. Flanigan, F. Romanov-Michailidis, N. A. White, T. Rovis, *Chem. Rev.* **2015**, *115*, 9307-9387.

(4) (a) P. Braunstein, F. Naud, *Angew. Chem. Int. Ed.* **2001**, *40*, 680-699. (b) W. H. Zhang, S. W. Chien, T. S. A. Hor, *Coord. Chem. Rev.* **2011**, *255*, 1991-2024.

(5) S. Hameury, P. de Fremont, P. Braunstein, *Chem. Soc. Rev.* **2017**, *46*, 632-733.

(6) (a) S. Hameury, P. de Fremont, P.-A. R. Breuil, H. Olivier-Bourbigou, P. Braunstein, *Dalton Trans.* **2014**, *43*, 4700-4710. (b) S. Hameury, P. de Frémont, P.-A. R. Breuil, H. Olivier-Bourbigou, P. Braunstein, *Organometallics* **2015**, *34*, 2183-2201.

(7) S. Hameury, P. de Fremont, P.-A. R. Breuil, H. Olivier-Bourbigou, P. Braunstein, *Inorg. Chem.* **2014**, *53*, 5189-5200.

(8) (a) G. van Koten, R. A. Gossage, *The Privileged Pincer-Metal Platform: Coordination Chemistry & Applications*, Springer International Publishing, **2015**. (b) G. van Koten, D. Milstein, *Organometallic Pincer Chemistry*, Springer Berlin Heidelberg, **2013**. (c) M. Asay, D. Morales-Morales, in *The Privileged Pincer-Metal Platform: Coordination Chemistry & Applications* (Eds.: van Koten, G.Gossage, R. A.), Springer International Publishing, Cham, **2016**, pp. 239-268.

(9) (a) P. Liu, M. Wesolek, A. A. Danopoulos, P. Braunstein, *Organometallics* **2013**, *32*, 6286-6297. (b) X. Ren, C. Gourlaouen, M. Wesolek, P. Braunstein, *Angew. Chem. Int. Ed.*,

12557 –12560.

(10) D. Yang, Y. Tang, H. Song, B. Wang, *Organometallics* **2016**, *35*, 1392-1398.

(11) (a) P.-A. R. Breuil, L. Magna, H. Olivier-Bourbigou, *Catal. Lett.* **2015**, *145*, 173-192. (b) Skupinska, J. *Chem. Rev.* **1991**, *91*, 613-648.

(12) (a) C. T. O'Connor, M. Kojima, *Catal. Today* **1990**, *6*, 329-349. (b) S. Z. Tasker, E. A. Standley, T. F. Jamison, *Nature* **2014**, *509*, 299-309.

(13) C. P. Newman, G. J. Clarkson, J. P. Rourke, *J. Organomet. Chem.* **2007**, *692*, 4962-4968.

(14) R. C. Poulten, I. López, A. Llobet, M. F. Mahon, M. K. Whittlesey, *Inorg. Chem.* **2014**, *53*, 7160-7169.

(15) J. W. Nugent, G. Espinosa Martinez, D. L. Gray, A. R. Fout, *Organometallics* **2017**, *36*, 2987-2995.

9. Supporting Information

Synthesis and Characterization of Nickel(II) Complexes with Oxygen- or Nitrogen-Functionalized NHC Hybrid Ligands and Catalytic Ethylene Oligomerization

Xiaoyu Ren,[a] Marcel Wesolek,[a] and Pierre Braunstein*[a]*

[a] *Laboratoire de Chimie de Coordination, Institut de Chimie (UMR 7177 CNRS), Université de Strasbourg, 4 rue Blaise Pascal, 67081 Strasbourg Cedex (France)*

E-mail: braunstein@unistra.fr

X-ray crystallography

Summary of the crystal data, data collection and refinement for structures of **4**, **5**, **7**, **8**, **11**, **13, 15, 17, 18, 20, 21, 26** and **27** are given in Table S1. The crystals were mounted on a glass fiber with grease, from Fomblin vacuum oil. Data sets were collected on a Bruker APEX II DUO diffractometer equipped with an Oxford Cryosystem liquid N_2 device, using Mo-Kα radiation (λ = 0.71073 Å). The crystal-detector distance was 38 mm. The cell parameters were determined (APEX2 software)[1] from reflections taken from three sets of 12 frames, each at 10 s exposure. The structures were solved by direct methods using the program SHELXS-97.[2] The refinement and all further calculations were carried out using SHELXL- 97.[3] The H-atoms were included in calculated positions and treated as riding atoms using SHELXL default parameters. The non-H atoms were refined anisotropically, using weighted full-matrix least-squares on F^2.

Summary of crystal data

Table S1. Crystal data for compounds.

	4	**5**	**7**
Chemical formula	$C_{19}H_{28}N_2O$	$C_{38}H_{56}Cl_2N_4NiO_2$	$C_{16}H_{28}Cl_2N_4NiO_2$
CCDC Number			
Formula Mass	300.43	730.47	438.03
Crystal system	monoclinic	monoclinic	monoclinic
a/Å	5.8130(3)	8.2693(3)	7.8997(2)
b/Å	15.5342(8)	15.2011(6)	12.6272(5)
c/Å	20.5647(10)	16.5342(6)	10.3467(4)
α/°	90	90	90
β/°	95.2330(10)	116.007(2)	99.579(2)
γ/°	90	90	90
Unit cell volume/Å^3	849.26(16)	1867.93(12)	1017.70(6)
Temperature/K	173(2)	173(2)	173(2)
Space group	*P 21/c*	*P 21/c*	*P 21/c*
Formula units / cell, *Z*	4	2	2
Absorption coefficient, μ/mm^{-1}	0.067	0.700	1.232
No. of reflections measured	19406	17165	7404
No. of independent reflections	4888	4507	2330
R_{int}	0.0384	0.0291	0.0365
Final R_1 values ($I > 2\sigma(I)$)	0.0697	0.0589	0.0275
Final $wR(F^2)$ values ($I > 2\sigma(I)$)	0.0983	0.0713	0.0366
Final R_1 values (all data)	0.1759	0.1171	0.0688
Final $wR(F^2)$ values (all data)	0.1905	0.1229	0.0807
Goodness of fit on F^2	1.040	1.074	1.191

	8	**11**	**13**
Chemical formula	$C_{38}H_{56}AgClN_4O_2$	$C_{38}H_{58}Cl_4N_4NiO_2$	$C_{16}H_{30}Cl_4N_4NiO$
CCDC Number			
Formula Mass	744.18	803.39	510.95
Crystal system	monoclinic	orthorhombic	monoclinic
a/Å	19.5274(8)	14.8204(3)	14.2659(8)
b/Å	16.9268(7)	16.7422(4)	10.6150(6)
c/Å	13.4692(6)	17.0557(4)	15.9193(8)
α/°	90	90	90
β/°	90.3800(10)	90	100.247(3)
γ/°	90	90	90
Unit cell volume/Å^3	4452.0(3)	4231.96(17)	2372.2(2)
Temperature/K	173(2)	173(2)	173(2)
Space group	*C 2/c*	*P 21 21 21*	*C 2/c*
Formula units / cell, *Z*	4	4	4
Absorption coefficient, μ/mm^{-1}	0.544	0.747	1.286
No. of reflections measured	28706	36383	9910
No. of independent reflections	7101	12330	2722
R_{int}	0.0259	0.0223	0.0772
Final R_1 values ($I > 2\sigma(I)$)	0.0293	0.0415	0.0511
Final $wR(F^2)$ values ($I > 2\sigma(I)$)	0.0365	0.0544	0.1019
Final R_1 values (all data)	0.0729	0.1016	0.1178
Final $wR(F^2)$ values (all data)	0.0755	0.1129	0.1603
Goodness of fit on F^2	1.053	1.037	1.096

For references, see p. 47

	15	**17**	**18**
Chemical formula	$C_{38}H_{53}F_{12}N_7NiO_2P_2$	$C_{38}H_{58}N_4O_2Br_4Ni$	$C_{38}H_{57}Br_3N_4NiO_2$
CCDC Number			
Formula Mass	988.52	981.23	900.31
Crystal system	triclinic	monoclinic	monoclinic
a/Å	11.8880(4)	17.8720(8)	14.2049(7)
b/Å	12.3384(4)	15.6603(8)	14.0845(7)
c/Å	17.2335(6)	17.6741(8)	24.0675(13)
α/°	80.6100(10)	90	90
β/°	78.0740(10)	115.5830(10)	107.1640(10)
γ/°	70.1870(10)	90	90
Unit cell volume/Å^3	2314.89(14)	4461.7(4)	4600.7(4)
Temperature/K	173(2)	173(2)	173(2)
Space group	*P -1*	*C c*	*P 21/c*
Formula units / cell, *Z*	2	4	4
Absorption coefficient, μ/mm^{-1}	0.577	4.051	3.059
No. of reflections measured	41786	24370	34268
No. of independent reflections	15926	11683	12061
R_{int}	0.0391	0.0293	0.0318
Final R_1 values ($I > 2\sigma(I)$)	0.0587	0.0372	0.0437
Final $wR(F^2)$ values ($I > 2\sigma(I)$)	0.1045	0.0663	0.0766
Final R_1 values (all data)	0.1427	0.0640	0.1036
Final $wR(F^2)$ values (all data)	0.1616	0.0724	0.1112
Goodness of fit on F^2	1.032	1.009	1.063

For references, see p. 47

	20	**21**	**26**
Chemical formula	$C_{42}H_{64}Cl_4N_6NiO_2$	$C_{21}H3_1AgClN_3O$	$C_{19}H_{29}Br_2N_3Ni$
CCDC Number			
Formula Mass	885.50	484.81	517.98
Crystal system	monoclinic	monoclinic	monoclinic
a/Å	34.0479(15)	8.6120(4)	29.1917(10)
b/Å	9.1932(4)	19.5331(10)	7.5175(2)
c/Å	15.3762(7)	15.3345(6)	21.4490(9)
α/°	90	90	90
β/°	101.9780(10)	117.272(2)	111.4300(10)
γ/°	90	90	90
Unit cell volume/Å^3	4708.1(4)	2292.81(19)	4381.5(3)
Temperature/K	173(2)	173(2)	173(2)
Space group	*C 2/c*	*P 21/c*	*P 21/c*
Formula units / cell, *Z*	4	4	8
Absorption coefficient, μ/mm^{-1}	0.679	1.010	4.540
No. of reflections measured	43227	34045	27093
No. of independent reflections	8905	6687	9832
R_{int}	0.0576	0.0315	0.1085
Final R_1 values ($I > 2\sigma(I)$)	0.0411	0.0246	0.0649
Final $wR(F^2)$ values ($I > 2\sigma(I)$)	0.0880	0.0338	0.1561
Final R_1 values (all data)	0.0897	0.0536	0.1394
Final $wR(F^2)$ values (all data)	0.1069	0.0565	0.1850
Goodness of fit on F^2	1.010	1.038	0.987

For references, see p. 47

	27
Chemical formula	$C_{20}H_{31}Br2N_3Ni$
CCDC Number	
Formula Mass	532.01
Crystal system	monoclinic
a/Å	9.6499(6)
b/Å	10.8404(7)
c/Å	21.4437(15)
α/°	90
β/°	92.515(5)
γ/°	90
Unit cell volume/Å^3	2241.0(3)
Temperature/K	173(2)
Space group	*P 21/c*
Formula units / cell, *Z*	4
Absorption coefficient, μ/mm^{-1}	5.479
No. of reflections measured	20686
No. of independent reflections	3935
R_{int}	0.0827
Final R_1 values ($I > 2\sigma(I)$)	0.0840
Final $wR(F^2)$ values ($I > 2\sigma(I)$)	0.1146
Final R_1 values (all data)	0.2449
Final $wR(F^2)$ values (all data)	0.2735
Goodness of fit on F^2	1.051

For references, see p. 47

REFERENCES

(1) Bruker AXS Inc Madison USA, **2006**.

(2) G. M. Sheldrick, *Acta Crystallogr. Sect. A: Found. Crystallogr.*, **1990**, *A46*, 467.

(3) G. M. Sheldrick, Universität Göttingen: Göttingen Germany, **1999**.

For references, see p. 47

CHAPITRE 2

Synthesis and Structural Characterization of Nickel(II) Complexes with Tritopic $N^{imine}C^{NHC}N^{amine}$ pincer Ligands

For references, see p. 47

This chapter is written in the form of a publication draft, the work being currently in progress. Some characterization data are still missing at this stage of the work.

My contribution to this work consisted of the bibliographic search, the experimental work and the preparation of the draft of the publication.

Synthesis and Structural Characterization of Nickel(II) Complexes with Tritopic $N^{imine}C^{NHC}N^{amine}$ pincer Ligands

Xiaoyu Ren,[a] Marcel Wesolek*[a] and Pierre Braunstein*[a]

[a] Laboratoire de Chimie de Coordination, Institut de Chimie (UMR 7177 CNRS), Université de Strasbourg, 4 rue Blaise Pascal, 67081 Strasbourg Cedex (France)

E-mail: braunstein@unistra.fr

Synopsis

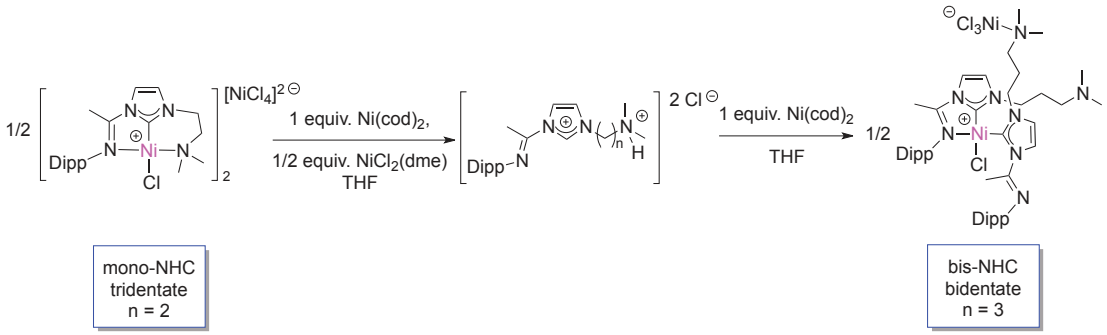

For references, see p. 47

1. Résumé en français

Des ligands tritopiques NCN de type pinceur contenant un carbène N-hétérocyclique (NHC) central flanqué de deux donneurs azotés différents (N^{imine} et N^{amine}) ont été synthétisés pour étudier leur potential de coordination dans des complexes du Ni(II). Le sel d'imidazolium [(ImH){C(Me)=NDipp}(C_2NMe_2)]Cl (**1**) et les sels d'imidazolium dans lesquels la fonction amine est protonée, [(ImH){C(Me)=NDipp}(C_2NHMe_2)]Cl_2 (**4**) et [(ImH){C(Me)=NDipp}(C_3NHMe_2)]Cl_2 (**5**), ont été synthétisés et l'influence de la longueur et de la nature (libre ou protonée) de la chaine alkyle du bras N^{amine} a été examinée. Un complexe du Ni(II) dinucléaire [Ni_2Cl_2{Im[C(Me)=NDipp](C_2NMe_2)}$_2$] **(2)** a été obtenu avec un réarrangement partiel de ligand par addition oxydante de **1** avec [Ni(1,5-cod)$_2$]. De plus, un produit secondaire [Ni_2Cl_3{Im[C(Me)=NDipp](C_2NMe_2)}{ImH[C(Me)=NDipp](C_2NMe_2)}] (**3**) a été isolé au cours du processus de cristallisation. Le sel [NiCl{Im[C(Me)=NDipp](C_2NMe_2)}]$_2$[$NiCl_4$] (**6**) possédant deux complexes de Ni(II) cationiques identiques contenant un pinceur tridenté, et un dianion $[NiCl_4]^{2-}$ a été obtenu par addition oxydante de **4** avec [Ni(1,5-cod)$_2$] suivi de l'addition de [$NiCl_2$(dme)]. La réaction de **5** avec [Ni(1,5-cod)$_2$] a donné un complexe dinucléaire du nickel(II), [Ni_2Cl_4{Im[C(Me)=NDipp](C_3NMe_2)}$_2$] (**7a**). La réaction d'abstraction de l'halogènure de **7a** à l'aide de $AgPF_6$ a conduit à un complexe mononucléaire de nickel(II), [NiCl{Im[C(Me)=NDipp](C_3NHMe_2)}$_2$][PF_6]$_2$Cl (**8**) sous forme de cristaux oranges stables à l'air. Dans les complexes d'Ag(I) avec ces ligands potentiellement tridentes, [AgCl{C(Me)=NDipp}(C_2NMe_2)] (**9**) et [AgCl{C(Me)=NDipp}(C_3NMe_2)] (**10**), obtenus avec de bons rendements, seule la fonction NHC est coordinée au métal. Un complexe dinucléaire du Ni(II) inattendu, [NiCl{Im[C(Me)=NDipp](C_2NMe_2)}]$_2$[Ag_2Br_4] (**11**), bis-NHC ponté par une entité $[Ag_2Br_4]^{2-}$ a été formé par réaction de transmétallation de [$NiBr_2$(dme)] avec **9**. Par ailleurs, des complexes mononucléaires du Ni(II), NiCl(NCMe){Im[C(Me)=NDipp](C_2NMe_2)}][BF_4]$_2$ (**12**) et [NiCl(NCMe){Im[C(Me)=NDipp](C_3NMe_2)}][BF_4]$_2$ (**13**), ont été obtenus lorsque [Ni(NCMe)$_6$](BF_4)$_2$ est utilisé comme précurseur dans les réactions de transmétallation avec **9** et **10**, respectivement.

Synthesis and Structural Characterization of Nickel(II) Complexes with Tritopic $N^{imine}C^{NHC}N^{amine}$ Pincer Ligands

*Xiaoyu Ren,[a] Marcel Wesolek[*a] and Pierre Braunstein[*a]*

For references, see p. 47

[a] *Laboratoire de Chimie de Coordination, Institut de Chimie (UMR 7177 CNRS), Université de Strasbourg, 4 rue Blaise Pascal, 67081 Strasbourg Cedex (France)*

E-mail: braunstein@unistra.fr

2. Abstract

Tritopic NCN pincer-type ligands containing a central N-heterocyclic carbene (NHC) donor flancked by two chemically-different nitrogen donors (N^{imine} and N^{amine}), have been prepared to investigate their potential in tridentate pincer Ni(II) complexes. The imidazolium salt [(ImH){C(Me)=NDipp}(C_2NMe_2)]Cl (**1**) and the N^{amine}-protonated imidazolium salts [(ImH){C(Me)=NDipp}(C_2NHMe_2)]Cl_2 (**4**) and [(ImH){C(Me)=NDipp}(C_3NHMe_2)]Cl_2 (**5**) were synthesized and the influence of the length and nature of the alkyl chain connecting the heterocyclic N atom to the N^{amine} donor was examined. The oxidative-addition reaction of **1** and [Ni(1,5-cod)$_2$] afforded a dinuclear bis-NHC Ni(II) complex [Ni_2Cl_2{Im[C(Me)=NDipp](C_2NMe_2)}$_2$] (**2**) in which partial ligand rearrangement has occurred. In addition, a byproduct, [Ni_2Cl_3{Im[C(Me)=NDipp](C_2NMe_2)}{ImH[C(Me)=NDipp](C_2NMe_2)}] (**3**)**,** was isolated during the crystallization procedure. A complex [NiCl{Im[C(Me)=NDipp](C_2NMe_2)}]$_2$[$NiCl_4$] (**6**) consisting of two tridentate $N^{imine}C^{NHC}N^{amine}$ pincer Ni(II) complex cations and one $[NiCl_4]^{2-}$ dianion was obtained by oxidative-addition of **4** to [Ni(1,5-cod)$_2$], followed by addition of [$NiCl_2$(dme)]. The reaction of **5** with [Ni(1,5-cod)$_2$] gave the dinickel(II) complex [Ni_2Cl_4{Im[C(Me)=NDipp](C_3NMe_2)}$_2$] (**7a**). Halide abstraction from **7a** with $AgPF_6$ afforded the mononuclear nickel(II) complex [NiCl{Im[C(Me)=NDipp](C_3NHMe_2)}$_2$][PF_6]$_2$Cl (**8**) as orange crystals. In the Ag(I) complexes prepared in good yields with the tritopic NCN ligands, [AgCl{C(Me)=NDipp}(C_2NMe_2)] (**9**) and [AgCl{C(Me)=NDipp}(C_3NMe_2)] (**10**), only monodentate behavior of the ligand was observed through the C^{NHC} donor. An unexpected Ni(II) complex [NiCl{Im[C(Me)=NDipp](C_2NMe_2)}]$_2$[Ag_2Br_4] (**11**) with a bis-NHC dinuclear unit bridged by a $[Ag_2Br_4]^{2-}$ core formed by transmetallation reaction of [$NiBr_2$(dme)] with **9**. In addition, mononuclear tritopic pincer Ni(II) complexes, Ni(NCMe){Im[C(Me)=NDipp](C_2NMe_2)}][BF_4]$_2$ (**12**) and [Ni(NCMe){Im[C(Me)=NDipp](C_3NMe_2)}][BF_4]$_2$ (**13**), were obtained when [Ni(NCMe)$_6$](BF_4)$_2$ was used as Ni(II) precursor in transmetallation with **9** and **10**, respectively.

3. Introduction

Since Shaw and Moulton[1] reported on the stabilization of transition metal complexes by tridentate

For references, see p. 47

chelates (**PCP**-type systems, Scheme 1), pincer platforms[2] in which the central σ-bound donor **E** is flanked by two side arm functionalities **E** (typical **ECE** architectures, Scheme 1), have been intensively developed because of the major contributions of the latter to the stability and electronic properties of their metal complexes. Neutral donors are often employed for **E**, with oxygen-, sulfur-, phosphorus- or nitrogen-donor atoms.[3] Owing to the diverse possibilities to fine-tune their electronic and steric properties, N-heterocyclic carbenes (NHCs) have been increasingly incorporated in pincer-type systems and this endeavor has generated new insights into the scope of hybrid ligands combining C^{NHC} and side arms donor groups in organometallic chemistry and catalysis.[4] Such functional NHC ligands are being increasingly used in molecular chemistry. In the late 1970s, van Koten *et al*.[5] developed the first examples of NCN pincer structures using a transmetallation protocol from the corresponding organolithium compounds. In the recent years, NCN pincer complexes have been much studied in organic and inorganic synthesis and have found numerous applications in catalysis, medicinal chemistry, photophysics and materials science.[6]

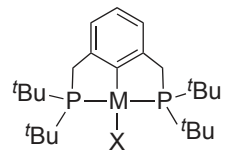

M = Ni, Pd, Pt, Rh, Ir
X = H, Cl, Br, CN, CO, etc

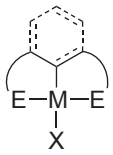

E = OR, SR, PR_2, NR_2, C^{NHC}, etc
M = transition metals
X = H, Cl, Br, CN, CO, etc

Scheme 1. PCP pincer-type complexes[1] (left) and general architecture of **ECE** pincer-type complexes (right).

In particular, nickel complexes with functional NHC ligands have been widely used as pre-catalysts in C−C coupling reactions, C−H bond activation and functionalization, oxidation of secondary alcohols, hydrosilylation, [2+2+2] cycloadditions, etc.[7] Although the donor groups in the side-arms of the pincer architecture may not always bind the metal centre in the final product, they can still play a major role in the course of reactions. The structural diversity that can be encountered, even when one **E** function remains constant, was recently illustrated with tritopic $N^{imine}C^{NHC}N$' ligand where the presence of different N' donor groups led to very different results.[8] Thus, when N = N^{imine} and N' = N^{amine} with a C3 spacer (eq. 1), a rare example of dinickel(I) complex containig a COD-derived bridging η^3-allyl-type complex was isolated and structurally characterized from the oxidative addition reaction of the corresponding imidazolium salts with $[Ni(1,5\text{-cod})_2]$ (cod = cycloocta-1,5-diene). It displays a monodentate C^{NHC} ligand with two dangling arms. Using a potentially bidentate $N^{imine}C^{NHC}$ ligand, Lavoie's group also observed monodentate C^{NHC} behaviour

For references, see p. 47

(eq. 2). When both donor groups **E** were imines, a similar reaction led to an unusual mononuclear imidazolyl nickel(II) pincer complex with a Ni-C_{sp3} bond (N' = N^{imine}, eq. 3).[9] Clearly, introduction of potential N' donor groups into a multidentate ligand will increase the structural diversity of the resulting coordination complexes. Inspired by these unexpected results, we decided to examine the influence (i) of different spacer lengths between the imidazole and N', and (ii) of the nature of the N' donor in potential $N^{imine}C^{NHC}N$' pincers on the structure and reactivity of nickel complexes.

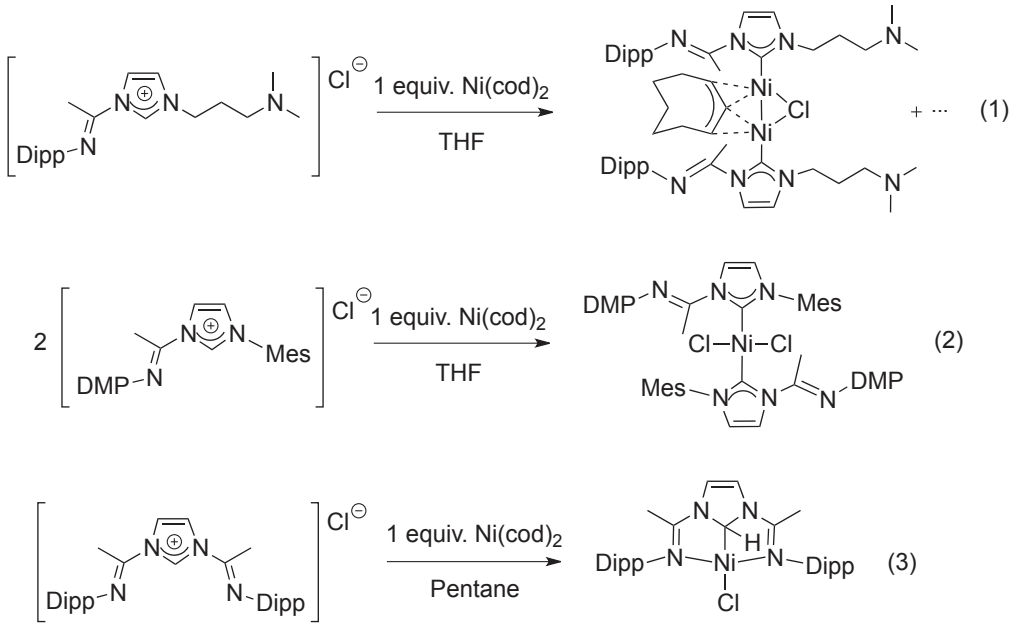

4. Results and discussion

Whereas the imidazolium salt [(ImH){C(Me)=NDipp}(C_2NMe_2)]Cl (**1**),[9] which contains a C2 spacer between the heterocycle and the amine group, was isolated as a white powder, the synthesis of the analogous salt with a single CH_2 spacer failed. Using the same synthetic procedure, a white precipitate was obtained but after it was dissolved for purification, an intractable yellow compound formed, possibly resulting from fragmentation of the imidazolium salt.[9c] The ^{1}H NMR spectrum (see SI) of the white powder showed the presence of the $C^{NHC}N^{imine}$ moiety, while the $ClCH_2NMe_2$ fragment undergoes a decomposition reaction. When salt **1** was reacted with [Ni(1,5-cod)$_2$] in THF at room temp. (eq. 4), we unexpectedly isolated a dinuclear nickel complex [Ni_2Cl_2{Im[C(Me)=NDipp](C_2NMe_2)}$_2$] (**2**) with an overall ligand to nickel ratio of 1:1, as established by X-ray diffraction (Figure 1). One functional NHC ligand is intact and C^{NHC}-bound to Ni in a monodentate fashion but the other underwent fragmentation of the N^{imid}–C^{imine} bond, leaving a C^{NHC},N^{amine}-chelate, while the liberated C(Me)=NDipp moiety acts as a bridge between the metals. A chlorido ligand is terminally bound to each Ni(II) center. This complex could possibly

For references, see p. 47

result from intermolecular hydrogen elimination between Ni(II) hydride intermediates formed by oxidative-addition of the N_2C-*H* bond to Ni(0). The breaking of the N^{imid}–C^{imine} bond that liberates the imine moiety could be triggered by the nucleophilic chloride ligand present in **2**.[11b] The shorter C2 spacer favors amine chelation over the C3 spacer (see eq. 1) since at least one amine group is chelating in **2**, which contributes to the driving force of the reaction. Interestingly, all the atoms from the ligands, except the imidazolium proton, are retained in the final product (synthesis with atom-economy).

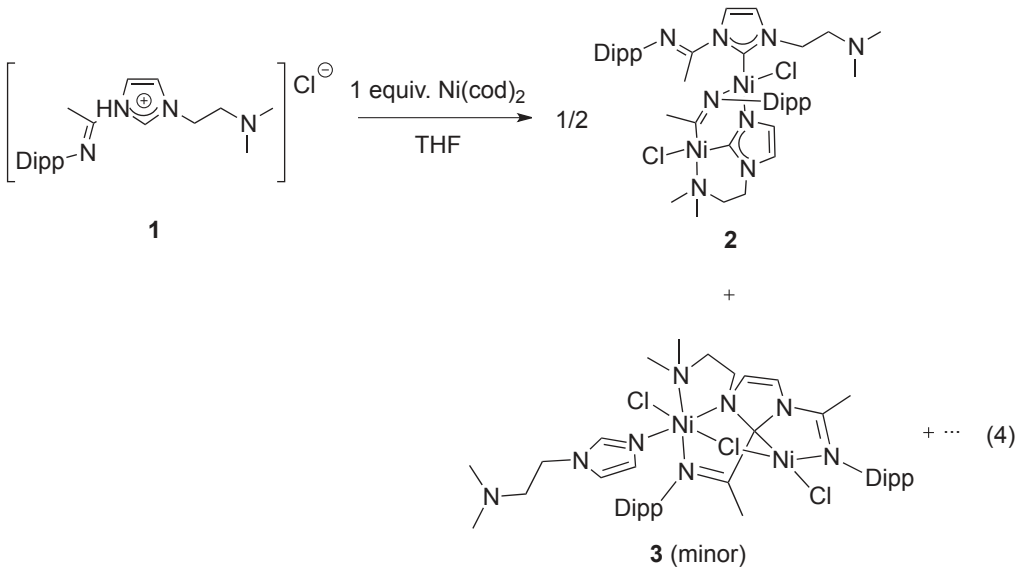

Both nickel centers in **2** have slightly distorted square planar coordination geometries. The nickel atoms, the bridging imine moiety and the C^{NHC},N^{amine} chelate form a six-membered ring in a boat conformation: atoms C22 and C29 and N5 and N8 are coplanar, while Ni1 and Ni2 are displaced away from that plane in the same direction. In the six-membered ring with boat conformation (Figure 1), the carbon atoms C22 and C29 and the nitrogen atoms N5 and N8, respectively, are almost symmetrically placed with respect to the Ni1···Ni2 axis, with nearly the same Ni−C (Ni2−C22 1.850(3) Å, Ni2−C29 1.849(3) Å) and Ni−N bond distances (Ni1−N5 1.911(2) Å, Ni1−N8 1.914(2) Å). The C−N bond distances C22−N5 1.341(3) Å and C29−N8 1.290(3) Å, are very different, the latter has some double bond character. A comparison of the C−N bond distances of the C(Me)=NDipp moieties between the one connecting the two nickel centres and the dangling imine in the intact ligand, shows that the former (C29−N8) is slightly longer than in the latter (C4−N3 1.265(3) Å). In contrast, the Ni−C^{NHC} bond distance in the intact ligand (Ni1−C1 1.912(3) Å) is slightly longer than in the fragmented ligand (Ni2−C22). A boat/chair conformation exchange may account for the complex ^{1}H NMR spectrum observed in solution (see

For references, see p. 47

SI) and is sufficiently slow on the NMR time scale to allow the observation of two conformers. Thus, in the ^{1}H NMR spectrum, four sets of backbone signals with two different intensities account for their presence. It is noteworthy that both amine spacers $CH_2CH_2NMe_2$ in compound **2** contain diastereotopic protons. For the dangling amine arm, this is due to its orientation with respect to the aryl group of the proximate Dipp. In the ^{13}C NMR spectrum, the carbon signals at δ 231.8 and δ 234.0 ppm belong to two conformers of complex **2** and are assigned to the quaternary carbon atoms of the bridging imine group (from the HMBC spectra). Furthermore, the four sets of CH_2CH_2 signals are consistent with the presence of these two conformers.

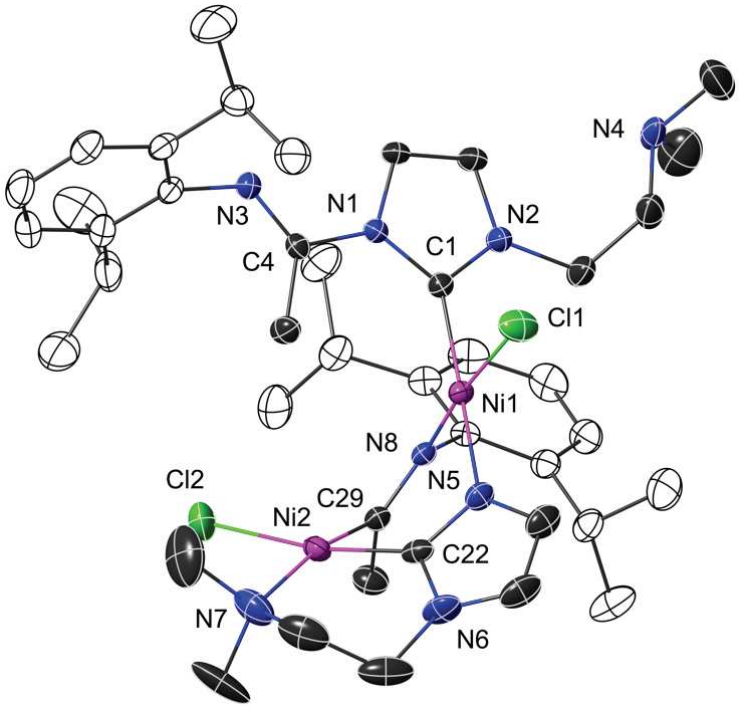

Figure 1. Structure of **2** with H atoms omitted for clarity. Thermal ellipsoids at the 30% probability level. Selected bond lengths (Å) and angles (deg): C1−N1 1.370(3), C1−N2 1.345(3), C4−N3 1.265(3), C22−N5 1.341(3), C22−N6 1.366(3), C29−N8 1.290(3), Ni1−C1 1.912(3), Ni1−N5 1.911(2), Ni1−N8 1.914(2), Ni2−C22 1.850(3), Ni2−C29 1.849(3), Ni2−N7 2.057(3), Ni1−Cl1 2.197(3), Ni2−Cl2 2.222(1), N1−C1−N2 104.1(2), N5−C22−N6 106.7(2), N5−Ni1−N8 87.7(1), C22−Ni2−C29 86.0(1).

A few dark red crystals of a byproduct, $[Ni_2Cl_3\{Im[C(Me)=NDipp](C_2NMe_2)\}\{ImH[C(Me)=NDipp](C_2NMe_2)\}]$ (**3**), were isolated once from the synthesis of **2** by slow evaporation of the toluene solution extracted from the crude reaction mixture. Its crystal structure revealed another dinuclear Ni(II) complex resulting from

For references, see p. 47

ligand transformations (Figure 2). Remarkably, one of the NHC ligands derived from **1** has coupled at its NHC carbon to the imine fragment, resulting from the splitting of the N^{imid}–C^{imine} bond of the other ligand, to give an imidazolyl sp^3 carbon. The corresponding N^{imine} N5 is bound to Ni2. The imidazole nitrogen N2 has become sp^3-hybridized and interacts directly with N2. The heterocycle that has lost its imine substituent as a result of N^{imid}–C^{imine} bond breaking is now directly bound to Ni2 via N6 while its amine group N8 is dangling. The square planar coordination sphere around the 16 electron Ni1 contains two chlorides (one of them is bridging to Ni2), and a N^{imine}–$C^{imidazolyl}$ 3 electron donor chelate. The 18 electron Ni2 center adopts an octahedral coordination geometry with two trans chlorides, a $N^{imidazolyl}$,N^{amine} 4 electron donor chelate, the N^{imid} donor N6 original and a N^{imine} donor N5 linked to the sp^3 carbon of the imidazolyl moiety. As shown in Figure 2, the C1−N1 (1.474(4) Å), C1−N2 (1.489(4) Å) distances correspond to single bonds, and are consistently longer than the C−N bonds in the delocalized imidazole ring (C36−N6 1.324(4) Å, C36−N7 1.342(5) Å). The C−N bond distances in the C(Me)=NDipp moieties (C4−N3 1.307(4) Å, C22−N5 1.284(4) Å) correspond to double bonds and are comparable to the C−N bond distance in the chelated C(Me)=NDipp (1.290(3) Å) group in **2**.

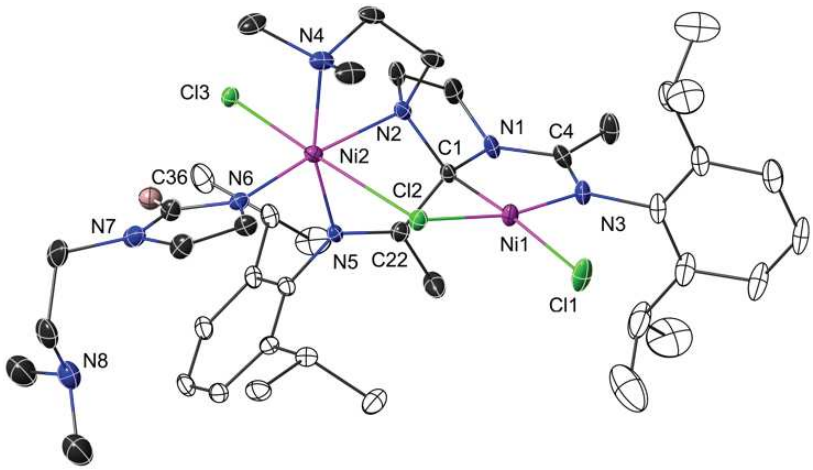

Figure 2. Structure of **3** with H atoms omitted for clarity. Thermal ellipsoids at the 30% probability level. Selected bond lengths (Å) and angles (deg): C1−N1 1.474(4), C1−N2 1.489(4), C1−C22 1.517(5), C4−N3 1.307(4), C22−N5 1.284(4), C36−N6 1.324(4), C36−N7 1.342(5), Ni1−C1 1.904(3), Ni1−N3 1.911(3), Ni2−N2 2.101(3), Ni2−N4 2.199(3), Ni2−N5 2.112(3), Ni2−N6 2.026(3), Ni1−Cl1 2.214(8), Ni1−Cl2 2.204(1), Ni2−Cl2 2.686(8), Ni2−Cl3 2.385(2); N1−C1−N2 103.0(3), N1−C1−Ni1 108.2(2), N2−C1−C22 108.1(3), C1−Ni1−Cl2 87.6(3), C1−Ni1−N3 84.3(9),

For references, see p. 47

Ni1−Cl2−Ni2 104.1(2), N2−Ni2−N4 85.1(3), N2−Ni2−N5 79.1(1), N4−Ni2−N6 92.9(8), N5−Ni2−N6 102.4(4), N6−C36−N7 111.7(3).

To our surprise, the $N^{imine}C^{NHC}N^{amine}$ potential pincer ligand with different spacer lengths (C2 and C3) of the *N*-amine-functionalized arms resulted in very different metal coordination spheres, even in different oxidation states of nickel. Thus, with the C3 spacer,[8] which was reported recently, a dinuclear Ni(I)−Ni(I) complex containing a bridging η^3-allyl-type ligand and a monodentate C^{NHC} donor formed as a result of the oxidative addition reaction of the imidazolium salt to [Ni(1,5-cod)$_2$] (eq. 1). In contrast, when the ligand with the C2 spacer was used under the same reaction conditions, a dinuclear Ni(II) complex was isolated as the major product, which contains a partially fragmented ligand. Cleavage of the $N^{imidazolyl}$–C^{amine} bond occurred in **2** and **3** and both fragments recombined with the nickel centers. The shorter arm *N*C$_2$NMe$_2$ appears more reactive and easier to be broken, while the *N*C$_3$NMe$_2$ side arm remained intact. Furthermore, 1,5-cod plays a key role in the formation of the cod-derived allyl-type ligand in the dinickel complex; it could also stabilize intermediates in the synthesis of compound **2**. Ligands differing only by the spacer lengths (C2 or C3) thus result in completely different reaction pathways and yield very different products.

We extended our investigation on the influence of the spacer length to related N' donors. The protonated imidazolium salts [(ImH){C(Me)=NDipp}(C$_2$NHMe$_2$)]Cl$_2$ (**4**) and [(ImH){C(Me)=NDipp}(C$_3$NHMe$_2$)]Cl$_2$ (**5**) (eq. 5) were synthesized in order to facilitate a one-pot access to NHC Ni(II) pincer complexes.

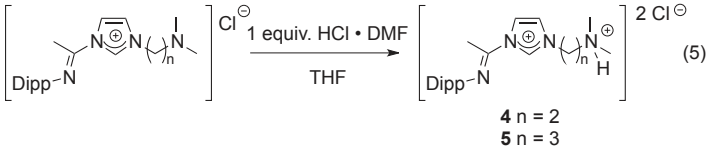

(5)

4 n = 2
5 n = 3

We used the same oxidative-addition reaction conditions as those adopted with **1** (eq. 4), but this time we have two types of protons (C*H* and N*H*) that could be potentially involved in the reaction with Ni(0) (eq. 6). A brown suspension was obtained and the ^{1}H NMR spectrum of the crude product showed broad paramagnetic signals. Crystals could not be obtained directly by a solvent/non solvent diffusion procedure but after two weeks in THF/Et$_2$O, green crystals of **6** were isolated (Figure 3). Two monocationic Ni(II) complexes are associated to a $[NiCl_4]^{2-}$ dianion. The coordination geometry around each nickel center is slightly distorted square planar and comprises

For references, see p. 47

the desired tridentate $N^{imine}C^{NHC}N^{amine}$ ligand and one chloride.

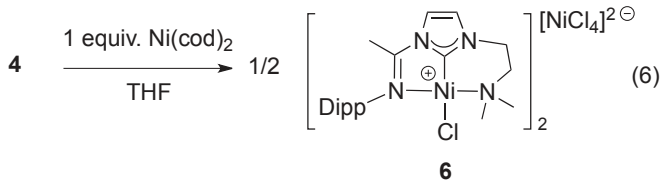

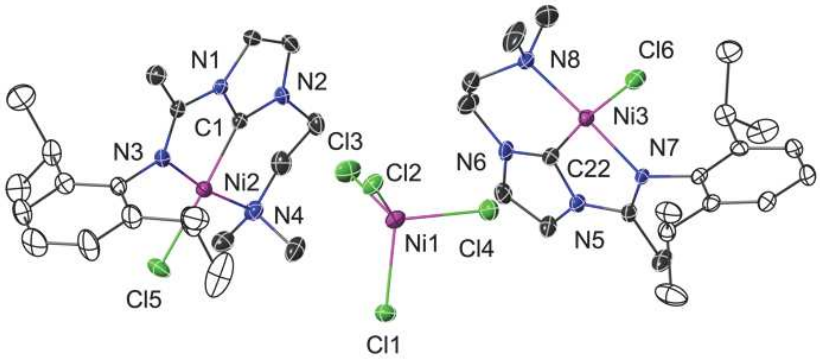

Figure 3. Structure of **6** with H atoms omitted for clarity. Thermal ellipsoids at the 30% probability level. Selected bond lengths (Å) and angles (deg): C1−N1 1.360(8), C1−N2 1.318(8), Ni2−C1 1.829(7), Ni2−N3 1.964(5), Ni2−N4 1.988(6), Ni2−Cl5 2.182(2), C22−N5 1.346(8), C22−N6 1.313(8), Ni3−C22 1.838(7), Ni3−N7 1.961(5), Ni3−N8 1.997(6), Ni3−Cl6 2.173(2), Ni1−Cl1 2.264(2), Ni1−Cl2 2.261(2), Ni1−Cl3 2.274(2), Ni1−Cl4 2.277(2); N1−C1−N2 105.9(6), C1−Ni2−N3 80.4(3), C1−Ni2−N4 89.8(3), N3−Ni2−N4 168.6(2), C1−Ni2−Cl5 173.6(2), N5−C22−N6 107.2(6), C22−Ni3−N7 80.3(3), C22−Ni3−N8 90.9(3), N7−Ni3−N8 171.2(2), C22−Ni3−Cl6 173.4(2).

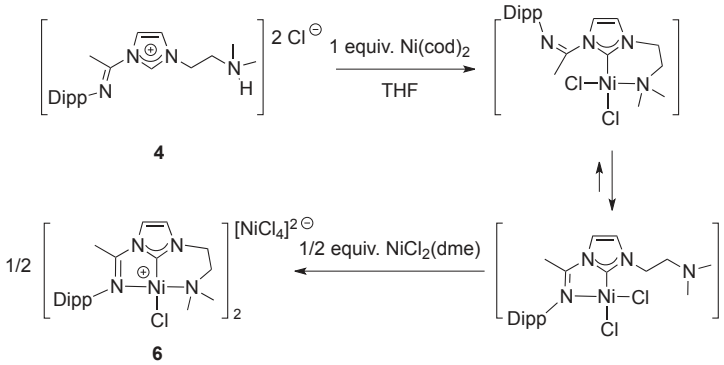

Scheme 2. Plausible pathway for the formation of **6**.

Formation of the $[NiCl_4]^{2-}$ dianion suggested that some decomposition occurred over 2 weeks to liberate enough chloride ions, and a plausible pathway is shown in Scheme 2. Reaction steps

For references, see p. 47

leading to **6** could consist of either reaction of the protonated arm $(CH_2)_2NHMe_2$ of the imidazolium salt **4** with [Ni(1,5-cod)$_2$] by proton transfer followed by oxidative-addition of the imidazolium proton N_2CH or first formation of a Ni-NHC hydride intermediate by oxidative-addition, followed by acid-base reaction between this hydride and the ammonium proton, liberating dihydrogen (not evidenced). A C^{NHC},N^{amine} bidentate mono-NHC Ni(II) complex would then readily react with [$NiCl_2$(dme)] to give **6**. We repeated the reaction and added half an equivalent of [$NiCl_2$(dme)] as a chloride abstractor and indeed, the tridentate mono-NHC Ni(II) cation was stabilized by the concomitant formation of the $[NiCl_4]^{2-}$ dianion and **6** was obtained in better yield within a few hours with rapid formation of crystals suitable for X-ray diffraction analysis.

We then extended these investigations to the precursor with a C3 spacer. The reaction of **5** with [Ni(1,5-cod)$_2$] (eq. 7) gave good yield (76-88%) of **7a** which, in the solid state, features a dinickel(II) structure with two different coordination modes (Figure 4). Ni1 displays a square planar coordination geometry involving one chloride and two C^{NHC} donors. Whereas one C^{NHC} ligand displays N^{imine}–Ni1 chelation and a dangling N^{amine} group, Ni2 has N^{amine}–Ni2 bound and a dangling N^{imine} group. Ni2 exhibits a tetrahedral coordination environment with three chlorides and the amine group. X-ray quality crystals were obtained by slow diffusion of Et_2O into a THF solution of the complex. Interestingly, a dinickel(II) isomer **7b** with the different location of the $[NiCl_3]^-$ unit was isolated from the crystallization in MeCN (Figure 4). A comparison between the reactions of equations **6** and **7** clearly demonstrates that the length of the spacer has a profound influence on the nature of the products.

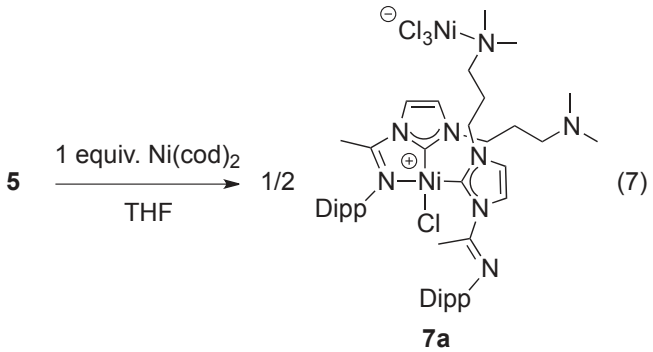

For references, see p. 47

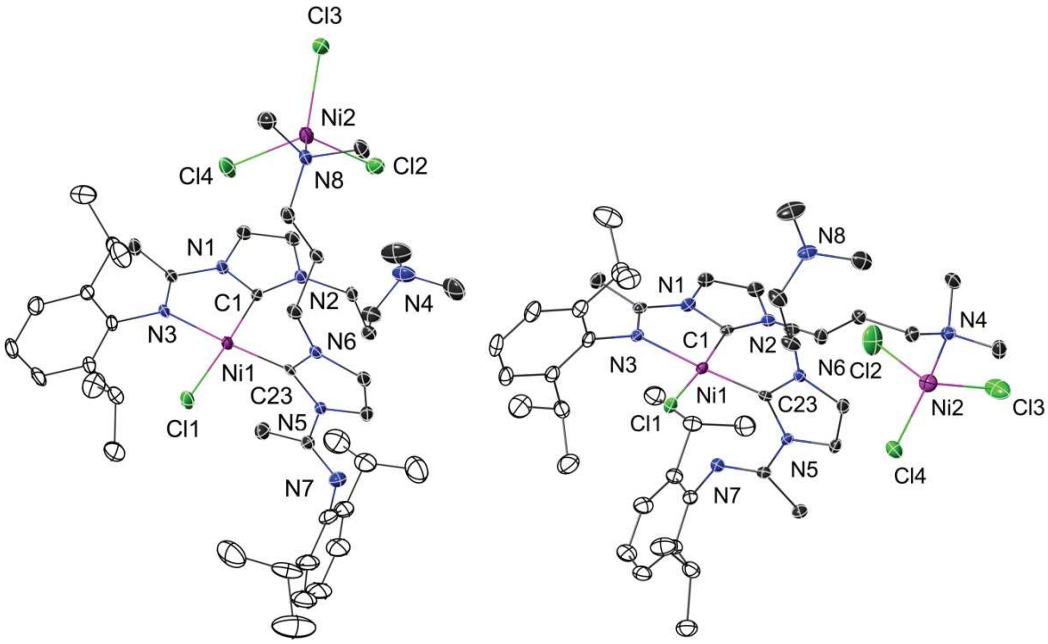

Figure 4. Structures of **7a** (left) and **7b** (right) with H atoms omitted for clarity. Thermal ellipsoids at the 30% probability level. Selected bond lengths (Å) and angles (deg): **7a**, C1−N1 1.361(4), C1−N2 1.341(4), Ni1−C1 1.880(3), C23−N5 1.370(4), C23−N6 1.343(4), Ni1−C23 1.861(3), Ni1−N3 1.960(2), Ni2−N8 2.042(3), N1−C1−N2 104.2(2), N5−C23−N6 104.9(2), C1−Ni1−C23 95.8(1), C23−Ni1−N3 176.7(4), N1−C1−Ni1 112.1(2), N2−C1−Ni1 143.7(2), N5−C23−Ni1 131.7(2), N6−C23−Ni1 123.4(2); **7b**, C1−N1 1.362(4), C1−N2 1.344(4), Ni1−C1 1.857(3), C23−N5 1.396(4), C23−N6 1.333(4), Ni1−C23 1.886(3), Ni1−N7 1.974(3), Ni2−N8 2.044(3), N1−C1−N2 105.1(3), N5−C23−N6 103.9(3), C1−Ni1−C23 94.0(4), C23−Ni1−N7 176.5(7), N1−C1−Ni1 128.5(2), N2−C1−Ni1 126.4(2), N5−C23−Ni1 111.7(2), N6−C23−Ni1 144.2(2).

A plausible pathway of the formation of **7a** is shown as Scheme 3. First, an oxidative-addition reaction would occur between $(CH_2)_3NHMe_2$ and [Ni(1,5-cod)$_2$]. An intermediate with two imidazolium cations bridged by $NiCl_2$ would form after the loss of cod and dihydrogen. Then two alternatives are conceivable: formation of a mononuclear bis-NHC Ni(II) by intramolecular oxidative addition reaction or of a bis-NHC Ni(II) polymer by intermolecular reaction. Furthermore, both Ni(II) complexes would undergo chloride redistribution and transfer to form the desired product with two NHCs in cis position.

For references, see p. 47

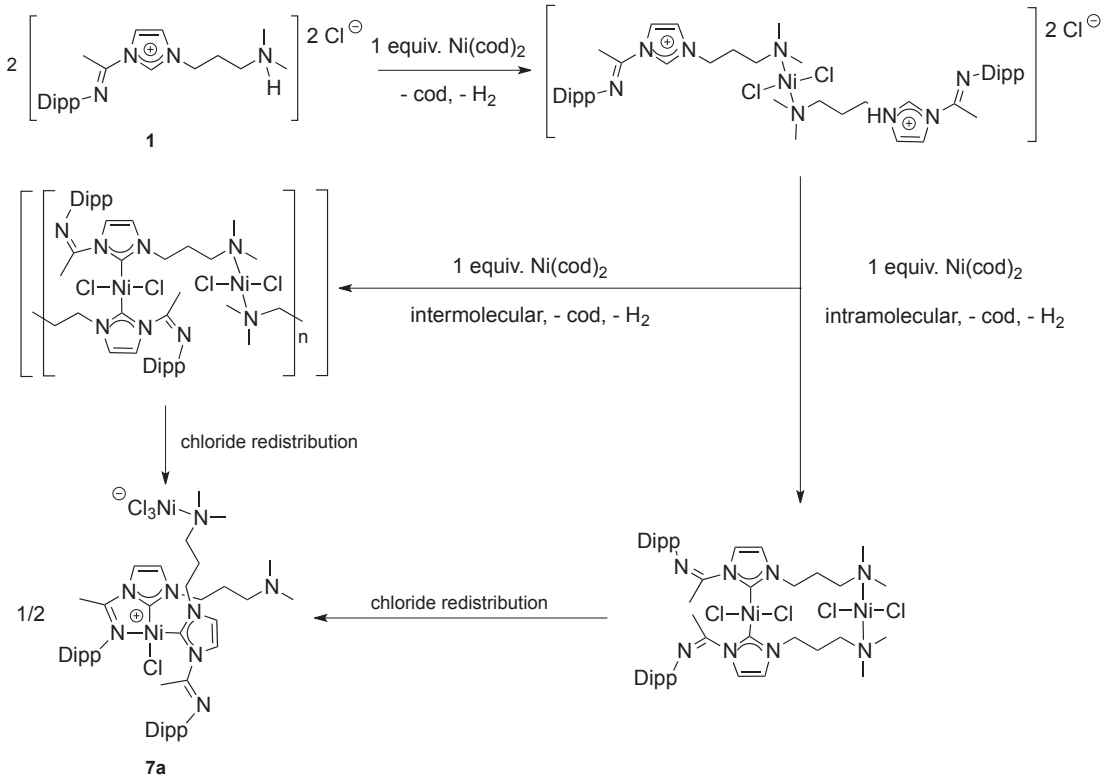

Scheme 3. Plausible mechanism of the formation of **7a**.

When we compare the formation of **6** and **7a** (**7b**), it appears that the $N^{imine}C^{NHC}N^{amine}$ ligand with NC_2NMe_2 side arm leads to a mono-NHC Ni(II) pincer complex **6**, whereas when a NC_3NMe_2 donor is used as a functional group, a bis-NHC Ni(II) complex is formed. A N^{amine} donor with shorter spacer length (C2) favors chelation compared to the C3 spacer.

To promote coordination of the dangling amine group of **7a**, halide abstraction by $AgPF_6$ was performed in THF and a yellow solution and a mixture of yellow ($NiCl_2$) and white (AgCl) precipitates were obtained. Few orange crystals formed after crystallization from THF/Et_2O and the analysis of [NiCl{Im[C(Me)=NDipp](C$_3$NHMe$_2$)}$_2$][PF6]$_2$Cl (**8**) by X-ray diffraction revealed the loss of poorly soluble $NiCl_2$ and protonation of the amine groups. Protonation may be due to the adventitious presence of traces of water. Consequently, no coordination of the dangling amine group was observed.

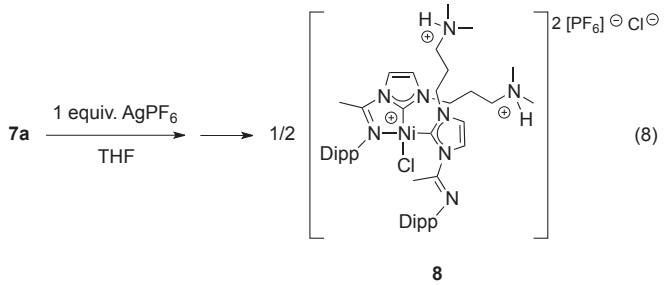

(8)

For references, see p. 47

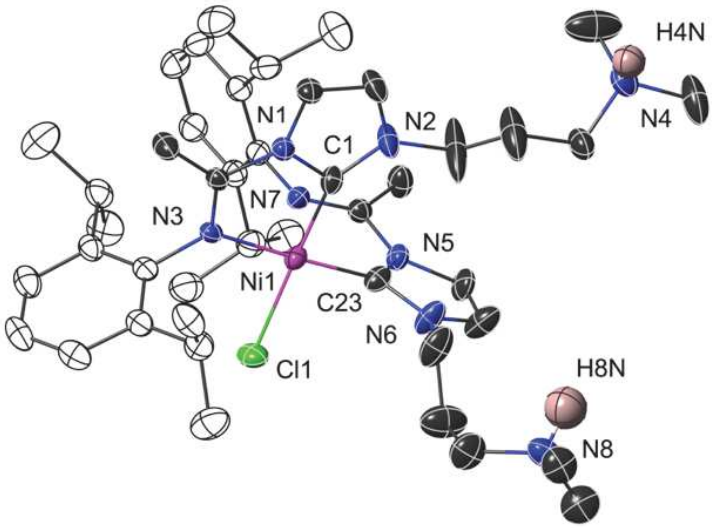

Figure 5. Structure of **8** with H atoms and $[PF_6]^-$ and Cl^- anions omitted for clarity. Thermal ellipsoids at the 40% probability level. Selected bond lengths (Å) and angles (deg): C1−N1 1.372(5), C1−N2 1.340(6), Ni1−C1 1.879(4), Ni1−N3 1.979(3), Ni1−C23 1.865(4), C23−N5 1.368(5), C23−N6 1.334(5), N1−C1−N2 103.8(3), N1−C1−Ni1 111.7(3), N2−C1−Ni1 144.5(3), C1−Ni1−Cl1 171.60(14), N5−C23−N6 104.8(3), N5−C23−Ni1 127.4(3), N6−C23−Ni1 127.8(3), C23−Ni1−N3 177.06(16).

Transmetallation Reactions

Considering the wide use of silver(I) complexes as transmetallating agents in the synthesis of transition metal NHC complexes, we prepared the mono-NHC silver complexes [AgCl{C(Me)=NDipp}(C_2NMe_2)] (**9**) and [AgCl{C(Me)=NDipp}(C_3NMe_2)] (**10**) (eq. 9, Figure 3) and used them for transmetallation reactions to Ni(II).

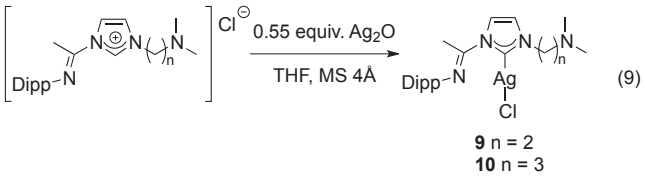

(9)

For references, see p. 47

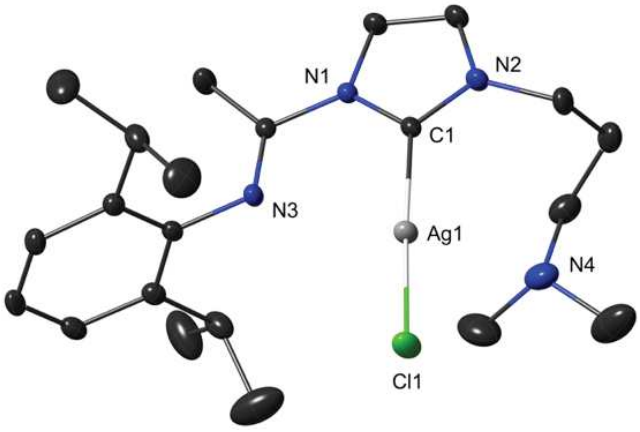

Figure 6. Structure of complex **10** with H atoms omitted for clarity. Thermal ellipsoids at the 30% probability level. Selected bond lengths (Å) and angles (deg): C1−N1 1.364(3), C1−N2 1.342(2), Ag1−C1 2.093(1), Ag1−Cl1 2.339(2), C1−Ag1−Cl1 176.1(1), N1−C1−Ag1 127.5(5), N2−C1−Ag1 128.3(6), N1−C1−N2 104.5(1).

As shown in Figure 6, compound **10** displays a nearly linear coordination geometry with a monodentate NHC donor ligand and a chloride forming a C1−Ag1−Cl1 angle of 176.1(1) Å. In the solid state, both functional groups in the side arms are dangling, with the N atoms directed toward the silver atom; however the Ag1···N3 (2.882 Å) and Ag1···N4 (3.113 Å) distances are too long to represent significant bonding interactions.

We first used $[NiCl_2(dme)]$ (which is poorly soluble) as the Ni(II) source for transmetallation but we were not able to isolate a pure crystalline product, instead green powders were obtained showing paramagnetic properties in ^{1}H NMR spectroscopy. However, reaction of $[NiBr_2(dme)]$ with **9** unexpectedly afforded a few yellow crystals of a dinuclear complex containing two bis-NHC Ni(II) units bridged by a $[Ag_2Br_4]^{2-}$ dianions, $[NiCl\{Im[C(Me)=NDipp](C_2NMe_2)\}]_2[Ag_2Br_4]$ (**11**). In its molecular structure (Figure 7), each nickel adopts a square planar coordination geometry with one C^{NHC},N^{imine}-chelating ligand (the amine group is coordinated to the $[AgBr_2]^-$ moiety), one C^{NHC} ligand (the imine and amine groups are dangling), and one chloride. It is noteworthy that the bromide ligand from the precursor $[NiBr_2(dme)]$ was replaced by chloride, and so allowing the formation of $[Ag_2Br_4]^{2-}$. In the centrosymmetric $[Ag_2Br_4]^{2-}$ core, the Ag1−Br2 and Ag1−Br2' distances involving the bridging bromides are as expected longer, 2.704(2) Å and 2.787(6) Å, respectively, than the terminal Ag−Br bond distances of 2.577(5) Å. The presence of the amine donor is clearly responsible for the retention of the silver halide complex in the final structure, in contrast with the situations encountered with non-functional NHC ligands.

For references, see p. 47

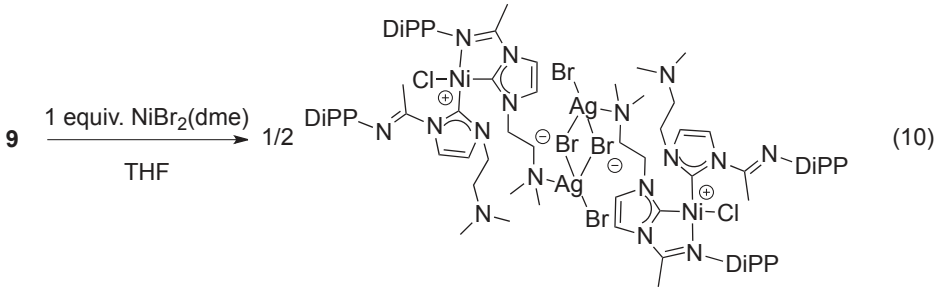

(10)

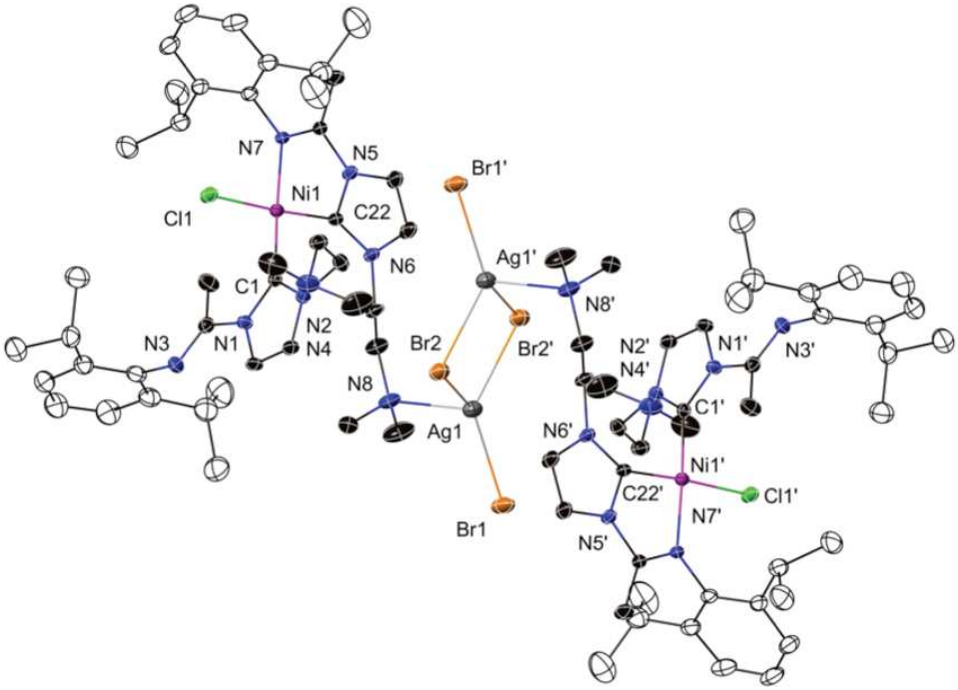

Figure 7. Structure of complex **11** with H atoms omitted for clarity. Thermal ellipsoids at the 40% probability level. Selected bond lengths (Å) and angles (deg): C1−N1 1.372(4), C1−N2 1.340(5), C1−Ni1 1.868(3), C22−N5 1.378(4), C22−N6 1.348(4), Ni1−C22 1.871(4), Ni1−N7 1.960(3), Ni1−Cl1 2.185(9), Ag1−N8 2.522(4), Ag1−Br1 2.577(5), Ag1−Br2 2.704(2), Ag1−Br2' 2.787(6), N1−C1−N2 104.9(3), N5−C22−N6 103.6(3), C1−Ni1−C22 96.8(1), C1−Ni1−Cl1 86.8(2), C22−Ni1−N7 82.2(9), N7−Ni1−Cl1 94.5(2).

To facilitate a better control of the reagents stoichiometry in transmetallation reactions, we then used $[Ni(NCMe)_6](BF_4)_2$ as starting material, which is much more soluble than $[NiX_2(dme)]$ (X = Cl, Br). Indeed, the desired mono-NHC tridentate Ni(II) complex with a C_2 spacer was obtained with this approach (eq. 11). The structure of **12** (Figure 8) features a Ni(II) center in a slightly distorted square planar coordination geometry (N3−Ni1−N4 angle of 170.5(6)°) with the 6 electron donor tridentate ($N^{imine}C^{NHC}N^{amine}$) ligand in a pincer-type coordination mode. An acetonitrile

For references, see p. 47

ligand completes the metal coordination sphere and two $[BF_4]^-$ anions compensate for the dicationic charge of the complex. A similar product **13** was isolated from the Ag(I) precursor containing a C3 spacer (Figure 8).

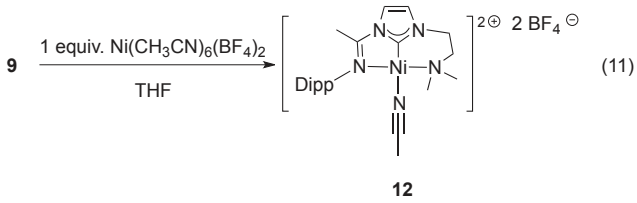

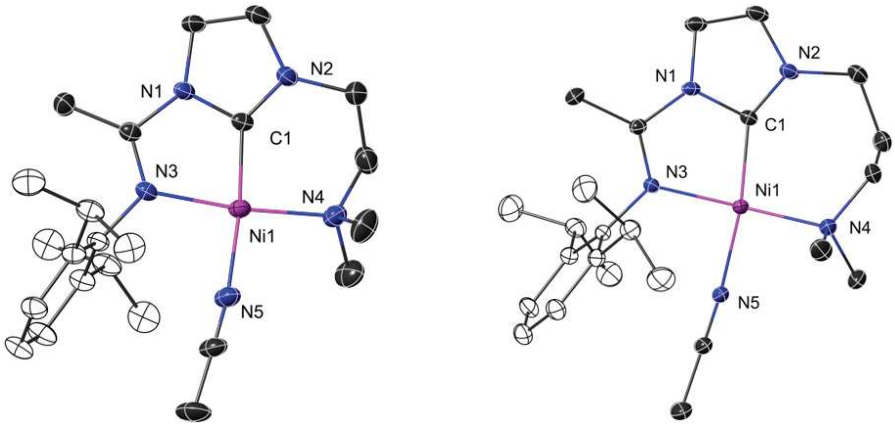

Figure 8. Structure of complex **12** (left) and **13** (right) with H atoms and two $[BF_4]^-$ anions omitted for clarity. Thermal ellipsoids at the 30% probability level. Selected bond lengths (Å) and angles (deg). **12**: C1−N1 1.351(4), C1−N2 1.317(4), Ni1−C1 1.819(3), Ni1−N3 1.949(2), Ni1−N4 1.974(3), Ni1−N5 1.902(3), N1−C1−N2 106.7(2), C1−Ni1−N3 80.8(1), C1−Ni1−N4 91.8(6), C1−Ni1−N5 171.5(9), N3−Ni1−N4 170.5(6); **13**: C1−N1 1.370(2), C1−N2 1.342(4), Ni1−C1 1.897(7), Ni1−N3 1.939(3), Ni1−N4 1.971(3), Ni1−N5 1.913(1), N1−C1−N2 104.1(7), C1−Ni1−N3 81.9(7), C1−Ni1−N4 100.0(5), C1−Ni1−N5 168.3(8), N3−Ni1−N4 163.9(2).

The pincer architecture of **12** is almost the same as that of the Ni(II) complex **6**, where a coordinated chloride replaces the acetonitrile molecule. The bond lengths and angles of the pincer moiety are similar, for instance, Ni−$C^{carbene}$ (1.819(3) Å in **12** and 1.838(7) Å in **6**), Ni−N^{imine} (1.949(2) Å in **12** and 1.964(5) Å in **6**), Ni−N^{amine} (1.974(3) Å in **12** and 1.997(6) Å in **6**), $C^{carbene}$–Ni–N^{imine} (80.3(3)° in **12** and 80.8(1)° in **6**) and $C^{carbene}$–Ni–N^{amine} (89.8(3)° in **12** and 91.8(6)° in **6**). The pincer ligand in complex **13** also adopts a similar bonding and C^{NHC},N^{amine} chelation leads to a seven-membered ring instead of the six-membered ring present in **12**. The Ni−$C^{carbene}$, Ni−N^{imine} , Ni−N^{amine} bond distances in **13** are similar to those in **12**, the angles $C^{carbene}$–Ni–N^{imine} are also very similar but the $C^{carbene}$–Ni–N^{amine} angle in **13** (C1−Ni1−N4 100.0(5)°) is significantly larger than in **12** (C1−Ni1−N4 91.8(6)°), due to the constraint associated

For references, see p. 47

with the seven-membered ring.

5. Conclusion

Our investigations on the oxidative-addition reactions of $N^{imine}C^{NHC}N'$ ($N' = N^{amine}$ or $N^{protonated\text{-}amine}$) pincer ligands to [Ni(1,5-cod)$_2$] have revealed completely different coordination behaviors which are dependent on the length of the spacer connecting the heterocycle with the amine or protonated-amine groups. The use of the $N^{imine}C^{NHC}N^{amine}$ ligand with the C2 spacer gave an unexpected dinuclear Ni(II) NHC complex **2** with a partially fragmented ligand, whereas formation of a dinuclear Ni(I)−Ni(I) NHC complex containing a bridging η^3-allyl-type ligand has been previously observed with the C3 spacer.[8] Interestingly, in compound **2**, the imine arm C(Me)=NDipp liberated from $N^{imine}C^{NHC}N^{amine}$ ligand becomes a bridging ligand, together with the remaining imidazole. A $N^{imidazole}$–C^{imine} bond cleavage has also been observed in a $N^{imine}C^{NHC}N^{imine}$ pincer ligand.[9c] Interestingly, when we used the same reaction conditions as above with $N^{imine}C^{NHC}N^{protonated\text{-}amine}$ pincer ligands, diverse coordination modes occurred that depend on the spacer length of the protonated-amine donors. Whereas a mono-NHC tridentate Ni(II) complex **6** was formed with the C2 spacer, a dinuclear bis-NHC Ni(II) complex **7a** and its isomer **7b** were isolated in the case of the C3 spacer. A shorter spacer length for the N^{amine} donor favors chelation to the metal and this orients the nature of the products formed. The synthesis of **6** provided a methodology for the formation of tridentate pincer transition metal complexes by an oxidative-addition reaction with protonated pincer type imidazolium salt and a zerovalent metal precursor. Finally, the isolation of compounds **12** and **13** demonstrates that transmetallation from a silver(I) complex is also a suitable procedure for the formation of tridentate transition metal complexes.

6. Experimental section

General methods

All manipulations involving organometallics were performed under nitrogen or argon in a Braun glove-box or using standard Schlenk techniques. Solvents were dried using standard methods and distilled under nitrogen prior use or passed through columns of activated alumina and subsequently purged with nitrogen or argon. The starting materials **1, 4** were prepared according to the literature. NMR spectra were recorded on Bruker spectrometers (AVANCE I − 300 MHz, AVANCE III − 400 MHz or AVANCE I − 500 MHz equipped with a cryogenic probe). Elemental analyses were performed by the “Service de microanalyses”, Université de Strasbourg.

For references, see p. 47

Preparation of [(ImH){C(Me)=NDipp}(C_2NMe_2)]Cl (1).

To a solution of 2-(1*H*-imidazol-1-yl)-*N*,*N*-dimethylethanamine (2.02 g, 14.4 mmol) in toluene (10 mL) was added dropwise (*E*)-*N*-(2,6-diisopropylphenyl)acetimidoyl chloride (3.42g, 14.4 mmol). The reaction mixture was stirred overnight at room temperature. Then the resulting precipitate was collected by filtration, and washed with Et_2O to give a white powder (4.78 g, 88%). ^{1}H NMR (300 MHz, $CDCl_3$) δ 12.07 (br, 1H, $CH^{imidazole}$), 8.15 (apparent t, $^{3,4}J$ = 1.8 Hz, 1H, $CH^{imidazole}$), 7.77 (br, 1H, $CH^{imidazole}$), 7.16 (br s, 3H, CH^{Ar}), 4.80 (br t, ^3J = 5.2 Hz, 2H, $CH_2CH_2NMe_2$), 3.04 (br, 2H, $CH_2CH_2NMe_2$), 2.59 (sept, ^3J = 6.9 Hz, 2H, CH^{iPr}), 2.52 (s, 3H, CH_3^{imine}), 2.44 (s, 6H, $CH_2CH_2NMe_2$), 1.14 (d, ^3J = 6.9 Hz, 6H, CH_3^{iPr}), 1.10 (d, ^3J = 6.9 Hz, 6H, CH_3^{iPr}). ^{13}C NMR (126 MHz, $CDCl_3$) δ 148.6 (C^{imine}), 140.7 ($C^{ipso\text{-}Ar}$), 139.1 ($CH^{imidazole}$), 136.6 ($C^{o\text{-}Ar}$), 125.6 ($CH^{p\text{-}Ar}$), 123.7 ($CH^{m\text{-}Ar}$), 123.2 ($CH^{imidazole}$), 117.2 ($CH^{imidazole}$), 58.2 ($CH_2CH_2NMe_2$), 47.4 ($CH_2CH_2NMe_2$), 45.2 ($CH_2CH_2NMe_2$), 28.6 (CH^{iPr}), 23.3 (CH_3^{iPr}), 23.0 (CH_3^{iPr}), 17.0 (CH_3^{imine}). Anal. calcd. for $C_{21}H_{33}ClN_4$: C, 66.91; H, 8.82; N, 14.86%; found: C, 65.97; H, 8.66; N, 14.77%.

Preparation of [Ni_2Cl_2{Im[C(Me)=NDipp](C_2NMe_2)}$_2$] (2).

To a suspension of [(ImH)(DippN=CMe)(C_2NMe_2)][Cl] (0.100 g, 0.265 mmol) in THF (15 mL) was added [Ni(cod)$_2$] (0.073 g, 0.265 mmol) at room temperature under magnetic stirring. The reaction mixture was stirred overnight. The solvent was evaporated under reduced pressure, and the solid was dissolved in toluene (10 ml). After filtration, the solution was slowly evaporated and X-ray quality orange-red crystals were obtained (0.030 g, yield isolated product 27%). Anal. calcd. for $C_{42}H_{64}Cl_2N_8Ni_2$: C, 58.03; H, 7.42; N, 12.89%; found: C, 58.25; H, 7.35; N, 12.57%.

In the ^{1}H NMR, four sets of backbone signals with two different intensities account for the presence of two conformers, are shown in Figures 3 and 4. It is noteworthy that the protons in the amine spacers $CH_2CH_2NMe_2$ in compound **2** are diastereotopic (Figure 5). Two carbon signals which belong to complex **2** and its conformer resonate in ^{13}C NMR at δ 231.8 ppm and δ 234.0 ppm, respectively, and they could be attributed to the quaternary carbon atoms of the imine groups coordinated directly to the nickel from the ^{13}C and HMBC NMR spectra (Figure 6-8). Additionally, in the ^{13}C NMR spectrum, four sets of CH_2 signals correspond to the existence of two conformers (Figure 9).

Preparation of [Ni_2Cl_3{Im[C(Me)=NDipp](C_2NMe_2)}{ImH[C(Me)=NDipp](C_2NMe_2)}] (3).

For references, see p. 47

Compound **3** was obtained during the crystallization of compound **2** as a byproduct. Satisfactory NMR or microanalysis data could not be obtained because of the irreproducible fragmentation and its very low yield. From the formula, the difference between the compound **3** and **2** is addition HCl.

Preparation of [(ImH){C(Me)=NDipp}(C_2NHMe_2)]Cl_2 (4).

A mixture of the imidazolium salt [(ImH){C(Me)=NDipp}(C_2NMe_2)]Cl **(1)** (1.000 g, 2.65 mmol) and [HCl·DMF] (0.291 g, 2.66 mmol) in THF was stirred overnight. The solvent was removed by filtration and the remaining white powder was washed with Et_2O (0.997 g, 91%). ^{1}H NMR (300 MHz, CD_2Cl_2): δ 13.01 (vbr s, 1H, $CH_2CH_2NHMe_2$), 12.31 (br s, 1H, $CH^{imidazole}$), 8.17 (br m, 1H, $CH^{imidazole}$), 7.77 (br s, 1H, $CH^{imidazole}$), 7.20-7.17 (br s, 3H, CH^{Ar}), 4.78 (t, ^3J = 5.5 Hz, 2H, $CH_2CH_2NHMe_2$), 3.03 (br, 2H, $CH_2CH_2NHMe_2$), 2.67 (sept, ^3J = 6.9 Hz, 2H, CH^{iPr},), 2.53 (s, 3H, CH_3^{imine}), 2.44 (s, 3H, $CH_2CH_2NHMe_2$), 1.17 (d, ^3J = 6.9 Hz, 6H, CH_3^{iPr}), 1.11 (d, ^3J = 6.9 Hz, 6H, CH_3^{iPr}). Anal. calcd. for $C_{21}H_{34}Cl_2N_4$: C, 61.01; H, 8.29; N, 13.55%; found: C, 56.29; H, 8.18; N, 12.90% (despite several attempts, no better analytical data could be obtained).

Preparation of [(ImH){C(Me)=NDipp}(C_3NHMe_2)]Cl_2 (5).

A mixture of the imidazolium salt [(ImH){C(Me)=NDipp}(C_3NMe_2)]Cl (1.000 g, 2.56 mmol) and [HCl·DMF] (0.280 g, 2.56 mmol) in THF was stirred overnight. The solvent was removed by filtration and the remaining white powder was washed with Et_2O (1.018 g, 93%). ^{1}H NMR (500 MHz, DMSO-d_6): δ 11.50 (vbr s, 1H, $CH_2CH_2CH_2NHMe_2$), 10.41 (br s, 1H, $CH^{imidazole}$), 8.51 (br s, 1H, $CH^{imidazole}$), 8.21 (br s, 1H, $CH^{imidazole}$), 7.29-7.21 (m, 3H, CH^{Ar}), 4.56 (t, ^3J = 6.9 Hz, 2H, $CH_2CH_2CH_2NHMe_2$), 3.26 (br, 2H, $CH_2CH_2CH_2NHMe_2$), 2.85 (br s, 6H, $CH_2CH_2CH_2NHMe_2$), 2.82 (sept, ^3J = 6.9 Hz, 2H, CH^{iPr}, overlapped with $CH_2CH_2CH_2NHMe_2$), 2.58 (br, 2H, $CH_2CH_2CH_2NHMe_2$), 2.41 (s, 3H, CH_3^{imine}), 1.20 (d, ^3J = 6.9 Hz, 6H, CH_3^{iPr}), 1.15 (d, ^3J = 6.9 Hz, 6H, CH_3^{iPr}). ^{13}C NMR (126 MHz, DMSO-d_6) δ 149.7 (C^{imine}), 141.0 ($C^{ipso\text{-}Ar}$), 137.6 ($CH^{imidazole}$), 136.4 ($C^{o\text{-}Ar}$), 125.0 ($CH^{p\text{-}Ar}$), 123.3 ($CH^{m\text{-}Ar}$), 123.1 ($CH^{imidazole}$), 118.5 ($CH^{imidazole}$), 52.8 ($CH_2CH_2CH_2NHMe_2$), 46.7 ($CH_2CH_2CH_2NHMe_2$), 41.9 ($CH_2CH_2CH_2NHMe_2$), 27.6 (CH^{iPr}), 24.1 ($CH_2CH_2CH_2NHMe_2$), 23.2 (CH_3^{iPr}), 22.9 (CH_3^{iPr}), 16.2 (CH_3^{imine}). Anal. calcd. for $C_{22}H_{36}Cl_2N_4$: C, 61.82; H, 8.49; N, 13.11%; found: C, 61.07; H, 8.36; N, 13.14%.

Preparation of [NiCl{Im[C(Me)=NDipp](C_2NMe_2)}]$_2$[$NiCl_4$] (6).

To a suspension of [(ImH){C(Me)=NDipp}(C_2NHMe_2)]Cl_2 (**4**) (0.100 g, 0.242 mmol) in THF (15 mL) was added [Ni(cod)$_2$] (0.067 g, 0.244 mmol) at room temperature under magnetic stirring. The

For references, see p. 47

reaction mixture was stirred 1 h, and then [$NiCl_2$(dme)] (0.027 g, 0.123 mmol) was added. The mixture was stirred overnight. The solvent was evaporated under reduced pressure, and replaced with MeCN (5 ml). After filtration, the filtrate was slowly concentrated and Et_2O (10 mL) was added to the green solution. Green, X-ray quality crystals were obtained (0.087 g, yield isolated product 67 %). Anal. calcd. for $C_{42}H_{64}Cl_6N_8Ni_3$: C, 47.15; H, 6.03; N, 10.47%; found: C, 43.83; H, 6.29; N, 10.06% (despite several attempts, no better analytical data could be obtained).

Preparation of [Ni_2Cl_4{Im[C(Me)=NDipp](C_3NMe_2)}$_2$] (7a).

To a suspension of [(ImH){C(Me)=NDipp}(C_3NHMe_2)]Cl_2 (**5**) (0.100 g, 0.234 mmol) in THF (15 mL) was added [Ni(cod)$_2$] (0.065 g, 0.236 mmol) at room temperature under magnetic stirring. The reaction mixture was stirred overnight. CH_2Cl_2 (2 mL) was added to the green suspension for complete dissolution, and then Et_2O (10 mL) was added slowly as non-solvent. Green, X-ray quality crystals were obtained (0.086 g, yield of isolated product 76%). Anal. calcd. for $C_{44}H_{68}Cl_4N_8Ni_2$: C, 54.58; H, 7.08; N, 11.57%; found: C, 54.02; H, 6.97; N, 11.85%.

Preparation of [Ni_2Cl_4{Im[C(Me)=NDipp](C_3NMe_2)}$_2$] (7b).

To a suspension of [(ImH){C(Me)=NDipp}(C_3NHMe_2)]Cl_2 (**5**) (0.100 g, 0.234 mmol) in THF (15 mL) was added [Ni(cod)$_2$] (0.065 g, 0.236 mmol) at room temperature under magnetic stirring. The reaction mixture was stirred overnight. The solvent was evaporated under reduced pressure, and then replaced with MeCN (5 ml) to redissolve the product. Et_2O (10 mL) was added to the green solution as a non-solvent and green, X-ray quality crystals were obtained (0.079 g, yield isolated product 70 %). Anal. calcd. for $C_{44}H_{68}Cl_4N_8Ni_2$: C, 54.58; H, 7.08; N, 11.57%; found: C, 52.56; 6.96, X; N, 10.41% (despite several attempts, no better analytical data could be obtained)..

Preparation of [NiCl{Im[C(Me)=NDipp](C_3NHMe_2)}$_2$][$PF6]_2$Cl (8).

To a suspension of [Ni_2Cl_4{Im[C(Me)=NDipp](C_3NMe_2)}$_2$] (**7a**) (0.030 g, 0.031 mmol) in THF (5 mL) was added a THF solution (5 mL) of $AgPF_6$ (0.008 g, 0.032 mmol) at room temperature under magnetic stirring. The reaction mixture was stirred for 3 h. Beige precipitates formed and an orange solution were obtained by filtration. Orange crystals were obtained by slow diffusion of Et_2O into THF solution. Because of the low yield of crystals, no NMR data was collected.

Preparation of [AgCl{Im[C(Me)=NDipp](C_2NMe_2)}] (9).

For references, see p. 47

A mixture of the imidazolium salt [(ImH){C(Me)=NDipp}(C_2NMe_2)]Cl (**1**) (0.200 g, 0.531 mmol), Ag_2O (0.68 g, 0.293 mmol) and molecular sieves in THF (10 mL) was stirred overnight under exclusion of light. The beige reaction mixture was then filtered through Celite and the filtrate was dried under reduced pressure. The resulting solid was washed with Et_2O to give as a beige powder (0.184 g, 72%). ^{1}H NMR (500 MHz, C_6D_6): δ 7.77 (d, ^3J = 1.8 Hz, 1H, $CH^{imidazole}$), 7.11-7.07 (m, 3H, CH^{Ar}), 6.36 (d, ^3J = 1.8 Hz, 1H, $CH^{imidazole}$), 3,81 (t, ^3J = 5.6 Hz, 2H, $CH_2CH_2NMe_2$), 2.71 (sept, ^3J = 6.9 Hz, 2H, CH^{iPr}), 2.47 (s, 3H, CH_3^{imine}), 2.18 (t, ^3J = 5.6 Hz, 2H, $CH_2CH_2NMe_2$), 1.91 (br s, 6H, $CH_2CH_2NMe_2$), 1.10 (d, ^3J = 6.9 Hz, 6H, CH_3^{iPr}), 1.05 (d, ^3J = 6.9 Hz, 6H, CH_3^{iPr}). ^{13}C NMR (126 MHz, C_6D_6): δ 184.2 ($C^{carbene}$), 153.2 (C^{imine}), 142.9 ($C^{ipso\text{-}Ar}$), 137.0 ($C^{o\text{-}Ar}$), 125.0 ($CH^{p\text{-}Ar}$), 123.7 ($CH^{m\text{-}Ar}$), 121.6 ($CH^{imidazole}$), 117.9 ($CH^{imidazole}$), 59.8 ($CH_2CH_2NMe_2$), 50.7 ($CH_2CH_2NMe_2$), 45.4 ($CH_2CH_2NMe_2$), 28.8 (CH^{iPr}), 23.5 (CH_3^{iPr}), 23.0 (CH_3^{iPr}), 18.4 (CH_3^{imine}). Anal. calcd. for $C_{21}H_{32}AgClN_4$: C, 52.13; H, 6.67; N, 11.58%; found: C, 52.09; H, 6.65; N, 11.67%.

Preparation of [AgCl{Im[C(Me)=NDipp](C_3NMe_2)}] (10).

A mixture of the imidazolium salt [(ImH){C(Me)=NDipp}(C_3NMe_2)]Cl (0.200 g, 0.515 mmol), Ag_2O (0.65 g, 0.280 mmol) and molecular sieves in THF (10 mL) was stirred overnight under exclusion of light. The beige reaction mixture was then filtered through Celite and the filtrate dried under reduced pressure. The resulting solid was washed with Et_2O to give as a beige powder (0.184 g, 76%). X-ray quality crystals were obtained by slow diffusion of pentane into THF solution. ^{1}H NMR (500 MHz, $CDCl_3$): δ 8.09 (d, ^3J = 1.5 Hz, 1H, $CH^{imidazole}$), 7.17-7.12 (m, 4H, $CH^{imidazole}$, CH^{Ar}), 4.35 (t, ^3J = 6.9 Hz, 2H, $CH_2CH_2CH_2NMe_2$), 2.67 (sept, ^3J = 6.9 Hz, 2H, CH^{iPr}), 2.54 (s, 3H, CH_3^{imine}), 2.29 (t, ^3J = 6.6 Hz, 2H, $CH_2CH_2CH_2NMe_2$), 2.25 (br s, 6H, $CH_2CH_2CH_2NMe_2$), 2.06-2.01 (m, 2H, $CH_2CH_2CH_2NMe_2$), 1.16 (d, ^3J = 6.9 Hz, 6H, CH_3^{iPr}), 1.14 (d, ^3J = 6.9 Hz, 6H, CH_3^{iPr}). ^{13}C NMR (126 MHz, C_6D_6): δ 184.2 ($C^{carbene}$), 153.2 (C^{imine}), 142.8 ($C^{ipso\text{-}Ar}$), 136.9 ($C^{o\text{-}Ar}$), 125.1 ($CH^{p\text{-}Ar}$), 123.7 ($CH^{m\text{-}Ar}$), 121.4 ($CH^{imidazole}$), 118.0 ($CH^{imidazole}$), 54.9 ($CH_2CH_2CH_2NMe_2$), 50.2 ($CH_2CH_2CH_2NMe_2$), 45.1 ($CH_2CH_2CH_2NMe_2$), 28.9 ($CH_2CH_2CH_2NMe_2$), 28.8 (CH^{iPr}), 23.5 (CH_3^{iPr}), 23.0 (CH_3^{iPr}), 18.4 (CH_3^{imine}). Anal. calcd. for $C_{22}H_{34}AgClN_4$: C, 53.07; H, 6.88; N, 11.25%; found: C, 52.96; H, 6.91; N, 11.09%.

Preparation of [NiCl{Im[C(Me)=NDipp](C_2NMe_2)}]$_2$[Ag_2Br_4] (11).

To a solution of [$NiBr_2$(dme)] (0.0019 g, 0.207 mmol) in THF (8 mL) was added a THF solution of [AgCl{Im[C(Me)=NDipp](C_2NMe_2)}] (**9**) (0.030 g, 0.062 mmol) at room temperature under magnetic stirring. The reaction mixture was stirred 3 h and a orange solution was obtained without

For references, see p. 47

precipitates. The yellow solution was concentrated to 3 mL and after slow evaporation, several yellow X-ray quality crystals were obtained by slow diffusion of Et_2O into THF solution. Because of the low yield of crystals, no NMR data was collected.

Preparation of [Ni(NCMe){Im[C(Me)=NDipp](C$_2$NMe$_2$)}][BF$_4$]$_2$ (12).

To a solution of $[Ni(NCMe)_6](BF_4)_2$ (0.099 g, 0.207 mmol) in THF (10 mL) was added a THF solution of [AgCl{Im[C(Me)=NDipp](C$_2$NMe$_2$)}] (**9**) (0.100 g, 0.207 mmol) at room temperature under magnetic stirring. The reaction mixture was stirred overnight. The solvent was evaporated under reduced pressure, and then replaced with MeCN (10 ml), giving a yellow solution and a white precipitate. After filtration, the filtrate was concentrated to 3 mL under reduced pressure and Et_2O (10 mL) was slowly added as non-solvent. X-ray quality yellow crystals were obtained (0.083 g, yield isolated product 65%). ^{1}H NMR (300 MHz, CD_3CN): δ 7.74 (d, ^3J = 1.7 Hz, 1H, $CH^{imidazole}$), 7.45-7.34 (m, 4H, $CH^{imidazole}$, CH^{Ar}), 4.25 (t, ^3J = 4.9 Hz, 2H, $CH_2CH_2NMe_2$), 3.34 (sept, ^3J = 6.7 Hz, 2H, CH^{iPr}), 3.06 (br t, ^3J = 4.9 Hz, 2H, $CH_2CH_2NMe_2$), 2.73 (br s, 6H, $CH_2CH_2NMe_2$), 2.27 (s, 3H, CH_3^{imine}), 1.96 (s, 3H, CH_3CN), 1.48 (d, ^3J = 6.7 Hz, 6H, CH_3^{iPr}), 1.19 (d, ^3J = 6.7 Hz, 6H, CH_3^{iPr}). ^{13}C NMR (126 MHz, CH_3CN) δ XX ($C^{carbene}$), 166.6 (C^{imine}), 143.0 ($C^{o\text{-}Ar}$), 138.2 ($C^{ipso\text{-}Ar}$), 130.5 ($CH^{p\text{-}Ar}$), 125.7 ($CH^{m\text{-}Ar}$), 125.3 ($CH^{imidazole}$), 121.1 ($CH^{imidazole}$), 61.1 ($CH_2CH_2NMe_2$), 50.3 ($CH_2CH_2NMe_2$), 45.9 ($CH_2CH_2NMe_2$), 29.3 (CH^{iPr}), 24.3 (CH_3^{iPr}), 23.9 (CH_3^{iPr}), 16.4 (CH_3^{imine}). Anal. calcd. for $C_{23}H_{35}B_2F_8N_5Ni$: C, 45.00; H, 5.75; N, 11.41%; found: C, 50.77; H, 6.67; N, 9.01% (despite several attempts, no better analytical data could be obtained).

Preparation of [Ni(NCMe){Im[C(Me)=NDipp](C$_3$NMe$_2$)}][BF$_4$]$_2$ (13).

To a solution of $[Ni(NCMe)_6](BF_4)_2$ (0.097 g, 0.203 mmol) in CH_2Cl_2 (10 mL) was added a CH_2Cl_2 solution of [AgCl{Im[C(Me)=NDipp](C$_3$NMe$_2$)}] **(10)** (0.100 g, 0.201 mmol) at room temperature under magnetic stirring. The reaction mixture was stirred overnight. After filtration, the filtrate was concentrated to 3 mL under reduced pressure, Et_2O (10 mL) was slowly added as non-solvent and red, X-ray quality crystals were obtained (0.077 g, yield isolated product 61%). ^{1}H NMR (400 MHz, CD_2Cl_2): δ 7.69 (d, ^3J = 1.8 Hz, 1H, $CH^{imidazole}$), 7.43 (m, 1H, $CH^{p\text{-}Ar}$), 7.34-7.32 (m, 2H, $CH^{m\text{-}Ar}$), 7.28 (d, ^3J = 1.8 Hz, 1H, $CH^{imidazole}$), 4.22 (t, ^3J = 5.1 Hz, 2H, $CH_2CH_2CH_2NMe_2$), 3.62 (sept, ^3J = 6.7 Hz, 2H, CH^{iPr}), 2.80-2.78 (br m, 8H, $CH_2CH_2CH_2NMe_2$, $CH_2CH_2NMe_2$), 2.34 (apparent t, ^3J = 5.1 Hz, ^3J = 5.4 Hz, 2H, $CH_2CH_2CH_2NMe_2$), 2.27 (s, 3H, CH_3^{imine}), 1.69 (br s, 3H, CH_3CN), 1.51 (d, ^3J = 6.7 Hz, 6H, CH_3^{iPr}), 1.22 (d, ^3J = 6.7 Hz, 6H, CH_3^{iPr}). Anal. calcd. for $C_{24}H_{37}B_2F_8N_5Ni$: C,

For references, see p. 47

45.91; H, 5.94; N, 11.15%; found: C, 35.24; H, 4.65; N, 7.62% (despite several attempts, no better analytical data could be obtained).

7. Acknowledgements

We are grateful to the China Scholarship Council for a PhD grant to X.R. We thank Marc Mermillon-Fournier for technical assistance, the CNRS and the MESR (Paris) for funding and Lydia Karmazin and Corinne Bailly from the Service de Radiocristallographie (UdS) for the determination of the crystal structures.

For references, see p. 47

8. References

(1) Albrecht, M.; van Koten, G. *Angew. Chem. Int. Ed.* **2001**, *40*, 3750-3781.

(2) (a) Morales-Morales, D.; Jensen, C. G. M., *The Chemistry of Pincer Compounds*, Elsevier Science, **2011**. (b) van Koten, G.; Gossage, R. A., *The Privileged Pincer-Metal Platform: Coordination Chemistry & Applications*, Springer International Publishing, **2015**.

(3) (a) van der Boom, M. E.; Milstein, D. *Chem. Rev.* **2003**, *103*, 1759-1792. (b) Pugh, D.; Danopoulos, A. A. *Coord. Chem. Rev.* **2007**, *251*, 610-641. (c) Mougang-Soumé, B.; Belanger-Gariépy, F.; Zargarian, D. *Organometallics* **2014**, *33*, 5990-6002. (d) Smith, J. B.; Miller, A. J. M. *Organometallics* **2015**. (e) Simler, T.; Danopoulos, A. A.; Braunstein, P. *Chem. Commun.* **2015**, *51*, 10699-10702. (f) Hameury, S.; de Fremont, P.; Braunstein, P. *Chem. Soc. Rev.* **2017**, *46*, 632-733.

(4) (a) Romain, C.; Miqueu, K.; Sotiropoulos, J.-M.; Bellemin-Laponnaz, S.; Dagorne, S. *Angew. Chem. Int. Ed.* **2010**, *49*, 2198-2201. (b) Simler, T.; Braunstein, P.; Danopoulos, A. A. *Chem. Commun.* **2016**, *52*, 2717-2720. (c) Charra, V.; de Frémont, P.; Braunstein, P. *Coord. Chem. Rev.* **2017**, *341*, 53-176.

(5) (a) Moulton, C. J.; Shaw, B. L. *J. Chem. Soc., Dalton Trans.* **1976**, 1020-1024. (b) van Koten, G.; Jastrzebski, J. T. B. H.; Noltes, J. G.; Spek, A. L.; Schoone, J. C. *J. Organomet. Chem.* **1978**, *148*, 233-245. (c) van Koten, G.; Timmer, K.; Noltes, J. G.; Spek, A. L. *J. Chem. Soc., Chem. Commun.* **1978**, 250-252.

(6) (a) Contel, M.; Stol, M.; Casado, M. A.; van Klink, G. P. M.; Ellis, D. D.; Spek, A. L.; van Koten, G. *Organometallics* **2002**, *21*, 4556-4559. (b) Nishiyama, H. *Chem. Soc. Rev.* **2007**, *36*, 1133-1141. (c) Suijkerbuijk, B. M. J. M.; Tooke, D. M.; Lutz, M.; Spek, A. L.; Jenneskens, L. W.; van Koten, G.; Klein Gebbink, R. J. M. *J. Org. Chem.* **2010**, *75*, 1534-1549. (d) Suijkerbuijk, B. M. J. M.; Schamhart, D. J.; Kooijman, H.; Spek, A. L.; van Koten, G.; Klein Gebbink, R. J. M. *Dalton Trans.* **2010**, *39*, 6198-6216. (e) Zhang, J.; Gao, W.; Lang, X.; Wu, Q.; Zhang, L.; Mu, Y. *Dalton Trans.* **2012**, *41*, 9639-9645. (f) Mancano, G.; Page, M. J.; Bhadbhade, M.; Messerle, B. A. *Inorg. Chem.* **2014**, *53*, 10159-10170. (g) Brown, R. M.; Borau Garcia, J.; Valjus, J.; Roberts, C. J.; Tuononen, H. M.; Parvez, M.; Roesler, R. *Angew. Chem. Int. Ed.* **2015**, *54*, 6274-6277. (h) Nair, A. G.; McBurney, R. T.; Walker, D. B.; Page, M. J.; Gatus, M. R. D.; Bhadbhade, M.; Messerle, B. A. *Dalton Trans.* **2016**, *45*, 14335-14342.

(7) (a) Díez-González, S.; Marion, N.; Nolan, S. P. *Chem. Rev.* **2009**, *109*, 3612-3676. (b) Cazin, C. S. J., *N-Heterocyclic Carbenes in Transition Metal Catalysis and Organocatalysis*, Springer

For references, see p. 47

Netherlands, **2010**. (c) Rosen, B. M.; Quasdorf, K. W.; Wilson, D. A.; Zhang, N.; Resmerita, A.-M.; Garg, N. K.; Percec, V. *Chem. Rev.* **2011**, *111*, 1346-1416. (d) Shao, D.-D.; Niu, J.-L.; Hao, X.-Q.; Gong, J.-F.; Song, M.-P. *Dalton Trans.* **2011**, *40*, 9012-9019. (e) Niu, J.-L.; Hao, X.-Q.; Gong, J.-F.; Song, M.-P. *Dalton Trans.* **2011**, *40*, 5135-5150. (f) Chen, C.; Qiu, H.; Chen, W. *J. Organomet. Chem.* **2012**, *696*, 4166-4172. (g) Tasker, S. Z.; Standley, E. A.; Jamison, T. F. *Nature* **2014**, *509*, 299-309. (h) Prakasham, A. P.; Ghosh, P. *Inorg. Chim. Acta* **2015**, *431*, 61-100. (i) Mu, H.; Pan, L.; Song, D.; Li, Y. *Chem. Rev.* **2015**, *115*, 12091-12137. (j) Henrion, M.; Ritleng, V.; Chetcuti, M. J. *ACS Catalysis* **2015**, *5*, 1283-1302. (k) Eberhardt, N. A.; Guan, H. *Chem. Rev.* **2016**, *116*, 8373-8426. (l) Gu, S.; Du, J.; Huang, J.; Guo, Y.; Yang, L.; Xu, W.; Chen, W. *Dalton Trans.* **2017**, *46*, 586-594. (m) Nair, A. G.; McBurney, R. T.; Gatus, M. R. D.; Walker, D. B.; Bhadbhade, M.; Messerle, B. A. *J. Organomet. Chem.* **2017**, *845*, 63-70.

(8) Ren, X.; Gourlaouen, C.; Wesolek, M.; Braunstein, P. *Angew. Chem. Int. Ed.* DOI: 10.1002/anie.201706581R1

(9) (a) Benhamou, L.; Chardon, E.; Lavigne, G.; Bellemin-Laponnaz, S.; César, V. *Chem. Rev.* **2011**, *111*, 2705-2733. (b) Luo, J.; Xin, T.; Wang, Y. *New J. Chem.* **2013**, *37*, 269-273. (c) Liu, P.; Wesolek, M.; Danopoulos, A. A.; Braunstein, P. *Organometallics* **2013**, *32*, 6286-6297.

For references, see p. 47

9. Supporting Information

Synthesis and Structural Characterization of Nickel(II) Complexes with Tritopic $N^{imine}C^{NHC}N^{amine}$ pincer Ligands

Xiaoyu Ren,[a] Marcel Wesolek,[a] and Pierre Braunstein*[a]*

[a] *Laboratoire de Chimie de Coordination, Institut de Chimie (UMR 7177 CNRS), Université de Strasbourg, 4 rue Blaise Pascal, 67081 Strasbourg Cedex (France)*

E-mail: braunstein@unistra.fr

For references, see p. 47

X-ray crystallography

Summary of the crystal data, data collection and refinement for structures of **2**, **3**, **6**, **7a, 7b, 8, 10**, **11**, **12** and **13** are given in Table S1. The crystals were mounted on a glass fiber with grease, from Fomblin vacuum oil. Data sets were collected on a Bruker APEX II DUO diffractometer equipped with an Oxford Cryosystem liquid N_2 device, using Mo-Kα radiation (λ = 0.71073 Å). The crystal-detector distance was 38 mm. The cell parameters were determined (APEX2 software)[1] from reflections taken from three sets of 12 frames, each at 10 s exposure. The structures were solved by direct methods using the program SHELXS-97.[2] The refinement and all further calculations were carried out using SHELXL- 97.[3] The H-atoms were included in calculated positions and treated as riding atoms using SHELXL default parameters. The non-H atoms were refined anisotropically, using weighted full-matrix least-squares on F^2.

For references, see p. 47

Summary of crystal data

Table S1. Crystal data for compounds.

	2	**3**	**6**	**7a • THF**
Chemical formula	$C_{42}H_{64}Cl_2N_8Ni_2$	$C_{42}H_{65}Cl_3N_8Ni_2$	$C_{42}H_{64}Cl_6N_8Ni_3$	$C_{44}H_{68}Cl_4N_8Ni_2$, • C_4H_8O
CCDC Number				
Formula Mass	869.33	905.79	1069.84	1040.38
Crystal system	monoclinic	monoclinic	monoclinic	triclinic
a/Å	9.7444(6)	13.8656(10)	17.4384(6)	13.4407(17)
b/Å	17.0424(10)	20.4096(14)	31.1958(11)	14.0456(18)
c/Å	26.4110(15)	17.2200(13)	20.2590(7)	19.832(3)
α/°	90	90	90	96.533(3)
β/°	91.9930(10)	90.787(3)	114.985(2)	100.230(3)
γ/°	90	90	90	112.191(3)
Unit cell volume/Å^3	4383.4(4)	4872.7(6)	9989.6(6)	3343.7(7)
Temperature/K	173(2)	103(2)	173(2)	173(2)
Space group	*P 21/c*	*P 21/c*	*P 21*	*P -1*
Formula units / cell, *Z*	4	4	8	2
Absorption coefficient, μ/mm^{-1}	1.020	0.973	4.558	0.756
No. of reflections measured	63533	63300	86431	59590
No. of independent reflections	10613	10012	33806	16036
R_{int}	0.0706	0.1005	0.0450	0.0627
Final R_1 values ($I > 2\sigma(I)$)	0.0548	0.0508	0.0460	0.0627
Final $wR(F^2)$ values ($I > 2\sigma(I)$)	0.0964	0.1087	0.0952	0.1463
Final R_1 values (all data)	0.0941	0.0875	0.0697	0.1087
Final $wR(F^2)$ values (all data)	0.1081	0.1288	0.1067	0.1613
Goodness of fit on F^2	1.076	1.082	1.031	1.000

For references, see p. 47

	7b	**8 • CH_2Cl_2**	**10**	**11 • 2 Et_2O**
Chemical formula	$C_{44}H_{68}Cl_4N_8Ni_2$	$C_{44}H_{70}ClN_8Ni$, 2(F_6P), Cl, CH_2Cl_2	$C_{22}H_{34}AgClN_4$	$C_{84}H_{128}Ag_2Br_4Cl_2N_{16}Ni_2$, 2($C_4H_{10}O$)
CCDC Number				
Formula Mass	968.28	1215.55	497.85	2233.96
Crystal system	orthorhombic	monoclinic	monoclinic	triclinic
a/Å	41.4354(19)	26.5990(7)	8.4886(8)	11.6854(9)
b/Å	13.8740(6)	12.3345(3)	19.7601(19)	14.5354(11)
c/Å	18.0086(8)	17.5971(4)	16.1890(12)	16.0920(12)
α/°	90	90	90	90.426(2)
β/°	90	103.406(2)	118.595(4)	95.984(2)
γ/°	90	90	90	99.225(2)
Unit cell volume/Å^3	10352.7(8)	5616.0(2)	2384.3(4)	2682.4(4)
Temperature/K	173(2)	173(2)	173(2)	173(2)
Space group	*P b c n*	*P 21/c*	*P 21/c*	*P -1*
Formula units / cell, *Z*	8	4	4	1
Absorption coefficient, μ/mm^{-1}	0.970	3.485	0.971	2.294
No. of reflections measured	54686	53481	31006	61958
No. of independent reflections	12443	9789	7592	12954
R_{int}	0.0461	0.0604	0.0333	0.0709
Final R_1 values ($I > 2\,\sigma(I)$)	0.0703	0.0653	0.0318	0.0458
Final $wR(F^2)$ values ($I > 2\,\sigma(I)$)	0.1336	0.1601	0.0643	0.1021
Final R_1 values (all data)	0.0963	0.0917	0.0552	0.0902
Final $wR(F^2)$ values (all data)	0.1422	0.1768	0.0734	0.1183
Goodness of fit on F^2	1.129	1.029	1.010	1.015

for references, see p. 76

	12	**13**
Chemical formula	$C_{23}H_{35}N_5Ni$, $2(BF_4)$	$C_{24}H_{37}N_5Ni$, $2(BF_4)$
CCDC Number		
Formula Mass	613.89	627.91
Crystal system	monoclinic	monoclinic
a/Å	12.8096(5)	12.6898(4)
b/Å	13.0115(5)	12.7224(4)
c/Å	19.5024(6)	20.9490(6)
α /°	90	90
β /°	119.769(2)	119.931(2)
γ /°	90	90
Unit cell volume/Å^3	2821.55(18)	2931.02(16)
Temperature/K	173(2)	173(2)
Space group	*P 21/c*	*P 21/c*
Formula units / cell, *Z*	4	4
Absorption coefficient, μ	0.763	0.736
No. of reflections measured	27535	33303
No. of independent reflections	6826	11084
R_{int}	0.0425	0.0312
Final R_1 values ($I > 2\ \sigma(I)$)	0.0527	0.0437
Final $wR(F^2)$ values ($I > 2\ \sigma(I)$)	0.1262	0.1014
Final R_1 values (all data)	0.0929	0.0739
Final $wR(F^2)$ values (all data)	0.1451	0.1154
Goodness of fit on F^2	1.014	1.015

for references, see p. 76

REFERENCES

(1) Bruker AXS Inc Madison USA, **2006**.

(2) G. M. Sheldrick, *Acta Crystallogr. Sect. A: Found. Crystallogr.*, **1990**, *A46*, 467.

(3) G. M. Sheldrick, Universität Göttingen: Göttingen Germany, **1999**.

for references, see p. 76

CHAPITRE 3

Tritopic NHC Precursors: Unusual Nickel Reactivity and Ethylene Insertion into a C_{sp3}-H Bond

This chapter is presented in the form of a publication. This article was published in *Angew. Chem. Int. Ed.* **2017**, 56, 12557–12560.

My contribution to this work consisted of the bibliographic search, the experimental work and the preparation of the draft of the publication. Dr. Christophe Gourlaouen performed the theoretical analysis.

Synthesis and Structural Characterization of Nickel(II) Complexes with Tritopic $N^{imine}C^{NHC}N^{amine}$ pincer Ligands

Xiaoyu Ren,[a] Christophe Gourlaouen,[b] Marcel Wesolek*[a] and Pierre Braunstein*[a]

[a] Laboratoire de Chimie de Coordination, Institut de Chimie (UMR 7177 CNRS), Université de Strasbourg, 4 rue Blaise Pascal, 67081 Strasbourg Cedex (France)
E-mail: braunstein@unistra.fr

[b] Laboratoire de Chimie Quantique, Institut de Chimie (UMR 7177 CNRS), Université de Strasbourg, 4 rue Blaise Pascal, 67081 Strasbourg Cedex (France)

Synopsis

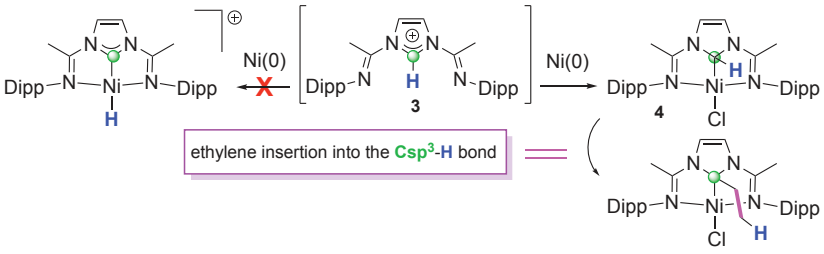

1. Résumé en français

Le chlorure d'imidazolium $[C_3H_3N(C_3H_6NMe_2)N\{C(Me)(=NDipp)\}]Cl$ (Dipp = 2,6-diisopropylphenyl) (**1**) précurseur potentiel d'un ligand tritopique de type pinceur $N^{imine}C^{NHC}N^{amine}$ a réagi avec $[Ni(1,5\text{-cod})_2]$ pour donner $[Ni(\mu\text{-}h^3\text{-}C_8H_{13})(\mu\text{-}Cl)\{Im[C(Me)=NDipp](C_3NMe_2)\}]_2$ (**2**), un complexe dinucléaire Ni(I)-Ni(I) possédant un rare exemple de ligand pontant du type η^3-allyl dérivé du 1,5-cod.

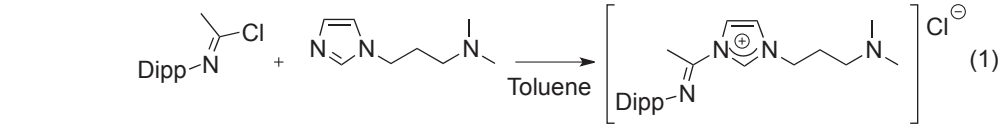

1

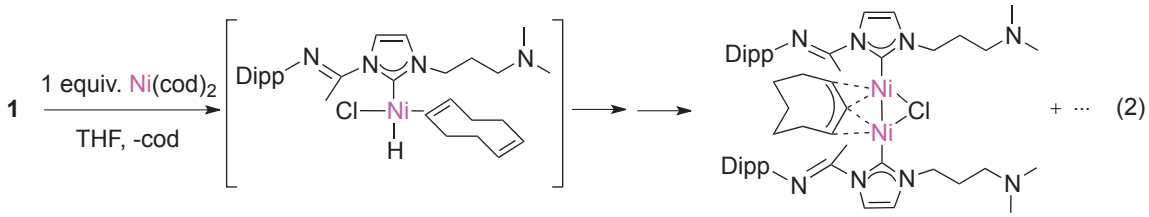

2

La formation implicite d'un intermédiaire Ni-hydrure provenant de l'addition oxydante du C-H de l'imidazolium n'a pas lieu avec le chlorure d'imidazolium symétrique $[C_3H_3N_2\{C(Me)(=NDipp)\}_2]Cl$ (**3**). Au lieu de cela, une liaison Ni-Csp^3 a été formée, conduisant au complexe neutre $[Ni\{C_3H_3N_2[C(Me)(=NDipp)]_2\}Cl]$ (**4**) contenant un ligand de type pinceur $N^{imine}CHN^{imine}$ dans lequel l'atome donneur central est un carbone de type Csp^3. Des études théoriques ont montré que ce fait hautement inhabituel dans la chimie NHC du nickel était dû aux contraintes stériques induites par les N-substituants qui empêchent la formation de la liaison Ni-H.

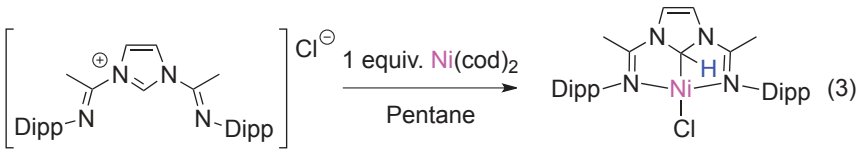

3 **4**

De manière remarquable, l'éthylène s'insère dans la liaison Csp^3-H sans formation de Ni-hydrure, ce qui suggère de nouvelles voies pour l'alkylation de liaisons C-H non activées.

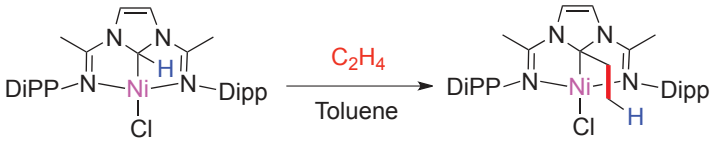

4 **6**

GDCh Communications Angewandte International Edition Chemie

Oxidative Addition

International Edition: DOI: 10.1002/anie.201706581
German Edition: DOI: 10.1002/ange.201706581

Tritopic NHC Precursors: Unusual Nickel Reactivity and Ethylene Insertion into a C(sp^3)–H Bond

Xiaoyu Ren, Christophe Gourlaouen, Marcel Wesolek, and Pierre Braunstein**

Abstract: *The imidazolium chloride $[C_3H_3N(C_3H_6NMe_2)N\{C(Me)(=NDipp)\}]Cl$ (**1**; Dipp = 2,6-diisopropyl phenyl), a potential precursor to a tritopic $N^{imine}C^{NHC}N^{amine}$ pincer-type ligand, reacted with $[Ni(cod)_2]$ to give the Ni^{I}-Ni^{I} complex **2**, which contains a rare cod-derived η^3-allyl-type bridging ligand. The implied intermediate formation of a nickel hydride through oxidative addition of the imidazolium C–H bond did not occur with the symmetrical imidazolium chloride $[C_3H_3N_2\{C(Me)(=NDipp)\}_2]Cl$ (**3**). Instead, a Ni–C(sp^3) bond was formed, leading to the neutral $N^{imine}CHN^{imine}$ pincer-type complex $Ni[C_3H_3N_2\{C(Me)(=NDipp)\}_2]Cl$ (**4**). Theoretical studies showed that this highly unusual feature in nickel NHC chemistry is due to steric constraints induced by the N substituents, which prevent Ni–H bond formation. Remarkably, ethylene inserted into the C(sp^3)–H bond of **4** without nickel hydride formation, thus suggesting new pathways for the alkylation of non-activated C–H bonds.*

Owing to their often unique stereoelectronic properties and easy tunability through wing-tip or remote (backbone) functionalization, N-heterocyclic carbenes (NHCs) have become ubiquitous in numerous branches of chemistry, with fast-growing applications in organic and inorganic synthesis, homogeneous and supported catalysis, medicinal chemistry, photophysics, and material science.[1] Reflecting the considerable interest for pincer-type ligands,[2] the number of such ligands containing NHC donor(s) has grown very fast in recent years. In addition to the NHC donor group, the N substituents forming the pincer system allow fine-tuning of the stability and electronic, catalytic, or photophysical properties of the resulting complexes. This is illustrated below by the unusual behaviour of an imidazolium C(sp^2)–H bond toward Ni^0 and subsequent insertion of ethylene into a C(sp^3)–H bond.

Since nickel is a cheap and versatile metal with considerable scope, for example, in catalytic C–C bond formation,[3] we examined the structural and chemical consequences of introducing amine and/or imine donors as N substituents in hybrid NHC ligands[4] and the possible occurrence of metal–ligand cooperation.[5] Imine donors are key contributors to the non-innocent redox behaviour[6] of the catalytically highly relevant 2,6-bis(imino)pyridines in base-metal complexes.[7] To access potentially tritopic $N^{imine}C^{NHC}N^{amine}$ pincer-type ligands, we prepared the imidazolium salt $[C_3H_3N(C_3H_6NMe_2)N\{C(Me)(=NDipp)\}]Cl$ (**1**; Dipp = 2,6-diisopropyl phenyl) according to Equation (1) (see the Supporting Information).

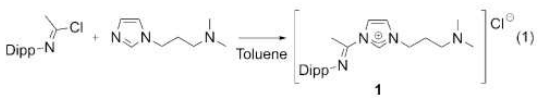

Since Ni^0 usually readily inserts into the C(sp^2)–H bond of imidazolium salts,[8–10] **1** was reacted with $[Ni(cod)_2]$ (cod = cycloocta-1,5-diene) in THF at room temperature [Eq. (2)]. The red-coloured complex **2** was isolated and characterized by X-ray diffraction (Figure 1).

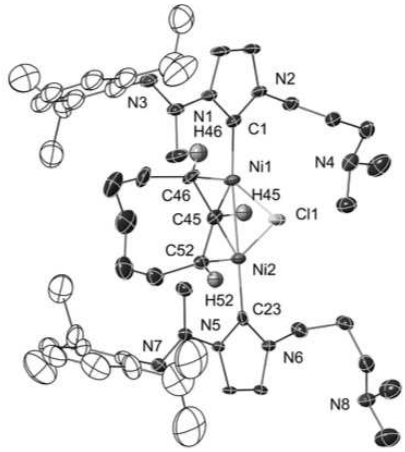

Figure 1. Structure of **2** with H atoms omitted for clarity, except for those on the η^3-cyclooctenyl moiety. Thermal ellipsoids are shown at 30% probability. Selected bond lengths [Å] and angles [deg]: Ni1–Ni2 2.415(1), C1–Ni1 1.868(7), C23–Ni2 1.857(6), C45–C46 1.467(9), C45–C52 1.443(9), C45–Ni1 2.159(6), C45–Ni2 2.142(6), C46–Ni1 1.920(8), C52–Ni2 1.921(6), Cl1–Ni1 2.234(2), Cl1–Ni2 2.235(2); N1-C1-N2 103.2(5), N5-C23-N6 103.0(5), C1-Ni1-Ni2 169.7(2), C23-Ni2-Ni1 167.2(2), C46-C45-C52 131.6(7).[19]

[*] X. Ren, Dr. M. Wesolek, Dr. P. Braunstein
Laboratoire de Chimie de Coordination
Institut de Chimie (UMR 7177 CNRS), Université de Strasbourg
4 rue Blaise Pascal, 67081 Strasbourg Cedex (France)
E-mail: wesolek@unistra.fr
braunstein@unistra.fr
Dr. C. Gourlaouen
Laboratoire de Chimie Quantique
Institut de Chimie (UMR 7177 CNRS), Université de Strasbourg
4 rue Blaise Pascal, 67081 Strasbourg Cedex (France)
Supporting information and the ORCID identification number(s) for the author(s) of this article can be found under: https://doi.org/10.1002/anie.201706581.

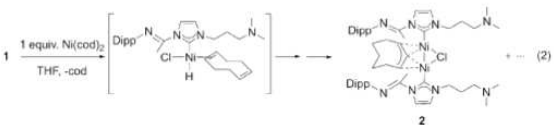

2

The formation of this unexpected dinuclear Ni^{I} complex should involve a reactive Ni^{II} hydride intermediate containing a η^2-coordinated 1,5-cod ligand, the insertion of which into the Ni–H bond and subsequent isomerization would lead to the bridging η^3-allyl moiety.[11] The Ni^{I}–Ni^{I} bond is further supported by a chloride, while a monodentate NHC is bound to each metal to form an almost linear C1-Ni-Ni-C23 array.[12c]

The Ni–Ni distance of 2.415(1) Å is consistent with metal–metal bonding between the two d^9 centres.[12a] To the best of our knowledge, there is only one precedent (Ru) for a cod-derived bridging η^3-allyl-type ligand,[13] and very few dinuclear Ni complexes with bridging allyl-type ligands have been reported.[12] The unexpected dangling nature of both N donors in the $N^{imine}C^{NHC}N^{amine}$ ligand of **2** prompted us to react the bis-imine imidazolium salt **3** with $[Ni(cod)_2]$ with the aim to form a $N^{imine}C^{NHC}N^{imine}$ pincer [Eq. (3)]. To our

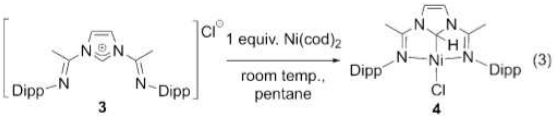

3 4

surprise, the imidazolium proton was not removed by oxidative addition and the imidazole C1 had instead become sp^3 hybridized. The square-planar Ni^{II} complex **4** thus contains a tridentate $N^{imine}CN^{imine}$ pincer ligand and a chloride (Figure 2). This behavior is exceptional for Ni^0 complexes;[14] they are usually highly competent for such C–H oxidative addition reactions, which represent an entry point for industrially important stoichiometric or catalytic C–C bond formation reactions.[15]

The Ni–C1 bond (1.828(3) Å) is rather short, the C1–N1 and C1–N2 distances correspond to single bonds, and the imidazole ring forms an angle of 64.0(1)° with the C1–H1

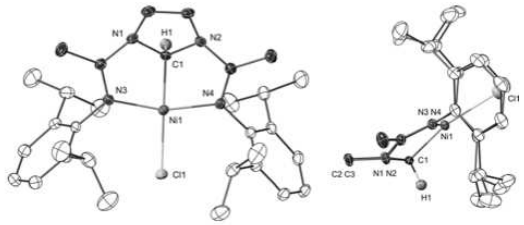

Figure 2. Views of the structure of **4** with H atoms omitted for clarity, except for the NC*H*N H atoms. Thermal ellipsoids are shown at 30% probability. Selected bond lengths [Å] and angles [deg]: C1–N1 1.448(3), C1–N2 1.446(3), C1–Ni 1.828(3), N3–Ni 1.929(2), N4–Ni 1.939(2), Cl1–Ni 2.236(7); N1-C1-Ni 104.6(2), N1-C1-Ni 113.3(2), N2-C1-Ni 112.9(2), H1-C1-Ni1 108.6.[19]

bond. In the ^{1}H NMR spectrum, the broad singlet at $\delta = 5.73$ (in $[D_8]$toluene) or septet (in CD_3CN, $^5J(H,H) = 1.1$ Hz) for C1–H1 and the ^{13}C NMR resonance of C1 at $\delta = 87.3$ ($^1J(C,H) = 159$ Hz) are consistent with such a $C(sp^3)$–H group (see the Supporting Information).[14]

The lack of oxidative addition of the imidazolium C1–H1 bond to Ni^0 in Equation (3) contrasts with the reaction of Equation (2), and is even more surprising considering the easy formation of the nickel hydride complex **5** with a closely related NHC phosphorus-based system.[16]

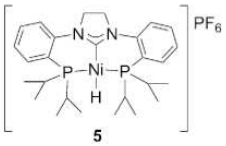

5

To shed some light on the reasons for our unusual findings, a comparative theoretical analysis was performed (see the Supporting Information) on both **4** and **5**. Neither ELF nor NCI analyses showed intramolecular interactions involving the C1–H1 proton in **4** (Figure 3 and the Supporting

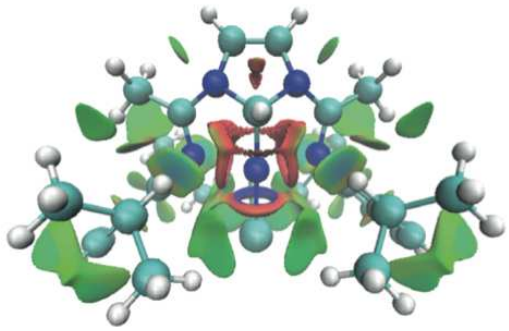

Figure 3. NCI analysis of complex **4**. Basins in red represent steric congestion, and those in green represent attractive van der Walls interactions.

Information), which is consistent with the structural and ^{1}H NMR data. The lack of Ni insertion into the imidazolium $N_2C(sp^2)$–H bond could be due either to the instability of the product compared to the reactants or to a transition state too high in energy. Whereas formation of **5** by Ni insertion into such a bond in the corresponding imidazolium salt **5a** is exothermic ($\Delta G = -15.1$ kcal mol^{-1}), going from **4** to **4a** (equivalent of **5**) is clearly disfavoured ($\Delta G = +24.4$ kcal mol^{-1}). Access to an NHC complex (**4b**) by HCl elimination from **4** would again be highly endothermic ($\Delta G = +48.9$ kcal mol^{-1}). Our experimental and theoretical results clearly establish a major reactivity difference between the $C(sp^2)$–H bond of the PCHP and $N^{imine}CHN^{imine}$ imidazolium precursors.

When tracing the origin of this difference (see Supporting Information), we noticed that in the carbenic forms **4a** and **4b**

(which have different oxidation state), the nickel atom remains out of the $N^{imine}C^{NHC}N^{imine}$ plane. Forcing the structure to be planar (**4c**) is strongly destabilizing ($\Delta G = +24.1$ kcal mol^{-1}) compared to **4b**: a considerable lengthening of the Ni–N^{imine} distance, from 1.922 Å in **4b** to 2.887 Å in **4c**, has to occur because of the rigidity of the ligand. The short imine C=N bond lengths and the sp^2 nature of the N*C*N carbon atom prevent N^{imine} coordination in **4c**. By contrast, when the metal is out of the heterocycle mean plane, N^{imine} coordination can occur with retention of the planarity of $C(sp^2)$ and of the N-C-N angles. Computational introduction of a second carbon atom (**4d**, see the Supporting Information) between the N^{imine} and the heterocycle is enough to reverse the balance, and formation of the carbene (**4e**) is now possible ($\Delta G = -1.0$ kcal mol^{-1}). Carbene formation is thus controlled by the binding of the pincer arms: if the ligand rigidity disfavours a planar structure as in **4**, the $N^{imine}C^{H}N^{imine}$ ligand will formally be reduced to give a 5-electron donor instead of a 6-electron donor $N^{imine}C^{NHC}N^{imine}$ pincer.

Reaction of a toluene solution of **4** with excess ethylene at room temperature yielded red needles of a new complex **6** in which one molecule of ethylene has inserted into the imidazolium $C(sp^3)$–H bond to give a C-ethyl moiety [Eq. (4)], while the pincer structure remains almost unaf-

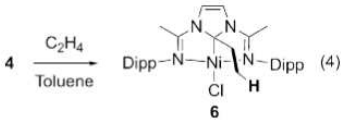

(4)

fected (Figure 4). There is excellent agreement between the experimental and calculated structures of **6**. Whereas with **5**, ethylene insertion occurred as expected into the Ni–H bond and was followed by ethyl migration to the C1 carbon,[16] we have no evidence for even the transient formation of a Ni hydride, and calculations clearly indicate that such a species would be too high in energy. Thus, another mechanism must be operative in our case. The steric constraints that trap the complex in a structure of type **4** may also weaken the Ni–N^{imine} bond and allow its opening. This facilitates access of an ethylene molecule and its subsequent insertion into the C–H bond. The computed intermediate **6a** (see the Supporting Information) is only $\Delta G = 9.4$ kcal mol^{-1} above the separated fragments (complex **4** and ethylene) and is thus accessible. In a control experiment, no reaction occurred when the imidazolium salt **3** was exposed to ethylene under the same conditions.

In conclusion, we have found that depending on the N functionalities present in tritopic NHC precursors, Ni^0 inserts into the $N_2C(sp^2)$–H bond to give an unprecedented dinuclear Ni^I complex with a cod-derived allyl-type bridging ligand. In contrast, no oxidative addition of this imidazolium C–H bond occurs when two lateral N^{imine} donors are present, owing to geometrical constraints in the pincer system. These constraints also account for the observations made in a PCP pincer system with Pd and Pt,[17] and a six-membered NHC with Ni.[14] The key role played by the ligand architecture in preventing the expected $N_2C(sp^2)$–H bond activation and favouring in **4** the formation of a covalent bond between the Ni^{II} centre and the $N_2C(sp^3)$–H carbon atom was demonstrated theoretically.

The alkylation of non-activated $C(sp^3)$–H bonds, as observed in the reaction of **4** with ethylene, remains a major challenge of considerable interest and relevance to organic synthesis and catalytic chain-growth processes.[18] Our results suggest that the partial decoordination of "strong pincers" may occur more frequently than expected and that new reactivity pathways may be accessible through suitable ligand design and metal–ligand cooperativity.

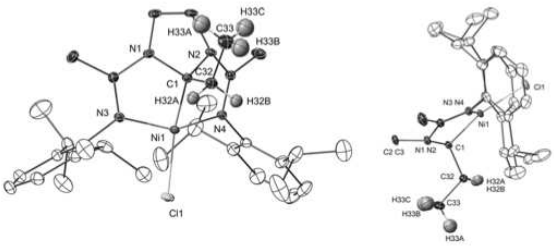

Figure 4. Views of the structure of complex **6** with H atoms omitted for clarity, except the ethyl H atoms on C32 and C33. Thermal ellipsoids are shown at 30% probability. Selected bond lengths [Å] and angles [deg]: C1–C32 1.534(2), C1–N1 1.460(2), C1–N2 1.471(2), C1–Ni1 1.867(2), N3–Ni1 1.936(1), N4–Ni1 1.948(1), Cl1–Ni1 2.2438(4); N1-C1-N2 102.7(1), N1-C1-Ni1 110.2(1), N2-C1-Ni1 110.2(1), C32-C1-Ni1 111.2(1).[19]

Acknowledgements

We are grateful to the China Scholarship Council for a PhD grant to X.R. We thank Marc Mermillon-Fournier for technical assistance, the CNRS and the MESR (Paris) for funding, and the Service de Radiocristallographie (UdS) for determination of the crystal structures.

Conflict of interest

The authors declare no conflict of interest.

Keywords: alkylation · N-heterocyclic carbenes · nickel · oxidative addition · pincer ligands

How to cite: *Angew. Chem. Int. Ed.* **2017**, *56*, 12557–12560
Angew. Chem. **2017**, *129*, 12731–12734

[1] Selected recent reviews: a) F. E. Hahn, M. C. Jahnke, *Angew. Chem. Int. Ed.* **2008**, *47*, 3122–3172; *Angew. Chem.* **2008**, *120*, 3166–3216; b) P. de Frémont, N. Marion, S. P. Nolan, *Coord. Chem. Rev.* **2009**, *253*, 862–892; c) S. Díez-González, N. Marion, S. P. Nolan, *Chem. Rev.* **2009**, *109*, 3612–3676; d) D. G. Gusev, *Organometallics* **2009**, *28*, 763–770; e) H. Jacobsen, A. Correa, A. Poater, C. Costabile, L. Cavallo, *Coord. Chem. Rev.* **2009**, *253*, 687–703; f) C. S. J. Cazin, *N-Heterocyclic Carbenes in Transition*

Metal Catalysis and Organocatalysis, Springer, Netherlands, **2010**; g) M. N. Hopkinson, C. Richter, M. Schedler, F. Glorius, *Nature* **2014**, *510*, 485 – 496; h) D. M. Flanigan, F. Romanov-Michailidis, N. A. White, T. Rovis, *Chem. Rev.* **2015**, *115*, 9307 – 9387; i) A. Nasr, A. Winkler, M. Tamm, *Coord. Chem. Rev.* **2016**, *316*, 68 – 124; j) E. Peris, *Chem. Rev.* **2017**, DOI: 10.1021/acs.chemrev.6b00695; k) S. Hameury, P. de Frémont, P. Braunstein, *Chem. Soc. Rev.* **2017**, *46*, 632 – 733; l) V. Charra, P. de Frémont, P. Braunstein, *Coord. Chem. Rev.* **2017**, *341*, 53 – 176.

[2] Selected examples: a) *The Chemistry of Pincer Compounds*, 1st ed. (Eds.: D. Morales-Morales, C. M. Jensen), Elsevier, Amsterdam, **2007**; b) D. Morales-Morales, *Mini-Rev. Org. Chem.* **2008**, *5*, 141 – 152; c) *Organometallic Pincer Chemistry* (Eds.: G. van Koten, D. Milstein), Springer, Berlin, **2013**; d) N. Darmawan, C.-H. Yang, M. Mauro, M. Raynal, S. Heun, J. Pan, H. Buchholz, P. Braunstein, L. De Cola, *Inorg. Chem.* **2013**, *52*, 10756 – 10765; e) T. Simler, A. A. Danopoulos, P. Braunstein, *Chem. Commun.* **2015**, *51*, 10699 – 10702; f) T. Simler, P. Braunstein, A. A. Danopoulos, *Angew. Chem. Int. Ed.* **2015**, *54*, 13691 – 13695; *Angew. Chem.* **2015**, *127*, 13895 – 13899; g) *The Privileged Pincer-Metal Platform: Coordination Chemistry & Applications* (Eds.: G. van Koten, R. A. Gossage, Springer, Berlin, **2015**; h) M. Asay, D. Morales-Morales, *Dalton Trans.* **2015**, *44*, 17432 – 17447; i) P. Ai, M. Mauro, L. De Cola, A. A. Danopoulos, P. Braunstein, *Angew. Chem. Int. Ed.* **2016**, *55*, 3338 – 3341; *Angew. Chem.* **2016**, *128*, 3399 – 3402; j) T. Simler, P. Braunstein, A. A. Danopoulos, *Chem. Commun.* **2016**, *52*, 2717 – 2720; k) P. J. Chirik, *Angew. Chem. Int. Ed.* **2017**, *56*, 5170 – 5181; *Angew. Chem.* **2017**, *129*, 5252 – 5265; l) R. Zhong, A. C. Lindhorst, F. J. Groche, F. E. Kühn, *Chem. Rev.* **2017**, *117*, 1970 – 2058.

[3] Selected examples: a) F. Speiser, P. Braunstein, L. Saussine, *Acc. Chem. Res.* **2005**, *38*, 784 – 793; b) S. Miyazaki, Y. Koga, T. Matsumoto, K. Matsubara, *Chem. Commun.* **2010**, *46*, 1932 – 1934; c) B. M. Rosen, K. W. Quasdorf, D. A. Wilson, N. Zhang, A.-M. Resmerita, N. K. Garg, V. Percec, *Chem. Rev.* **2011**, *111*, 1346 – 1416; d) W. Keim, *Angew. Chem. Int. Ed.* **2013**, *52*, 12492 – 12496; *Angew. Chem.* **2013**, *125*, 12722 – 12726; e) T. Mesganaw, N. K. Garg, *Org. Process Res. Dev.* **2013**, *17*, 29 – 39; f) S. Z. Tasker, E. A. Standley, T. F. Jamison, *Nature* **2014**, *509*, 299 – 309; g) M. Henrion, V. Ritleng, M. J. Chetcuti, *ACS Catal.* **2015**, *5*, 1283 – 1302; h) H. Mu, L. Pan, D. Song, Y. Li, *Chem. Rev.* **2015**, *115*, 12091 – 12137; i) A. P. Prakasham, P. Ghosh, *Inorg. Chim. Acta* **2015**, *431*, 61 – 100.

[4] a) P. Braunstein, F. Naud, *Angew. Chem. Int. Ed.* **2001**, *40*, 680 – 699; *Angew. Chem.* **2001**, *113*, 702 – 722; b) W.-H. Zhang, S. W. Chien, T. S. A. Hor, *Coord. Chem. Rev.* **2011**, *255*, 1991 – 2024.

[5] J. R. Khusnutdinova, D. Milstein, *Angew. Chem. Int. Ed.* **2015**, *54*, 12236 – 12273; *Angew. Chem.* **2015**, *127*, 12406 – 12445.

[6] a) P. J. Chirik, K. Wieghardt, *Science* **2010**, *327*, 794 – 795; b) P. J. Chirik, *Acc. Chem. Res.* **2015**, *48*, 1687 – 1695.

[7] a) B. L. Small, M. Brookhart, A. M. A. Bennett, *J. Am. Chem. Soc.* **1998**, *120*, 4049 – 4050; b) S. Mecking, *Angew. Chem. Int. Ed.* **2001**, *40*, 534 – 540; *Angew. Chem.* **2001**, *113*, 550 – 557; c) M. W. Bouwkamp, A. C. Bowman, E. Lobkovsky, P. J. Chirik, *J. Am. Chem. Soc.* **2006**, *128*, 13340 – 13341; d) V. C. Gibson, C. Redshaw, G. A. Solan, *Chem. Rev.* **2007**, *107*, 1745 – 1776; e) D. Takeuchi, *Dalton Trans.* **2010**, *39*, 311 – 328; f) B. Burcher, P.-A. R. Breuil, L. Magna, H. Olivier-Bourbigou in *Iron Catalysis II* (Ed.: E. Bauer), Springer, Cham, **2015**, pp. 217 – 257.

[8] T. Steinke, B. K. Shaw, H. Jong, B. O. Patrick, M. D. Fryzuk, *Organometallics* **2009**, *28*, 2830 – 2836.

[9] S. Gründemann, M. Albrecht, A. Kovacevic, J. W. Faller, R. H. Crabtree, *J. Chem. Soc. Dalton Trans.* **2002**, 2163 – 2167.

[10] A. C. Badaj, G. G. Lavoie, *Organometallics* **2012**, *31*, 1103 – 1111.

[11] a) H. Bönnemann, C. Krüger, Y.-H. Tsay, *Angew. Chem. Int. Ed. Engl.* **1976**, *15*, 46 – 47; *Angew. Chem.* **1976**, *88*, 50 – 51; b) P. Braunstein, T. Faure, M. Knorr, T. Stährfeldt, A. DeCian, J. Fischer, *Gazz. Chem. Ital.* **1995**, *125*, 35 – 50; c) N. A. Eberhardt, H. Guan, *Chem. Rev.* **2016**, *116*, 8373 – 8426.

[12] a) R. Hanko, *Angew. Chem. Int. Ed. Engl.* **1985**, *24*, 704 – 705; *Angew. Chem.* **1985**, *97*, 707 – 708; b) M. J. Chetcuti in *Comprehensive Organometallic Chemistry II*, *Vol. 9* (Eds.: E. W. Abel, F. G. A. Stone, G. Wilkinson), Pergamon, Oxford, **1995**, pp. 107 – 191; c) D. P. Hruszkewycz, J. Wu, J. C. Green, N. Hazari, T. J. Schmeier, *Organometallics* **2012**, *31*, 470 – 485; d) J. Wu, A. Nova, D. Balcells, G. W. Brudvig, W. Dai, L. M. Guard, N. Hazari, P.-H. Lin, R. Pokhrel, M. K. Takase, *Chem. Eur. J.* **2014**, *20*, 5327 – 5337.

[13] J. A. Cabeza, I. del Río, M. Gille, M. C. Goite, E. Pérez-Carreño, *Organometallics* **2008**, *27*, 609 – 616.

[14] R. M. Brown, J. Borau Garcia, J. Valjus, C. J. Roberts, H. M. Tuononen, M. Parvez, R. Roesler, *Angew. Chem. Int. Ed.* **2015**, *54*, 6274 – 6277; *Angew. Chem.* **2015**, *127*, 6372 – 6375.

[15] a) W. Keim, *Angew. Chem. Int. Ed. Engl.* **1990**, *29*, 235 – 244; *Angew. Chem.* **1990**, *102*, 251 – 260; b) S. Sengupta, M. Leite, D. S. Raslan, C. Quesnelle, V. Snieckus, *J. Org. Chem.* **1992**, *57*, 4066 – 4068; c) J. F. Hartwig, *Organotransition Metal Chemistry: From Bonding to Catalysis*, University Science Books, Sausalito, **2010**; d) A. R. Ehle, Q. Zhou, M. P. Watson, *Org. Lett.* **2012**, *14*, 1202 – 1205; e) R. H. Crabtree, *The Organometallic Chemistry of the Transition Metals*, Wiley, Hoboken, **2014**.

[16] T. Steinke, B. K. Shaw, H. Jong, B. O. Patrick, M. D. Fryzuk, J. C. Green, *J. Am. Chem. Soc.* **2009**, *131*, 10461 – 10466.

[17] B. Pan, S. Pierre, M. W. Bezpalko, J. W. Napoline, B. M. Foxman, C. M. Thomas, *Organometallics* **2013**, *32*, 704 – 710.

[18] a) J. A. Labinger, J. E. Bercaw, *Nature* **2002**, *417*, 507 – 514; b) J. D. Lawrence, M. Takahashi, C. Bae, J. F. Hartwig, *J. Am. Chem. Soc.* **2004**, *126*, 15334 – 15335; c) T. W. Lyons, M. S. Sanford, *Chem. Rev.* **2010**, *110*, 1147 – 1169; d) J. Wencel-Delord, T. Droge, F. Liu, F. Glorius, *Chem. Soc. Rev.* **2011**, *40*, 4740 – 4761; e) S. H. Cho, J. Y. Kim, J. Kwak, S. Chang, *Chem. Soc. Rev.* **2011**, *40*, 5068 – 5083; f) K. M. Engle, T.-S. Mei, M. Wasa, J.-Q. Yu, *Acc. Chem. Res.* **2012**, *45*, 788 – 802; g) D. A. Colby, A. S. Tsai, R. G. Bergman, J. A. Ellman, *Acc. Chem. Res.* **2012**, *45*, 814 – 825; h) G. Rouquet, N. Chatani, *Angew. Chem. Int. Ed.* **2013**, *52*, 11726 – 11743; *Angew. Chem.* **2013**, *125*, 11942 – 11959; i) Y. Aihara, N. Chatani, *J. Am. Chem. Soc.* **2014**, *136*, 898 – 901; j) J. B. Smith, A. J. M. Miller, *Organometallics* **2015**, *34*, 4669 – 4677; k) R. Zhou, H. Liu, H. Tao, X. Yu, J. Wu, *Chem. Sci.* **2017**, *8*, 4654 – 4659.

[19] CCDC 1409335, 1409336, 1409337, 1409338, 1409339 and 1409340 contain the supplementary crystallographic data for this paper. These data can be obtained free of charge from The Cambridge Crystallographic Data Centre.

Manuscript received: June 28, 2017
Accepted manuscript online: July 31, 2017
Version of record online: August 31, 2017

2. Supporting Information

Tritopic NHC Precursors: Unusual Nickel Reactivity and Ethylene Insertion into a C_{sp3}-H Bond

Xiaoyu Ren,[a] Christophe Gourlaouen,[b] Marcel Wesolek,[a] and Pierre Braunstein*[a]*

[a] Laboratoire de Chimie de Coordination, Institut de Chimie (UMR 7177 CNRS), Université de Strasbourg, 4 rue Blaise Pascal, 67081 Strasbourg Cedex (France)

E-mail: braunstein@unistra.fr

[b] Laboratoire de Chimie Quantique, Institut de Chimie (UMR 7177 CNRS), Université de Strasbourg, 4 rue Blaise Pascal, 67081 Strasbourg Cedex (France)

3. Experimental Procedures & Results and Discussion

Synthesis and characterization

3.1 General methods

All manipulations involving organometallics were performed under nitrogen or argon in a Braun glove-box or using standard Schlenk techniques. Solvents were dried using standard methods and distilled under nitrogen prior use or passed through columns of activated alumina and subsequently purged with nitrogen or argon. The starting materials **1**[1,2] and **3**[2] were prepared according to the literature.

Preparation of [(ImH){C(Me)=NDipp}(C_3NMe_2)]Cl (1).

To a solution of 3-(1*H*-imidazol-1-yl)-*N*,*N*-dimethylpropan-1-amine (6.50 g, 42.4 mmol) in toluene (10 mL) was added dropwise (*E*)-*N*-(2,6-diisopropylphenyl)acetimidoyl chloride (10.08 g, 42.4 mmol). The reaction mixture was stirred overnight at room temperature. A precipitate formed that was collected by filtration, and washed with Et_2O to give a white powder (15.5 g, 93%). ^{1}H NMR (300 MHz, $CDCl_3$): δ 12.20 (apparent t, $^{3,4}J$ = 1.3 Hz, 1H, $CH^{imidazole}$), 8.17 (apparent t, $^{3,4}J$ = 1.8 Hz, 1H, $CH^{imidazole}$), 7.58 (apparent t, $^{3,4}J$ = 1.6 Hz, 1H, $CH^{imidazole}$), 7.16 (br s, 3H, CH^{Ar}), 4.69 (t, ^3J = 6.8 Hz, 2H, $CH_2CH_2CH_2NMe_2$), 2.59 (sept, ^3J = 6.8 Hz, 2H, CH^{iPr}), 2.55 (s, 3H, CH_3^{imine}), 2.52 (t, ^3J = 6.8 Hz, 2H, $CH_2CH_2CH_2NMe_2$), 2.31 (s, 6H, $CH_2CH_2CH_2NMe_2$), 2.35−2.26 (m, partly overlapped, 2H, $CH_2CH_2CH_2NMe_2$), 1.14 (d, ^3J = 6.8 Hz, 6H, CH_3^{iPr}), 1.10 (d, ^3J = 6.8 Hz, 6H, CH_3^{iPr}). ^{13}C NMR (126 MHz, $CDCl_3$) δ 148.8 (C^{imine}), 140.7 ($C^{ipso\text{-}Ar}$), 139.3 ($CH^{imidazole}$), 136.6 ($C^{o\text{-}Ar}$), 125.7 ($CH^{p\text{-}Ar}$), 123.7 ($CH^{m\text{-}Ar}$), 123.2 ($CH^{imidazole}$), 117.2 ($CH^{imidazole}$), 55.1 ($CH_2CH_2CH_2NMe_2$), 48.4 ($CH_2CH_2CH_2NMe_2$), 45.0 ($CH_2CH_2CH_2NMe_2$), 28.6 (CH^{iPr}), 27.7 ($CH_2CH_2CH_2NMe_2$), 23.3 (CH^{iPr}), 23.0 (CH_3^{iPr}), 17.2 (CH_3^{imine}). Anal. calcd. for $C_{22}H_{35}N_4Cl$: C, 67.58; H, 9.02; N, 14.33%; found: C, 66.78; H, 9.21; N, 14.43% (despite several attempts, no better carbon analysis could be obtained).

Preparation of [Ni(μ-h3-C8H13)(μ-Cl){Im[C(Me)=NDipp](C3NMe2)}]2 (2).

To a suspension of [(ImH){C(Me)=NDipp}(C_3NMe_2)]Cl (0.100 g, 0.256 mmol) in THF (20 mL) was added [Ni(cod)$_2$] (0.071 g, 0.258 mmol) at room temperature under magnetic stirring. After the reaction mixture was stirred for 24 h, the solvent was

evaporated under reduced pressure, and then pentane was added (10 ml). After filtration, the filtrate was slowly evaporated and X-ray quality dark red crystals were obtained (0.058 g, yield isolated product 47%). Anal. calcd. for $C_{52}H_{81}ClN_8Ni_2$: C, 64.31; H, 8.41; N, 11.54%; found: C, 61.87; H, 8.19; N, 10.35% (despite several attempts, no better carbon analysis could be obtained).

The ^{1}H NMR spectrum of compound **2** in C_6D_6 presents four sets of sharp signals that could be clearly attributed to CH_3^{imine}, CH_3^{amine} and the backbones of the NHC ligand. The pattern of the ^{1}H NMR spectrum was similar in toluene-d_8 and THF-d_8. From the comparison between the enlarged views of the backbone resonances (Figure S2, S5 and S7), two sets of peaks (a and d) have always the same intensities, irrespective of the solvent used, but the ratio between these isomers depends on the solvent. In the ^{13}C NMR spectrum, three carbene signals around δ 196 ppm were observed (Figure S3, the intensity of the fourth carbene signal is too small to be seen).

Preparation of [ImH{C(Me)=NDipp}2]Cl (3).

This salt was prepared according to the literature.[2]

Preparation of [NiCl{ImH[C(Me)=NDipp]2}] (4).

To a suspension of **3** (0.100 g, 0.197 mmol) in pentane (20 mL) was added $[Ni(cod)_2]$ (0.055 g, 0.197 mmol) at room temperature and magnetic stirring was maintained for 24 h. The solvent was removed by filtration and the solid was extracted with toluene (4 ml) and X-ray quality orange-red crystals were obtained (0.069 g, yield of isolated product 62%). ^{1}H NMR (500 MHz, toluene-d_8): δ 7.09-6.94 (m, 6H, $CH^{p\text{-Ar}}$, $CH^{m\text{-Ar}}$ and toluene-d_8), 5.73 (s, 1H, C_{sp3}-$H^{imidazole}$), 5.59 (s, 2H, C_{sp2}-$H^{imidazole}$), 3.86 (sept, ^3J = 6.9 Hz, 2H, $CH^{i\text{Pr}}$), 3.02 (sept, ^3J = 6.9 Hz, 2H, $CH^{i\text{Pr}}$), 1.80 (d, ^3J = 6.9 Hz, 6H, $CH_3^{i\text{Pr}}$), 1.55 (d, ^3J = 6.9 Hz, 6H, $CH_3^{i\text{Pr}}$), 1.19 (d, ^3J = 6.9 Hz, 6H, $CH_3^{i\text{Pr}}$), 1.10 (d, ^3J = 6.9 Hz, 6H, $CH_3^{i\text{Pr}}$, overlapped with CH_3^{imine}), 1.09 (s, 6H, CH_3^{imine}). ^{13}C NMR (126 MHz, toluene-d_8) δ 162.1 (C^{imine}), 142.3, 141.8, 141.0 ($C^{o\text{-Ar, }ipso\text{-Ar}}$), 126.6 ($CH^{p\text{-Ar}}$), 123.6, 123.1 ($CH^{m\text{-Ar}}$), 117.5 ($C_{sp2}$-$H^{imidazole}$), 87.3 ($C_{sp3}$-$H^{imidazole}$, ^1J(C,H) = 159 Hz), 29.0, 28.8 ($CH^{i\text{Pr}}$), 24.7, 24.5, 24.0, 23.3 ($CH_3^{i\text{Pr}}$), 14.1 (CH_3^{imine}). Anal. calcd. for $C_{31}H_{43}N_4ClNi$: C, 65.80; H, 7.66; N, 9.90%; found: C, 60.43; H, 7.27; N, 8.59% (despite several attempts, no better carbon analysis could be obtained).

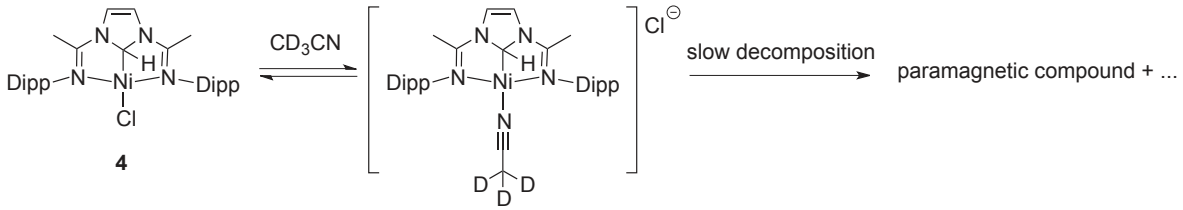

The ^{1}H NMR spectrum of compound **4** in CD_3CN presents two sets of signals which correspond to symmetrical compounds with a long range coupling (^{5}J = 1.1 Hz) between the CH_3^{imine} and C_{sp3}-$H^{imidazolyl}$ protons (Figure S9 and S11). If one set of signals (a) could be compound **4**, the other (b) could be attributed to the compound in which the chloride ligand has been substituted by CD_3CN. These compounds are not stable over longer periods of time (days), and give intractable paramagnetic compounds. In ^{13}C NMR, there are also two sets of signals consistent with the presence of two similar compounds (Figure S12).

Preparation of [NiCl{ImEt[C(Me)=NDipp]2}] (6).

To a solution of **4** (0.100 g, 0.177 mmol) in toluene (10 mL) was added excess ethylene at room temperature. After several days, X-ray quality red crystals were obtained from the toluene solution (0.084 g, isolated yield 80%). ^{1}H NMR (500 MHz, toluene-d_8): δ 7.10-6.94 (m, 6H, $CH^{p\text{-Ar}}$, $CH^{m\text{-Ar}}$ and toluene-d_8), 5.55 (s, 2H, C_{sp2}-$H^{imidazole}$), 3.95 (sept, ^{3}J = 6.9 Hz, 2H, $CH^{i\text{Pr}}$), 3.21 (sept, ^{3}J = 6.9 Hz, 2H, $CH^{i\text{Pr}}$), 2.33 (q, ^{3}J = 7.3 Hz, 2H, CH_2^{Et}), 1.73 (d, ^{3}J = 6.9 Hz, 6H, $CH_3^{i\text{Pr}}$), 1.53 (d, ^{3}J = 6.9 Hz, 6H, $CH_3^{i\text{Pr}}$), 1.23 (d, ^{3}J = 6.9 Hz, 6H, $CH_3^{i\text{Pr}}$), 1.15 (s, 6H, CH_3^{imine}), 1.11 (d, ^{3}J = 6.9 Hz, 6H, $CH_3^{i\text{Pr}}$), 1.02 (t, ^{3}J = 7.3 Hz, 3H, CH_3^{Et}). ^{13}C NMR (126 MHz, toluene-d_8) δ 164.6 (C^{imine}), 142.4, 141.9, 141.6 ($C^{o\text{-Ar, }ipso\text{-Ar}}$), 126.6 ($CH^{p\text{-Ar}}$), 123.7, 123.0 ($CH^{m\text{-Ar}}$), 117.2 ($C_{sp2}$-$H^{imidazole}$), 92.9 ($C_{sp3}$-^{imidazole}), 32.3 ($CH_2^{Et}$), 28.9, 28.8 ($CH^{i\text{Pr}}$), 25.1, 24.3, 23.9, 23.3 ($CH_3^{i\text{Pr}}$), 14.5 (CH_3^{imine}), 7.4 (CH_3^{Et}). Anal. calcd. for $C_{33}H_{47}N_4ClNi$ + 0.5 toluene: C, 68.50; H, 8.03; N, 8.75%; found: C, 67.86; H, 7.79; N, 8.09%.

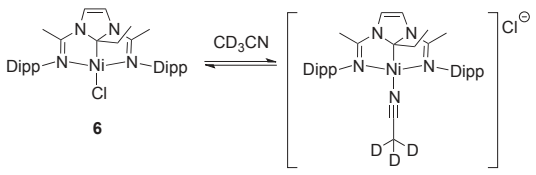

The ^{1}H and ^{13}C NMR, there are also two sets of signals consistent with the presence of two similar compounds (Figure S13 and S14). One set of signals (a) is assigned to **6**, and the other one (b) could be attributed to a compound in which the chloride ligand has

been substituted by CD_3CN. The CD_3CN solution remains stable for a long period of time.

3.2 Partial NMR spectra.

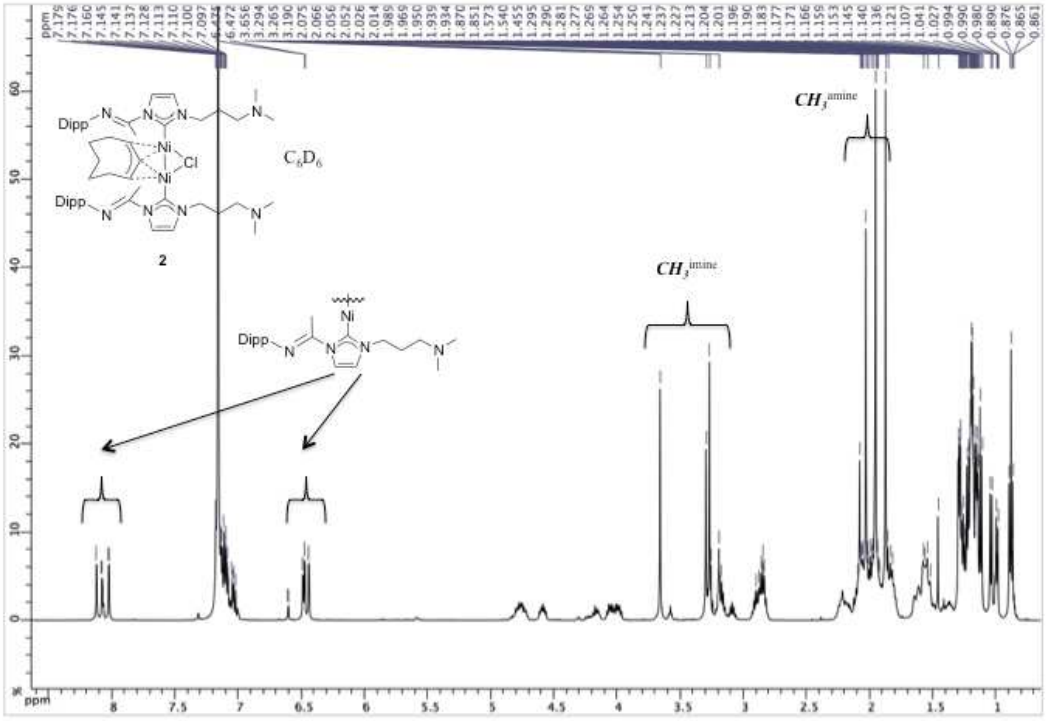

Figure S1. ^1H NMR spectrum of **2** in C_6D_6.

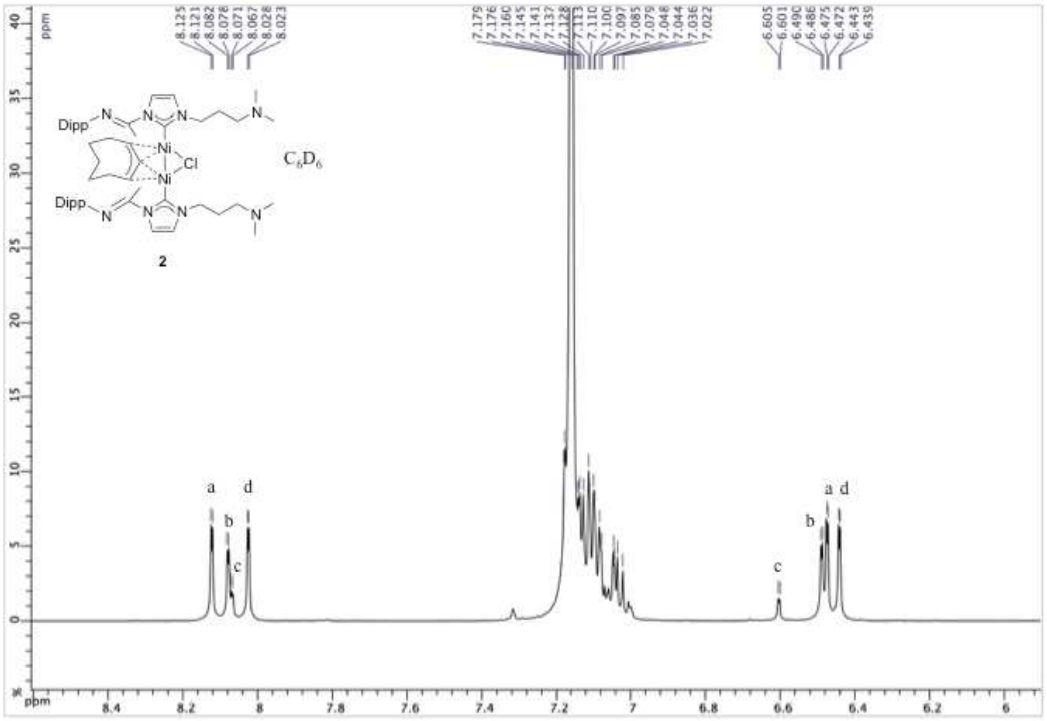

Figure S2. Partial ^{1}H NMR spectrum of 2 in C_6D_6.

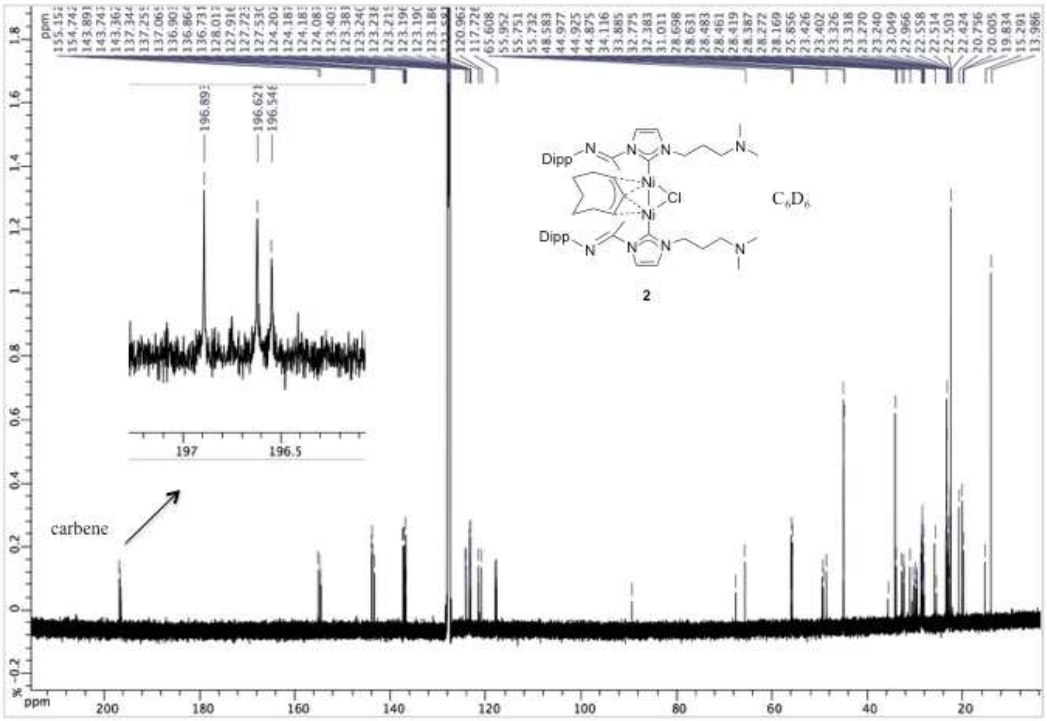

Figure S3. ^{13}C NMR spectrum of **2** in C_6D_6.

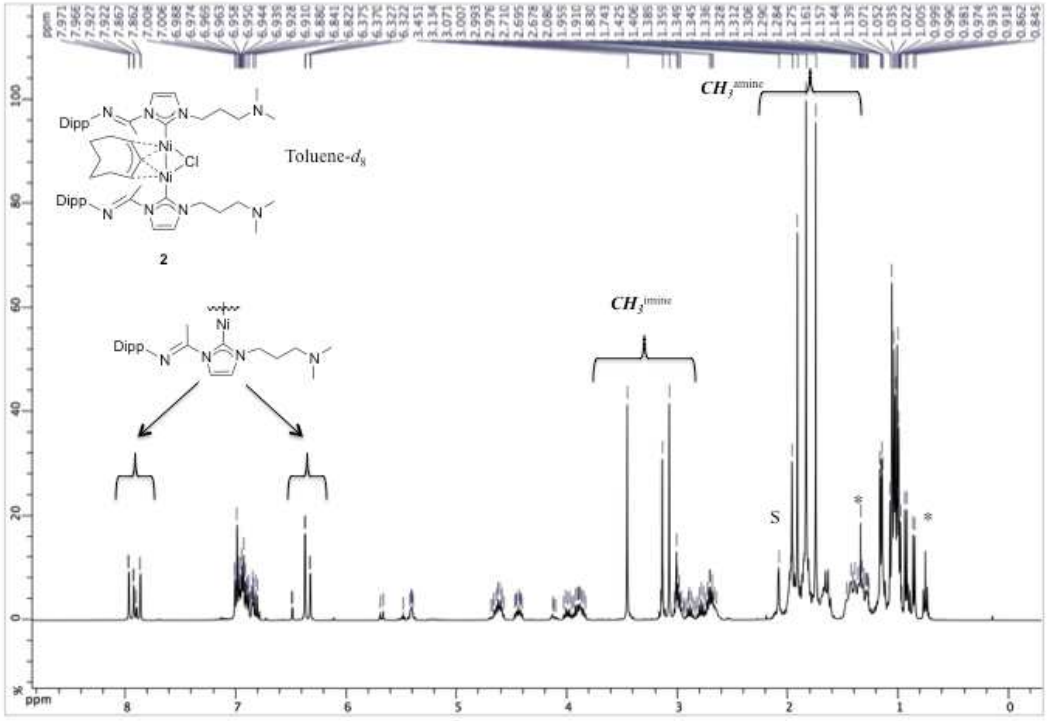

Figure S4. ^{1}H NMR spectrum of **2** in toluene-d_8.

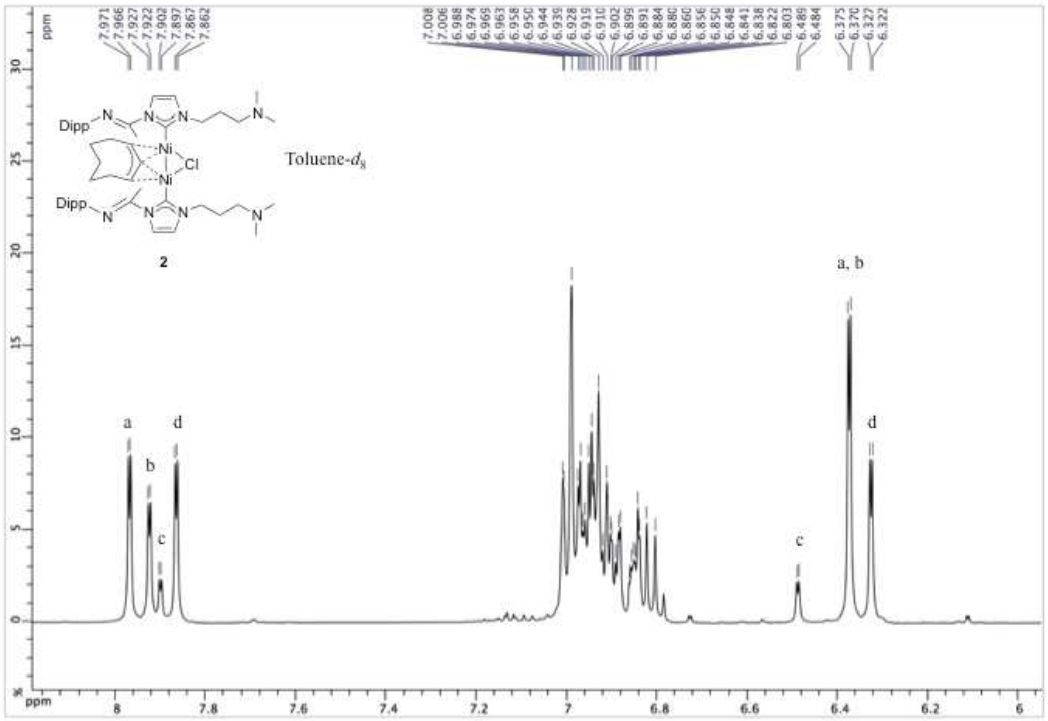

Figure S5. Partial ^{1}H NMR spectrum of **2** in toluene-d_8.

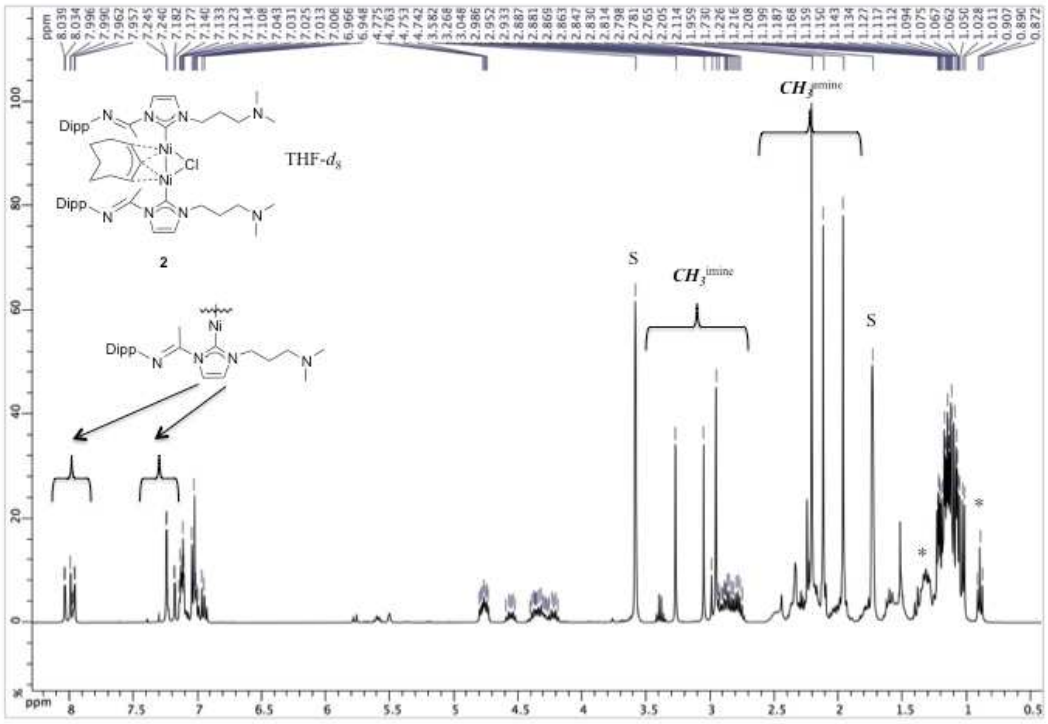

Figure S6. ^{1}H NMR spectrum of **2** in THF-d_8.

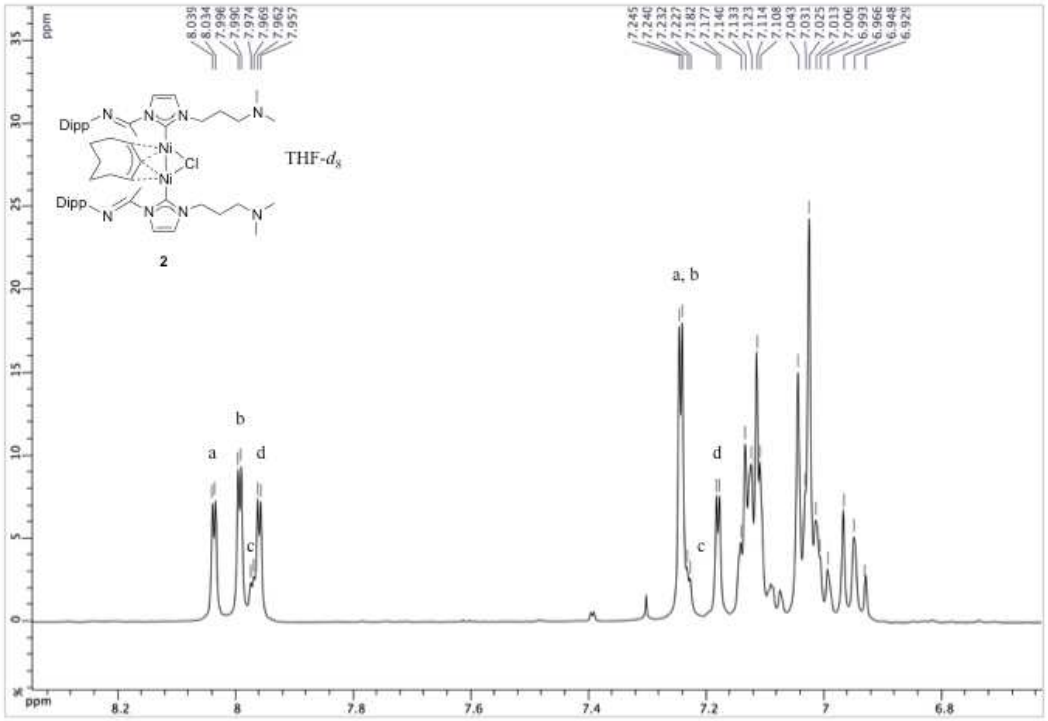

Figure S7. Partial ^{1}H NMR spectrum of **2** in THF-d_8.

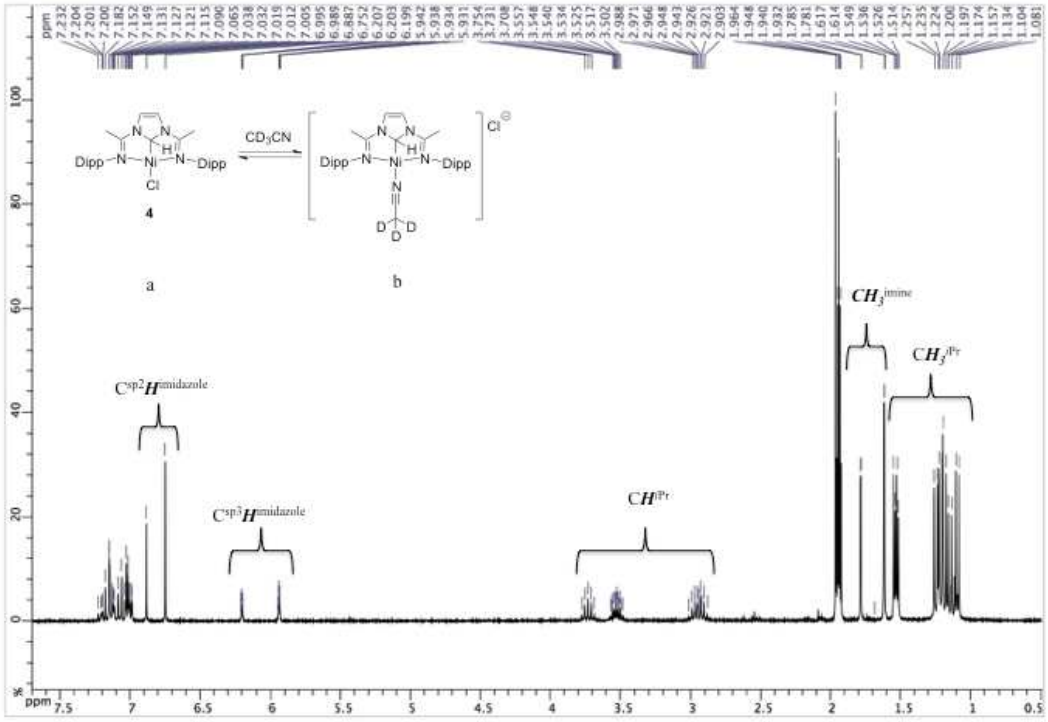

Figure S8. ^{1}H NMR spectrum of **4** in CD_3CN.

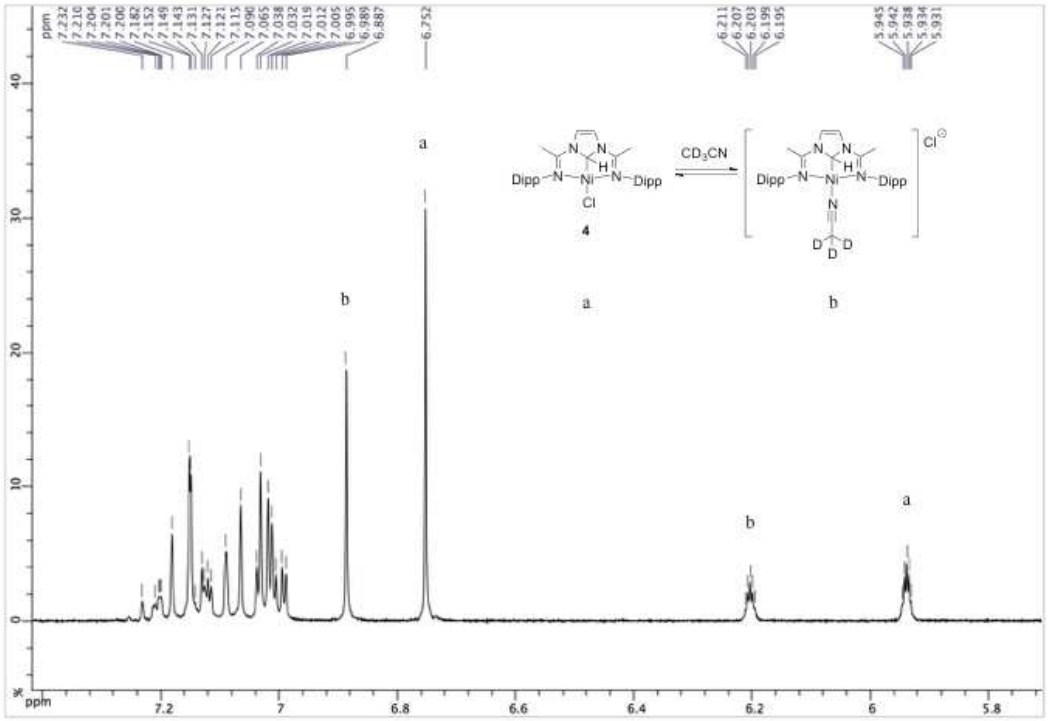

Figure S9. Partial ^{1}H NMR spectrum of **4** in CD_3CN.

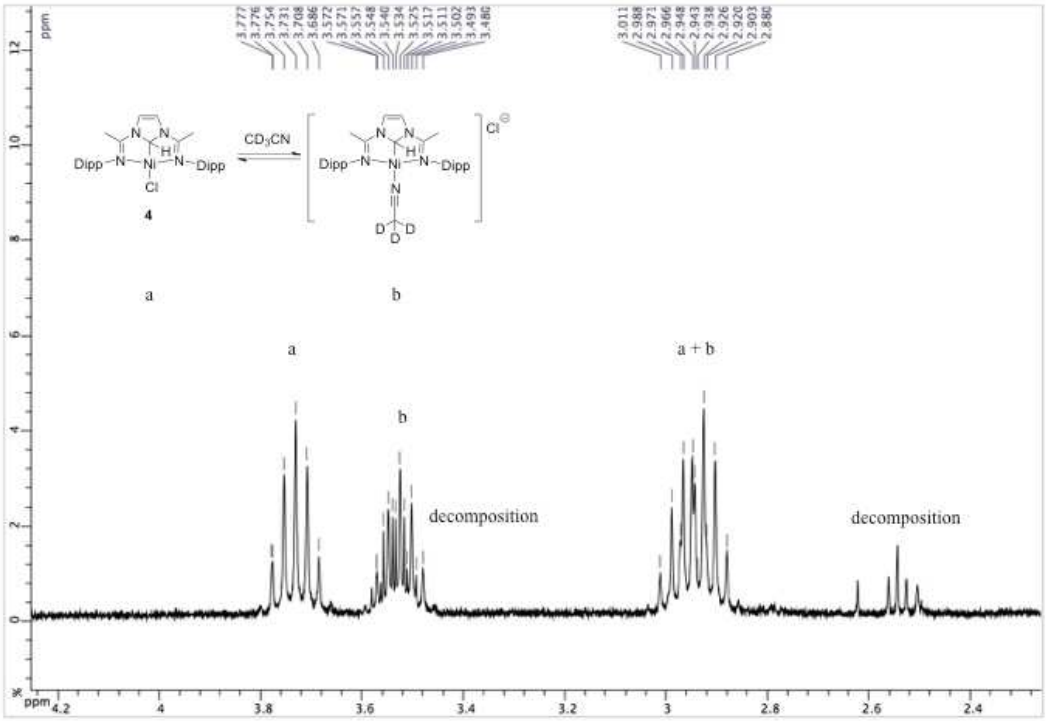

Figure S10. Partial ^{1}H NMR spectrum of **4** in CD_3CN.

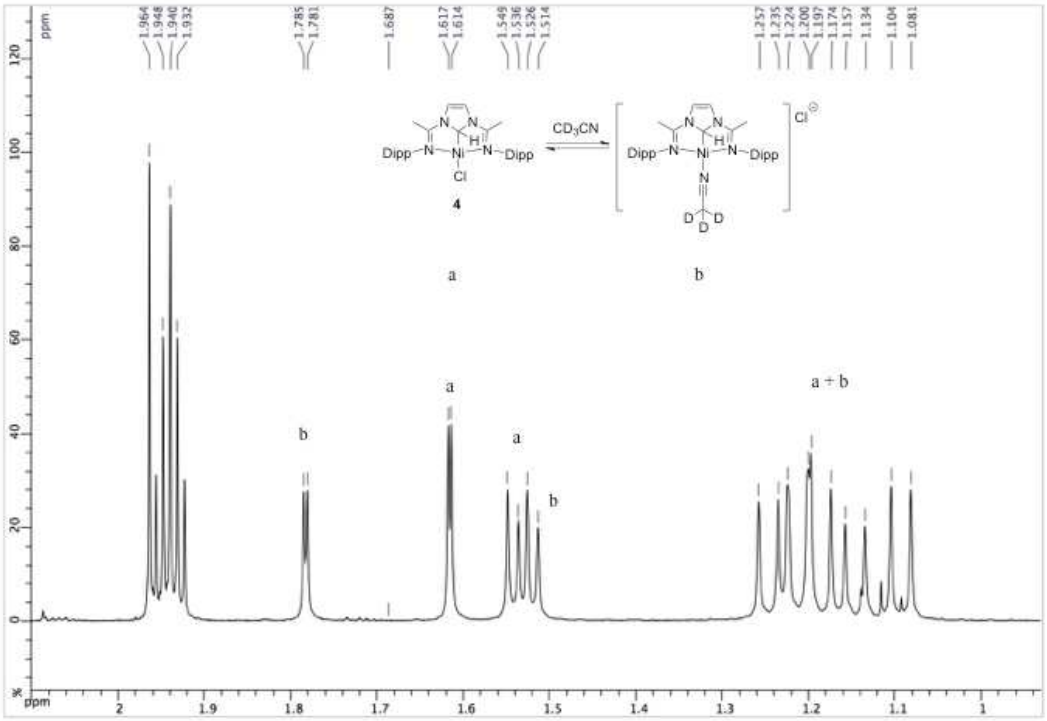

Figure S11. Partial ^{1}H NMR spectrum of **4** in CD_3CN.

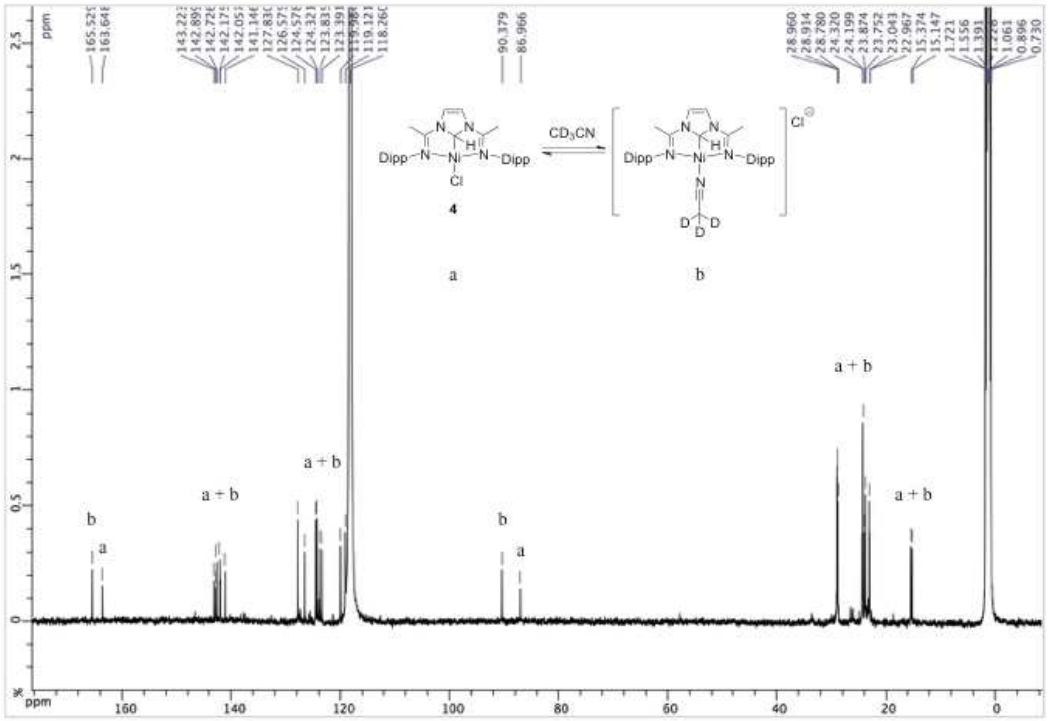

Figure S12. ^{13}C NMR spectrum of **4** in CD_3CN.

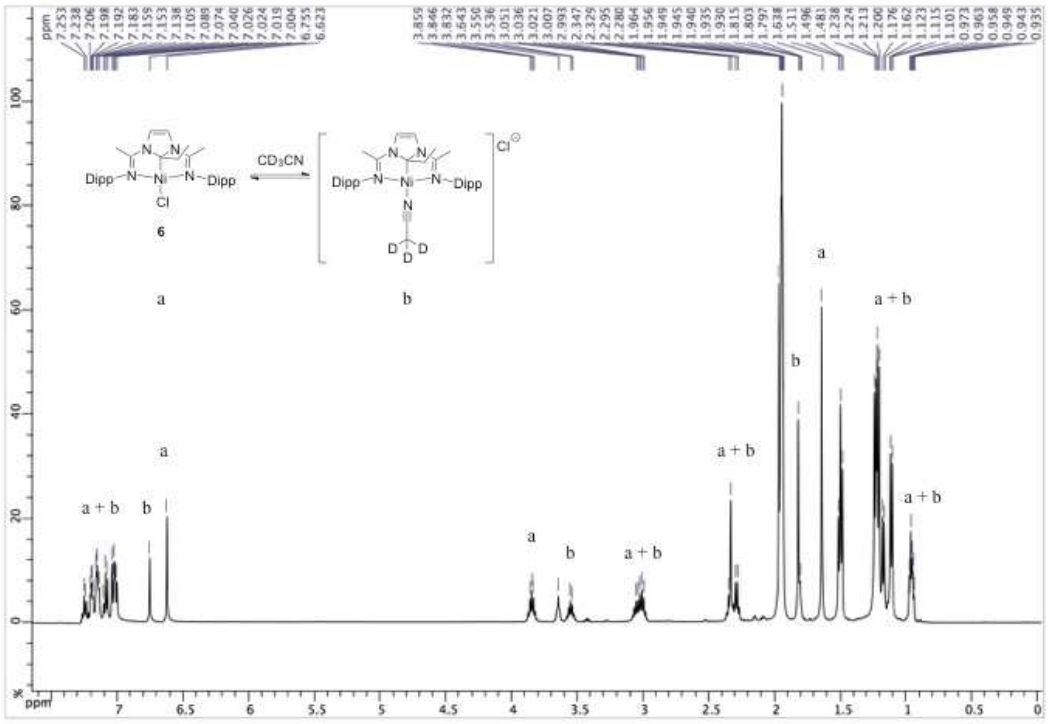

Figure S13. ^{1}H NMR spectrum of **6** in CD_3CN.

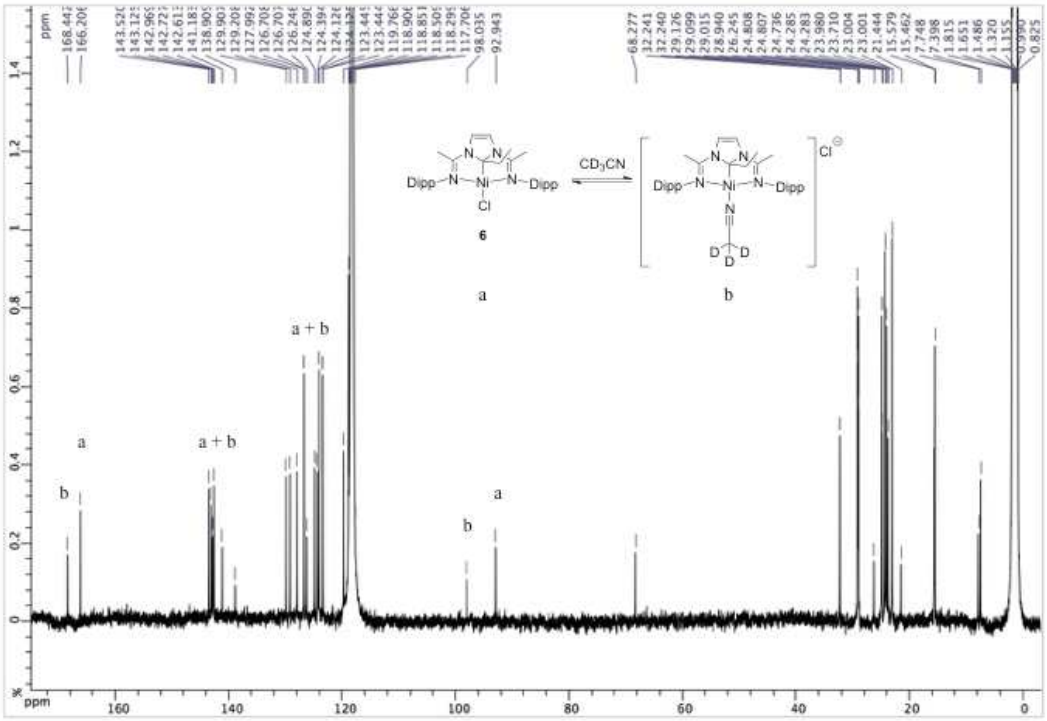

Figure S14. ^{13}C NMR spectrum of **6** in CD_3CN.

4. X-ray crystallography

4.1 General methods

The crystals were mounted on a glass fiber with grease, from Fomblin vacuum oil. Data sets were collected on a Bruker APEX II DUO diffractometer equipped with an Oxford Cryosystem liquid N_2 device, using Mo-Kα radiation (λ = 0.71073 Å). The crystal-detector distance was 38 mm. The cell parameters were determined (APEX2 software)[3] from reflections taken from three sets of 12 frames, each at 10 s exposure. The structures were solved by direct methods using the program SHELXS-97.[4] The refinement and all further calculations were carried out using SHELXL-97.[5] The H-atoms were included in calculated positions and treated as riding atoms using SHELXL default parameters. The non-H atoms were refined anisotropically, using weighted full-matrix least-squares on F^2.

The following special comments apply to the models of the structures:

For **2**, the complex contains a C^{NHC}-bound ligand coordinated to each nickel centre, and a chloride and h^3-cyclooctadienyl bridge the Ni−Ni bond. A squeeze was made. The

residual electron density was assigned to half a molecule of ether. The space group ($P\ 2_1\ 2_1\ 2_1$) is chiral. The Flack parameter is 0.009(10). There are two Alerts B in the checkcif because the ellipsoids of one isopropyl (C34, C35, C36) are large but R1 = 7.7%.

For **4**, one tridentate ligand and one chloride are coordinated to the nickel. The asymmetric unit contains one molecule of acetonitrile. All hydrogen atoms were found, including the hydrogen on C1, which was placed at a fixed distance de 1.0000 Å. The distances C1−N1 and C1−N2 are about 1.44 Å, consistent with single bonds, which is consistent with the value of 167° for the C1−Ni1−Cl1 angle.

For 6, a squeeze was made. The residual electron density was assigned to one molecule of toluene.

4.2 Summary of crystal data

Summary of the crystal data, data collection and refinement for the structures of **2**, **4**•$NCCH_3$ and **6** are given in Table S1.

Table S1. Crystal data for compounds **2**, **4**•$NCCH_3$ and **6**.

	2	**4**•$NCCH_3$	**6**
Chemical formula	$C_{52}H_{81}ClN_8Ni_2$	$C_{31}H_{43}ClN_4Ni$, C_2H_3N	$C_{33}H_{47}ClN_4Ni$
CCDC Number	1556328	1556329	1556330
Formula Mass	971.11	606.91	593.90
Crystal system	orthorhombic	monoclinic	monoclinic
a/Å	10.2247(10)	16.6848(11)	10.9976(3)
b/Å	22.638(2)	12.9898(8)	17.5999(5)
c/Å	25.267(2)	15.5125(10)	20.6626(6)
α/°	90	90	90
β/°	90	101.450(2)	109.9350(10)
γ/°	90	90	90
Unit cell volume/Å^3	5848.6(10)	3295.1(4)	3759.74(19)
Temperature/K	173(2)	173(2)	173(2)
Space group	*P 21 21 21*	*P 21/c*	*P 21/c*
Formula units / cell, *Z*	4	4	4
Absorption coefficient, μ/mm^{-1}	0.727	0.699	0.610
No. of reflections measured	31945	32709	44572
No. of independent reflections	14026	7953	10952
R_{int}	0.0646	0.0941	0.0439
Final R_1 values ($I > 2\sigma(I)$)	0.0777	0.0518	0.0446
Final $wR(F^2)$ values ($I > 2\sigma(I)$)	0.1389	0.1038	0.1040
Final R_1 values (all data)	0.1302	0.1140	0.0665
Final $wR(F^2)$ values (all data)	0.1527	0.1237	0.1106
Goodness of fit on F^2	1.007	0.995	1.048

5. Modelisation

5.1 Computational details

All calculations were performed with GAUSSIAN 09 rev. D01 package[6] at DFT level of theory (B3LYP functional[7]). All atoms were described using the Pople's 6-31+G** basis sets.[8, 9] All structures were fully optimized and the nature of the encountered stationary points was checked through a frequency calculations. Gibbs free energies were extracted from these calculations. ELF topological analysis [10,11] and Non-Covalent Interactions [12] were computed using the GAUSSIAN wavefunction of these optimized structures.

5.2 Structural analysis

The agreement between experimental and theoretical structures of **4** is very good (see Table S2). The ELF analysis performed on the optimized structure shows that the bond between the nickel atom and the carbon has some covalent character, the cation contributing to the ELF valence basin (Figure S15, Table S3). There are no interactions between the cation and the hydrogen atom hold by the carbanionic carbon. Similarly, the NCI analysis (Figure 17) does not show any weak interactions between the metal and the ligand, only dispersive interactions are present between the methyl hydrogen of the isopropyl groups and the chloride.

Table S2. Experimental (RX) and theoretical structures (Theo) of **4** and computed neutral complex (**4b**) and its planar version (**4c**). Bond lengths are in Å and angles in degrees.

	4 RX	**4** Theo	**4b**	**4c**
C1-C2	1.329	1.353	1.356	1.345
C2-N1	1.414	1.413	1.407	1.403
N1-C4	1.362	1.370	1.374	1.415
N1-C3	1.446	1.460	1.428	1.409
C3-H	1.000	1.104	-	-
C3-Ni	1.827	1.853	1.803	1.752
Ni-N2	1.939	1.973	1.922	2.829
Ni-Cl	2.236	2.245	-	-
H-C3-Ni	108.7	109.2	-	-
C2-N1-C4	131.9	131.3	131.8	126.0
C3-N1-C4	112.5	112.8	113.8	123.3
C3-Ni-Cl	167.0	169.8	-	-
C2-N1-C3-Ni	131.1	130.9	130.1	180.0
C2-N1-C3-C4	-153.6	-152.3	-157.6	-180.0

Table S3. Electronic populations and atomic contribution to some of complex **4** ELF valence basins.

Basin X1-X2	Population	Atom X1 contribution	Atom X2 contribution
C3-Ni	1.80	1.46	0.32
Ni-Cl	0.92	0.12	0.79
C3-H	2.10	1.12	0.98

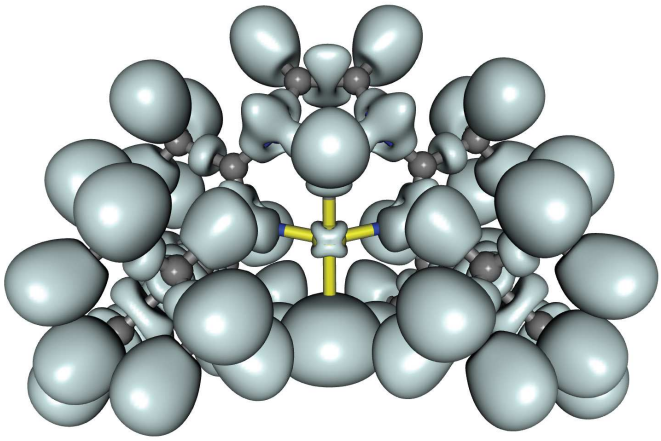

Figure S15. ELF analysis of complex **4**.

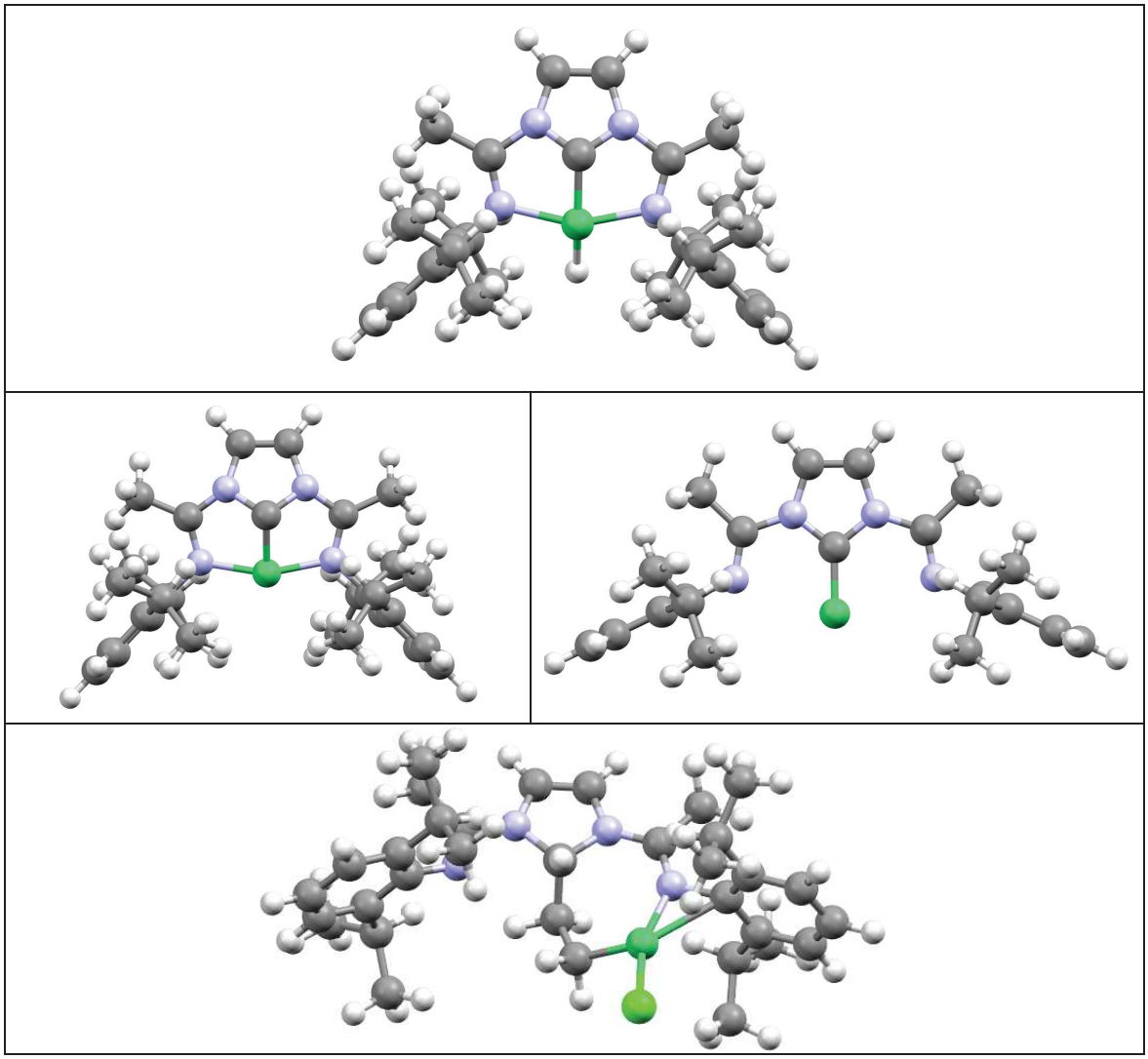

Figure S16. Structures of **4a** (top), **4b** (centre, left), **4c** (centre, right) and **6a** (bottom).

In Figure S16, the structure of **4a** was obtained by removing the chlorine anion of **4** from the metal centre and displacing the H atom from the heterocycle towards the metal,

which remain Ni(II). **4b** was obtained by removing the H^+ from **4a** in which the metal is reduced into a Ni(0) species. To check that the structure of **4b** is not due to the choice of the starting geometry, the structure of **4b** was forced to be planar, leading to **4c**. To evaluate the influence of a longer spacer on the thermodynamic balance of the carbene formation, the theoretical structures **4d** and **4e** were calculated (Figure S17). We aimed at retaining the electronic conjugation between the nitrogen of the heterocycle and that of the imine and also the ligand rigidity. This was achieved by introducing a cyclopentadienyl derivative. **4d** is the equivalent of **4**, and **4e** is the equivalent of **4b**. So in **4d**, the oxidation state of the metal is (+II) while it is zero in **4e**. **6a** was obtained in the search of the ethylene insertion mechanism and the Ni atom is in the +II oxidation state. All the structures are local minima characterised by a complete set of real frequencies.

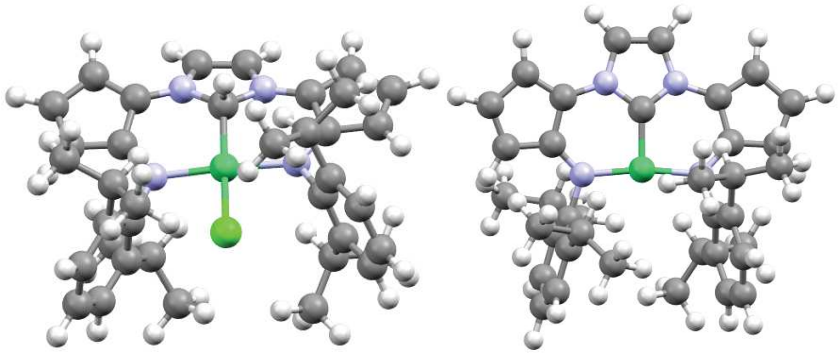

Figure S17. Structures of the theoretical molecules **4d** (left) and **4e** (right).

Further information and the ORCID identification number(s) for the author(s) of this article can be found under: https ://doi.org/10.1002/anie.201706581.

6. References

(1) J. Luo, T. Xin, Y. Wang, *New Journal of Chemistry*, **2013**, *37*, 269.

(2) (a) P. Liu, M. Wesolek, A. A. Danopoulos, P. Braunstein, *Organometallics*, **2013**, *32*, 6286; (b) L. Benhamou, E. Chardon, G. Lavigne, S. Bellemin-Laponnaz, V. César, *Chem. Rev.*, **2011**, *111*, 2705.

(3) Bruker AXS Inc Madison USA, **2006**.

(4) G. M. Sheldrick, *Acta Crystallogr. Sect. A: Found. Crystallogr.*, **1990**, *A46*, 467.

(5) G. M. Sheldrick, Universität Göttingen: Göttingen Germany, **1999**.

(6) Gaussian 09, Revision D.01, M. J. Frisch, G. W. Trucks, H. B. Schlegel, G. E. Scuseria, M. A. Robb, J. R. Cheeseman, G. Scalmani, V. Barone, G. A. Petersson, H. Nakatsuji, X. Li, M. Caricato, A. Marenich, J. Bloino, B. G. Janesko, R. Gomperts, B. Mennucci, H. P. Hratchian, J. V. Ortiz, A. F. Izmaylov, J. L. Sonnenberg, D. Williams-Young, F. Ding, F. Lipparini, F. Egidi, J. Goings, B. Peng, A. Petrone, T. Henderson, D. Ranasinghe, V. G. Zakrzewski, J. Gao, N. Rega, G. Zheng, W. Liang, M. Hada, M. Ehara, K. Toyota, R. Fukuda, J. Hasegawa, M. Ishida, T. Nakajima, Y. Honda, O. Kitao, H. Nakai, T. Vreven, K. Throssell, J. A. Montgomery, Jr., J. E. Peralta, F. Ogliaro, M. Bearpark, J. J. Heyd, E. Brothers, K. N. Kudin, V. N. Staroverov, T. Keith, R. Kobayashi, J. Normand, K. Raghavachari, A. Rendell, J. C. Burant, S. S. Iyengar, J. Tomasi, M. Cossi, J. M. Millam, M. Klene, C. Adamo, R. Cammi, J. W. Ochterski, R. L. Martin, K. Morokuma, O. Farkas, J. B. Foresman, and D. J. Fox, Gaussian, Inc., Wallingford CT, 2016.

(7) A. D. Becke, *J. Chem. Phys.*, **1993**, *98*, 5648.

(8) P. C. Hariharan, J. A. Pople, *Theor. Chem. Acc.*, **1973**, *28*, 213.

(9) V. A. Rassolov, J. A. Pople, M. A. Ratner, T. L. Windus, *J. Chem. Phys.*, **1998**, *109*, 1223.

(10) S. Noury, X. Krokidis, F. Fuster, B. Silvi, TopMod Package, 1997. This package is available on the web site of the Laboratoire de Chimie Théorique, Université Pierre et Marie Curie (UMR 7616 CNRS/UPMC), URL: http://www.lct.jussieu.fr.

(11) S. Noury, X. Krokidis, F. Fuster and B. Silvi, *Comput. Chem.* **1999**, *23*, 597.

(12) J. Contreras-García, E. R. Johnson, S. Keinan, R. Chaudret, J.-P. Piquemal, D. N. Beratan and W. Yang J. Chem. *Theory Comput.* **2011**, *7*, 625.

CHAPITRE 4

Synthesis and Structural Characterization of Cu(I), Cr(III) and Ir(I) Complexes with Tritopic $N^{imine}C^{NHC}N^{amine}$ pincer Ligands and Catalytic Ethylene Oligomerization

This chapter is written in the form of a publication draft, some additional work being currently in progress. Some characterization data are still missing at this stage.

My contribution to this work consisted of the bibliographic search, the experimental work and the preparation of the draft of the publication.

Synthesis and Structural Characterization of Cu(I), Cr(III) and Ir(I) Complexes with Tritopic $N^{imine}C^{NHC}N^{amine}$ pincer Ligands and Catalytic Ethylene Oligomerization

Xiaoyu Ren,[a] Marcel Wesolek*[a] and Pierre Braunstein*[a]

[a] Laboratoire de Chimie de Coordination, Institut de Chimie (UMR 7177 CNRS), Université de Strasbourg, 4 rue Blaise Pascal, 67081 Strasbourg Cedex (France)

E-mail: braunstein@unistra.fr

Synopsis

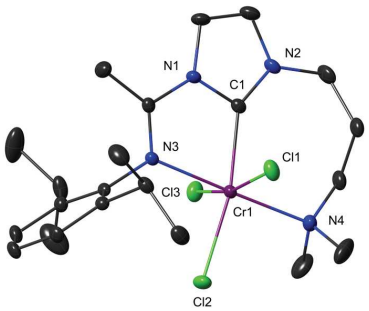

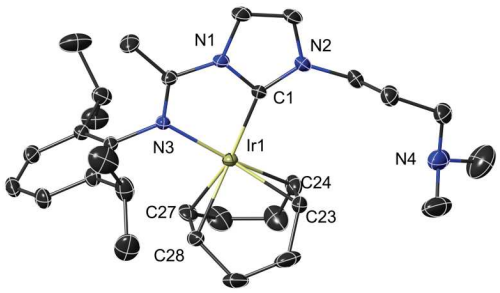

1. Résumé en français

Les chlorures d'imidazolium [(ImH){C(Me)=NDipp}(C_2NMe_2)]Cl (**1**) et [(ImH){C(Me)=NDipp}(C_3NMe_2)]Cl (**2**) ont été préparés en tant que précurseurs de ligands de type pinceur tritopique pour la synthèse de complexes de métaux de transition. Les complexes mononucléaire du cuivre(I) [CuCl{Im[C(Me)=NDipp](C_2NMe_2)}] (**3**) et [CuCl{Im[C(Me)=NDipp](C_3NMe_2)}] (**4**) ont été préparés respectivement par réaction de **1** et **2** avec du mesitylcuivre(I). Les complexes de l'argent(I) [AgCl{Im[C(Me)=NDipp](C_2NMe_2)}] (**5**) et [AgCl{Im[C(Me)=NDipp](C_3NMe_2)}] (**6**) ont été préparés respectivement par réaction de **1** et **2** avec Ag_2O en présence de tamis moléculaire. Un complexe dinucléaire du cuivre(I) contenant une structure primaire de type échelle, formée d'atomes de cuivre et d'iode, Cu_4I_4[(Im){C(Me)=NDipp}(C_3NMe_2)]$_2$ (**7**) a été obtenu par déprotonation de **2** en utilisant le mélange sodium trimethylsilylamide/CuI. Les réactions de transmétallation de complexes d'argent avec soit [$CrCl_2(THF)_2$] soit [$CrCl_3(THF)_3$], ont donné, avec des rendements raisonnables, les mêmes complexes du chrome(III), à savoir *mer*-$CrCl_3$[(Im){C(Me)=NDipp}(C_2NMe_2)] (**8**) et *mer*-$CrCl_3$[(Im){C(Me)=NDipp}(C_3NMe_2)] (**9**) en partant respectivement de **5** et de **6**. De plus, des réactions de transmétallation des complexes d'argent ont aussi été tentées avec un précurseur de l'iridium(I), [Ir(μ-Cl)(cod)]$_2$ (cod = 1,5-cycloocadiene). En partant respectivement de **5** et de **6**, des complexes monodentés de l'Ir(I), Ir(cod)Cl[(Im){C(Me)=NDipp}(C_3NMe_2)] (**10**) et Ir(cod)Cl[(Im){C(Me)=NDipp}(C_3NMe_2)] (**11**), ont été isolés sous forme de cristaux jaunes avec de bons rendements. Les complexes bidenté de l'Ir(I) [Ir(cod){(Im)[C(Me)=NDipp](C_2NMe_2)}]BF_4 (**12**) et [Ir(cod){(Im)[C(Me)=NDipp](C_3NMe_2)}]BF_4 (**13**) ont été obtenus par abstraction de l'halogènure dans les complexes **10** et **11**.

Synthesis and Structural Characterization of Cu(I), Cr(III) and Ir(I) Complexes with Tritopic $N^{imine}C^{NHC}N^{amine}$ pincer Ligands and Catalytic Ethylene Oligomerization

Xiaoyu Ren,[a] Marcel Wesolek[*a] and Pierre Braunstein*[*a]*

[a] *Laboratoire de Chimie de Coordination, Institut de Chimie (UMR 7177 CNRS), Université de Strasbourg, 4 rue Blaise Pascal, 67081 Strasbourg Cedex (France)*

E-mail: braunstein@unistra.fr

2. Abstract

The imidazolium chlorides [(ImH){C(Me)=NDipp}(C_2NMe_2)]Cl (**1**) and [(ImH){C(Me)=NDipp}(C_3NMe_2)]Cl (**2**) were prepared as precursors to pincer-type tritopic $N^{imine}C^{NHC}N^{amine}$ ligands in transition metal complexes. The mononuclear Cu(I) complexes [CuCl{Im[C(Me)=NDipp](C_2NMe_2)}] (**3**) and [CuCl{Im[C(Me)=NDipp](C_3NMe_2)}] (**4**) were prepared by reaction of **1** and **2** with mesitylcopper(I), respectively. The Ag(I) complexes [AgCl{Im[C(Me)=NDipp](C_2NMe_2)}] (**5**) and [AgCl{Im[C(Me)=NDipp](C_3NMe_2)}] (**6**) were prepared by reaction of **1** and **2**, respectively, with Ag_2O in the presence of molecular sieves. A Cu(I) dinuclear complex containing a ladder-type skeleton formed by copper and iodine atoms, Cu_4I_4[(Im){C(Me)=NDipp}(C_3NMe_2)]$_2$ (**7**) was obtained by deprotonation of **2** using sodium trimethylsilylamide/CuI. Silver transmetalation reactions from **5** and **6** to either [$CrCl_2(THF)_2$] or [$CrCl_3(THF)_3$] gave the same chromium(III) complexes, *mer*-$CrCl_3$[(Im){C(Me)=NDipp}(C_2NMe_2)] (**8**) and *mer*-$CrCl_3$[(Im){C(Me)=NDipp}(C_3NMe_2)] (**9**), respectively, in reasonable yields. Moreover, silver transmetalation reactions were also attempted with an Ir(I) precursor [Ir(μ-Cl)(cod)]$_2$ (cod = 1,5-cycloocadiene) and monodentate Ir(I) complexes Ir(cod)Cl[(Im){C(Me)=NDipp}(C_3NMe_2)] (**10**), and Ir(cod)Cl[(Im){C(Me)=NDipp}(C_3NMe_2)] (**11**) could be isolated as yellow crystals in good yields, starting from **5** and **6,** respectively. Bidentate Ir(I) complexes [Ir(cod){(Im)[C(Me)=NDipp](C_2NMe_2)}]BF_4 (**12**) and [Ir(cod){(Im)[C(Me)=NDipp](C_3NMe_2)}]BF_4 (**13**) were obtained by halide abstraction of **10** and **11**.

3. Introduction

Since the first isolation of stable crystalline *N*-heterocyclic carbene (NHC) reported by Arduengo

and co-workers in 1991,[1] the synthesis of diverse *N*-functionalized NHCs and their complexation chemistry has attracted increasing attention. The class of hybrid ligands[2] containing at least one NHC donor group is rapidly expanding, and research in this area is fueled, in particular, by the diversity and tunability of the ligand electronic and steric properties resulting from the introduction of an additional functionality, donor group, such as an oxygen-,[3] a sulfur-,[4] a phosphorus-,[5] or a nitrogen-based[6] donor group. In the latter case, amine and imine groups predominate.[6i-k] The rich coordination chemistry of transition metal complexes containing *N*-functionalized NHC ligands has led to numerous applications, ranging from homogeneous catalysis[7] to photophysics.[8]

The study of transition metal complexes stabilized by pincer ligands has also enjoyed spectacular developments, with numerous applications in e.g. stoichiometric and catalytic transformations.[9] It is therefore not surprising that attempts to combine within the same ligand system the specific features of NHC and pincer chemistries would generate considerable research efforts. Among the ECE pincer-type ligands, where C represents an anionic or neutral carbon donor and E a neutral donor group, those with a central NHC donor flanked by two potential donors E, *i.e.* $EC^{NHC}E$ pincer ligands, have indeed been particularly successful. Their development has been further triggered by the diversity of side arms that can be installed at the N atom(s) of a NHC backbone, not only in terms of the nature of the donor group E but also of the length of the connecting spacer between them. Both these parameters, together with the NHC donor, are expected to play a major role in the stabilization of pincer complexes and the tuning of their stereoelectronic properties.

Chromium complexes have been very successfully applied to the catalytic oligomerization of ethylene, achieving in particular the industrially highly relevant formation of trimers and tetramers with high selectivity.[10] The remarkable results obtained with bis(diphenylphosphino)amine-type ligands[11] have been accompanied by the development of a range of multidentate ligands in order to further improve the activity and selectivity of chromium-based catalytic system. Thus, diverse Cr complexes with PNP,[12] PNC,[12f, 13] PCN,[14] CNC,[15] NPN,[16] NCN[17] pincer ligands have been reported. Some of those containing a central C^{NHC} donor have been associated with N donor functions and found interesting catalytic applications. In particular, Cr(II/III) complexes with bidentate or tridentate NHC ligands containing one or two imine donor(s) have been reported by Lavoie and co-workers and applied to ethylene polymerization (**A**-**D**, Scheme 1).[18] As seen when comparing complexes **A** and **B**, coordination of the imine group may depend on subtle changes in the ligand backbone so that pincer behaviour is not always observed. Nakada and co-workers mentioned a silver transmetallation reaction between the AgBr complex with a bis(oxazolinyl)benzimidazole

ligand and $CrCl_2$ to afford a tridentate NHC Cr(III) complex (**E**, Scheme 1).[17b] Our group isolated diverse bidentate Cr(II/III) complexes with amidine- or amidinate-functionalized N-heterocyclic carbene ligands (**F**-**H**, Scheme 1).[6m] An interesting extension of this class of potential pincer ligands, discussed in the present chapter, consists of $N^{imine}C^{NHC}N^{'}$ systems where two chemically-different N donor functions flank the central NHC. Their use allows a finer tuning of the metal coordination sphere.

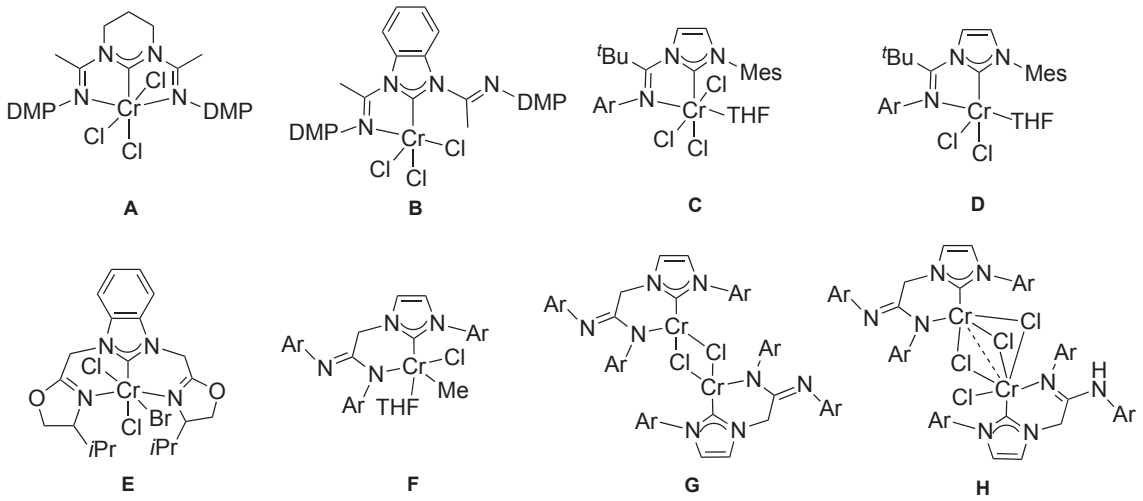

Scheme 1. Selected Cr complexes containing functional NHC donor ligands of the $NC^{NHC}N$ or NC^{NHC} type.

As part of our general interest in the catalytic oligomerization of ethylene directed toward the formation of short chain linear α-olefins (LAOs), we previously described $N^{imine}C^{NHC}N^{amine}$ pincer-type nickel complexes prepared by oxidative addition reactions of imidazolium salts to Ni(0) or by transmetallation of the corresponding Ag(I) complexes. These complexes were shown to exhibit diverse coordination behaviors and catalytic properties. Herein, we extend the use of such multifunctional ligands and describe the synthesis and properties of copper, silver, chromium and iridium complexes containing a $N^{imine}C^{NHC}N^{amine}$ tritopic ligand. Related iridium complexes have been used for catalytic alkane activation by both H transfer and direct activation without sacrificial acceptor.[19]

4. Results and discussion

Synthesis and structure of Cu(I) and Ag(I) complexes. In view of the successful use of silver(I)

and copper(I) NHC complexes as transmetalating agents in the synthesis of a broad range of NHC transition metal complexes,[7c] we first prepared the imidazolidene copper(I) complexes CuCl[(Im){C(Me)=NDipp}(C_2NMe_2)] (Im = $C_3H_2N_2$) (**3**) and CuCl[(Im){C(Me)=NDipp}(C_3NMe_2)] (**4**) containing a tritopic $N^{imine}C^{NHC}N^{amine}$ ligand, with a $(CH_2)_2$ or a $(CH_2)_3$ spacer between the heterocycle and the amine group, respectively (eq. 1).

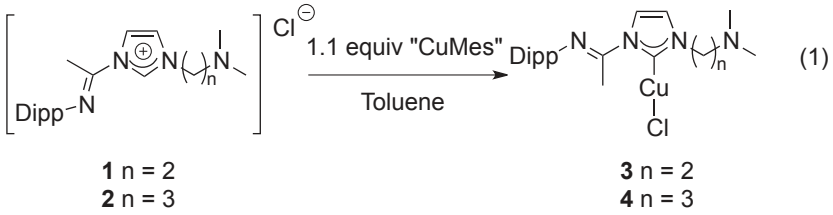

1 n = 2
2 n = 3

3 n = 2
4 n = 3

These mononuclear Cu(I) complexes were obtained by reaction of the corresponding imidazolium salts [(ImH){C(Me)=NDipp}(C_2NMe_2)]Cl (**1**) and [(ImH){C(Me)=NDipp}(C_3NMe_2)]Cl (**2**), respectively, with mesityl copper(I) in toluene. In both cases, a similar transformation occurred with the release of one equivalent of mesitylene. A single-crystal X-ray diffraction analysis of complex **3** (Figure 2 and ESI), which crystallizes in the monoclinic system ($P2_1/c$ space group), revealed that the *N*-functionalized arms are pendent, with the N atoms pointing away from the copper centre. Consequently, the latter presents a nearly linear coordination geometry (C1−Cu1−Cl1 177.2(7)°). The related silver(I) complexes AgCl[(Im){C(Me)=NDipp}(C_2NMe_2)] (**5**) and AgCl[(Im){C(Me)=NDipp}(C_3NMe_2)] (**6**) were also prepared by reactions with imidazolium salts and silver oxide for subsequent transmetallation purpose (eq. 2).

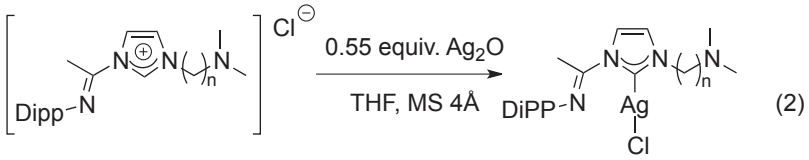

1 n = 2
2 n = 3

5 n = 2
6 n = 3

An X-ray diffraction analysis of compound **6** (monoclinic system, $P2_{1/c}$ space group) (Figure 1) also reveals a monodentate NHC bonding for the ligand, with two dangling functional groups. However, the N atoms are now pointing toward the silver atom but the Ag1···N3 (2.882 Å) and Ag1···N4 (3.113 Å) distances are too long to represent significant bonding interactions. The Ag−C1 and Ag1−Cl1 bond lengths (2.091(2) Å and 2.339(6) Å) are slightly longer than Cu1−C1 and Cu1−Cl1 (1.892(2) Å and 2.095(6) Å), consistent with the larger covalent radius of Ag (1.45 Å) *vs*. Cu (1.32 Å).[20]

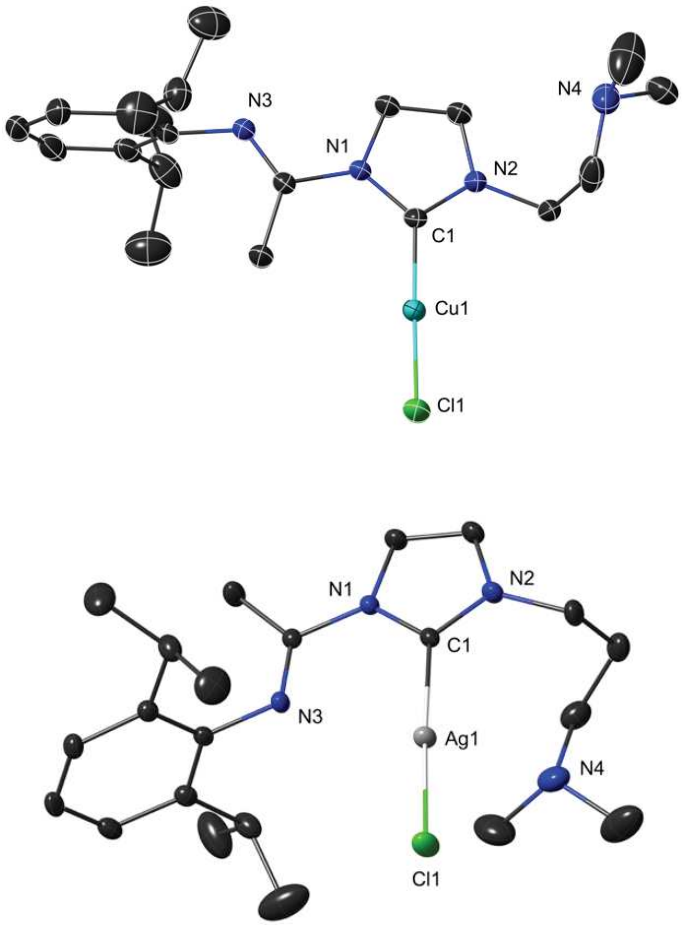

Figure 1. Views of the structures of **3** (top) and **6** (bottom) with H atoms omitted for clarity. Thermal ellipsoids at the 40% (**3**) and 30% (**6**) probability levels. Selected bond lengths (Å) and angles (deg): **3**, Cu1−C1 1.892(2), Cu1−Cl1 2.095(6), C1−N1 1.368(3), C1−N2 1.340(3); N1−C1−N2 104.1(2), N1−C1−Cu1 131.0(2), N2−C1−Cu1 124.7(2), C1−Cu1−Cl1 177.2 (7); **6**, Ag1−C1 2.091(2), Ag1−Cl1 2.339(6), C1−N1 1.364(3), C1−N2 1.342(2); N1−C1−N2 104.3(2), N1−C1−Ag1 127.4(1), N2−C1−Ag1 128.2(2).

In addition to the reaction with the mesityl copper(I) precursor, formation of Cu(I) NHC complexes was also achieved by deprotonation of the imidazolium salt using the mixture sodium trimethylsilylamide/CuI (eq. 3).

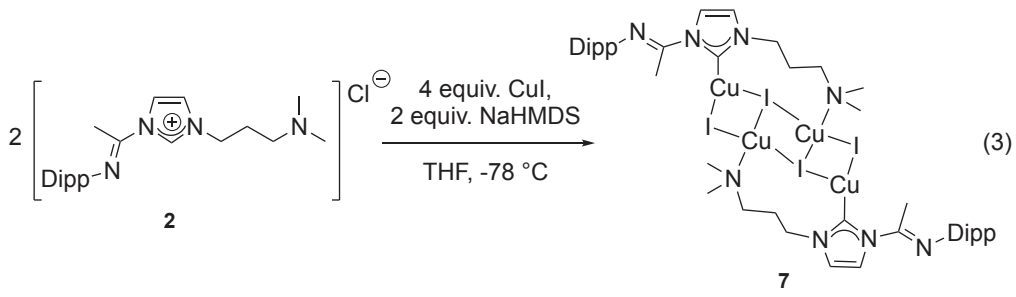

(3)

A pale yellow powder of the product, $Cu_4I_4[(Im)\{C(Me)=NDipp\}(C_3NMe_2)]_2$ (**7**), was isolated in 65% yields, and colourless crystals suitable for X-ray diffraction analysis were obtained by slow diffusion of pentane into a THF solution (Figure 2 and ESI). The complex crystallizes in the monoclinic system ($P2_1/c$ space group) and the asymmetric unit contains half a molecule of this complex. The four coplanar copper centres and the four doubly bridging iodine atoms form a ladder-type structure. There are two bridging, bidentate organic ligands, through the C^{NHC} and N^{amine} donors, while the imine groups remain uncoordinated. The structure reveals two types of Cu(I) ions in different chemical and coordination environments: Cu1 adopts a distorted trigonal planar geometry formed by C1, I1 and I2' (C1−Cu1−I1 102.8(2)°, C1−Cu1−I2' 134.7(2)°), whereas Cu2 has a slightly distorted tetrahedral coordination geometry involving N4, I1, I1' and I2 (N4−Cu2−I1 116.2(2)°, N4−Cu2−I2 107.7(2)°, N4−Cu2−I1' 109.8(2)°). The iodide ligands feature different bonding modes: I1 displays a μ_3-mode with a triangular pyramidal geometry, whereas I2 adopts a μ_2-bonding mode. The Cu−I distances range from 2.496(9)−2.706(1) Å and the shortest Cu−Cu distance, Cu1−Cu2' 2.655(1) Å, is similar to those in other ladder-type Cu(I)-I polynuclear complexes.[21] Among the Cu(I)-halide coordination complexes and polymers,[22] those with a Cu_4I_4 core often display photoluminescence,[23] photo(thermo)chromism,[24] and catalytic activity.[25] It is interesting to note that the structure of **7** is closely related to that of a tetranuclear Ag(I) complex containing two bridging NHC,thioether ligands.[26] When the Cu(I) complexes **3**, **4** and **7** were used as precursors for transmetallation reactions to Ni(II), green paramagnetic powders were obtained but no single crystals could be obtained, which precluded their identification.

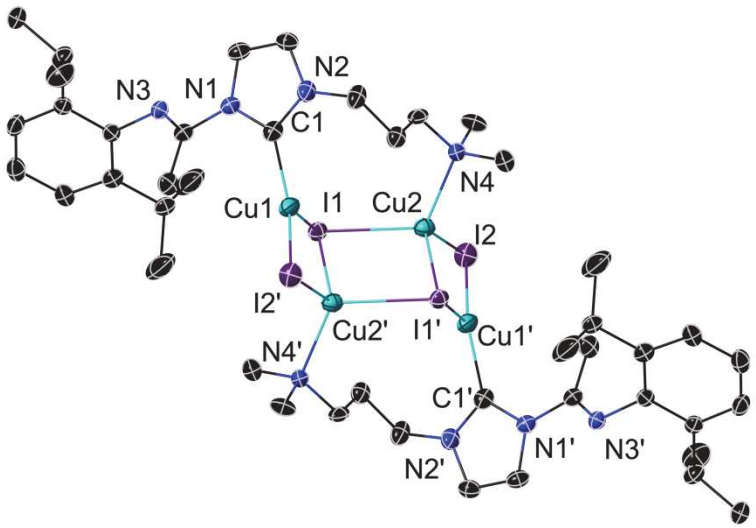

Figure 2. View of the structure of **7** with H atoms omitted for clarity. Thermal ellipsoids at the 40% probability levels. Selected bond lengths (Å) and angles (deg): Cu1−C1 1.928(7), Cu1−I1 2.706(1), Cu1−I2' 2.496(1), Cu2−N4 2.114(6), Cu2−I1 2.684(1), Cu2−I2 2.655(1), C1−N1 1.378(9), C1−N2 1.329(9), Cu1−Cu2' 2.655(1); N1−C1−N2 103.6(6), N1−C1−Cu1 129.2(5), N2−C1−Cu1 126.0(6), C1−Cu1−I1 102.8(2), C1−Cu1−I2' 134.7(2), I1−Cu1−I2' 122.4(4), Cu1−I1−Cu2 97.6(3), N4−Cu2−I1 116.2(2), N4−Cu2−I2 107.7(2), N4−Cu2−I1' 109.8(2).

Synthesis and structure of Cr complexes. The synthesis of chromium complexes with $N^{imine}C^{NHC}N^{amine}$ pincer ligands was attempted in order to investigate their catalytic properties in ethylene oligomerization. First, a one pot reaction was carried out at low temperature consisting in the deprotonation of the imidazolium salt **2** by NaHMDS followed by the addition of a Cr(II) or Cr(III) reagent (see Experimental section). However, analysis by NMR spectroscopy was precluded by the paramagnetism of the reaction mixture and attempts to crystallize a pure product failed, may be due to the instability and reactivity of the free carbene intermediate. We then used the transmetallation procedure based on Ag(I) complexes and a THF solution of the Cr(II) precursor $[CrCl_2(THF)_2]$ was added dropwise to a THF solution of AgCl[(Im){C(Me)=NDipp}(C_2NMe_2)] (**5**) (eq. 4).

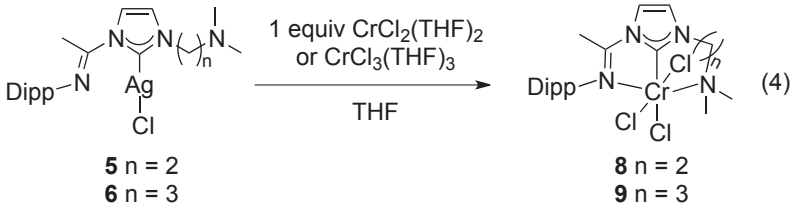

5 n = 2
6 n = 3

8 n = 2
9 n = 3

Surprisingly, a Cr(III) complex was isolated as dark blue crystals, *mer*-$CrCl_3$[(Im){C(Me)=NDipp}(C_2NMe_2)] (**8**). Their analysis by X-ray diffraction (triclinic system, P_{-1} space group) established the presence of a tridentate $N^{imine}C^{NHC}N^{amine}$ pincer ligand and of three meridional chlorides, forming a slightly distorted octahedral coordination sphere around the hexacoordinated chromium centre. The C^{NHC},N^{imine} and C^{NHC},N^{amine} chelates form five- and six-membered rings, respectively (Figure 3).

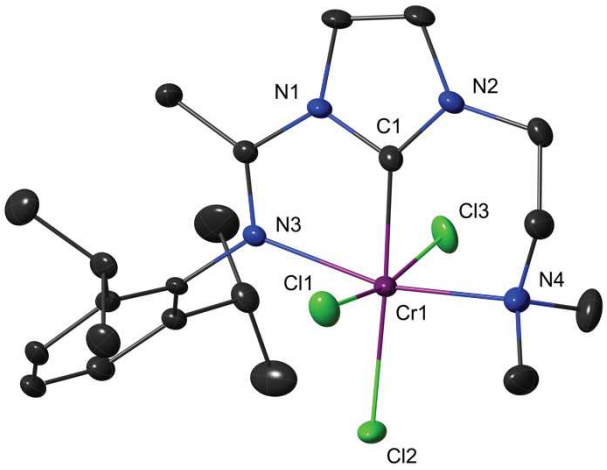

Figure 3. View of the structure of **8** with H atoms omitted for clarity. Thermal ellipsoids at the 30% probability levels. Selected bond lengths (Å) and angles (deg): Cr1−C1 1.982(3), Cr1−N3 2.203(2), Cr1−N4 2.199(2), Cr1−Cl1 2.299(9), Cr1−Cl2 2.328(8), Cr1−Cl3 2.339(9), C1−N1 1.359(3), C1−N2 1.327(3); N1−C1−N2 105.9(2), N1−C1−Cr1 117.2(2), N2−C1−Cr1 136.5(2), C1−Cr1−N3 75.9(9), C1−Cr1−N4 88.0(1), C1−Cr1−Cl1 88.2(8), C1−Cr1−Cl2 173.6(9), C1−Cr1−Cl3 80.9(8), N3−Cr1−N4 163.1(8).

During the reaction, a characteristic silver mirror formed on the inner surface of the reaction vessel, which strongly supports the occurrence of a redox reaction. The nature of **8** suggested that it could be obtained directly by treatment of the Ag(I) complex **5** with [$CrCl_3(THF)_3$]. Therefore, the same procedure as with [$CrCl_2(THF)_2$] was followed and a dark blue solution and a white precipitate were obtained. From the solution, dark blue crystals were isolated and a comparison of their cell parameters confirmed the formation of **8**. It is noteworthy that only bidentate behaviour and formation of a five-membered chelate was observed for the bis-imine NHC ligand in the Cr(III) complex **B** (Scheme 1) whereas tridentate coordination of the $N^{imine}C^{NHC}N^{amine}$ pincer ligand is observed in **8** with formation of five- and six-membered ring chelates. Such comparisons highlight the major influence of the lateral functions in these potential pincer-type systems.

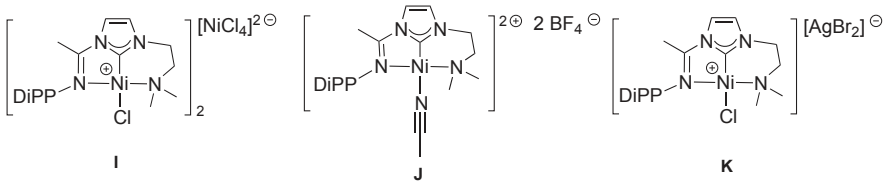

Scheme 2. Ni(II) complexes containing the tridentate $N^{imine}C^{NHC}N^{amine}$ pincer ligand

A comparison of the metrical data in Cr(III) complex **8** with those in the recently reported Ni(II) complexes **I**, **J** and **K** (Scheme 2), containing the same tridentate skeleton, shows that the C–C and C–N bond lengths in the pincer ligand are very similar. In contrast, the bond distances between the metal center and the coordinated atoms are longer in **8** than in the corresponding Ni(II) complexes, and the Cr1–C1, Cr1–N3 and Cr1–N4 bond lengths are in agreement with the expected values based on the difference between the covalent radii of chromium (1.39 Å) and nickel (1.24 Å).[20]

Considering the six-membered ring formed by chelation of the C^{NHC} and N^{amine} donors in **8**, we wondered whether a longer spacer would still favour chelation. We therefore used AgCl[(Im){C(Me)=NDipp}(C_3NMe_2)] (**6**) as precursor, under similar conditions (eq. 4).

The complex *mer*-$CrCl_3$[(Im){C(Me)=NDipp}(C_3NMe_2)] (**9**) was isolated and its structure was elucidated by X-ray diffraction analysis (Figure 4). It is similar to that of **8**, but with a seven-membered ring resulting from chelation of the C^{NHC},N^{amine} donors. The C3 spacer still allows stabilization of the complex by chelation whereas bridging behaviour was observed for this ligand in the Cu(I) complex **7**. The bond distances in **8** and **9** are almost the same, but the angles at chromium are affected by the coordination of N4 and are more relaxed than in **8**, resulting is a lesser distortion of the metal coordination sphere. In particular the C1−Cr1−N4 and N3−Cr1−N4 angles open up from 88.0(1)° and 163.1(8)° in **8** to 101.9(9)° and 178.6(8)° in **9**, respectively.

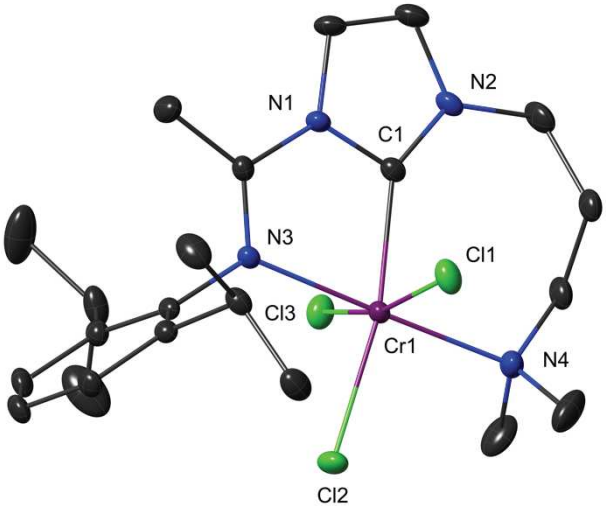

Figure 4. View of the structure of **9** with H atoms omitted for clarity. Thermal ellipsoids at the 30% probability levels. Selected bond lengths (Å) and angles (deg): Cr1−C1 2.081(2), Cr1−N3 2.182(2), Cr1−N4 2.188(2), Cr1−Cl1 2.339(7), Cr1−Cl2 2.324(7), Cr1−Cl3 2.325(7), C1−N1 1.372(3), C1−N2 1.334(3); N1−C1−N2 104.1(2), N1−C1−Cr1 111.9(2), N2−C1−Cr1 144.0(2), C1−Cr1−N3 77.0(8), C1−Cr1−N4 101.9(9), C1−Cr1−Cl1 82.4(7), C1−Cr1−Cl2 167.7(7), C1−Cr1−Cl3 84.4(6), N3−Cr1−N4 178.6(8).

Ethylene oligomerization catalysis

The catalytic activities of the tridentate $N^{imine}C^{NHC}N^{amine}$ Cr(III) complexes **8** and **9** towards ethylene oligomerization in toluene were studied in the presence of 400 equivalents methylaluminoxane (MAO) as cocatalyst. The influence of spacer length between N^{amine} and N^{NHC}, the quantity of co-catalyst and the starting reaction temperature was examined.

As shown in Table 1, the compound **8** was low active (1700 g C_2H_4/(g Cr·h)) and produced small amounts of polyethylenes (25 wt %). Moreover, precatalyst **8** gave rise to a selective system, affording mainly hexenes (23 wt%) with a high selectivity for α-olefins (>93%) (entry 1). The Cr(III) complex **9** with a longer alkyl linker between two nitrogens (N^{amine} and N^{NHC}) was tested under similar conditions and exhibited a three times higher productivity (5200 g C_2H_4/(g Cr·h), entry 2) and only 25 wt % of polyethylenes, and a similar selectivity in the formation of oligomers as the complex **8**. Increasing the quantity of the co-catalyst (574 equiv.) was expected to enhance the activity of the catalysis and a better productivity (7200 g C_2H_4/(g Cr·h), entry 3) with almost the same selectivity as with 400 equiv. of MAO were obtained. Furthermore, a higher initial reaction temperature is beneficial to the ethylene oligomerization, with a much higher ethylene consumption (11.1 g) and productivity (9200 g C_2H_4/(g Cr·h), entry 4).

entry	complex	ethylene consumed[a]	productivity[b]	selectivity[c]								
				C_4	C_6	C_8	C_{10}	C_{10}+	1-C_4	1-C_6	1-C_8	PE
1	8	2.1	1700	20	23	17	11	4	99	95	93	25
2	9	6.3	5200	16	25	23	21	12	99	91	85	3
3[d]	9	8.7	7200	13	24	25	23	12	98	85	72	3
4[e]	9	11.1	9200	15	23	23	21	13	99	92	86	5
5												

Conditions: amount of catalyst: 4×10^{-5} mol, amount of cocatalyst (MAO): 1.6×10^{-2} mol (400 equiv.), T = 30–35 °C, solvent: chlorobenzene, total volume: 20 mL, 10 bar C_2H_4, reaction time 35 min., every test was repeated at least twice.

[a] equal to the quantity of ethylene introduced minus the unreacted ethylene collected at the end of the reaction (see experimental), expressed in g;

[b] expressed in g C_2H_4/(g Cr·h);

[c] expressed in %, calculated by GC analysis;

[d] amount of cocatalyst (MAO): 2.3×10^{-2} mol (574 equiv.);

[e] T = 60 °C

Synthesis and structure of Ir complexes. The reaction of AgCl[(Im){C(Me)=NDipp}(C_2NMe_2)] (**5**) or AgCl[(Im){C(Me)=NDipp}(C_3NMe_2)] (**6**) with 0.5 equiv. [Ir(μ-Cl)(cod)]$_2$ in THF led to the isolation of yellow powders in good yield (eq. 5).

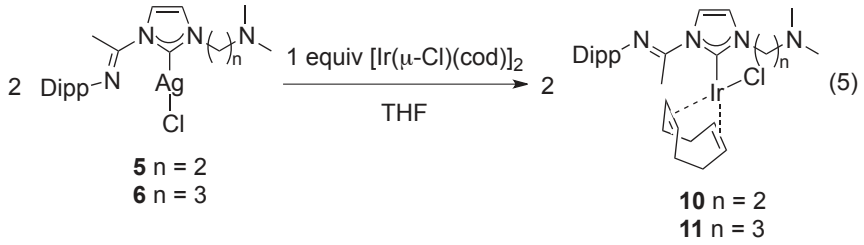

5 n = 2
6 n = 3

10 n = 2
11 n = 3

The mononuclear Ir(I) complex Ir(cod)Cl[(Im){C(Me)=NDipp}(C_3NMe_2)] (**11**) was shown by X-ray diffraction analysis to contain a monodentate NHC ligand (Figure 5). The square planar coordination geometry of the d^8 centre is defined by a chloride ligand, a bidentate 1,5-cyclooctadiene and a C^{NHC}-bound $N^{imine}C^{NHC}N^{amine}$ ligand of which the potential N-donors are dangling, their lone pairs pointing away from the iridium center, similarly to the situation previously encountered in a $N^{imine}C^{NHC}N^{imine}$ Ir(I) complex.[17c] The coordination of the C^{NHC} donor to the iridium center in solution was evidenced by a low-field resonance at δ 182.5 ppm in the $^{13}C\{^1H\}$ NMR spectrum in C_6D_6. The ^1H NMR resonances of the NHC backbone (NC*H*C*H*N)

protons at δ 7.61 and 6.56 ppm consist of two doublets with ^{3}J = 2.0 Hz, and are associated with ^{13}C NMR resonances at δ 122.0 and 118.9 ppm, respectively (HMQC experiment). Four broad peaks at δ 5.00, 2.93, 2.18 and 1.63 ppm are attributed to the cod protons. The methyl protons on the pendent arms resonate at δ 3.05 (CH_3^{imine}) and 2.01 (CH_3^{amine}) ppm.

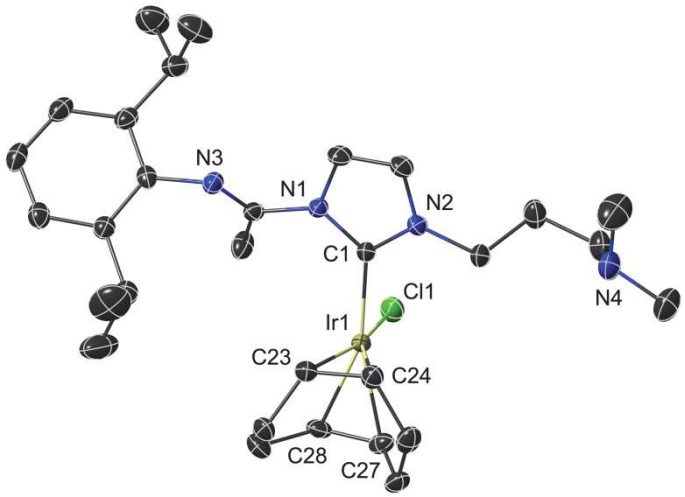

Figure 5. View of the structure of **11** with H atoms omitted for clarity. Thermal ellipsoids at the 60% probability levels. Selected bond lengths (Å) and angles (deg): Ir1−C1 2.029(2), Ir1−Cl1 2.367(4), C1−N1 1.378(2), C1−N2 1.355(2), N1−C1−N2 103.7(1), N1−C1−Ir1 129.2(1), N2−C1−Ir1 126.4(1).

In attempts to promote ligand chelation by coordination of a side arm in addition to the C^{NHC} donor and examine which of the two potential N donors would be preferred, **10** and **11** were reacted with a stoichiometric amount of $AgBF_4$ and the corresponding cationic complexes [Ir(cod){(Im)[C(Me)=NDipp](C$_2$NMe$_2$)}]BF_4 (**12**) and [Ir(cod){(Im)[C(Me)=NDipp](C$_3$NMe$_2$)}]BF_4 (**13**) were isolated, respectively (eq. 6).

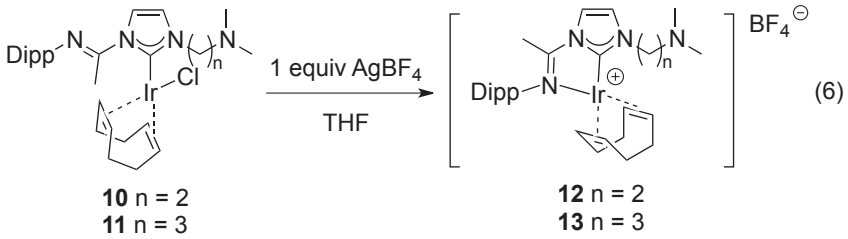

10 n = 2
11 n = 3

12 n = 2
13 n = 3

The structure of **13** was determined by X-ray diffraction (space group *P*-1) (Figure 6) and the cationic complex contains an iridium center in a distorted square planar coordination environment consisting of a bidentate cod molecule and a five-membered ring N^{imine},C^{NHC} chelate. Coordination

of the N^{imine} donor is favoured over N^{amine} by both the higher s character of the N-Ni bond and the size of the resulting chelate ring. The ^{1}H NMR resonances of the backbone protons NC*H*C*H*N appear as two doublets with ^{3}J = 1.5 Hz, and are low field-shifted to δ 8.26 and 7.71 ppm compared to δ 7.61 and 6.56 ppm in compound **11**. In contrast, the 1,5-cyclooctadiene protons are shifted upfield. The resonance of the CH_3^{imine} protons is upfield-shifted to δ 2.39 ppm compared to the pendent CH_3^{imine} whereas the resonance of the CH_3^{amine} protons are almost unchanged. The Ir–C^{NHC} distances of 2.029(2) Å (**11**) and 2.027(2) Å (**13**) are almost identical within experimental error and the reported average for other known Ir(I)–C^{NHC} bonds is 2.04 Å.

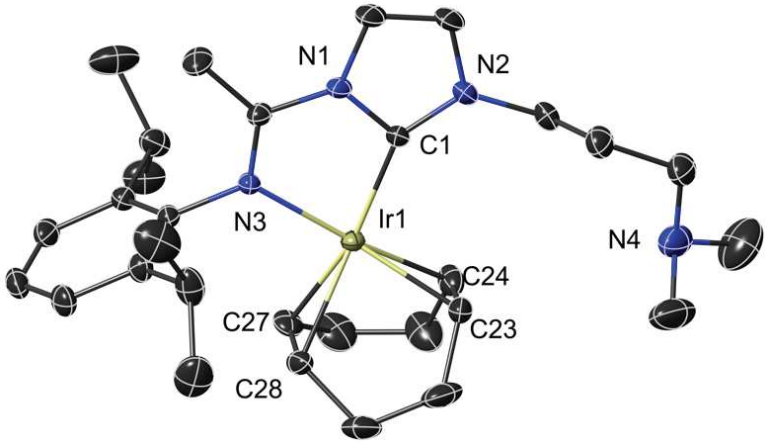

Figure 8. View of the structure of **13** with H atoms and $[BF_4]^-$ anion omitted for clarity. Thermal ellipsoids at the 70% probability levels. Selected bond lengths (Å) and angles (deg): Ir1−C1 2.027(2), Ir1−N3 2.099(2), C1−N1 1.386(3), C1−N2 1.340(3); N1−C1−N2 103.6(2), N1−C1−Ir1 112.7(1), N2−C1−Ir1 143.7(2), C1−Ir1−N3 77.8(8).

The analytical and spectroscopic data for **12** point to a structure similar to that of **13**.

5. Conclusion

A comparative study of the coordination behaviour of tritopic $N^{imine}C^{NHC}N^{amine}$ ligands to copper, chromium and iridium complexes has revealed interesting similarities and differences. In all cases, C^{NHC} coordination was observed, sometimes alone, or associated with amine or imine coordination, or both in the case of pincer formation. The two methodologies chosen to form Cu(I) complexes, i.e. reaction of imidazolium salt with mesityl copper(I) or deprotonation of imidazolium salt by trimethylsilylamide/CuI, have yielded complexes with very different structures. In the former case, mononuclear Cu(I) complexes with two dangling side arms were obtained whereas in the latter case, a tetranuclear ladder-type Cu(I) complex with $C^{NHC}N^{amine}$ bridging behaviour of the ligand was isolated. Such structures illustrate how functional ligands can favour the formation of polynuclear

Cu(I)-halide complexes. When transmetallation reactions from Cu(I) to Ni(II) were attempted with all our Cu(I) complexes, green paramagnetic solids were formed that were not characterized further. The $N^{imine}C^{NHC}N^{amine}$ ligands with different lengths of the spacer connecting the amine donor to the heterocycle were unambiguously shown to coordinate to Cr(III) in a pincer-type fashion. Whether starting from a Cr(II) or a Cr(III) precursor, the same complex was obtained and an unexpected redox reaction occurred during the Ag(I) transmetallation reaction with $[CrCl_2(THF)_2]$. Lavoie and co-workers mentioned the synthesis of Cr(II)/(III) complexes (**C** and **D** in Scheme 1) by Cu(I) transmetallation reaction using Cr(II)/(III) precursors with bidentate $N^{imine}C^{NHC}$ ligand. Incorporating an amine donor in the bidentate $N^{imine}C^{NHC}$ ligand impacts the geometric constraints of the tridentate system but the reasons for the occurrence of a redox reaction are still unclear. However, related phenomena have been previously encountered when Cr(II) complexes were reacted with Grignard reagents.[27]

In the case of Ir(I) chemistry, coordination of the $N^{imine}C^{NHC}N^{amine}$ ligand could be modified from C^{NHC} monodentate behaviour with both imine and amine donors pendent to bidentate $C^{NHC}N^{amine}$ coordination after halide abstraction to liberate an additional coordination site. Selective coordination of the N^{amine} donor was observed, the N^{imine} group remaining dangling. Clearly, both electronic and geometric parameters are involved in pincer formation.

6. Experimental section

General Considerations. All manipulations involving organometallics were performed under nitrogen or argon in a Braun glove-box or using standard Schlenk techniques. Solvents were dried using standard methods and distilled under nitrogen prior use or passed through columns of activated alumina and subsequently purged with nitrogen or argon. The starting materials **1**-**2** and **5**-**6** were prepared according to the literature. $[CrCl_2(THF)_2]$ and $[CrCl_3(THF)_3]$ were prepared by continuous Soxhlet extraction of commercial anhydrous $CrCl_2$ with THF under argon for 24−48 h. Mesityl copper(I) was obtained from commercial source and used as received. NMR spectra were recorded on Bruker spectrometers (AVANCE I − 300 MHz, AVANCE III − 400 MHz or AVANCE I − 500 MHz equipped with a cryogenic probe). Elemental analyses were performed by the "Service de microanalyses", Université de Strasbourg.

Preparation of [(ImH){C(Me)=NDipp}(C_2NMe_2)]Cl (1).

Description in the text of Chapter 2.

Preparation of [(ImH){C(Me)=NDipp}(C_3NMe_2)]Cl (2).

Description in the ESI of Chapter 3.

Preparation of [CuCl{Im[C(Me)=NDipp](C_2NMe_2)}] (3).

To a solution of [(ImH){C(Me)=NDipp}(C_2NMe_2)]Cl (0.100 g, 0.265 mmol) in toluene (5 mL) was added dropwise a solution of mesityl copper(I) (0.049 g, 0.268 mmol) in toluene (5 mL). The reaction mixture was stirred overnight at room temperature. The solution was concentrated under reduced pressure and then 10 mL Et_2O were added to precipitate the product. After removal of the solvent by filtration, a yellow powder was obtained (0.085 g, 73%). ^{1}H NMR (400 MHz, C_6D_6): δ 7.73 (d, ^3J = 1.2 Hz, 1H, $CH^{imidazole}$), 7.23-7.16 (br m, 3H, CH^{Ar}, overlapped with C_6D_6), 6.30 (br, 1H, $CH^{imidazole}$), 3.63 (t, ^3J = 5.6 Hz, 2H, $CH_2CH_2NMe_2$), 2.80 (sept, ^3J = 6.9 Hz, 2H, CH^{iPr}), 2.60 (s, 3H, CH_3^{imine}), 2.18 (t, ^3J = 5.6 Hz, 2H, $CH_2CH_2NMe_2$), 2.06 (s, 6H, $CH_2CH_2NMe_2$), 1.19 (d, ^3J = 6.9 Hz, 6H, CH_3^{iPr}), 1.12 (d, ^3J = 6.9 Hz, 6H, CH_3^{iPr}). ^{13}C NMR (100 MHz, C_6D_6): δ 179.0 ($C^{carbene}$), 153.2 (C^{imine}), 142.8 ($C^{ipso\text{-}Ar}$), 137.1 ($C^{o\text{-}Ar}$), 125.1 ($CH^{p\text{-}Ar}$), 123.7 ($CH^{m\text{-}Ar}$), 121.6 ($CH^{imidazole}$), 117.1 ($CH^{imidazole}$), 59.7 ($CH_2CH_2NMe_2$), 49.7 ($CH_2CH_2NMe_2$), 45.5 ($CH_2CH_2NMe_2$), 28.8 (CH^{iPr}), 23.5 (CH_3^{iPr}), 22.9 (CH_3^{iPr}), 18.8 (CH_3^{imine}) Anal. calcd. for $C_{21}H_{32}ClCuN_4$: C, 57.39; H, 7.34; N, 12.57%; found: C, 53.01; H, 6.88; N, 11.31% (despite several attempts, no better analytical data could be obtained).

Preparation of [CuCl{Im[C(Me)=NDipp](C_3NMe_2)}] (4).

To a solution of [(ImH){C(Me)=NDipp}(C_3NMe_2)]Cl (0.100 g, 0.256 mmol) in toluene (5 mL) was added dropwise a solution of mesityl copper(I) (0.047 g, 0.257 mmol) in toluene (5 mL). The reaction mixture was stirred overnight at room temperature. The solvent was concentrated under reduced pressure and 10 mL Et_2O were added to precipitate the product. After removal of the solvent by filtration, a yellow powder was obtained (0.079 g, 68%). ^{1}H NMR (400 MHz, C_6D_6): δ 7.69 (d, ^3J = 1.2 Hz, 1H, $CH^{imidazole}$), 7.16 (br s, 3H, CH^{Ar}), 6.19 (br, 1H, $CH^{imidazole}$), 3.83 (t, ^3J = 6.7 Hz, 2H, $CH_2CH_2CH_2NMe_2$), 2.80 (sept, ^3J = 6.9 Hz, 2H, CH^{iPr}), 2.56 (s, 3H, CH_3^{imine}), 2.04 (s, 6H, $CH_2CH_2CH_2NMe_2$), 1.85 (t, ^3J = 6.5 Hz, 2H, $CH_2CH_2CH_2NMe_2$), 1.56 (apparent t, $^{3,4}J$ = 6.7 Hz, $^{3,4}J$ = 6.5 Hz, 2H, $CH_2CH_2CH_2NMe_2$), 1.18 (d, ^3J = 6.9 Hz, 6H, CH_3^{iPr}), 1.12 (d, ^3J = 6.9 Hz, 6H, CH_3^{iPr}). ^{13}C NMR (100 MHz, C_6D_6): δ 179.2 ($C^{carbene}$), 152.9 (C^{imine}), 142.8 ($C^{ipso\text{-}Ar}$), 137.0 ($C^{o\text{-}Ar}$), 125.1 ($CH^{p\text{-}Ar}$), 123.8 ($CH^{m\text{-}Ar}$), 121.3 ($CH^{imidazole}$), 117.3 ($CH^{imidazole}$), 55.0 ($CH_2CH_2CH_2NMe_2$), 49.7 ($CH_2CH_2CH_2NMe_2$), 45.1 ($CH_2CH_2CH_2NMe_2$), 28.9 (CH^{iPr}), 28.8 ($CH_2CH_2CH_2NMe_2$), 23.5 (CH_3^{iPr}), 22.9 (CH_3^{iPr}), 18.8 (CH_3^{imine}). Anal. calcd. for $C_{22}H_{34}ClCuN_4$: C, 57.39; H, 7.34; N,

12.75%; found: C, 55.07; H, 7.17; N, 11.47% . Despite numerous attempts, no better analytical data could be obtained.

Preparation of [AgCl{Im[C(Me)=NDipp](C$_2$NMe$_2$)}] (5).

Description in the text of Chapter 2.

Preparation of [AgCl{Im[C(Me)=NDipp](C$_3$NMe$_2$)}] (6).

Description in the text of Chapter 2.

Preparation of [Cu$_4$I$_4${Im[C(Me)=NDipp](C$_3$NMe$_2$)}] (7).

To a solution of CuI (0.098 g, 0.515 mmol) in THF (5 mL) was added dropwise a solution of NaHMDS (0.047g, 0.256 mmol) in THF (3 mL) at −78 °C. The reaction mixture was slowly brought to room temperature and stirred for 1 h. The solution was added dropwise to a solution of [(ImH){C(Me)=NDipp}(C$_3$NMe$_2$)]Cl (0.100 g, 0.256 mmol) in THF (5 mL) at −78 °C. The reaction mixture was slowly brought to room temperature and stirred overnight. A yellow solution was obtained by filtration through Celite and the solvent was removed under reduced pressure. The product was washed with pentane (3x5 mL) to give a pale yellow powder (0.127 g, 68%). ^{1}H NMR (500 MHz, toluene-d_8): δ 7.71 (d, ^3J = 1.8 Hz, 1H, CH^{imidazole}), 7.09-6.97 (m, 3H, CH^{Ar}), 6.20 (d, ^3J = 1.8 Hz, 1H, CH^{imidazole}), 3.96 (apparent t, ^3J = 6.7 Hz, 2H, CH_2CH$_2$CH$_2$NMe$_2$), 2.84 (sept, ^3J = 6.9 Hz, 2H, CH^{iPr}), 2.69 (s, 3H, CH$_3^{imine}$), 1.99 (s, 6H, CH$_2$CH$_2$CH$_2$N*Me*$_2$), 1.91 (apparent t, ^3J = 6.4 Hz, 2H, CH$_2$CH$_2$CH_2NMe$_2$), 1.77 (m, 2H, CH$_2$CH_2CH$_2$NMe$_2$), 1.11 (d, ^3J = 6.9 Hz, 6H, CH$_3^{iPr}$), 1.09 (d, ^3J = 6.9 Hz, 6H, CH$_3^{iPr}$). ^{13}C NMR (126 MHz, Toluene-d_8) δ 185.9 (C^{carbene}), 153.7 (C^{imine}), 143.2 (C$^{ipso\text{-}Ar}$), 137.2 (C$^{o\text{-}Ar}$), (CH$^{p\text{-}Ar}$), 123.6 (CH$^{m\text{-}Ar}$), 121.2 (CH^{imidazole}), 116.7 (CH^{imidazole}), 55.6 (CH$_2$CH$_2$*C*H$_2$NMe$_2$), 49.1 (*C*H$_2$CH$_2$CH$_2$NMe$_2$), 45.5 (CH$_2$CH$_2$CH$_2$N*Me*$_2$), 28.8 (CH^{iPr}), 28.6 (CH$_2$*C*H$_2$CH$_2$NMe$_2$), 23.6 (CH$_3^{iPr}$), 23.1 (CH$_3^{iPr}$), 18.8 (CH$_3^{imine}$). Despite several attempts, no better microanalysis data could be obtained.

Preparation of [CrCl$_3${Im[C(Me)=NDipp](C$_2$NMe$_2$)}] (8).

Method A: To a solution of **5** (0.100 g, 0.207 mmol) in THF (5 mL) was added dropwise a solution of [CrCl$_2$(THF)$_2$] (0.055 g, 0.206 mmol) in THF (5 mL). The reaction mixture was stirred overnight at room temperature. A dark blue solution was obtained after filtration through Celite. The solvent was concentrated to ca. 3 mL under reduced pressure and then Et$_2$O (8 mL) was added as non-solvent. Dark blue crystals formed from crystallization (0.077 g, 75%).

Method B: To a solution of **5** (0.100 g, 0.207 mmol) in THF (5 mL) was added dropwise a solution of [$CrCl_3(THF)_3$] (0.078 g, 0.208 mmol) in THF (5 mL). The reaction mixture was stirred overnight at room temperature. A dark blue solution was obtained after filtration through Celite. The solvent was concentrated to ca. 3 mL under reduced pressure and then Et_2O (8 mL) was added as non-solvent. Dark blue crystals formed from crystallization (0.082 g, 80%). Anal. calcd. for $C_{21}H_{32}Cl_3CrN_4$: C, 50.56; H, 6.47; N, 11.23%; found: C, 40.44; H, 6.63; N, 7.90% (despite several attempts, no better analytical data could be obtained).

Preparation of [$CrCl_3${Im[C(Me)=NDipp](C_3NMe_2)}] (9).

Method A: To a solution of **6** (0.100 g, 0.201 mmol) in THF (5 mL) was added dropwise a solution of [$CrCl_2(THF)_2$] (0.054 g, 0.202 mmol) in THF (5 mL). The reaction mixture was stirred overnight at room temperature. A green solution was obtained after filtration through Celite. The solvent was concentrated to ca. 3 mL under reduced pressure and then Et_2O (8 mL) was added and green crystals were collected (0.081 g, 79%).

Method B: To a solution of **6** (0.100 g, 0.201 mmol) in THF (5 mL) was added dropwise a solution of [$CrCl_3(THF)_3$] (0.075 g, 0.200 mmol) in THF (5 mL). The reaction mixture was stirred overnight at room temperature. A green solution was obtained after filtration through Celite. The solvent was concentrated to ca. 3 mL under reduced pressure and then Et_2O (8 mL) was added as non-solvent and green crystals were collected (0.073 g, 68%). Anal. calcd. for $C_{22}H_{34}Cl_3CrN_4$: C, 51.52; H, 6.68; N, 10.92%; found : C, 49.68; H, 6.89; N, 9.41% (despite several attempts, no better analytical data could be obtained).

Preparation of [IrCl(cod){Im[C(Me)=NDipp](C_2NMe_2)}] (10).

To a solution of **5** (0.100 g, 0.207 mmol) in THF (5 mL) was added dropwise a solution of [Ir(μ-Cl)(cod)]$_2$ (0.070g, 0.104 mmol) in THF (5 mL). The reaction mixture was stirred overnight at room temperature. A yellow solution was obtained after filtration through Celite. The solvent was concentrated to ca. 3 mL under reduced pressure and then Et_2O (8 mL) was added as non-solvent and yellow crystals were collected (0.122 g, 87%). ^{1}H NMR (300 MHz, CD_3CN): δ 7.61 (d, ^3J = 2.2 Hz, 1H, $CH^{imidazole}$), 7.29-7.24 (m, 3H, CH^{Ar}), 7.21 (d, ^3J = 2.2 Hz, 1H, $CH^{imidazole}$), 4.19 (t, ^3J = 6.4 Hz, 2H, $CH_2CH_2NMe_2$), 3.77 (br m, 4H, CH^{cod}), 3.09 (sept, ^3J = 6.8 Hz, 2H, CH^{iPr}), 2.81 (t, ^3J = 6.4 Hz, 2H, $CH_2CH_2NMe_2$), 2.48 (s, 3H, CH_3^{imine}), 2.27 (s, 6H, $CH_2CH_2NMe_2$), 2.15 (s, 3H, CH_3CN, overlapped with CH_2^{cod}), 2.15 (br m, 4H, CH_2^{cod}), 1.72 (br m, 4H, CH_2^{cod}), 1.20 (d, ^3J = 6.8 Hz, 6H, CH_3^{iPr}), 1.10 (d, ^3J = 6.8 Hz, 6H, CH_3^{iPr}). ^{13}C NMR (126 MHz, C_6D_6): δ 182.5 ($C^{carbene}$), 155.4

(C^{imine}), 143.3 ($C^{ipso\text{-}Ar}$), 137.5 ($C^{o\text{-}Ar}$), 125.1 ($CH^{p\text{-}Ar}$), 123.7 ($CH^{m\text{-}Ar}$), 122.0 ($CH^{imidazole}$), 118.9 ($CH^{imidazole}$), 83.9 (CH^{cod}), 59.6 ($CH_2\mathit{C}H_2NMe_2$), 50.7 (CH^{cod}), 49.9 ($\mathit{C}H_2CH_2NMe_2$), 45.4 ($CH_2CH_2N\mathit{Me}_2$), 34.2 (CH_2^{cod}), 30.0 (CH_2^{cod}), 28.7 (CH^{iPr}), 23.6 (CH_3^{iPr}), 23.3 (CH_3^{iPr}), 22.8 (CH_3^{imine}). Anal. calcd. for $C_{29}H_{44}ClIrN_4$: C, 51.50; H, 6.56; N, 8.28%; found: C, 46.8; H, 6.28; N, 6.74% (despite several attempts, no better analytical data could be obtained).

Preparation of [IrCl(cod){Im[C(Me)=NDipp](C$_3$NMe$_2$)}] (11).

To a solution of **6** (0.100 g, 0.201 mmol) in THF (5 mL) was added dropwise a solution of $[Ir(\mu\text{-}Cl)(cod)]_2$ (0.068g, 0.101 mmol) in THF (5 mL). The reaction mixture was stirred overnight at room temperature. A yellow solution was obtained after filtration through Celite. The solvent was concentrated to ca. 3 mL under reduced pressure and then Et_2O (8 mL) was added as non-solvent and yellow crystals were collected (0.119 g, 86%). ^{1}H NMR (300 MHz, C_6D_6): δ 7.68 (d, ^3J = 2.1 Hz, 1H, $CH^{imidazole}$), 7.18-7.14 (m, 3H, CH^{Ar}), 6.37 (d, ^3J = 2.1 Hz, 1H, $CH^{imidazole}$), 5.01 (br s, 2H, CH^{cod}), 4.50 (br s, 2H, $C\mathit{H}_2CH_2CH_2NMe_2$), 3.11 (s, 3H, CH_3^{imine}), 2.96 (br m, 4H, CH^{iPr} overlapped with CH^{cod}), 2.22 (br m, 4H, $CH_2CH_2C\mathit{H}_2NMe_2$ overlapped with CH_2^{cod}), 2.11 (s, 6H, $CH_2CH_2CH_2N\mathit{Me}_2$), 2.07 (br m, 4H, CH_2^{cod}), 1.65 (br, m, 4H, $CH_2C\mathit{H}_2CH_2NMe_2$ overlapped with CH_2^{cod}), 1.18 (d, ^3J = 6.9 Hz, 6H, CH_3^{iPr}), 1.14 (d, ^3J = 6.9 Hz, 6H, CH_3^{iPr}). ^{13}C NMR (126 MHz, C_6D_6): δ 182.4 ($C^{carbene}$), 155.1 (C^{imine}), 143.3 ($C^{ipso\text{-}Ar}$), 137.5 ($C^{o\text{-}Ar}$), 125.1 ($CH^{p\text{-}Ar}$), 123.7 ($CH^{m\text{-}Ar}$), 122.4 ($CH^{imidazole}$), 118.2 ($CH^{imidazole}$), 83.9 (CH^{cod}), 55.3 ($CH_2CH_2\mathit{C}H_2NMe_2$), 50.5 ($CH^{cod}$), 49.2 ($\mathit{C}H_2CH_2CH_2NMe_2$), 44.9 ($CH_2CH_2CH_2N\mathit{Me}_2$), 34.1 ($CH_2^{cod}$), 30.2 ($CH_2^{cod}$), 28.7 ($CH^{iPr}$), 27.8 ($CH_2\mathit{C}H_2CH_2NMe_2$), 23.9 ($CH_3^{iPr}$), 23.3 ($CH_3^{iPr}$), 22.6 ($CH_3^{imine}$). Anal. calcd. for $C_{30}H_{46}ClIrN_4$: C, 52.19; H, 6.72; N, 8.12%; found: C, 51.55; H, 6.63; N, 8.34%.

Preparation of [Ir(cod){Im[C(Me)=NDipp](C$_2$NMe$_2$)}] (12).

To a solution of **10** (0.100 g, 0.148 mmol) in THF (5 mL) was added dropwise a solution of $AgBF_4$ (0.029 g, 0.149 mmol) in THF (5 mL). The reaction mixture was stirred overnight at room temperature. A dark green-blue solution was obtained after filtration through Celite. The solvent was concentrated to ca. 3 mL under reduced pressure and then Et_2O (8 mL) was added as non-solvent and dark blue crystals were collected (0.085 g, 79%). ^{1}H NMR (500 MHz, C_6D_6): δ 8.36 (d, ^3J = 2.3 Hz, 1H, $CH^{imidazole}$), 7.83 (d, ^3J = 2.3 Hz, 1H, $CH^{imidazole}$), 7.00-6.90 (m, 3H, CH^{Ar}), 4.33 (m, 2H, CH^{cod}), 3.69 (t, ^3J = 6.7 Hz, 2H, $C\mathit{H}_2CH_2NMe_2$), 3.64 (m, 2H, CH^{cod}), 2.91 (sept, ^3J = 6.7 Hz, 2H, CH^{iPr}), 2.50 (t, ^3J = 6.7 Hz, 2H, $CH_2C\mathit{H}_2NMe_2$), 2.45 (s, 3H, CH_3^{imine}), 2.07 (s, 6H, $CH_2CH_2N\mathit{Me}_2$), 1.98 (m br, 2H, CH_2^{cod}), 1.80 (m br, 2H, CH_2^{cod}), 1.56 (m br, 2H, CH_2^{cod}), 1.39 (m

br, 2H, CH_2^{cod}), 1.12 (d, ^3J = 6.7 Hz, 6H, CH_3^{iPr}, overlapped with Et_2O), 0.91 (d, ^3J = 6.9 Hz, 6H, CH_3^{iPr}). ^{13}C NMR (126 MHz, C_6D_6) δ 173.1 ($C^{carbene}$), 171.5 (C^{imine}), 141.9 ($C^{o\text{-}Ar}$), 137.7 ($C^{ipso\text{-}Ar}$), 128.7 ($CH^{p\text{-}Ar}$), 126.5 ($CH^{imidazole}$), 124.3 ($CH^{m\text{-}Ar}$), 120.5 ($CH^{imidazole}$), 88.2 (CH^{cod}), 63.6 (CH^{cod}), 59.3 ($CH_2CH_2NMe_2$), 48.1 ($CH_2CH_2NMe_2$), 45.7 ($CH_2CH_2NMe_2$), 33.7 (CH_2^{cod}), 29.6 (CH_2^{cod}), 28.5 (CH^{iPr}), 25.1 (CH_3^{iPr}), 23.4 (CH_3^{iPr}), 16.6 (CH_3^{imine}). Anal. calcd. for $C_{29}H_{44}BF_4IrN_4$: C, 47.86; H, 6.09; N, 7.70%; found: C, 44.56; H, 5.94; N, 6.98% (despite several attempts, no better analytical data could be obtained).

Preparation of [Ir(cod){Im[C(Me)=NDipp](C$_3$NMe$_2$)}] (13).

To a solution of **11** (0.100 g, 0.145 mmol) in THF (5 mL) was added dropwise a solution of $AgBF_4$ (0.029 g, 0.149 mmol) in THF (5 mL). The reaction mixture was stirred overnight at room temperature. A dark green-blue solution was obtained after filtration through Celite. The solvent was concentrated to ca. 3 mL under reduced pressure and then Et_2O (8 mL) was added as non-solvent and dark blue crystals were collected (0.089 g, 83%). ^{1}H NMR (500 MHz, C_6D_6): δ 8.29 (d, ^3J = 2.1 Hz, 1H, $CH^{imidazole}$), 7.79 (d, ^3J = 2.1 Hz, 1H, $CH^{imidazole}$), 7.00-6.91 (m, 3H, CH^{Ar}), 4.46 (br m, 2H, CH^{cod}), 3.71 (t, ^3J = 7.3 Hz, 2H, $CH_2CH_2CH_2NMe_2$), 3.65 (br m, 2H, CH^{cod}), 2.94 (sept, ^3J = 6.9 Hz, 2H, CH^{iPr}), 2.41 (s, 3H, CH_3^{imine}), 2.29 (t, ^3J = 6.4 Hz, 2H, $CH_2CH_2CH_2NMe_2$), 2.05 (s, 6H, $CH_2CH_2CH_2NMe_2$), 2.02 (br m, 2H, CH_2^{cod}, overlapped with $CH_2CH_2CH_2NMe_2$), 1.91-1.86 (m, 2H, $CH_2CH_2CH_2NMe_2$), 1.81 (br m, 2H, CH_2^{cod}), 1.60 (br m, 2H, CH_2^{cod}), 1.42 (br m, 2H, CH_2^{cod}), 1.13 (d, ^3J = 6.9 Hz, 6H, CH_3^{iPr}), 0.94 (d, ^3J = 6.9 Hz, 6H, CH_3^{iPr}). ^{13}C NMR (126 MHz, C_6D_6) δ 173.2 ($C^{carbene}$), 171.1 (C^{imine}), 141.9 ($C^{o\text{-}Ar}$), 137.7 ($C^{ipso\text{-}Ar}$), 128.7 ($CH^{p\text{-}Ar}$), 125.7 ($CH^{imidazole}$), 124.3 ($CH^{m\text{-}Ar}$), 121.0 ($CH^{imidazole}$), 88.2 (CH^{cod}), 64.0 (CH^{cod}), 55.5 ($CH_2CH_2CH_2NMe_2$), 47.3 ($CH_2CH_2CH_2NMe_2$), 45.1 ($CH_2CH_2CH_2NMe_2$), 33.8 (CH_2^{cod}), 29.6 (CH_2^{cod}), 28.5 (CH^{iPr}), 28.4 ($CH_2CH_2CH_2NMe_2$), 25.1 (CH_3^{iPr}), 23.3 (CH_3^{iPr}), 16.5 (CH_3^{imine}). Anal. calcd. for $C_{30}H_{46}BF_4IrN_4$: C, 48.58; H, 6.25; N, 7.55%; found: C, 48.51; H, 6.42; N, 7.51%.

7. Acknowledgements

We are grateful to the China Scholarship Council for a PhD grant to X.R. We thank Marc Mermillon-Fournier for technical assistance, the CNRS and the MESR (Paris) for funding and Lydia Karmazin and Corinne Bailly from the Service de Radiocristallographie (UdS) for the determination of the crystal structures.

8. References

(1) A. J. Arduengo, R. L. Harlow, M. Kline, *J. Am. Chem. Soc.* **1991**, *113*, 361-363.

(2) a) W.-H. Zhang, S. W. Chien, T. S. A. Hor, *Coord. Chem. Rev.* **2011**, *255*, 1991-2024; b) P. Braunstein, F. Naud, *Angew. Chem. Int. Ed.* **2001**, *40*, 680-699.

(3) S. Hameury, P. de Fremont, P. Braunstein, *Chem. Soc. Rev.* **2017**, *46*, 632-733.

(4) C. Fliedel, P. Braunstein, *J. Organomet. Chem.* **2014**, *751*, 286-300.

(5) S. Gaillard, J.-L. Renaud, *Dalton Trans.* **2013**, *42*, 7255-7270.

(6) a) M. Pellei, V. Gandin, M. Marinelli, C. Marzano, M. Yousufuddin, H. V. R. Dias, C. Santini, *Inorg. Chem.* **2012**, *51*, 9873-9882; b) G. Huang, H. Sun, X. Qiu, Y. Shen, J. Jiang, L. Wang, *J. Organomet. Chem.* **2011**, *696*, 2949-2957; c) C.-C. Tai, M.-S. Yu, Y.-L. Chen, W.-H. Chuang, T.-H. Lin, G. P. A. Yap, T.-G. Ong, *Chem. Commun.* **2014**, *50*, 4344-4346; d) S. Warsink, S. Y. de Boer, L. M. Jongens, C.-F. Fu, S.-T. Liu, J.-T. Chen, M. Lutz, A. L. Spek, C. J. Elsevier, *Dalton Trans.* **2009**, 7080-7086; e) A. R. Naziruddin, C.-S. Zhuang, W.-J. Lin, W.-S. Hwang, *Dalton Trans.* **2014**, *43*, 5335-5342; f) A. A. D. Tulloch, S. Winston, A. A. Danopoulos, G. Eastham, M. B. Hursthouse, *Dalton Trans.* **2003**, 699-708; g) A. M. Magill, D. S. McGuinness, K. J. Cavell, G. J. P. Britovsek, V. C. Gibson, A. J. P. White, D. J. Williams, A. H. White, B. W. Skelton, *J. Organomet. Chem.* **2001**, *617–618*, 546-560; h) D. Yang, Y. Tang, H. Song, B. Wang, *Organometallics* **2016**, *35*, 1392-1398; i) R. M. Brown, J. Borau Garcia, J. Valjus, C. J. Roberts, H. M. Tuononen, M. Parvez, R. Roesler, *Angew. Chem. Int. Ed.* **2015**, *54*, 6274-6277; j) J. Deng, H. Gao, F. Zhu, Q. Wu, *Organometallics* **2013**, *32*, 4507-4515; k) J. L. Drake, H. Z. Kaplan, M. J. T. Wilding, B. Li, J. A. Byers, *Dalton Trans.* **2015**, *44*, 16703-16707; l) X. Wang, H. Chen, X. Li, *Organometallics* **2007**, *26*, 4684-4687; m) S. Conde-Guadano, M. Hanton, R. P. Tooze, A. A. Danopoulos, P. Braunstein, *Dalton Trans.* **2012**, *41*, 12558-12567; n) W. B. Cross, C. G. Daly, Y. Boutadla, K. Singh, *Dalton Trans.* **2011**, *40*, 9722-9730.

(7) a) S. Díez-González, N. Marion, S. P. Nolan, *Chem. Rev.* **2009**, *109*, 3612-3676; b) A. Nasr, A. Winkler, M. Tamm, *Coord. Chem. Rev.* **2016**, *316*, 68-124; c) C. S. J. Cazin, *N-Heterocyclic Carbenes in Transition Metal Catalysis and Organocatalysis*, Springer Netherlands, **2010**; d) D. M. Flanigan, F. Romanov-Michailidis, N. A. White, T. Rovis, *Chem. Rev.* **2015**, *115*, 9307-9387; e) E. Peris, *Chem. Rev.* **2017**; f) V. Charra, P. de Frémont, P. Braunstein, *Coord. Chem. Rev.* **2017**, *341*, 53-176; g) W. A. Herrmann, C. Köcher, *Angew. Chem. Int. Ed. Engl.* **1997**, *36*, 2162-2187; h) W. A. Herrmann, *Angew. Chem. Int.*

Ed. **2002**, *41*, 1290-1309; i) N. Marion, S. Díez-González, S. P. Nolan, *Angew. Chem. Int. Ed.* **2007**, *46*, 2988-3000.

(8) R. Visbal, M. C. Gimeno, *Chem. Soc. Rev.* **2014**, *43*, 3551-3574.

(9) a) G. van Koten, R. A. Gossage, *The Privileged Pincer-Metal Platform: Coordination Chemistry & Applications*, Springer International Publishing, **2015**; b) G. van Koten, D. Milstein, *Organometallic Pincer Chemistry*, Springer Berlin Heidelberg, **2013**; c) M. Asay, D. Morales-Morales, in *The Privileged Pincer-Metal Platform: Coordination Chemistry & Applications* (Eds.: G. van Koten, R. A. Gossage), Springer International Publishing, Cham, **2016**, pp. 239-268; d) D. Morales-Morales, C. M. Jensen, Elsevier Science B.V., Amsterdam, The Netherlands, **2007**.

(10) a) J. T. Dixon, M. J. Green, F. M. Hess, D. H. Morgan, *J. Organomet. Chem.* **2004**, *689*, 3641-3668; b) D. S. McGuinness, *Chem. Rev.* **2011**, *111*, 2321-2341; c) T. Agapie, *Coord. Chem. Rev.* **2011**, *255*, 861-880; d) P. W. N. M. van Leeuwen, N. D. Clément, M. J. L. Tschan, *Coord. Chem. Rev.* **2011**, *255*, 1499-1517.

(11) a) C. Fliedel, A. Ghisolfi, P. Braunstein, *Chem. Rev.* **2016**, *116*, 9237-9304; b) A. Bollmann, K. Blann, J. T. Dixon, F. M. Hess, E. Killian, H. Maumela, D. S. McGuinness, D. H. Morgan, A. Neveling, S. Otto, M. Overett, A. M. Z. Slawin, P. Wasserscheid, S. Kuhlmann, *J. Am. Chem. Soc.* **2004**, *126*, 14712-14713; c) M. J. Overett, K. Blann, A. Bollmann, J. T. Dixon, F. Hess, E. Killian, H. Maumela, D. H. Morgan, A. Neveling, S. Otto, *Chem. Commun.* **2005**, 622-624; d) K. Blann, A. Bollmann, J. T. Dixon, F. M. Hess, E. Killian, H. Maumela, D. H. Morgan, A. Neveling, S. Otto, M. J. Overett, *Chem. Commun.* **2005**, 620-621.

(12) a) M. Mastalir, S. R. M. M. de Aguiar, M. Glatz, B. Stöger, K. Kirchner, *Organometallics* **2016**; b) A. Alzamly, S. Gambarotta, I. Korobkov, *Organometallics* **2013**, *32*, 7204-7212; c) A. Alzamly, S. Gambarotta, I. Korobkov, *Organometallics* **2014**, *33*, 1602-1607; d) D. S. McGuinness, P. Wasserscheid, W. Keim, C. Hu, U. Englert, J. T. Dixon, C. Grove, *Chem. Commun.* **2003**, 334-335; e) T. Simler, G. Frison, P. Braunstein, A. A. Danopoulos, *Dalton Trans.* **2016**, *45*, 2800-2804; f) T. Simler, P. Braunstein, A. A. Danopoulos, *Organometallics* **2016**.

(13) T. Simler, A. A. Danopoulos, P. Braunstein, *Chem. Commun.* **2015**, *51*, 10699-10702.

(14) J. E. Radcliffe, A. S. Batsanov, D. M. Smith, J. A. Scott, P. W. Dyer, M. J. Hanton, *ACS Catalysis* **2015**, *5*, 7095-7098.

(15) D. S. McGuinness, V. C. Gibson, D. F. Wass, J. W. Steed, *J. Am. Chem. Soc.* **2003**, *125*,

12716-12717.

(16) a) S. Liu, R. Peloso, R. Pattacini, P. Braunstein, *Dalton Trans.* **2010**, *39*, 7881-7883; b) S. Liu, R. Pattacini, P. Braunstein, *Organometallics* **2011**, *30*, 3549-3558.

(17) a) Z. Liu, W. Gao, X. Liu, X. Luo, D. Cui, Y. Mu, *Organometallics* **2011**, *30*, 752-759; b) Y. Uetake, T. Niwa, M. Nakada, *Tetrahedron: Asymmetry* **2015**, *26*, 158-162; c) P. Liu, M. Wesolek, A. A. Danopoulos, P. Braunstein, *Organometallics* **2013**, *32*, 6286-6297.

(18) a) J. A. Thagfi, G. G. Lavoie, *Organometallics* **2012**, *31*, 7351-7358; b) T. G. Larocque, A. C. Badaj, S. Dastgir, G. G. Lavoie, *Dalton Trans.* **2011**, *40*, 12705-12712.

(19) F. He, L. Ruhlmann, J.-P. Gisselbrecht, S. Choua, M. Orio, M. Wesolek, A. A. Danopoulos, P. Braunstein, *Dalton Trans.* **2015**, *44*, 17030-17044.

(20) B. Cordero, V. Gomez, A. E. Platero-Prats, M. Reves, J. Echeverria, E. Cremades, F. Barragan, S. Alvarez, *Dalton Trans.* **2008**, 2832-2838.

(21) a) R.-Y. Wang, X. Zhang, Q.-F. Yang, Q.-S. Huo, J.-H. Yu, J.-N. Xu, J.-Q. Xu, *J. Solid State Chem.* **2017**, *251*, 176-185; b) W. Liu, K. Zhu, S. J. Teat, G. Dey, Z. Shen, L. Wang, D. M. O'Carroll, J. Li, *J. Am. Chem. Soc.* **2017**, *139*, 9281-9290.

(22) R. Peng, M. Li, D. Li, *Coord. Chem. Rev.* **2010**, *254*, 1-18.

(23) a) S.-Q. Bai, L. Jiang, A. L. Tan, S. C. Yeo, D. J. Young, T. S. Andy Hor, *Inorganic Chemistry Frontiers* **2015**, *2*, 1011-1018; b) Q. Benito, A. Fargues, A. Garcia, S. Maron, T. Gacoin, J.-P. Boilot, S. Perruchas, F. Camerel, *Chem. Eur. J.* **2013**, *19*, 15831-15835; c) A. Lapprand, M. Dutartre, N. Khiri, E. Levert, D. Fortin, Y. Rousselin, A. Soldera, S. Jugé, P. D. Harvey, *Inorg. Chem.* **2013**, *52*, 7958-7967.

(24) X.-c. Shan, F.-l. Jiang, D.-q. Yuan, H.-b. Zhang, M.-y. Wu, L. Chen, J. Wei, S.-q. Zhang, J. Pan, M.-c. Hong, *Chem. Sci.* **2013**, *4*, 1484-1489.

(25) M. S. Deshmukh, A. Yadav, R. Pant, R. Boomishankar, *Inorg. Chem.* **2015**, *54*, 1337-1345.

(26) C. Fliedel, P. Braunstein, *Organometallics* **2010**, *29*, 5614-5626.

(27) P. Ai, A. A. Danopoulos, P. Braunstein, *Organometallics* **2015**, *34*, 4109-4116.

9. Supporting Information

Synthesis and Structural Characterization of Cu(I), Cr(III) and Ir(I) Complexes with Tritopic $N^{imine}C^{NHC}N^{amine}$ pincer Ligands and Catalytic Ethylene Oligomerization

Xiaoyu Ren,[a] Marcel Wesolek,[a] and Pierre Braunstein*[a]*

[a] *Laboratoire de Chimie de Coordination, Institut de Chimie (UMR 7177 CNRS), Université de Strasbourg, 4 rue Blaise Pascal, 67081 Strasbourg Cedex (France)*

E-mail: braunstein@unistra.fr

X-ray crystallography

Summary of the crystal data, data collection and refinement for structures of **3**, **7**, **8**, **9**, **11**, **13** are given in Table S1. The crystals were mounted on a glass fiber with grease, from Fomblin vacuum oil. Data sets were collected on a Bruker APEX II DUO diffractometer equipped with an Oxford Cryosystem liquid N_2 device, using Mo-Kα radiation (λ = 0.71073 Å). The crystal-detector distance was 38 mm. The cell parameters were determined (APEX2 software)[1] from reflections taken from three sets of 12 frames, each at 10 s exposure. The structures were solved by direct methods using the program SHELXS-97.[2] The refinement and all further calculations were carried out using SHELXL- 97.[3] The H-atoms were included in calculated positions and treated as riding atoms using SHELXL default parameters. The non-H atoms were refined anisotropically, using weighted full-matrix least-squares on F^2.

The following special comments apply to the models of the structures:

For **3**, the carbons C13, C14 and hydrogens of C12 are disordered on two positions. This structure is good with R1=3.9%.

For **7**, this is the copper complex with two ligands, four copper and four iodine. Each iodine is coordinated to two copper. The asymmetric unit contains half a molecule of this complex. This structure is correct : R1=5.5%.

For **8**, a squeeze was made. The residual electron density was assigned to one molecule of THF. This structure is correct : R1=5%.

For **9**, the chromium is coordinated to one ligand and to three chlorides. The asymmetric unit contains also two molecules of toluene. The methylenes : C19 and C20 are disordered on two positions. The hydrogens of C18 are also disordered on two position. One toluene (C30, C31, C32, C33, C34, C35, C36) is disordered on two positions. This structure is correct : R1=5%.

For **11**, this structure is good : R1=1.9%.

For **13**, the asymmetric unit contains a THF molecule in addition. The structure is good (R1=2,6%).

Summary of crystal data

Table S1. Crystal data for compounds.

	3	**7**	**8**
Chemical formula	$C_{21}H_{32}ClCuN_4$	$C_{44}H_{68}Cu_4I_4N_8$	$C_{21}H_{32}Cl_3CrN_4$
CCDC Number			
Formula Mass	439.49	1470.82	498.85
Crystal system	monoclinic	monoclinic	triclinic
a/Å	11.5696(5)	15.7098(8)	9.2760(10)
b/Å	11.3251(5)	8.6227(2)	10.6492(12)
c/Å	17.3683(8)	22.1783(10)	15.4308(17)
α/°	90	90	94.943(2)
β/°	91.4890(10)	119.744(3)	105.109(2)
γ/°	90	90	96.726(2)
Unit cell volume/Å^3	2274.95(18)	2608.5(2)	1450.6(3)
Temperature/K	173(2)	173(2)	173(2)
Space group	*P 21/c*	*P 21/c*	*P -1*
Formula units / cell, *Z*	4	2	2
Absorption coefficient, μ/mm^{-1}	1.090	4.013	0.683
No. of reflections measured	21300	14983	26545
No. of independent reflections	5494	5963	7041
R_{int}	0.0331	0.0836	0.0619
Final R_1 values ($I > 2\sigma(I)$)	0.0399	0.0555	0.0507
Final $wR(F^2)$ values ($I > 2\sigma(I)$)	0.0903	0.1164	0.1081
Final R_1 values (all data)	0.0614	0.1020	0.0978
Final $wR(F^2)$ values (all data)	0.0984	0.1559	0.1184
Goodness of fit on F^2	1.029	1.096	0.961

	9 • 2 Toluene	**11**	**13 • THF**
Chemical formula	$C_{22}H_{34}Cl_3CrN_4$, $2(C_7H_8)$	$C_{30}H_{46}ClIrN_4$	$C_{30}H_{46}IrN_4$, BF_4, C_4H_8O
CCDC Number			
Formula Mass	697.15	690.36	813.82
Crystal system	orthorhombic	triclinic	triclinic
a/Å	11.6017(4)	8.4032(4)	10.1636(5)
b/Å	18.8201(7)	11.1493(5)	10.9789(5)
c/Å	32.9818(11)	16.7862(7)	17.0720(9)
α/°	90	105.2100(10)	107.6610(10)
β/°	90	104.4890(10)	92.2080(10)
γ/°	90	96.0040(10)	100.5780(10)
Unit cell volume/Å^3	7201.4(4)	1444.74(11)	1775.30(15)
Temperature/K	173(2)	173(2)	173(2)
Space group	*P b c a*	*P -1*	*P -1*
Formula units / cell, *Z*	8	2	2
Absorption coefficient, μ/mm^{-1}	0.571	4.739	3.813
No. of reflections measured	82448	41189	57054
No. of independent reflections	8673	10898	12293
R_{int}	0.0795	0.0229	0.0215
Final R_1 values ($I > 2\sigma(I)$)	0.0502	0.0199	0.0257
Final $wR(F^2)$ values ($I > 2\sigma(I)$)	0.1003	0.0424	0.0629
Final R_1 values (all data)	0.0861	0.0254	0.0297
Final $wR(F^2)$ values (all data)	0.1120	0.0441	0.0647
Goodness of fit on F^2	1.022	1.068	1.092

For references, see p. 129

REFERENCES

(1) Bruker AXS Inc Madison USA, **2006**.

(2) G. M. Sheldrick, *Acta Crystallogr. Sect. A: Found. Crystallogr.*, **1990**, *A46*, 467.

(3) G. M. Sheldrick, Universität Göttingen: Göttingen Germany, **1999**.

For references, see p. 129

CONCLUSION GÉNÉRALE

Dans cette thèse, nous avons développé la synthèse d'une série de nouveaux ligands NHC fonctionnalisés par un groupe éther et/ou par un azote d'un groupement amine ou imine représentés dans le Schéma 1. Les complexes du nickel et du chrome correspondants ont été caractérisés et leurs propriétés catalytiques évaluées dans la réaction d'oligomérisation de l'éthylène. Avec le ligand de type pinceur « tritopique » $N^{imine}C^{NHC}N^{amine}$ des complexes de l'Ir(I) bidentes ont été caractérisés et leurs propriétés catalytiques sont en cours d'études.

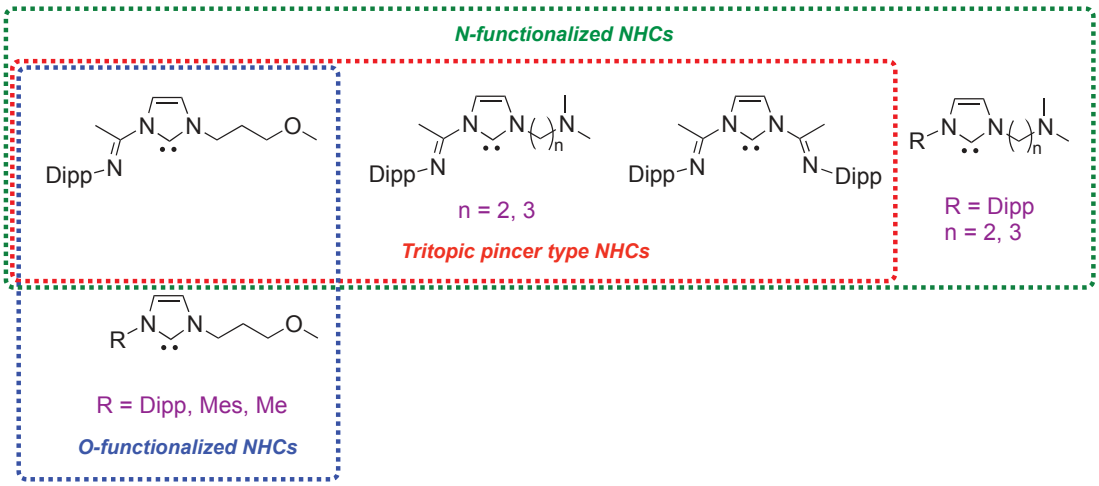

Schéma 1. Différents types de ligands NHC utilisés dans cette thèse.

Dans la première partie de notre travail nous nous sommes focalisés sur un ligand NHC possédant une fonctionnalité éther avec un espaceur C_3 entre l'hétérocycle et la fonction éther et nous avons étudié son pouvoir chélatant. Nous avons mis au point une synthèse indirecte des complexes mono- ou bis-NHC du Ni(II) en contrôlant la quantité de base utilisée. En introduisant une fonctionnalité amine à la place de l'éther, nous avons montré que celle-ci avait un pouvoir coordinant plus important.

Dans la seconde partie du travail, nous avons utilisé des ligands « tritopiques » avec trois atomes donneurs différents, N^{imine}, N^{amine} et C^{NHC}, et nous avons examiné leur mode de coordination. Les modes pontant, chélatant, monodentate, bidentate et tridentate ont été observés et caractérisés qui soulignent la polyvalence de tels systèmes. De plus, la longueur de l'espaceur connectant l'amine à l'azote hétérocyclique change de façon spectaculaire le cours de la réaction. Dans le cas de l'espaceur C_2 (**1**), on observe la fragmentation d'un des ligands avec la formation concomittante d'un complexe dinucléaire du Ni(II) (**3**). Par contre, dans le cas de

l'espaceur C_3 (**2**), un complexe (**4**) allyl-η^3 Ni(I)-Ni(I) se forme par insertion du 1,5 cyclooctadiène dans la liaison Ni-H d'un intermédiaire, réaction suivie d'une isomérisation. Au départ des sels d'imidazolium protonés, quand l'espaceur est C_2 (**5**) on isole un complexe (**7**) du Ni(II) mono-NHC « tritopique », tandis que quand l'espaceur est C_3 (**6**), on isole un complexe (**8**) dinucléaire du Ni(II) bis-NHC.

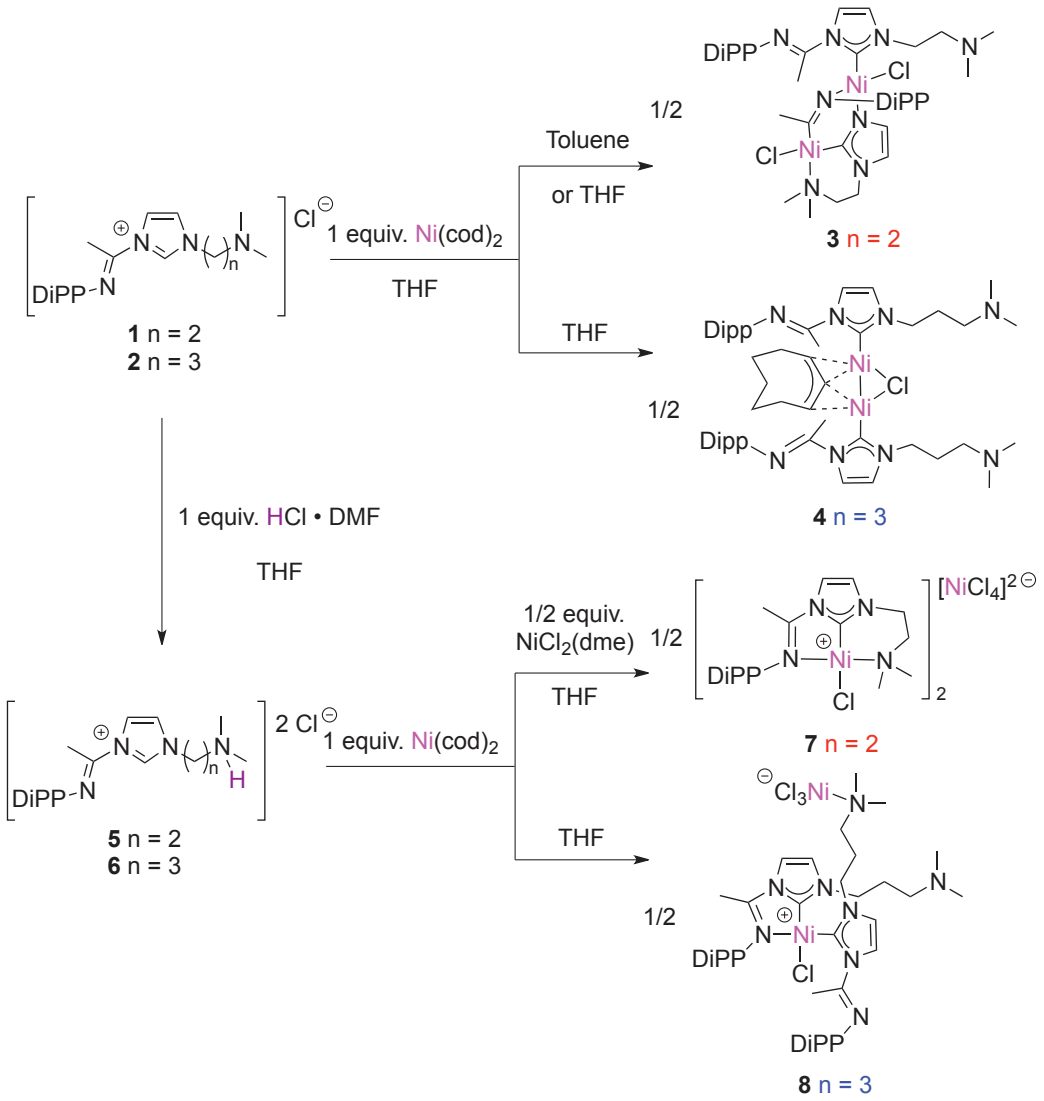

Schéma 2. Différents complexes du Ni obtenus par réaction des ligands « tritopiques » avec des espaceurs C_2 et C_3 libres ou protonés et $[Ni(cod)_2]$.

Dans le cas de l'imidazolium (**9**) fonctionnalisé avec deux imines, l'activation du proton C-H de l'hétérocycle ne s'est étonnamment pas produite mais un complexe (**10**) remarquable du Ni(II) possédant un ligand sp^3 imidazolyl chélaté avec le deux

groupements imine s'est formé. De manière inattendue, lors du traitement de ce complexe du nickel imidazolyle avec un excès d'éthylène en solution, un complexe (**11**) a été obtenu qui résulte de l'insertion de l'éthylène dans la liaison C1-H1 du cycle imidazole. Ce fait excitant puisqu'il implique la réactivité d'un carbone Csp^3 permet d'envisager de nouveaux mécanismes en ce qui concerne l'insertion de l'éthylène.

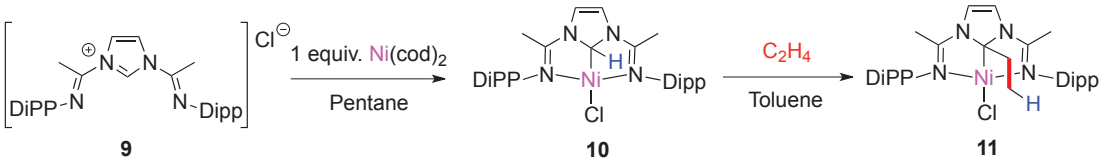

9 **10** **11**

Schéma 3. Synthèse du complexe bis-imine de Ni(II) et insertion d'éthylène dans la liaison Csp^3-H.

Enfin nous avons également examiné la synthèse de complexes d'autres métaux de transition avec ces ligands pinceurs « tritopique », tels que le chrome (Schéma 4)

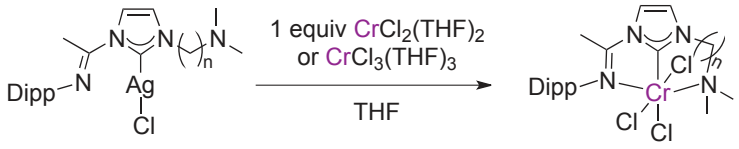

12 n = 2
13 n = 3

14 n = 2
15 n = 3

Schéma 4. Synthèse de complexes « tritopic » $N^{imine}C^{NHC}N^{amine}$ du Cr (III).

et l'iridium (Schéma 5)

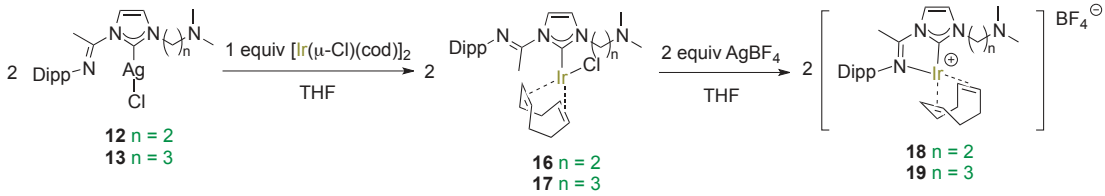

12 n = 2
13 n = 3

16 n = 2
17 n = 3

18 n = 2
19 n = 3

Schéma 5. Synthèse de complexes $N^{imine}C^{NHC}N^{amine}$ de l'Ir (I).

Durant cette thèse, des compétences expérimentales dans la manipulation et la caractérisation de composés très réactifs, sensibles à l'air, ont pu être acquises. Cette thèse m'a donné l'occasion d'élargir considérablement mes connaissances dans la chimie organométallique et la chimie de coordination.

Xiaoyu REN

Synthèse et réactivité de complexes métalliques porteurs de ligands carbéniques N-hétérocycliques fonctionnels

Résumé

Des ligands hydrides potentiellement bidentes (possédant un donneur N-hétérocyclique (NHC) associé à un groupement donneur éther ou amine) ainsi que des ligands tritopiques de type pinceur (possédant un groupement (NHC) flanqué de deux types de donneurs azotés différents N^{imine} et N^{amine})ont été préparés et utilisés pour la coordination de métaux de transition tels que le Ni, Cr, Cu et Ir. L'influence de la longueur de la chaine alkylée $-(CH_2)_2-$ ou $-(CH_2)_3-$ reliant le groupe éther ou amine au groupe hétérocyclique (NHC) a été examinée. Dans le but d'accéder aux complexes des métaux de transition différentes méthodologies ont été adoptées : a) déprotonation préalable du sel d'imidazolium suivie de l'addition des précurseurs métalliques correspondants ; b) transmétallation à partir des complexes (NHC) de l'argent correspondants ; c) réaction d'addition oxydante des sels d'imidazolium ou de leurs sels protonés avec du Ni(0). Une série de complexes du Ni(II) et du Cr(III) a été testée dans la réaction catalytique d'oligomérisation de l'éthylène.

Mots clés : carbènes N-hétérocycliques, ligands tritopiques de type pinceur, addition oxydante, alkylation, Ni, Cr, Ir, Cu, Ag, oligomérisation de l'éthylène.

Résumé en anglais

Potentially bidentate hybrid ligands (containing a NHC donor associated with an ether or an amine) and tridentate NCN pincer-type ligands (containing a central NHC donor flancked by two chemically-different nitrogen donors (N^{imine} and N^{amine})) have been prepared and used for coordination to transition metals, such as Ni, Cr, Cu, Ir. The influence of the length of the alkyl chain, $-(CH_2)_2-$ or $-(CH_2)_3-$ connecting the ether or the amine group to the heterocycle NHC was examined. In order to have access to the transition metal complexes, several methodologies were adopted: a) deprotonation of the corresponding imidazolium salts followed by addition of transition metal precursors; b) transmetalation from NHC silver complexes; c) oxidative-addition reaction of Ni(0) with imidazolium salts or the corresponding protonated salts. A series of Ni(II), Cr(III) complexes were tested in the catalytic ethylene oligomerization reaction.

Keywords: N-heterocyclic carbenes, tritopic pincer ligands, oxidative addition, alkylation, Ni, Cr, Ir, Cu, Ag, ethylene oligomerization.